SEISMIC SITE RESPONSE OF ALLUVIAL VALLEYS AND EFFECTS ON A SUSPENSION BRIDGE

BY

MOHSEN M. M. RASSEM, B.Sc., M.Sc.

A Thesis

Submitted to the School of Graduate studies

in Partial Fulfilment of the Requirements

for the Degree of

Doctor of Philosophy

McMaster University

SEISMIC SITE RESPONSE OF ALLUVIAL VALLEYS AND EFFECTS ON A SUSPENSION BRIDGE

TO MY PARENTS AND MY WIFE AZZA

DOCTOR OF PHILOSOPHY (1992)
(Civil Engineering and Engineering Mechanics)

McMaster University
Hamilton, Ontario

TITLE:	Seismic site response of alluvial valleys and effects on a suspension bridge
AUTHOR:	Mohsen M. M. Rassem, B.Sc. (Cairo University) M.Sc. (Cairo University)
SUPERVISORS:	Professor A.C. Heidebrecht Professor A. Ghobarah
NUMBER OF PAGES:	xv, 195

ABSTRACT

A study has been conducted on the seismic site response of alluvial valleys with limited width and the effects of spatially varying surface motions in these valleys on the response of a suspension bridge. The intent of this investigation is to extend the work carried out by seismologists on the two-dimensional seismic response of alluvial valleys to include the effects of stiffness variation with depth and non-linear behaviour of soils which were mainly considered by engineers in a one-dimensional perspective. One objective is to provide engineers with useful guidelines to predict the valley response at different sites. Another objective is to analyze the potential of soil conditions and subsurface topographic structure in alluvial valleys for producing significant variations in the bridge response to a multiple-support excitation.

A simplified engineering model (frame model) has been developed to predict the non-linear seismic response of symmetrical valleys. The proposed model is a one-dimensional model which accounts for the limited horizontal extent of soil in a two-dimensional valley. The frame model provides valuable insight into the dynamic behaviour of the alluvial valley by identifying the vibration modes of significance and their variation in the horizontal and vertical directions. Response results from the frame model show good agreement with those results from the two-dimensional finite-element model of the valley.

Effect of the key parameters governing the spatial variations of motions at different sites in the valley has been analyzed. This includes the effect of soil type, valley geometry and control motion characteristics in rock. It is found that the two-dimensional effect from the valley edges extends toward the centre up to a distance after which only one dimension, the depth, governs the response. The soil amplification varies from one soil type to another, depending on the stiffness of soil and the amount of damping existing during excitation. The magnitude of the surface spectral acceleration at a site depends on the proximity of the local-amplification period at site to the dominant period of the input rock record. Finally, the free-field surface motions in a hypothetical valley are applied to the Humber suspension bridge in U.K. It is concluded that the inclusion of the multiple-support excitation case in the analysis is significant when soil conditions and topography produce noticeable variations in the intensity of support motions in the period range of interest for the bridge response.

ACKNOWLEDGEMENTS

I would like to express my sincere gratitude to my supervisors Dr. A.C. Heidebrecht and Dr. A. Ghobarah for their guidance, advice and interest during the course of this research.

Special thanks are due to Dr. J.C. Wilson and Dr. M. Dokainish, members of my supervisory committee, for their valuable comments and suggestions.

Many thanks to my wife Azza for her help, understanding and encouragement towards the completion of this thesis. Special thanks to my parents for their support and inspiration.

Particular acknowledgement is due to McMaster University for providing the financial support for the research work.

TABLE OF CONTENTS

TABLE OF CONTENTS (continued)

TABLE OF CONTENTS (continued)

TABLE OF CONTENTS (continued)

LIST OF FIGURES

LIST OF FIGURES (continued)

LIST OF FIGURES (continued)

LIST OF FIGURES (continued)

LIST OF FIGURES (continued)

LIST OF TABLES

CHAPTER 1
INTRODUCTION

1.1 GENERAL

The general understanding of earthquake ground motions, the manner in which they propagate through the earth, descriptions of their characteristics at a certain location and methods for incorporating this information into engineering designs have been the subject of considerable interest and research. The characteristics of earthquake shaking at a given site in a particular event will depend on a number of factors including:

1. The source mechanism of the earthquake
2. The distance of the site from the main zone of energy release
3. The geological characteristics of the rocks along the wave transmission path from source to site
4. The effects of wave interference
5. The local soil conditions at the site

The energy released from a source mechanism will travel in the form of seismic waves through the rock formation where some energy absorption takes place. The seismic waves will be reflected and refracted as they approach the zone of special interest. The motions will be further modified as they pass from the underlying rock formation through different soil deposits until they reach the ground surface where structures are founded. The significant characteristics of ground motions that affect the intensity of shaking and the extent of damage to structures include:

1. The maximum amplitude of ground acceleration, velocity and displacement
2. The frequency content of the excitation

3. The duration of strong-phase shaking

Analysis of the source mechanism and the effects of transmission path geology on earthquake waves is the main area of interest for seismologists. The effects of local site conditions on the characteristics of ground motions have been the focus of research by both seismologists and geotechnical engineers. This is because of the concentration of human population in sediment-filled valleys and because of the common observation that ground motion at the surface of sediments is larger than on nearby hard rocks (e.g. Gutenberg, 1957). The aim of the seismological and geotechnical studies is the definition of the design earthquake input which is of main interest to the structural engineer. Once a suitable support-excitation history has been established, the calculation of the stresses and deflections in a given structure is a problem of structural dynamics and on occasion soil-structure interaction.

Site-response problems involve the determination of the effects of local soil conditions on the temporal and spatial variation of all the motions within a site from a specified control motion at some control point within the site, where an observed or estimated motion is available. Soil parameters and geologic conditions that may cause significant effect on the characteristics of the ground motions at a site include:

1. Depth of soil layers above the bedrock
2. Variation of soil type and properties (shear modulus, mass density and material damping) along the depth
3. Non-linear variation of soil properties under strong earthquakes
4. Lateral irregularity and surface topography at the site

Mathematically, the site-response problem is one of wave propagation in a continuous medium. Soil amplification theories are useful as an engineering tool for obtaining reasonable estimates of motions, when applied with proper judgment. As in many other engineering problems, and particularly in the areas of geotechnology and earthquake engineering, there is a substantial amount of uncertainty in all phases of the analysis. Special consideration must be given to the selection of an appropriate control motion with characteristics consistent with the location where it is specified. However, the estimation of the control motion and the wave pattern contributing to it is still a major problem to establish and far-reaching assumptions have to be made. Moreover, the estimation of soil properties and their variation with level of strains should be considered in any mathematical model. Finally, the establishment of boundaries and boundary conditions should also be taken into consideration. Actual soft surface layers are not infinitely flat but laterally confined in the form of sediment-filled valley or basin. The finite lateral extent of surface layers introduces additional effects such as the generation of surface waves at the edge and the resonance in lateral direction and tends to increase the amplitude as well as the duration of ground motion (Aki, 1988). This will create spatially varying ground motions at the soil surface of the valley. These spatial variations are of particular significance in the assessment of the seismic response of long structures such as dams, bridges or life-line systems. The relative movements at different support points may contribute significantly to the response and dynamic stresses in such structures. The main concern in this thesis will be focused on the evaluation of the seismic site response of alluvial valleys and the effects of the free-field surface motions in a valley on the dynamic response of a long-span suspension bridge.

1.2 LITERATURE REVIEW

1.2.1 Effects of Site Conditions on Ground Motions

Seismic waves propagating through near-surface soil layers can amplify and produce free-field ground motions much larger and with different characteristics than those recorded at the rock base. The combined effects of earthquakes and local site conditions are commonly referred to as site response effects. Numerous examples of recent earthquakes where site effects were observed are available. For example, during the 1985 Mexico City earthquake, site amplification caused substantial damage and collapse of many buildings (Romo and Seed, 1986; Seed et al, 1987). Records of damage during the 1989 Loma Prieta, California, earthquake also indicate that site response effects were the major cause of failure of many facilities (Astaneh et al, 1990). Detailed studies of the relationship between building damage and soil conditions were provided by Seed (1986).

The estimation of site specific ground motion parameters for seismic design studies is one of the more complex and challenging problems of earthquake engineering. Apparent differences in the main interests of seismologists and geotechnical engineers have been reported by Finn (1991). For example, geotechnical engineers recognized the importance of non-linear effects at most soil sites during strong shaking, following the pioneering studies of ground response during the Niigata earthquake of 1964 by Seed and Idriss (1969). On the other hand, seismologists tend to find a good correlation between weak and strong motions at a given site, namely, similar amplification for both, implying that non-linearities are not important as the first order effect in most cases (Aki, 1988). Reviews by seismologists such as Sanchez-Sesma (1987), Aki (1988) and Faccioli (1991) have shown that the effects of surface and buried topography on ground motions can be significant from both the seismological and engineering points of view. However, geotechnical engineers have mainly relied on the one-dimensional analysis to predict surface motions at any site, overlooking the effects of surface topography and the limited lateral extent of soil in sediment-filled valleys.

The one-dimensional approach is based on Kanai's (1952) assumption that the main response in a soil deposit is caused by the upward propagation of shear waves from the underlying rock formation. Analytical procedures based on this concept incorporating non-linear soil behaviour in a linear iterative scheme in the frequency domain were introduced by Schnabel et al (1972) in the SHAKE program. The computer program SIREN, developed by J.W. Pappin (Henderson et al, 1989a), solves the one-dimensional problem in the time domain using finite differences in a true non-linear model. In the SIREN program, the soil is represented as a series of lumped masses connected by non-linear springs. The non-linear springs are formulated as an assemblage of elastic-plastic springs which exhibit hysteretic damping in accordance with the Masing principles (Pyke, 1979). SIREN program was used by Heidebrecht et al (1990) and Henderson et al (1990) for the analysis of site response effects for structures located on clay sites and sand sites, respectively. They showed that, depending on the site and the nature and level of the rock excitation, the expected base shears can be well in excess of the values specified by the National Building Code of Canada (NBCC) 1990.

For non-vertical incidence of body waves, the situation becomes complicated because of the coupling between primary (P) and shear (SV) waves in plane, as they reflect and refract at soil layer interfaces. Solutions for body waves with arbitrary angles of incidence have been obtained for stratified soils without lateral irregularities. The fundamental work was done by Thomson (1950) and Haskell (1960; 1962) who developed an efficient matrix method for computing the frequency-dependent transmission coefficients in a layered linear continuum for incident SH, SV and P-waves, where the SH waves are those shear waves associated with out-of-plane motion. Silva (1976) extended the Thomson-Haskell method to include damping in the soil layers. Huang (1984) developed a two-dimensional model considering inclined body waves propagating horizontally in homogeneous layered soil overlying a half-space.The system was assumed to be linear and the problem was studied in the frequency domain. Based on the three-dimensional wave equation, Wolf (1985) formulated transfer and dynamic stiffness matrices of horizontal surface layers and of half-space for in-plane (P, SV waves) and out-of-plane (SH waves) motions with different angles of incidence. Uniform linear material properties were assumed for the horizontal surface layers.

The finite lateral extent of soil surface layers in a sediment-filled valley has been the subject of numerous studies. The sediment-basement rock interface generates surface waves and may trap body waves in the alluvium (Aki, 1988). These waves amplify the motion and increase the duration over that predicted by the one-dimensional analysis. There are several well-documented examples of valleys or basins that were shaken by earthquakes where such effects were clearly observed. A case in which the irregularities of the subsurface topography appear to have influenced significantly the motion of the overlying sediments is the response of the Caracas valley, Venezuela, to the July 29, 1967 earthquake. A significant feature of the earthquake was the concentration of damage to certain types of structures in localized areas (Seed et al, 1970; 1972). This damage concentration was attributed to the site effects. During the Lima, Peru, earthquake of November 9, 1974, ground-motion accelerograms recorded at two sites with nearly the same epicentral distance display pronounced dissimilarities (Zahradnik and Hron, 1987). The first site, located on top of a weakly horizontally varying surface structure, experienced only minor shaking. The second site, on top of the La Molina sediment-filled valley, was subjected to a remarkably strong and prolonged ground motion that can be explained by the combined effect of the complex bedrock topology and the soft subsurface sediments. The 1971 San Fernando, California, earthquake data demonstrated clearly that the excitation of surface waves in deep sedimentary basins of the San Fernando and the Los Angeles areas had a pronounced effect on the amplitude and duration of the ground motion (Hanks, 1975; Vidale and Helmberger, 1988). Variations in the response at different sites of the Mexico City valley to the September 19, 1985 Mexican earthquake have also been observed (Finn and Nichols, 1988; Bard et al, 1988).

A variety of approaches were developed to predict the motions in an alluvial valley analytically. Exact analytical solutions are available for the case of SH waves incident on a semi-cylindrical (Trifunac, 1971) and a Semi-elliptical (Wong and Trifunac, 1974) sediment-filled valleys. Lee (1984) obtained solutions for the three-dimensional cases of P, SH and SV plane waves incident on a semi-spherical valley.

Finite difference (Harmsen and Harding, 1981) and finite element (Ohtsuki and Harumi, 1983) have been used to show a strong generation of Rayleigh waves at the edge of sediment-filled valleys when P and SV waves are incident. The finite element method has the advantage of modelling very irregular soil configurations considering the hysteretic behaviour of soil (e.g. Joyner and Chen, 1975; joyner, 1975). A finite-element computer program "FLUSH" was developed by Lysmer et al (1975) to take into account the strong non-linear effects which occur in soil subjected to strong earthquake motions. This was achieved by a combination of the equivalent linear method described by Seed and Idriss (1969) and the method of complex response in the frequency domain. The input excitation to the finite element model in FLUSH program is specified by an acceleration time history at the rigid baserock which does not have to be horizontal.

The boundary methods are well suited to deal with wave propagation problems because they avoid the introduction of fictitious boundaries and reduce by one the dimensionality of the problem, which yield numerical advantages. Boundary methods were applied to various problems of diffraction of elastic waves (e.g. Sanchez-Sesma and Esquivel, 1979; Wong, 1982; Dravinski, 1983; Bravo et al, 1988). Moreover, a hybrid method that combines the finite element discretization and the boundary integral representation has been introduced by Khair et al (1989) to simulate the three-dimensional scattering of obliquely incident P and SV waves by cylindrical alluvial valleys. Khair et al (1991) applied the same hybrid method to investigate the scattering of SH and Rayleigh waves in a cylindrical alluvial valley.

Ray methods (Hong and Helmberger, 1977) have also been used to study the ground motion in sediment-filled basins. They appear to give good results for the case of incident SH waves. Sanchez-Sesma et al (1988) presented a simple representation of wave field as a sum of rays in a triangular basin under incident SH waves. Ray methods, however, are incapable of dealing with the cases in which plane waves, such as P and SV waves, are incident on alluvial valleys.

Aki and Larner (1970) presented a method which can be considered as a particular case of approximation to the complete system of solutions. In the Aki-Larner method, the wave field in each layer is expressed as a superposition of plane harmonic waves including inhomogeneous plane waves. The boundary condition is met in the horizontal wave-number domain taking advantage of the fast Fourier transform. This method has found many applications in seismology, mainly due to its flexibility to model an elastic field. The Aki-Larner method has been extended to the time domain by Bard and Bouchon (1980a, b; 1985) and to the case of vertically inhomogeneous layers by Bard and Gariel (1986).

Bard and Bouchon (1980a) considered two types of alluvial valley geometry in plane: a cosine-shaped valley and a valley having flat bottom and bounded by steep edges (trapezoidal). Both valleys are symmetrical in plane and have the same depth at the centre and the same total width at the top surface. The results showed that, in the case of SH waves incident vertically from below on the valley, Love waves are generated at the edge of the valley and propagated back and forth between both edges. The amplitude of Love waves is the largest at the valley centre because of the constructive interference of waves from both edges. It was also pointed out that Love waves are generated in the cosine-shaped valley more strongly than in the flat-bottom valley. The flat-bottom valley, on the other hand, produces stronger one-dimensional response because of the broader width over which the sediment depth is constant. Bard and Bouchon (1980b) extended their study of SH waves in sediment-filled valleys to vertically incident P and SV waves using the same two types of valley geometry. They found that the behaviour of the motion is qualitatively similar to that for SH waves. The edge of the valley generates Rayleigh waves which are trapped between the two edges and increases the amplitude of motion as well as its duration.

The numerical results of Bard and Bouchon (1985) on the elastic response of symmetrical and homogeneous sediment-filled valleys show the existence of specific two-dimensional resonance patterns in relatively deep valleys, regardless of the incident wave field. They classified the patterns into three categories: the anti-plane shear modes (SH), the in-plane shear modes (SV) and the in-plane "bulk" modes (P). These resonances affect the valley as a whole and are associated with large amplifications and with long duration of motion. The three fundamental modes (in-plane shear, anti-plane shear and bulk), which are the most important ones, are characterized by an in-phase motion for the main component (horizontal transverse to the valley axis, horizontal parallel to the valley axis and vertical, respectively). The corresponding amplification is maximum at the valley centre and regularly decreases toward the edges, where it vanishes. An important result of their study is that both the two-dimensional resonant frequencies and amplification values differ substantially from their "classical" one-dimensional estimates.

The above characteristics of resonance patterns are in perfect agreement with the experimental observations of King and Tucker (1984) and Tucker and King (1984). The experiments of King and Tucker (1984) on the sediments of Chusal Valley in the Garm (Tadjikistan) region indicate that the ratio of valley to rock motion depends strongly on frequency and the location of the valley site and to a lesser extent on azimuth and incidence of the input signal.

One of the recent papers that extended the Aki-Larner method to the prediction of seismic motion in an arbitrary arrangement of a three-dimensional sedimentary basin was presented by Uebayashi et al (1992). The results of their analysis pointed out that the seismic motions in the three-dimensional wavefield are greater in spatial variation and larger in maximum amplitude than those in the two-dimensional wavefield at all sites in the basin. These differences were mainly attributed to the local surface waves generated at the periphery of the basin. It was concluded that the three-dimensional irregular subsurface structures must be taken into account when predicting seismic ground motions in sedimentary basins.

1.2.2 Response of Suspension Bridges to Varying Input Excitations

Complete seismic analysis of critical structures, particularly with long spans such as suspension bridges, requires realistic predictions of the free-field ground motions at all the interface points on the supporting foundation under design earthquake conditions. Time histories differ slightly in wave form at sequential points because of wave propagation differential velocities and because of irregularities in rock and soil structure. The effects in the input support motions show up as phase shifts and as variations in amplitude and frequency.

Seismic response of long structures, and in particular suspension bridges, to differential ground motions has been considered by many investigators. Bogdanoff et al (1965) were among the first investigators to consider the transmission time of a seismic disturbance in considering the response of a long-span suspension bridge. Their suspension bridge model was a simplified spring-mass arrangement, and they analyzed the random response in terms of extreme values. They utilized a random input to the structure which was assumed to propagate from one end of the structure to the other at a constant velocity causing phase delays at the support points of the bridge. It was concluded that the phasing of support motions is very important in long-span structures and that the propagating input resulted in a much more severe response than the case of simultaneous uniform support excitations.

Studies of the influence of various parameters on the dynamic response of single- and multi-span bridges supported on an elastic half-space were carried out by Abdel-Ghaffar and Trifunac (1977) and Werner et al (1979) for the case of incident plane SH-waves. Soil-structure interaction was introduced in their analyses which showed the dynamic response to be dependent on the phase differences in the input ground motions applied to the bridge foundations and on the direction of incidence as well as the excitation frequency of the seismic waves.

In the deterministic approach to the dynamic analysis of structures, the ground motion input is completely specified in advance and the dynamic structural response can be determined in the time domain, where the variation with time or maximum values of particular response quantities are obtained. Multiple-support seismic excitation techniques (Clough and Penzien, 1975) are used to obtain the dynamic response of a structure to a varying input motion at its supports. Altinisik and Severn (1981) and Dumanoglu and Severn (1984) are among the papers dealing with deterministic approaches in multiple-support seismic excitation problems. They showed that the finite speed of the travelling wave and the finite travel time, in turn, produce a quasi-static displacement in addition to the normal dynamic displacement. The additional quasi-static displacement is caused by the differential movement of the foundations and is time-dependent. This causes stresses which are added to the dynamic stresses caused by inertia forces. Dumanoglu and Severn (1985b, c, d) applied their travelling wave approach to the finite-element models of two modern suspension bridges with box-girders, flexible towers and inclined hangers: the Bosporus bridge in Turkey and the Humber bridge in U.K. with main spans of 1074 m and 1410 m, respectively. A single acceleration record was assumed to propagate with different finite speeds from one support to another without change in frequency or amplitude. They used a multiple-support excitation time-history analysis based on the modal response of the bridges to obtain the total response that include the dynamic as well as the quasi-static effects of vibration. They showed that the quasi-static effect becomes significant for lower speeds of wave propagation and may lead, when added to the dynamic response, to total response values in some parts of the bridge that are higher than those obtained under the uniform support excitation assumption.

A simple and approximate response spectrum technique was proposed for the multiple-support excitation problem by Rutenberg and Heidebrecht (1987). Time lag effects were considered under the travelling wave assumption. The response spectrum approach showed good agreement with the time history analysis by Dumanoglu and Severn (1984), when applied to the multiple-support excitation of single- and three-bay frames. Rassem et al (1990) applied the above response spectrum technique to the multiple-support excitation of the Humber suspension bridge in U.K. They showed that while the dynamic response is lower under the travelling wave assumption, the quasi-static effects are likely to increase the response. The net effect depends on the ratio of the reduced dynamic displacement to the maximum differential motion.

Another approach to determine the structural dynamic response to a varying input motion is by using the stochastic analysis, in which the input motion and the required response quantities are described in statistical or probabilistic terms. The stochastic analysis has the advantage of reducing the large amount of information produced in the time domain analysis of structures into statistical parameters relating this information together. However, the statistical parameters of response, in themselves, are not indicative of the maximum response values which are significant in determining the damaging potential of the excitations. Any input excitation can be expressed as a sum of harmonic functions to which the structural system response can be easily obtained. Although all information about time is lost in the frequency domain, the frequency content of the response becomes much clearer and the analysis is simpler. The solution in the frequency domain is the approach used in the stochastic method. In fact, the stochastic analysis can be summarized as the determination of what is called the spectral density function of the output once the spectral density of the input is given. In this approach, the ground motions at different stations are modelled as random processes with a given spectral density and the spatial variation is described by a correlation function. Recorded earthquake data collected from strong ground motion arrays are required to evaluate the spectral density and correlation function.

Abdel-Ghaffar and Rubin investigated the vertical response (1983a) and the lateral response (1983b) of the Golden Gate suspension bridge in California, when subjected to correlated or uncorrelated multiple-support excitations. The analysis was performed using the frequency-domain random-vibration approach. The ground motion inputs were taken from an array of time histories recorded during the Imperial Valley, California, earthquake of October 15, 1979. They took into account not only the differences in ground motion inputs but also the correlation among the various input motions. They showed that the uncorrelated ground inputs over-estimate the bridge response. In addition, they pointed out that a relatively large number of modes is necessary to obtain a reasonable representation of the response and that uniform ground motion over the entire span in the analysis of these long structures does not represent the worst possible conditions.

Instead of assuming different seismic inputs acting simultaneously at the supports of the Golden Gate bridge, Abdel-Ghaffar and Stringfellow (1984a, b) used only one array record from the October 15, 1979 Imperial Valley earthquake as the input to the left anchorage of the bridge. The single input record was assumed to propagate with different speeds with no change in shape. They analyzed the vertical and lateral responses of the bridge in the time domain (deterministic) as well as in the frequency domain (stochastic) under different wave propagation velocities. They concluded that the shear wave propagation velocity can have a significant effect on the response which is somehow different than the effect of using different simultaneous multiple array inputs. They also pointed out that the frequency domain analysis yields results which are roughly the same as those found in the time domain.

Dumanoglu and Severn (1990) studied the applicability of stochastic methods for determining the seismic response of the Humber and Bosporus suspension bridges. They showed that this depends on whether the input function contains significant frequency components coinciding with the natural frequencies of the structure. They concluded that the stochastic approach gives acceptable results when the limited duration of the input record is extended by adding trailing zeros to allow values of response quantities to appear sufficiently frequently to permit statistical concepts to apply.

A response spectrum was developed by Der Kiureghian and Neuenhofer (1992) for the seismic analysis of linear multi-degree-of-freedom, multiply-supported structures subjected to spatially varying ground motions. The method is based on the fundamental principles of random vibration theory and considers the variations of ground motion due to wave passage, loss of coherency with distance and variation of local soil conditions. The former two effects are modelled in terms of a coherency function, whereas the local soil effect is considered in terms of its influence on the response spectral shape at each individual support point. It was found that in most cases the spatial variability tends to reduce the response in relation to the case of uniform support motions. However, under certain conditions (rapid loss of coherency) it was found that the response may actually amplify due to an increase in the quasi-static component of response.

Several analyses of (SMART-1) array recordings in Taiwan have been performed to derive engineering guidelines for assessing the influence of spatial variations of ground motions on the dynamic response of extended structures. The research performed by earthquake engineers on SMART-1 data, since it began operation in September 1980, has led, among other results, to the construction of various coherency models of wave propagation as functions of separation distance of the structural supports and of the frequency. One of the recent examples is the coherency model presented by Hao (1989) which allows the simulation and interpolation of realistic spatially correlated multiple ground motions compatible with prescribed ground motion properties and given response spectra. He developed a computer program to perform this task as well as to utilize these simulated ground motions as the multiple inputs to solve the structural response including soil-structure interaction effects. He demonstrated that often there is a general reduction in structural response when multiple inputs are used due to the phase differences in the inputs. The conclusion was that the seismic multiple inputs at support points must not only possess realistic characteristics individually but they must also be properly cross-correlated with each other.

1.3 OBJECTIVES AND SCOPE

Although available seismological studies provide valuable insight into the qualitative features of seismic response of sedimentary valleys, these approaches are incapable of providing a realistic quantitative response evaluation that can be relied upon by engineers in making decisions regarding their structural design at different sites in the valley. This is because, in the majority of their analyses, seismologists disregarded the effects of variation of soil stiffness with depth as well as the non-linear behaviour of soil deposits under strong earthquakes. The effects of these parameters are of much interest to engineers but were so far mainly included in a one-dimensional scope. Therefore, it is of interest to extend the work carried out by seismologists on alluvial valleys in the two-dimensional field to more realistic representation of the problem by including the stiffness variation with depth and non-linear behaviour of soils. This will integrate the seismological and engineering perspectives to gain more physical insight into the dynamic behaviour of alluvial valleys. In addition, useful guidelines will be provided for engineers to predict surface ground motions in a sedimentary valley which has a limited lateral extent in plane, under different conditions of valley dimensions, soil types and rock motion characteristics. The objectives of the present investigation regarding the analysis of the seismic site response of alluvial valleys can be summarized as follows:

1. To provide guidelines on the limitations of using the one-dimensional approach to obtain the free-field motions in valleys with limited width.
2. To identify the main parameters governing the spatial variations of surface seismic motions in alluvial valleys.
3. To develop a simple engineering model capable of predicting the non-linear seismic site response of alluvial valleys, based on the understanding of their performance in plane.
4. To examine the sensitivity of the valley response, which is obtained from different engineering models, to small variations in dynamic soil properties in order to account for the uncertainty in establishing these properties.
5. To analyze the influence of valley dimensions on the seismic site response as well as on the validity of the engineering models.
6. To investigate the influence of soil type and input rock motion characteristics (maximum amplitude and frequency content) on the seismic response of valleys.

The analyses carried out by many investigators on the multiple-support excitation of suspension bridges were not directly related to site topographic effects. The focus was rather on analyzing the response to spatially varying ground motions that are correlated, uncorrelated or travelling according to some assumptions of ground motion models which overlooked the spatial variations due to topographic effects in sedimentary valleys. To evaluate the possible effects of soil conditions and subsurface topographic structure in alluvial valleys, the case of extended long-span suspension bridge is investigated. The surface motions in a hypothetical valley will be applied to the suspension bridge to achieve the following objectives:

1. To develop more realistic varying input motions at the supports of a long-span suspension bridge by utilizing the analytical model of the valley. The purpose is to analyze the linear dynamic response of the bridge to spatially varying excitations which are different in amplitude and frequency.
2. To examine the influence of parameters such as soil type and bridge support locations in the valley on the multiple-support input motion to the bridge and the potential for producing significant variation in the bridge response.

The scope of the present study is confined to valleys and rock motions with the following limitations:

1. The alluvial valley is symmetrical in plane and bounded by rigid rock. The valley has a limited width relative to its depth.
2. The soil continuum can be divided into horizontal layers, each of which has homogeneous and isotropic material properties.
3. The non-linear response of soil is obtained through an iterative linear approach. In each iteration, linear elastic response is assumed, provided that soil properties are compatible with the effective shear strain amplitudes from the previous iteration.
4. The input control motion is selected as a given accelerogram representing a horizontal (or vertical) component of excitation and acting along the rock boundary of the alluvial valley. This is assumed to be sufficiently accurate for engineering purposes, since many uncertainties are involved in identifying the wave pattern contribution to a given control motion.

1.4 THESIS ORGANIZATION

To accomplish the stated objectives, the study is organized as follows:

1. In chapter 2, two existing engineering models (one-dimensional and two-dimensional

finite element) for symmetrical valleys, in plane, are reviewed and a new one (frame model) is developed to represent the alluvial valley response under earthquake motions in rock.

2. In chapter 3, the key parameters that are expected to govern the seismic response of alluvial valleys are presented: soil type, valley geometry and control motion characteristics in rock.
3. In chapter 4, the sensitivity of the horizontal seismic response of the valley, resulting from the engineering models, is examined for the variation in soil-layer discretization and the variation in dynamic soil properties.
4. In chapter 5, the influence of valley dimensions on the horizontal seismic site response as well as on the validity of the engineering models is investigated. Limitations on the use of the one-dimensional approach to predict the valley response are discussed.
5. In chapter 6, the influence of soil type and uniform rock motion characteristics on the horizontal seismic site response of the valley is analyzed. In addition, the valley response to a travelling motion in rock is addressed and results are compared with the case of uniform rock excitation.
6. In chapter 7, the free-field horizontal surface motions in a hypothetical wide valley are applied to the supports of the Humber suspension bridge in the U.K. The linear dynamic response of the bridge to the spatially varying excitations at its supports is analyzed for different soil conditions and various cases of support locations.
7. A summary of the analysis, conclusions of this study and recommendations for future work are provided in chapter 8.

CHAPTER 2

ENGINEERING MODELS AND DYNAMICS OF THE VALLEY

2.1 INTRODUCTION

The problem of investigating the spatial variations of surface seismic motions that arise in alluvial valleys requires an analytical model capable of accounting for the complexities involved in the soil conditions, valley geometry and input rock motions. In general, site-response problems are ill-posed and unique solutions can only be obtained by the introduction of restrictive assumptions leading to the development of the required models.

The analysis performed in this study is for a symmetrical alluvial valley, in the two-dimensional plane, with horizontal soil surface and bounded by rigid rock. Two engineering models are reviewed for predicting the seismic motions developed in the valley under the influence of a uniform control motion acting in plane along the rock boundary. In addition a third model that accounts for the horizontal and vertical responses is developed. The first model is based on the one-dimensional approach which has enjoyed popularity among practising engineers, in spite of the restrictions that may be relevant. The second is based on the finite-element method which is believed to provide the most accurate analytical solution to the dynamic-response problem of the valley, since the irregularities of the rock boundaries and soil properties are best simulated using this model. The third model, namely the frame model, is basically developed by modifying the one-dimensional model to consider the effect of the limited horizontal extent of the soil in the valley. Numerical examples that compare vibration modes of the horizontal response of the valley from the last two approaches are provided. In addition, the horizontal response calculations using the frame model are presented.

2.2 THE ONE - DIMENSIONAL MODEL

The current approach to most site-response problems is to use the one-dimensional model, for simplicity, regardless of how far the soil may extend horizontally. Although this model may be valid near or at the centre of a valley with large horizontal dimensions, it will fail in approximating the response near the edges of the valley, where the effects of the sloping rock boundaries are significant.

2.2.1 Assumptions

The following are the main assumptions used in the one-dimensional analysis:

1. The ground motions developed near the surface of a soil deposit during an earthquake may be attributed primarily to the upward propagation of shear waves from an underlying rock formation (Idriss and Seed, 1968).
2. The ground surface, the rock surface and the boundaries between soil layers are horizontal and extend infinitely in the lateral direction.

In such cases, the ground motions induced by the seismic excitation at the base are only the result of shear deformations in the soil, and the deposit may be considered as a one-dimensional shear beam. The one-dimensional model can also predict the surface vertical response under the assumption of upward propagation of P-waves.

Further idealized conditions are assumed to obtain a simple mathematical representation of the model. These assumptions involve treating the soil continuum as a linear visco-elastic system consisting of layers, each of which has homogeneous and isotropic material properties (Schnabel et al, 1972).

2.2.2 Methods of Analysis

The one-dimensional model can be used to obtain the resulting motion at a point on the soil surface by considering the response of a soil column located underneath that point, as shown in Fig. 2-1. The following two methods may be used for the analysis :

a. The finite-difference approach (lumped-mass model), suggested by Seed and Idriss (1969), where the soil column is discretized into lumped masses, one at each layer boundary, connected by shear springs. These springs represent the shear stiffness properties of the soil between any two discrete masses. The approach is idealized in Fig. 2-2 (a).

b. The wave-propagation approach (continuous model) which is based on the solution of the wave equation and shown in Fig. 2-2 (b). This approach was presented by Tsai and Housner (1970).

Program SHAKE, introduced by Schnabel et al (1972), is employed in this study to calculate the response of the one-dimensional analysis. The program is based on the continuous solution to the wave equation for vertical propagation of shear waves, as shown in Fig. 2-2 (b). Hysteretic damping in the soil is included in the complex shear modulus terms. The system transfer functions are obtained in the frequency domain and multiplied by the Fourier transform of the input bedrock motion to obtain the Fourier transform of the surface motion. An inverse transformation then gives the time history of the output motion. The non-linearity of the shear modulus and damping is accounted for by the use of equivalent linear soil properties (Idriss and Seed, 1968 ; Seed and Idriss, 1970) using an iterative procedure to obtain values for shear modulus and damping compatible with the effective strains in each layer.

2.3 THE TWO - DIMENSIONAL FINITE - ELEMENT MODEL

The finite-element method is a numerical procedure by means of which the actual soil continuum is represented by an assemblage of elements interconnected at a finite number of nodal points as shown in Fig. 2-3. Excitations along the rock boundary are specified as boundary conditions and the resulting motions in the valley are computed. Output motions are free to have two in-plane components regardless of the direction of the input motion component.

In earthquake - response evaluations, the governing equation of motion is:

$$[M]\ \{\ddot{u}\} + [C]\ \{\dot{u}\} + [K]\ \{u\} = \{Q(t)\} \qquad [2.1]$$

in which,

[M] = mass matrix for the assemblage of elements

[C] = damping matrix of the system

[K] = overall stiffness matrix of the system

{ u } = nodal displacements vector (dots denote differentiation with respect to time), and

{Q(t)} = earthquake load vector

The solution of equation [2.1] may be performed in the time domain by modal superposition (Clough and Chopra, 1966 ; Idriss and Seed, 1966) or by direct integration (Dibaj and Penzien, 1969 ; Idriss et al, 1973).

Program FLUSH, by Lysmer et al (1975), is used for the two-dimensional modelling of the valley under consideration, where equation [2.1] is solved in the frequency domain. The rock boundary is assumed to be rigid and translate horizontally or vertically according to a given acceleration time history. The program applies the method of complex response where the earthquake motion is decomposed into a complex series of harmonic motions using the fast Fourier transform technique, by Cooley and

Tukey (1965). The harmonic response to each term in the complex input series is obtained independently and the complete solution follows by simple superposition in the frequency domain. The damping can be introduced by using complex moduli in the formation of the stiffness matrix [K]. The response can then be obtained in the time domain by the inverse Fourier transform.

The solution procedure makes extensive use of superposition and therefore is applicable only to linear visco-elastic systems. However, the large shear deformations which occur in soils during strong earthquakes introduce significant non-linear effects. This problem has been solved by Seed and Idriss (1969) by the introduction of the equivalent linear method. According to this method an approximate non-linear solution can be obtained by a linear analysis provided the stiffness and damping used are compatible with the effective shear strain amplitudes at all points of the system. This can be achieved in iterative linear steps. The response from the last iteration is taken as being the non-linear response.

2.4 THE PROPOSED FRAME MODEL

Being a simple approach, the one-dimensional analysis does not consider the limited horizontal extent of the soil layers in an alluvial valley. Furthermore, it lacks the continuity of displacements between any two adjacent soil columns with different depths. A new model for the valley is developed in this section to modify the response resulting from the one-dimensional model by adding the effect of the sloping rock boundary. This will create variation in the motion with the horizontal direction, leading to a more realistic representation of the seismic behaviour of the valley.

2.4.1 Main Assumptions and Limitations

The new model of the valley is originally based on the one-dimensional approach with modifications to consider the limited horizontal extent of the soil. In the model development, the following assumptions are adopted :

1. The soil continuum can be divided into horizontal layers, each of which is homogeneous and isotropic.
2. The valley is symmetrical about the z-axis of the x-z plane, as shown in Fig. 2-4, and bounded by rigid rock where the input motion is uniform. This will lead to an antisymmetrical loading in the case when the horizontal component of the control motion is used and symmetrical loading when the vertical component is in effect. Consequently, the soil response at the line of symmetry of the valley will be in the same direction as the input motion component in the underlying rock. The frame model will be thus capable of producing only one component of motion in the same direction as the input component (horizontal or vertical).

2.4.2 Horizontal Undamped Free Vibration Response of a Soil Layer

To investigate the horizontal undamped free vibration response of the symmetrical valley shown in Fig. 2-4, the valley is divided into N layers with uniform soil properties for each layer. The origin of the x-axis is at the centre line of the valley. The local z-axis of each layer points downward and its origin is located at the top of the layer. Consider an infinitesimal cube of dimensions dx , dz and unit thickness. The deformation gradients in the x-direction of the cube in a layer, with thickness, h , and breadth at mid-height, $2B$, are shown in Fig. 2-5. The horizontal displacement response in this layer as a function of the local coordinates x and z and the time, t , is termed $u(x,z,t)$. The derivatives $\partial u/\partial z$ and $\partial u/\partial x$ are the shear strain and axial strain in the x-direction, respectively. The axial strain, $\partial u/\partial x$, is induced due to the limited width of valley.

The stresses acting on that cube are illustrated in Fig. 2-6, where τ_{zx} and σ_x are the shear stress and axial stress, respectively, in the x-direction. They are given by

$$\tau_{zx} = G \frac{\partial u}{\partial z} \qquad [2.2]$$

and

$$\sigma_x = (\lambda + 2G) \frac{\partial u}{\partial x} \qquad [2.3]$$

in which, G is the shear modulus and λ is Lamé's constant. The modulus $(\lambda+2G)$ can be expressed as

$$\lambda + 2G = 2G \frac{1-\nu}{1-2\nu} \qquad [2.4]$$

where, ν is Poisson's ratio.

The net forces acting in the x-direction on the cube are shown in Fig. 2-7. The inertia force, I_x, is given as

$$I_x = \rho \frac{\partial^2 u}{\partial t^2} dx.dz \qquad [2.5]$$

in which, ρ is the mass density. The net shear force, S_x, is expressed as

$$S_x = \frac{\partial \tau}{\partial z} dz.dx = G \frac{\partial^2 u}{\partial z^2} dx.dz \qquad [2.6]$$

and the net axial force, N_x, is given by

$$N_x = \frac{\partial \sigma_x}{\partial x} dx.dz = (\lambda + 2G) \frac{\partial^2 u}{\partial x^2} dx.dz \qquad [2.7]$$

Dynamic equilibrium in the x-direction gives

$$S_x + N_x - I_x = 0 \qquad [2.8]$$

Substituting for the forces in equation [2.8] and omitting dx.dz lead to

$$G \frac{\partial^2 u}{\partial z^2} + (\lambda + 2G) \frac{\partial^2 u}{\partial x^2} = \rho \frac{\partial^2 u}{\partial t^2} \qquad [2.9]$$

Variables can be separated in the above equation using the substitution

$$u(x,z,t) = g(x)\, f(z)\, \psi(t) \qquad [2.10]$$

Substituting [2.10] into [2.9] and dividing by $[\rho\, g(x)\, f(z)\, \psi(t)]$ give

$$\frac{d^2\psi / dt^2}{\psi(t)} = \frac{(\lambda + 2G)}{\rho\, g(x)} . \frac{d^2 g}{dx^2} + \frac{G}{\rho\, f(z)} . \frac{d^2 f}{dz^2} \qquad [2.11]$$

Since the left-hand side of equation [2.11] is a function of the time, t, only, whereas the right-hand side depends on x and z which are independent from t, each side should equal a constant. This constant of separation is taken as $(-\omega^2)$ and leads to

$$\frac{d^2\psi}{dt^2} + \omega^2 \psi(t) = 0 \qquad [2.12]$$

which has the solution

$$\psi(t) = \exp(i \omega t) \qquad [2.13]$$

where, ω is the circular frequency of the horizontal vibration and $i = \sqrt{-1}$. Equating the right-hand side of equation [2.11] to $(-\omega^2)$ and rearranging give

$$\frac{1}{f(z)} . \frac{d^2 f}{dz^2} = - \frac{(\lambda + 2G)}{G.g(x)} . \frac{d^2 g}{dx^2} - \frac{\rho \omega^2}{G} \qquad [2.14]$$

Again, this can be solved by equating each side of the equation to a constant $(-p^2)$. This will result into two simple differential harmonic equations

$$\frac{d^2 f}{dz^2} + p^2 f(z) = 0 \qquad [2.15]$$

and

$$\frac{d^2 g}{dx^2} + q^2 g(x) = 0 \qquad [2.16]$$

where, p^2 and q^2 are constants that should satisfy the relationship

$$\omega^2 = p^2 \frac{G}{\rho} + q^2 \frac{\lambda + 2G}{\rho} \qquad [2.17]$$

The first term on the right-hand side of equation [2.17] represents the effect of shear stiffness of the soil on the resulting frequency, while the second term gives the effect of the sloping rock boundary. This indicates an increase in the overall horizontal stiffness of the valley when the limited lateral extent of the soil is considered. The Solution of equation [2.15] is

$$f(z) = E \exp(ipz) + F \exp(-ipz) \qquad (0 \le z \le h) \qquad [2.18]$$

Similarly, the solution of equation [2.16] can be written as

$$g(x) = C \exp(iqx) + D \exp(-iqx) \qquad (|x| \le B) \qquad [2.19]$$

where , C, D, E and F are constants to be determined from the boundary conditions, compatibility of displacements and continuity of shear stresses along layer interfaces. The function f (z) represents the variation of the horizontal vibration modes with the depth and the function g (x) describes the modal variation with the x-direction, which occurs due to the rock boundary constraint.

The horizontal component of uniform motion in the rock excites the horizontal modes of vibration with symmetrical variation about the z-axis due to the valley symmetry. In this case, g(x) is an even function, i.e.

$$g(x) = g(-x) \qquad [2.20]$$

Hence, the odd part in equation [2.19] must vanish and the variation of the mode shape with x becomes

$$g(x) = \cos(qx) \qquad [2.21]$$

Only one boundary condition is needed to define the constant q . If the breadth of the layer at its mid-height is 2B, then at x = $\pm$ B the relative displacement is zero. Thus, q can be expressed as

$$q = \frac{(2j-1)\pi}{2B} \qquad , j = 1,2,3,.... \qquad [2.22]$$

The resulting mode shapes in one layer can now be written as

$$u_{k,j}(x,z) = \left[\cos(q_j x)\right]\left[E\exp(ip_k z) + F\exp(-ip_k z)\right] \qquad [2.23]$$

where, $\quad$ j = 1,2,3,...

and $\quad$ k = 1,2,3,...

Equation [2.23] shows that the vibration modes of significance to the horizontal response can have several shapes of variation with the horizontal direction depending on the value of j. Also, for each j-variation there will exist different variations of the mode shapes with depth, which will be called, for short, the k-variations. Hence, $u_{k,j}$ (x, z) describes the horizontal displacement of the mode having k-variation with depth and j-variation with the horizontal direction.

2.4.3 Dynamic - Stiffness Matrix of a Soil Layer

Since the variation of the horizontal displacement with x is completely defined in equations [2.21] and [2.22] and is always a unit at x = 0 , the term describing the modal variation with z , in equation [2.23], needs only to be evaluated at the centre line of the valley. Thus, at x = 0 , u(x,z) in equation [2.23] will be denoted as u(z) , for the sake of conciseness, and is given by

$$u(z) = E\exp(ipz) + F\exp(-ipz) \qquad [2.24]$$

The amplitude, $\tau(z)$, describing the variation of the shear stress with z can be calculated from equation [2.2] and [2.24] as

$$\tau(z) = ipG\,[E\exp(ipz) - F\exp(-ipz)] \qquad [2.25]$$

Determining the modal variation with z is pursued by developing a dynamic stiffness matrix relating u(z) and $\tau(z)$ at the top and bottom of one layer. The horizontal layer of constant material properties shown in Fig. 2-8 represents the basic element for analyzing a layered valley. The displacement and stress at the top of the layer (subscript 1) follow from equations [2.24] and [2.25], when $z = 0$, as

$$\begin{Bmatrix} u_1 \\ \tau_1 \end{Bmatrix} = \begin{bmatrix} 1 & 1 \\ ipG & -ipG \end{bmatrix} \begin{Bmatrix} E \\ F \end{Bmatrix} \qquad [2.26]$$

Similarly, when $z = h$, the displacement and stress at the bottom of the layer (subscript 2) can be written as

$$\begin{Bmatrix} u_2 \\ \tau_2 \end{Bmatrix} = \begin{bmatrix} \exp(iph) & \exp(-iph) \\ ipG\exp(iph) & -ipG\exp(-iph) \end{bmatrix} \begin{Bmatrix} E \\ F \end{Bmatrix} \qquad [2.27]$$

By omitting the vector containing the constants E and F between equations [2.26] and [2.27], the state vector at the bottom of the layer can be related to that at the top by the following equation

$$\begin{Bmatrix} u_2 \\ \tau_2 \end{Bmatrix} = [T] \begin{Bmatrix} u_1 \\ \tau_1 \end{Bmatrix} \qquad [2.28]$$

in which, [T] is the transfer matrix, given by

$$[T] = \frac{1}{pG} \begin{bmatrix} pG\cos(ph) & \sin(ph) \\ -p^2G^2\sin(ph) & pG\cos(ph) \end{bmatrix} \qquad [2.29]$$

When assembling the stiffness matrix, the applied loads are defined in the global-coordinate system. Hence, τ_1 and τ_2 , defined in the local coordinate system, can be expressed globally by introducing the external load amplitudes $Q_1 = -\tau_1$ and $Q_2 = \tau_2$. Thus, equation [2.28] can be rearranged to become

$$\begin{Bmatrix} Q_1 \\ Q_2 \end{Bmatrix} = [s] \begin{Bmatrix} u_1 \\ u_2 \end{Bmatrix} \qquad [2.30]$$

in which, [s] is the dynamic-stiffness matrix of the layer, given as

$$[s] = \frac{pG}{\sin(ph)} \begin{bmatrix} \cos(ph) & -1 \\ -1 & \cos(ph) \end{bmatrix} \qquad [2.31]$$

By expanding sin (ph) and cos (ph) in a Taylor series and neglecting higher-order terms, they may be written as

$$\sin(ph) = ph \qquad [2.32]$$

and

$$\cos(ph) = 1 - \frac{1}{2}p^2h^2 \qquad [2.33]$$

The constant p^2 can be obtained from equation [2.17] as

$$p^2 = \frac{1}{G}[\rho\,\omega^2 - q^2(\lambda+2G)] \qquad [2.34]$$

The constant q is given by equation [2.22] as

$$q = \frac{(2j-1)\pi}{2B} \qquad , j = 1,2,3,.... \qquad [2.35]$$

Substituting equations [2.32] through [2.35] into equation [2.31] leads to the discrete dynamic-stiffness matrix of the layer which can be written as

$$[s] = \frac{G}{h}\begin{bmatrix} 1 & -1 \\ -1 & 1 \end{bmatrix} + (\lambda+2G).\frac{h}{2}\left(\frac{(2j-1)\pi}{2B}\right)^2\begin{bmatrix} 1 & 0 \\ 0 & 1 \end{bmatrix}$$

$$- \omega^2 \frac{\rho h}{2}\begin{bmatrix} 1 & 0 \\ 0 & 1 \end{bmatrix} \qquad [2.36]$$

The first and third terms of the right-hand side of equation [2.36] are associated with the lateral shear stiffness and the mass matrix of the soil layer, respectively. The second term is a new term describing the lateral axial stiffness of the layer due to the existence of the sloping rock boundary. It is clear from the second term that this new added stiffness vanishes as the breadth, 2B , approaches infinity, leading to the stiffness matrix of the regular one-dimensional model which assumes unlimited lateral extent of the soil layers.

2.4.4 The Frame Model for Horizontal Response

For a symmetric valley consisting of N layers, as shown in Fig. 2-4, the discrete dynamic-stiffness matrices of the layers may be assembled together to form the overall dynamic-stiffness matrix. This will be used to evaluate the horizontal response at the centre line of a valley subjected to a horizontal component of uniform control motion at the rock boundary. The dynamic-stiffness matrix can be expressed as

$$[S] = (\ [K^V] + [K^H]\ ) - \omega^2[M] \qquad [2.37]$$

in which,

$[\ K^V\ ]$ = stiffness matrix containing the effect of shear stiffness of the soil (tridiagonal)

$[\ K^H\ ]$ = stiffness matrix containing the added stiffness due to the limited extent of soil (diagonal)

[M] = lumped-mass matrix (diagonal)

These matrices are defined as follows

$$[K^V]_{NxN} = \begin{bmatrix} k_1{}^a & -k_1{}^a & 0 & 0 & 0 & 0 \\ -k_1{}^a & k_1{}^a+k_2{}^a & -k_2{}^a & 0 & 0 & 0 \\ 0 & \dots & \dots & \dots\dots & 0 & 0 \\ 0 & 0 & \dots & \dots\dots & \dots & 0 \\ 0 & 0 & 0 & \dots\dots & \dots & -k_{N-1}{}^a \\ 0 & 0 & 0 & 0 & -k_{N-1}{}^a & k_{N-1}{}^a+k_N{}^a \end{bmatrix} \qquad [2.38]$$

$$[K^H]_{NxN} = \begin{bmatrix} k_1{}^b & 0 & 0 & 0 & 0 & 0 \\ 0 & k_2{}^b & 0 & 0 & 0 & 0 \\ 0 & 0 & \dots & 0 & 0 & 0 \\ 0 & 0 & 0 & \dots & 0 & 0 \\ 0 & 0 & 0 & 0 & \dots & 0 \\ 0 & 0 & 0 & 0 & 0 & k_N{}^b \end{bmatrix} \qquad [2.39]$$

$$[M]_{NxN} = \begin{bmatrix} m_1 & 0 & 0 & 0 & 0 & 0 \\ 0 & m_2 & 0 & 0 & 0 & 0 \\ 0 & 0 & \dots & 0 & 0 & 0 \\ 0 & 0 & 0 & \dots & 0 & 0 \\ 0 & 0 & 0 & 0 & \dots & 0 \\ 0 & 0 & 0 & 0 & 0 & m_N \end{bmatrix} \qquad [2.40]$$

where,

$$k_m{}^a = \frac{G_m}{h_m} \qquad [2.41]$$

$$k_m{}^b = \frac{1}{2}\left[\frac{(2j-1)\pi}{2}\right]^2 \left[\frac{h_{m-1}}{B_{m-1}^2}(\lambda+2G)_{m-1} + \frac{h_m}{B_m^2}(\lambda+2G)_m\right] \qquad [2.42]$$

$$m_m = \frac{1}{2}\,[\rho_{m-1}h_{m-1} + \rho_m h_m] \qquad [2.43]$$

in which, the subscript m denotes the layer number ($m = 1,2,\ldots N$)

The above forms of the mass and stiffness matrices indicate that the valley may be idealized, making use of symmetry, as the frame model shown in Fig. 2-9 (a). The soil-layer masses, m_m , are lumped at the top of each layer and connected to each other by vertical columns which represent the lateral shear stiffness properties of the soil, k_m^a. Furthermore, the masses are connected to the sloping rock boundaries by horizontal axial links representing the lateral axial stiffness, k_m^b , due to the limited horizontal extent of the soil. Due to symmetry, half the stiffnesses, k_m^a and k_m^b , and half the masses, m_m, are shown in Fig. 2-9 (a), since only one half of the frame is illustrated. The soil masses can only move in the lateral direction, which means one horizontal degree of freedom for each mass.

2.4.5 The Frame Model for Vertical Response

The frame model can also be used to calculate the vertical soil response at the centre line of a symmetric valley subjected to a vertical component of uniform control motion at the rock boundary. The variation of the vertical mode shapes with x is obtained using equations similar to equations [2.21] and [2.22]. The dynamic-stiffness matrix in this case will have the same form as the one obtained for the horizontal response in equation [2.37]. The only modifications that need to be considered are substituting G for $(\lambda+2G)$ and vice versa, in the stiffness matrices. Hence, the forms of the stiffness matrices in equations [2.38] and [2.39] will hold after replacing k_m^a and k_m^b with k_m^c and k_m^d , respectively, where,

$$k_m{}^c = \frac{(\lambda + G)_m}{h_m} \qquad [2.44]$$

and

$$k_m{}^d = \frac{1}{2}\left[\frac{(2j-1)\pi}{2}\right]^2 \left[\frac{h_{m-1}}{B_{m-1}^2} G_{m-1} + \frac{h_m}{B_m^2} G_m\right] \qquad [2.45]$$

in which, k_m^c represents the vertical axial stiffness of the soil and k_m^d describes the shear stiffness that arises in the vertical direction due to the limited lateral extent of the soil.

The frame model for vertical response of the valley is shown in Fig. 2-9 (b). The lumped masses can only move vertically and are attached to each other by columns resisting axial deformations in the vertical direction. The vertical links between the soil masses and the sloping rock boundaries represent the shear stiffness resisting the vertical shear deformations in the soil. However, this shear stiffness arising from the existence of the sloping rock boundary will have a very little impact on the resulting vertical response, since its resistance to the vertical deformations is so small when compared to the resistance from the vertical axial stiffness of the soil. Hence, the influence of the sloping rock boundary on the horizontal seismic response of the alluvial valley is much more visible than the influence on the vertical response. Consequently, the frame model will be primarily used in this analysis to compute the horizontal seismic response of the valley.

2.5 VIBRATION MODES FOR HORIZONTAL RESPONSE OF THE VALLEY

The evaluation of the dynamic behaviour of the alluvial valley is based on the study of the shapes of the vibration modes, the periods at which they occur and their contribution to the dynamic response. This is achieved by considering the mode shapes resulting from the two-dimensional finite-element model and comparing with the results from the frame model.

2.5.1 Mode Shapes Using the 2-D Model

A two-dimensional finite-element mesh is created for the alluvial symmetric valley, half of which is shown in Fig. 2-10. Dimensions of the valley are $B = 300$ m, $d = 100$ m and $L = 100$ m, where B is half the breadth at the top surface of the valley, d is the depth at the centre line and L is the length of the horizontal projection of the sloping rock boundary. Two categories of soil deposits are selected for this study:

(a) Normally to lightly over-consolidated clay (NC)

(b) Dense sand (DS)

These categories are selected to represent two classes of soil, the first is a soft profile and the second is a stiff profile. The G_o profiles versus the depth z of the above two soil types are reproduced from Elhamadi et al (1990) in Fig. 2-11, in which G_o represents the value of the shear modulus of soil at very low shear strain levels.

The valley is divided into a number of horizontal layers, each of which has homogeneous and isotropic soil properties, with Poisson's ratio $\nu = 0.4$. The shear modulus of each layer is selected to be the G_o value at its mid-height. Dividing the valley into vertical columns will constitute, with the horizontal layers, the required mesh of plane-strain elements which have unit thickness in the x-z plane. Program SAP IV, by Bathe et al (1973), is used to obtain the mode shapes and periods of the valley for each soil type. The nodes on the rock boundary are fixed while the nodes on the axis of symmetry are free to move in the x-direction only. The latter constraint is made to take advantage of the symmetry, ensuring that the model will produce only the vibration modes of significance to the horizontal response of the valley under a horizontal component of uniform motion in the rock. All other nodes are free to move in both x- and z-directions.

The first five major modes are plotted in Fig. 2-12 for profile (NC) and in Fig. 2-13 for profile (DS). Although the modes are plotted out of the valley plane, they in fact represent in-plane vibrations in the horizontal (x-axis) direction. The plotted modes are not necessarily the first five modes in a descending order of periods. In fact, they are described as major modes because they have the largest participation in the horizontal response. For soil profile (NC), the five major modes are modes number 1, 4, 6, 9 and 12, while for soil profile (DS), they are modes number 1, 2, 3, 4 and 5 in a descending order of periods. Each mode in Fig. 2-12 and Fig. 2-13 is denoted as mode (k, j) where k represents the k-variation of the mode with z and j describes the j-variation with x .

For the soil profile (NC) the k-variation is similar to the variation of the mode shapes of a cantilever beam with height, while for (DS), it is similar to the frame mode shapes. This means that the top layers in (NC) are very soft compared to the bottom layers. On the other hand, for (DS) the ratio of the increase of stiffness with depth is much smaller than that in (NC). The j-variation in both profiles resembles the shape of the cosine curve expressed in equations [2.21] and [2.22] describing the variation of the mode shapes with x due to the existence of the sloping rock boundary. In general, the vibration modes described herein confirm the characteristics of the two-dimensional resonance patterns (in-plane shear modes), described by Bard and Bouchon (1985), for sediment-filled valleys.

2.5.2 Comparison with Results from the Frame Model

The mode shapes determined by the frame model for horizontal response of the valley may be obtained by implementing the frame model, shown in Fig. 2-9 (a), in program SAP IV, by Bathe et al (1973). The shear stiffness, k_m^a ,of the frame columns and the masses, m_m , are calculated using equations [2.41] and [2.43], respectively. For each value of j , where j = 1,2,3,.... , the axial stiffnesses, k_m^b , of the links are calculated using equation [2.42]. The j-variation of any vibration mode of the valley may be expressed for the m^{th} layer, using equations [2.21] and [2.22], as

$$(\phi_j)_m = \cos\left[\frac{(2j-1)\pi}{2}\frac{x}{B_m}\right] \qquad [2.46]$$

where, B_m , is half the breadth of the m^{th} layer, measured at its mid-height. It is to be noted that the value of $(\phi_j)_m$ at $x = 0$ is always a unit, and thus the frame model is analyzed, using program SAP IV, at $x = 0$ to determine the frame modes, or in other words the variation of the valley modes with z , at the axis of symmetry. In a valley consisting of N layers, there are N horizontal degrees of freedom, one at each mass, and N frame modes associated with each j-variation. These N modes describe the k-variations of the valley modes with depth and are denoted by $\{\phi_k\}$ where $k = 1,2,\ldots,N$. The natural circular frequencies, ω_k , of these modes can be calculated from the frequency equation of the frame system (Clough and Penzien, 1975). The frequency equation may be written, by setting the determinant of the dynamic-stiffness matrix in equation [2.37] equal to zero

$$\left| [K^V] + [K^H] - \omega_k^2[M] \right| = 0 \qquad [2.47]$$

The corresponding mode shapes, $\{\phi_k\}$, may be obtained from

$$\left([K^V] + [K^H] - \omega_k^2[M] \right) \{\Phi_k\} = \{0\} \qquad [2.48]$$

where, the k^{th} mode shape is expressed as

$$\{\Phi_k\} = \begin{Bmatrix} (\Phi_k)_1 \\ (\Phi_k)_2 \\ \cdot\cdot \\ \cdot\cdot \\ (\Phi_k)_N \end{Bmatrix} \qquad [2.49]$$

in which, $(\phi_k)_m$ represents the value of the frame mode associated with the m^{th} mass. This is the value of the valley mode (k,j) at $x = 0$. Consequently, the value of the valley mode (k,j) at any point on the top interface of the m^{th} layer may be written as

$$(\phi_{kj})_m = (\phi_k)_m \, (\phi_j)_m \tag{2.50}$$

Since the support motions tend to excite strongly only the lowest modes of vibration in the frame system, it is sufficient to solve equations [2.47] and [2.48] for the first few k-modes associated with each j-variation. Furthermore, the first few j-variations need only be considered. These are the modes having the most significant participation in the response.

In order to calculate the modal participation factor, Γ_k, associated with the mode (k,j), the second dimension missing from the frame model has to be included to assure that each frame mode has its proper share of participation in the response. This means that the sum of the products of the masses at all points in the valley and the corresponding mode shape values have to be considered in calculating Γ_k. The modal participation factor associated with the k^{th} frame mode, before modification is written as

$$\Gamma_k = \frac{\sum_{m=1}^{N} m_m \, (\phi_k)_m}{\sum_{m=1}^{N} m_m \, (\phi_k)_m^2} \tag{2.51}$$

To introduce the missing second dimension effect to equation [2.51], each term in the numerator has to be multiplied times the area under the associated j-variation, $(\phi_j)_m$, expressed in equation [2.46]. Moreover, each term in the denominator is multiplied times the area under the curve $(\phi_j)_m^2$. Consequently, the modified Γ_k may be rewritten as

$$\Gamma_k = \frac{\sum_{m=1}^{N} m_m \, (\phi_k)_m \int_{-B_m}^{B_m} (\phi_j)_m \, dx}{\sum_{m=1}^{N} m_m \, (\phi_k)_m^2 \int_{-B_m}^{B_m} (\phi_j)_m^2 \, dx} \tag{2.52}$$

where,

$$\int_{-B_m}^{B_m} (\phi_j)_m \, dx = (-1)^{j-1} \frac{4B_m}{(2j-1)\pi} \qquad [2.53]$$

and

$$\int_{-B_m}^{B_m} (\phi_j)_m^2 \, dx = B_m \qquad [2.54]$$

Thus, Γ_k may be expressed in its final form as

$$\Gamma_k = (-1)^{j-1} \frac{4}{(2j-1)\pi} \frac{\sum_{m=1}^{N} m_m (\phi_k)_m B_m}{\sum_{m=1}^{N} m_m (\phi_k)_m^2 B_m} \qquad [2.55]$$

From equation [2.55] , when j increases the corresponding Γ_k will decrease. This modification has been incorporated in program SAP IV to calculate the proper values of the modal participation factors for the frame model.

Two valleys are considered for the comparison study of the frame and the 2-D vibration modes. The dimensions of the two valleys are shown in Fig. 2-14 and Fig. 2-15. Valley (1) is the same as that shown in Fig. 2-10, while valley (2) is a wide and shallow one. The same soil profiles (DS) and (NC), described before, are used. For the sake of comparison, the same number of horizontal layers is considered in the frame and the 2-D models. The shear modulus of each layer is chosen to be the G_o value at its mid-height as given by Fig. 2-11. Program SAP IV is utilized to obtain the mode shapes, the periods and the modal participation factors of the valleys from both models.

Samples of the major modes are presented in Fig. 2-14 and Fig. 2-15 for valleys (1) and (2), respectively, for the (DS) profile. Fig. 2-16 and Fig. 2-17 present the corresponding results for the (NC) profile. The scale in the figures is distorted to give a clear picture of the variation of the mode shapes with both directions. Each mode is denoted as mode (k,j), where k stands for the k-variation and j denotes the j-variation. The j-variation is illustrated at three depths of the valley, the first is at the top surface, the second is at the mid-depth and the third is at the top of the bottom layer in the valley. The modal variation with x follows equation [2.46] at any depth. The k-variation describes the modal variation with z at the centre line of the valley, where $x = 0$. In general, it can be seen that the agreement is good between the two models, particularly when comparing the shapes of the k-variations. The periods and the modal participation factors of the major modes obtained from both models are listed in tables 2-1 and 2-2 for valley (1) and in tables 2-3 and 2-4 for valley (2). These are the modes with significant contribution to the horizontal response of the valley. They are selected as those modes having the ratio $|\Gamma_k/\Gamma_1| > 10\ \%$. Other modes with smaller ratio are of negligible participation in the response. The modes are listed in the tables in a descending order of their periods. The frame mode numbers are presented as modes (k,j) and the corresponding modes having the same k- and j-variations from the 2-D model almost occur at the same periods with participation comparable to those of the frame modes. The modes of major participation are mainly those with $j=1$ and/or $k=1$. Some cross modes with $j>1$ and $k>1$ also have important contribution to the response, particularly in valley (1) where the ratio B/d is relatively small which allows higher k-variations associated with higher j-variations to take part in the response. It is observed that the number of modes with major participation in the response of the (NC) profile is more than that in the case of the (DS) profile. This is mainly because the soft profile of (NC) along the depth allows more k-variations to participate in the response. This is more apparent with the first j-variation. It is further noted that the larger breadth of valley (2) permits more j-variations , with closely-spaced periods, to participate, particularly when $k=1$, as shown in tables 2-3 and 2-4.

Since the motions of the frame model are restricted in the horizontal direction only, the horizontal modes of significant participation are the first few modes encountered in the analysis and thus are picked out faster than in the 2-D approach. This is more visible in wider valleys, such as valley (2) in table 2-4, where 134 modes are needed in the finite-element model to extract only 12 modes of major contribution. This can also be explained on the grounds that the second dimension of the valley has to be represented by a large mesh in the finite-element approach, while it is only represented by links in the frame model.

2.6 HORIZONTAL RESPONSE CALCULATIONS USING THE FRAME MODEL

Since the frame model is based on the modal dynamic behaviour of the valley, the horizontal response will be computed by mode superposition in the time domain. This will require the modification of program SAP IV to accommodate the modified modal participation factors given in equation [2.55]. The program is also improved to permit different damping ratios for different modes and to calculate the displacement and/or acceleration response at points in the valley with different x-coordinates. The mode superposition will impose the assumption of a linear soil system. This can be treated by using the equivalent linear method which approximates the real non-linear behaviour of the soil by solving in a linear iterative procedure, updating the soil properties to be compatible with the effective shear strain in each linear step.

2.6.1 Modal Analysis Technique

The unknown relative displacement vector $\{u\}$ in the equation of motion of the system [2.1] can be obtained as the sum of the k-modal displacement vectors of the system

$$\{u\}_{Nx1} = \sum_{k=1}^{N} y_k(t)\ \{\Phi_k\}_{Nx1} \qquad [2.56]$$

where, k denotes the mode number and $y_k(t)$ is the unknown modal amplitude or the normal coordinate associated with the k^{th} mode. This involves a coordinate transformation such that the set of coupled differential equations in [2.1] is converted into a set of uncoupled ordinary differential equations by modal decomposition. Furthermore, the summation in equation [2.56] may be truncated by including only the first few modes of significant contribution to the response. Thus, the response analysis of the frame system having N unknown degrees of freedom can be carried out for only a few normal coordinates, reducing the number of the unknowns to the number of the modes actually required in the response.

The procedure of decoupling the equations of motion for earthquake-response analysis is described by Clough and Penzien (1975). Using the orthogonality conditions, the equation of motion associated with the k^{th} mode, for a given j-variation, is

$$\ddot{y}_k + 2\ \beta_k\ \omega_k\ \dot{y}_k + \omega_k^2\ y_k = -\Gamma_k\ \ddot{u}_r(t) \qquad [2.57]$$

where, $\ddot{u}_r(t)$ is the horizontal acceleration describing the uniform input excitation in the rock. The natural circular frequency, the modal participation factor and the modal damping ratio of the k^{th} mode are termed ω_k , Γ_k and β_k , respectively.

In equation [2.57] it is assumed that the damping matrix of the system is of a form which satisfies the same orthogonality conditions as the mass and stiffness matrices. Two kinds of damping may exist in the soil system, viscous and hysteretic. The viscous dissipation of energy depends on the velocity of motion or rate of strain and the effects on the entire system vary with the frequency of motion. Hysteretic damping involves frictional loss of energy that is largely independent of frequency but depends on the magnitude of displacement or strain. Experimental evidence seems to indicate that the internal dissipation of energy in the soil is mostly of a hysteretic nature. Consequently, the viscous damping effects may be negligible, particularly when high strains are developed in the soil due to high intensity of motion.

Roesset et al (1973) demonstrated that the responses to a steady-state harmonic motion with frequency Ω of two SDOF (single degree of freedom) systems, with the same mass and stiffness but one with viscous damping ratio, β ,and the other with hysteretic damping ratio, D , are equal at resonance (i.e. $\Omega/\omega=1$), when $D = \beta$, where ω is the natural circular frequency of both systems. They also showed that, when $D = \beta$, the differences in the responses of the two systems to a transient excitation are negligible in the frequency range of interest to practical applications. Accordingly, for a SDOF system as represented by the modal equation [2.57], considering the modal damping ratio as entirely viscous while it may be in part viscous and in part hysteretic, is of little practical importance, provided that the contributions of each component's damping of the system to the modal values are properly computed.

The contribution of the hysteretic damping ratios of the different layers, D_m, to the energy dissipation of the k^{th} mode may thus be represented by the equivalent viscous damping ratio, β_k . Neglecting the viscous damping effects, β_k will include only the hysteretic losses and can be calculated using the weighted modal damping rule, described by Roesset et al (1973). The rule was expressed by Desai and Christian (1977), as

$$\beta_k = \frac{\sum_{m=1}^{N} \{\phi_{km}\}^T [K_m] \{\phi_{km}\} D_m}{\{\phi_k\}^T [K] \{\phi_k\}} \qquad [2.58]$$

where, m denotes the layer or element number. [K] is the overall stiffness matrix of the system and $[K_m]$ is the stiffness matrix of the m^{th} layer. $\{\phi_{km}\}$ is the portion of the k^{th} mode shape, $\{\phi_k\}$, that involves nodes of element m . The modal damping ratio, β_k , in equation [2.58] is thus the weighted average of the damping in all elements where the weighting factors are the proportions of the strain energy for mode k stored in the individual elements. It is worthwhile noticing that the calculation can be simplified when the mode shapes are orthonormalized with respect to the mass matrix, because

$$\{\phi_k\}^T [K] \{\phi_k\} = \omega_k^2 \qquad [2.59]$$

For each j-variation of the valley there is a number of k-modal equations, given by equation [2.57] which can be solved for the unknown $y_k(t)$ .Thus, summing the k-modal displacement vectors in equation [2.56] will give the contribution of only one j-variation to the relative displacement vector, $\{u\}$, evaluated at $x = 0$. The relative total displacement vector can be then obtained by adding the contributions from the number of j-variations, M_1 , considered in the analysis

$$\{u_{tot}\} = \sum_{j=1}^{M_1} \sum_{k=1}^{M_2} y_k(t) \{\phi_k\} \qquad [2.60]$$

where, M_2 is the number of k-variations considered for each j . The absolute acceleration response at any point on the top interface of the m^{th} layer can be obtained from

$$\ddot{U}_m(x,t) = \ddot{u}_r + \sum_{j=1}^{M_1} \sum_{k=1}^{M_2} \ddot{y}_k(t) \left(\phi_k\right)_m \cos\left(\frac{(2j-1)\pi}{2} \frac{x}{B_m}\right) \qquad [2.61]$$

where, $(\phi_k)_m$ is the k-modal value associated with the m^{th} mass of the frame.

2.6.2 The Equivalent Linear Method

The superposition of the mode responses requires a linear system throughout the analysis. However, an iterative linear solution may be used to simulate the non-linear behaviour of the soil system. The equivalent linear method, suggested by Seed and Idriss (1969), starts with a set of curves that relate the secant shear modulus, G, and the hysteretic damping ratio, D , to the level of strain, γ , for different types of soil (Seed and Idriss, 1970). Fig. 2-18 shows the general form of these curves. As the excitation and correspondingly the levels of strain increase, the shear modulus decreases and the effective internal damping increases. There is therefore a shift in the amplification peaks toward longer periods, accompanied by a reduction in the peak amplification values due to the increased energy dissipation. The iterative procedure using the frame approach proceeds as follows:

1. An initial assumption of the shear modulus and the damping ratio is made for each layer.
2. The structural properties of the frame elements are computed for each j-variation and incorporated in the modified version of program SAP IV. It is to be noted that the j-variation affects only the calculations of the axial stiffnesses of the horizontal links in the frame.
3. The program, using the mode-superposition method, calculates the horizontal displacement response, u_m, associated with each mass, m_m, at $x = 0$. The calculation of this response is given in equation [2.60].
4. The shear strain history, γ_m, in the m^{th} layer can be computed from

$$\gamma_m(t) = \frac{u_{m+1}(t) - u_m(t)}{h_m} \qquad [2.62]$$

   The effective shear strain amplitude in each layer is calculated as a percentage of the maximum strain developed in that layer. An empirical percentage of 65% is widely used in other approaches where the linear iterative procedure is applied. The effective strains are used to select improved values of the shear modulus and the damping ratio for each layer, for the next iteration.

5. The operation is repeated until strain-compatible soil properties are obtained within a given error limit. Convergence usually occurs within 3 to 5 iterations.
6. The response from the last iteration is taken as being the non-linear response. The modified SAP IV can also compute the absolute acceleration at any point in the valley at the top interface of a layer, using equation [2.61].

2.7 SUMMARY

Two existing models for the symmetrical alluvial valley were reviewed and a new one was introduced. The assumptions and methods of analysis of the three engineering models were discussed. The simple one-dimensional approach ignores the effects of the limited horizontal extent of the soil which can be significant to the resulting ground motions in the valley. Being an elaborate model, on the other hand, the two-dimensional finite-element model considers the complexities that may be encountered in the site-response problem of the valley.

The new frame model was developed to compensate for the deficiency of the regular one-dimensional approach without sacrificing its simplicity. The proposed model was introduced to predict the non-linear response of symmetrical alluvial valleys which are bounded by rigid rock and have limited width in plane. The soil continuum is divided into horizontal layers, each having uniform properties. The separation of the valley mode shapes into variations with depth (the k-variations) and variations with the horizontal direction (the j-variations) led to the development of the model to describe the modal variations with depth.

Identifying the contribution of each mode to the solution provides valuable insight into the dynamic behaviour of the valley system and its response. In addition, the summation of the modal contributions does not have to extend to all modes. In general, the vibration modes resulting from the frame model are in good agreement with the results from the 2-D analysis. The number of modes that have significant participation in the response and the shapes of their k- and j-variations depend on the valley dimensions and the soil profile. The frame model selects those modes with major participation faster than does the finite element.

Program SAP IV is modified to accommodate the frame model and calculate the response by mode superposition. The resulting motions from the frame model are representative of the valley response at the axis of symmetry. The response at other points in the valley can be obtained by making use of the modal variations with the horizontal direction. The equivalent linear method has been applied to the analysis to account for the non-linear behaviour of the soil by ensuring strain-compatible properties.

Table 2-1 Periods and modal participation factors of major modes

Valley (1) - Profile (DS)
[B=300 m, d=100 m, L=100 m]

Frame Model			2-D Model		
mode number (k , j)	period (sec)	$\lvert\Gamma_k/\Gamma_1\rvert$	mode number	period (sec)	$\lvert\Gamma_k/\Gamma_1\rvert$
1 , 1	0.54	1.00	1	0.53	1.00
1 , 2	0.29	0.30	2	0.30	0.30
2 , 1	0.23	0.33	3	0.23	0.38
1 , 3	0.20	0.16	4	0.21	0.17
2 , 2	0.18	0.16	5	0.18	0.15
3 , 1	0.15	0.20	9	0.15	0.20
2 , 3	0.13	0.12	10	0.13	0.14
4 , 1	0.11	0.14	16	0.11	0.13

Table 2-2 Periods and modal participation factors of major modes

Valley (1) - Profile (NC)
[B=300 m, d=100 m, L=100 m]

Frame Model			2-D Model		
mode number (k , j)	period (sec)	$\lvert\Gamma_k/\Gamma_1\rvert$	mode number	period (sec)	$\lvert\Gamma_k/\Gamma_1\rvert$
1 , 1	1.59	1.00	1	1.56	1.00
1 , 2	1.24	0.26	4	1.26	0.24
1 , 3	1.08	0.12	6	1.01	0.11
2 , 1	0.87	0.52	9	0.85	0.56
2 , 2	0.71	0.19	12	0.73	0.17
3 , 1	0.61	0.33	16	0.60	0.34
3 , 2	0.53	0.15	20	0.54	0.14
4 , 1	0.47	0.24	23	0.46	0.26
4 , 2	0.41	0.14	26	0.42	0.13
5 , 1	0.37	0.21	31	0.36	0.22
5 , 2	0.33	0.11	34	0.34	0.12
6 , 1	0.30	0.16	39	0.30	0.14
7 , 1	0.25	0.13	51	0.24	0.13
8 , 1	0.22	0.11	59	0.21	0.12

Table 2-3 Periods and modal participation factors of major modes

Valley (2) - Profile (DS)
[B=1000 m, d=40 m, L=100 m]

Frame Model			2-D Model		
mode number (k , j)	period (sec)	$\lvert \Gamma_k / \Gamma_1 \rvert$	mode number	period (sec)	$\lvert \Gamma_k / \Gamma_1 \rvert$
1 , 1	0.34	1.00	1	0.34	1.00
1 , 2	0.33	0.33	2	0.33	0.38
1 , 3	0.31	0.20	3	0.32	0.25
1 , 4	0.30	0.14	4	0.31	0.18
1 , 5	0.27	0.11	5	0.29	0.11
2 , 1	0.13	0.34	21	0.13	0.38
2 , 2	0.12	0.11	22	0.12	0.11
3 , 1	0.08	0.20	43	0.08	0.22
4 , 1	0.05	0.13	62	0.05	0.13

Table 2-4: Periods and modal participation factors of major modes

Valley (2) - Profile (NC)
[B=1000 m, d=40 m, L=100 m]

Frame Model			2-D Model		
mode number (k , j)	period (sec)	$\lvert\Gamma_k/\Gamma_1\rvert$	mode number	period (sec)	$\lvert\Gamma_k/\Gamma_1\rvert$
1 , 1	1.06	1.00	7	1.03	1.00
1 , 2	1.03	0.33	8	1.02	0.34
1 , 3	1.01	0.20	10	0.99	0.21
1 , 4	0.98	0.14	12	0.92	0.16
2 , 1	0.53	0.47	28	0.52	0.49
2 , 2	0.52	0.16	29	0.50	0.15
3 , 1	0.36	0.31	45	0.35	0.33
4 , 1	0.27	0.25	61	0.26	0.26
5 , 1	0.21	0.21	79	0.20	0.23
6 , 1	0.17	0.16	96	0.17	0.17
7 , 1	0.14	0.13	115	0.14	0.12
8 , 1	0.11	0.13	134	0.11	0.13

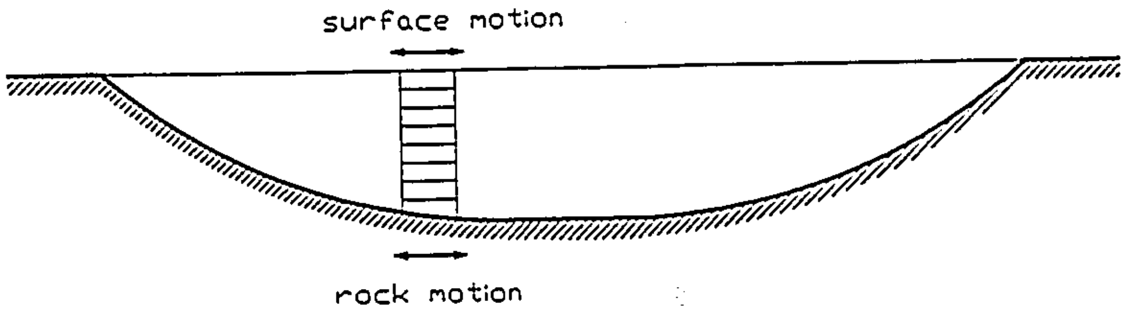

Fig. 2-1 One-dimensional soil column in a valley

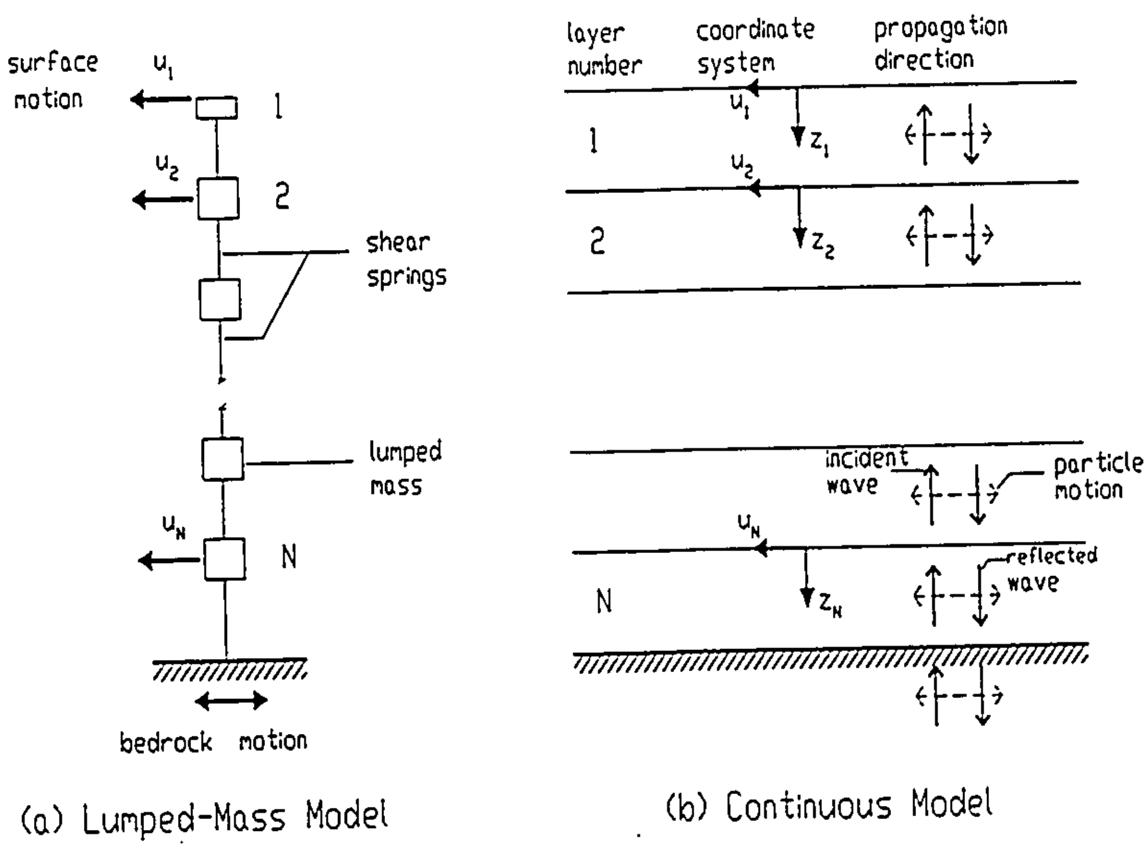

Fig. 2-2 One-dimensional models for a system of N soil layers

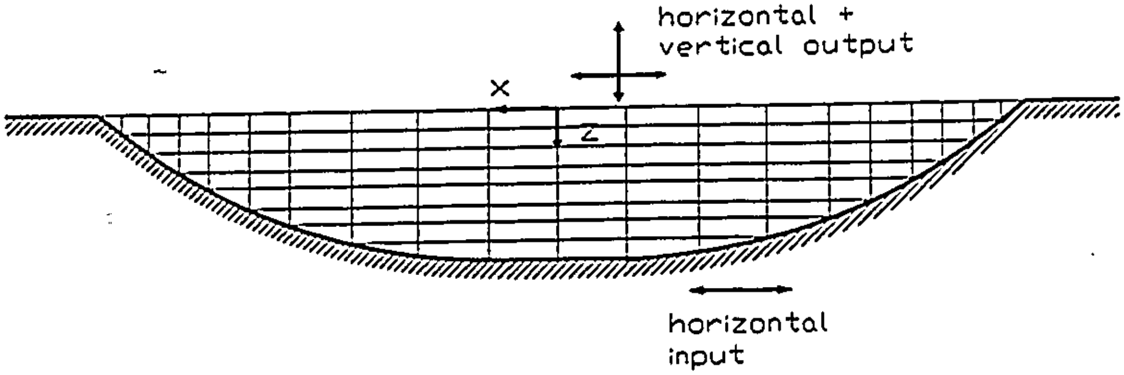

Fig. 2-3 The two-dimensional finite-element model

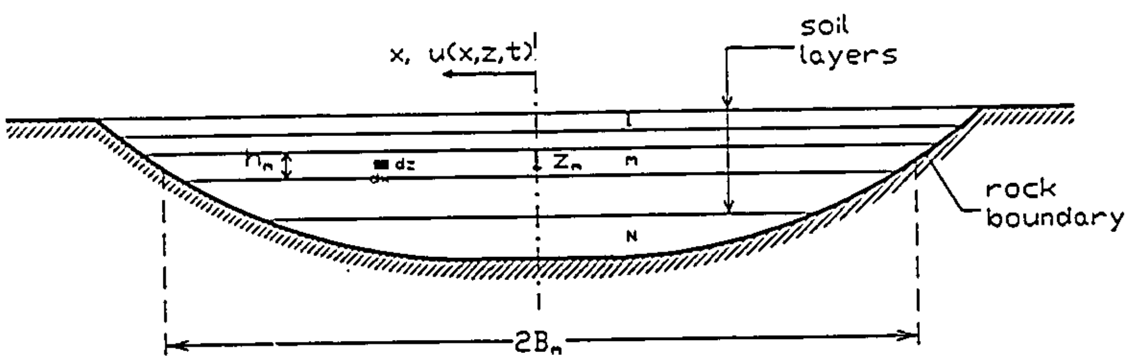

Fig. 2-4 Symmetric valley

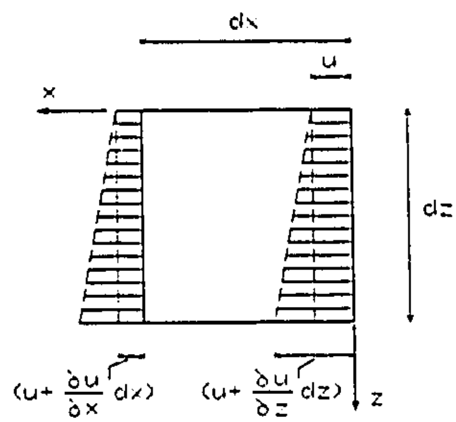

Fig. 2-5 Lateral deformation gradients in a cube of soil

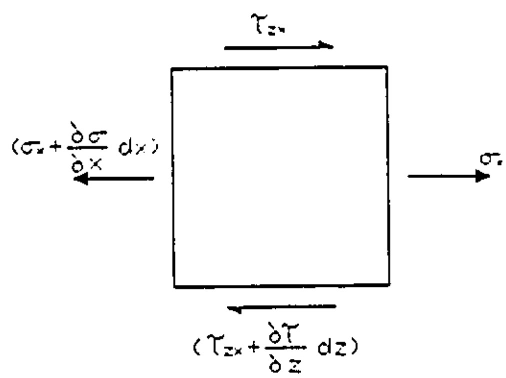

Fig. 2-6 Stresses in the x-direction

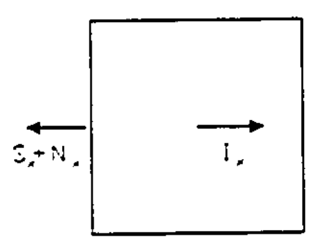

Fig. 2-7 Forces in the x-direction

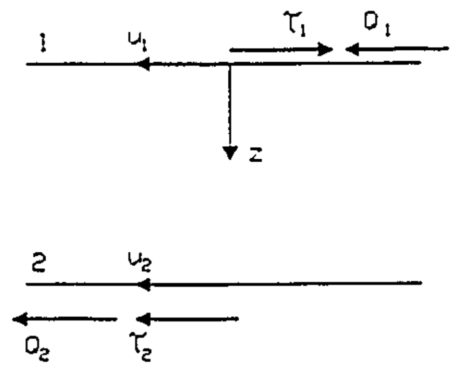

Fig. 2-8 State of displacements and stresses at the interfaces of a layer

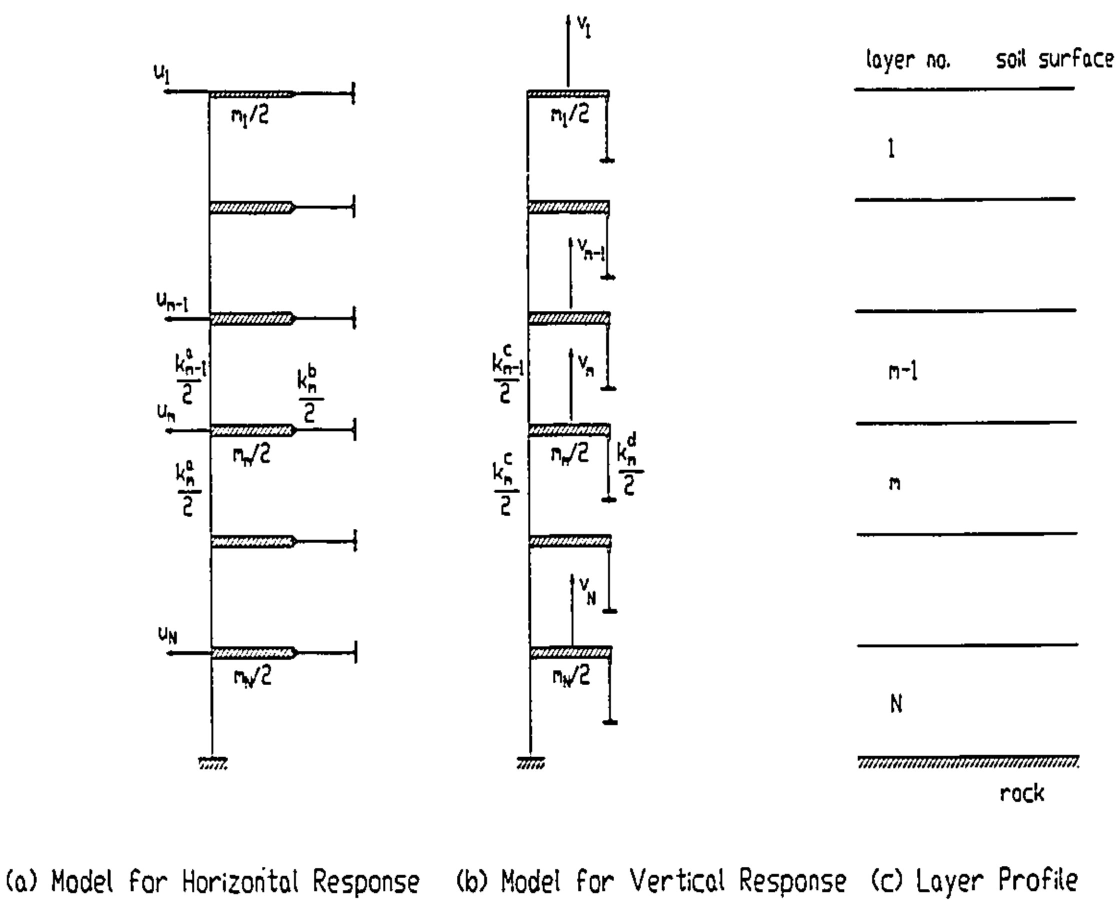

Fig. 2-9 The frame model of the valley

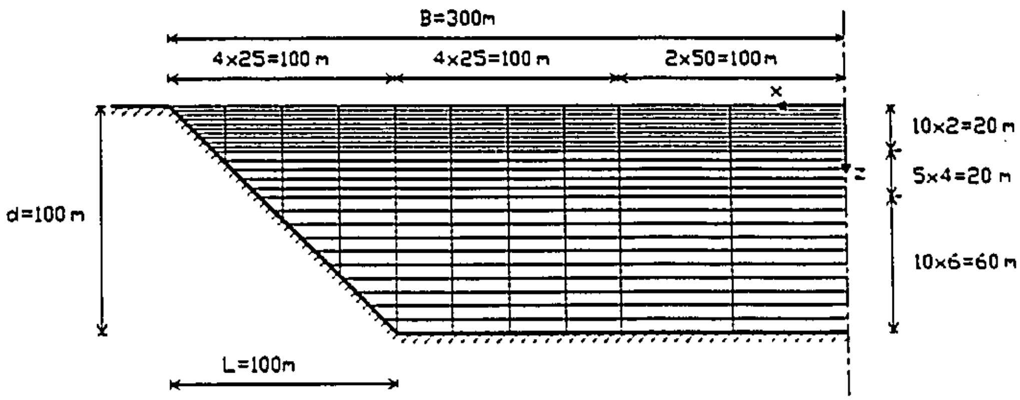

Fig. 2-10 Finite-element mesh of half the valley

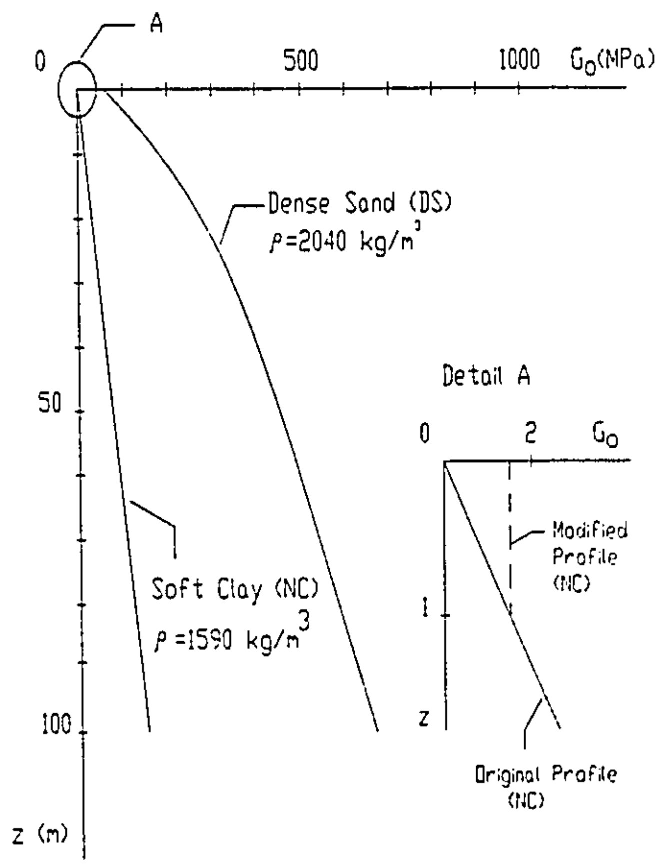

Fig. 2-11 Variation of shear modulus, G_o , with depth for soil profiles (NC) and (DS)

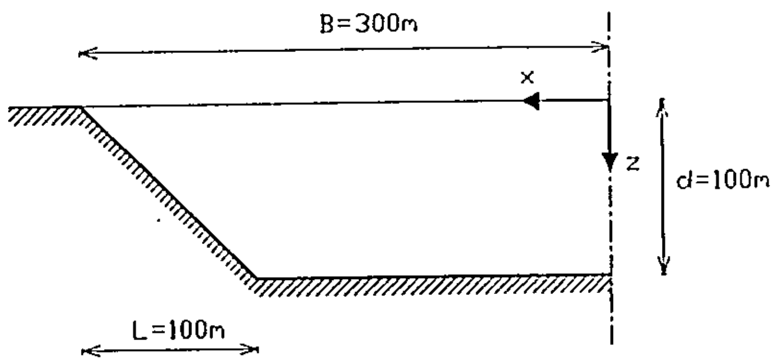

(a) Valley dimensions

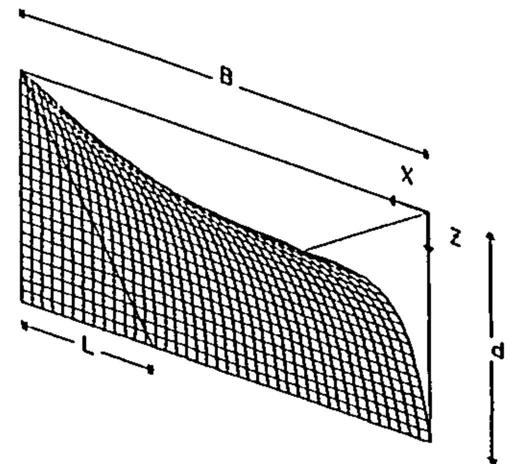

(b) Mode 1,1 - Period = 1.56 s

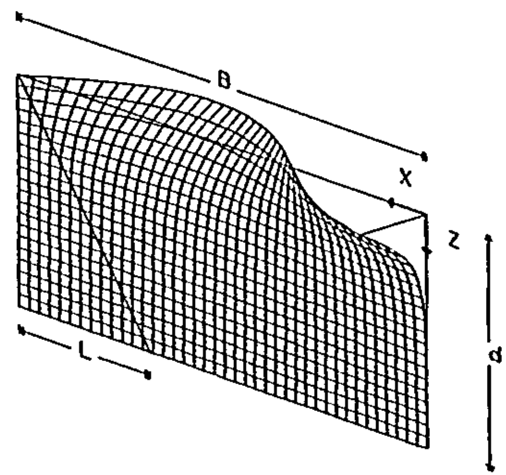

(c) Mode 1,2 - Period = 1.26 s

Fig. 2-12 Major modes from 2-D analysis
Soil profile : NC

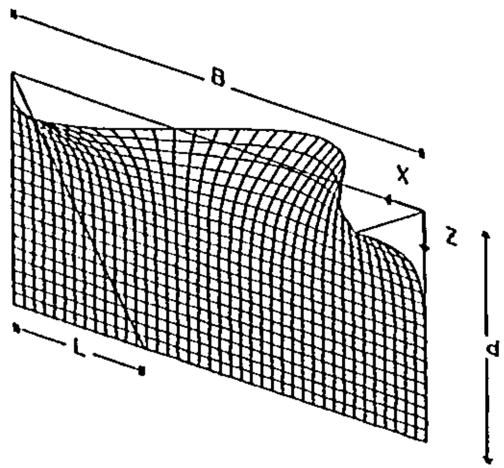

(d) Mode 1,3 - Period = 1.01 s

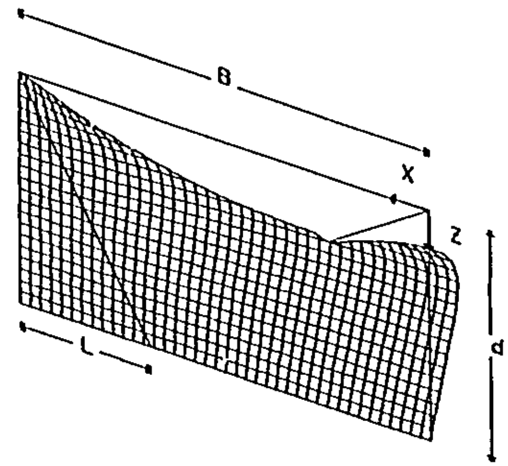

(e) Mode 2,1 - Period = 0.85 s

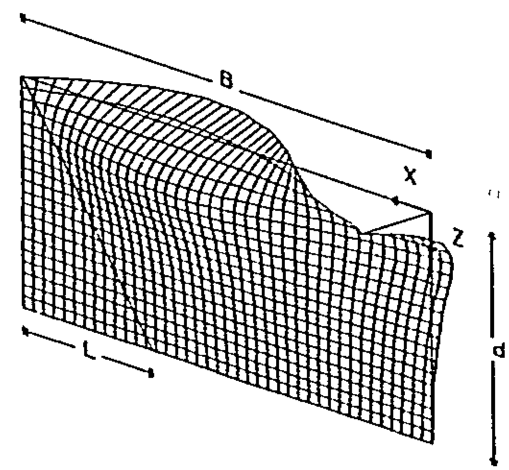

(f) Mode 2,2 - Period = 0.73 s

Fig. 2-12 (Cont'd) Major modes from 2-D analysis
Soil profile : NC

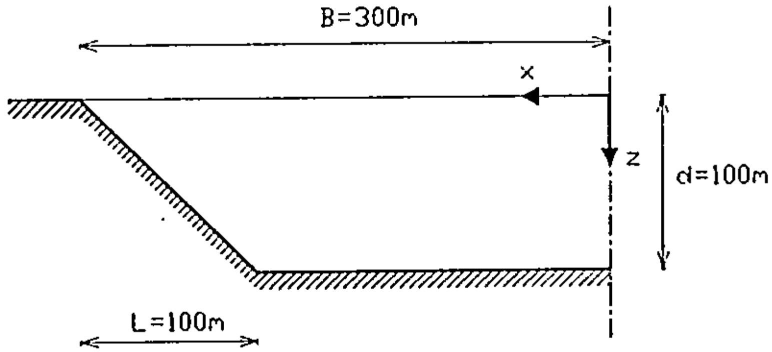

(a) Valley dimensions

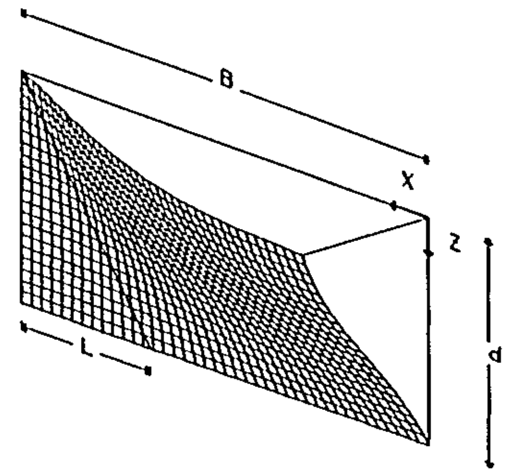

(b) Mode 1,1 - Period = 0.53 s

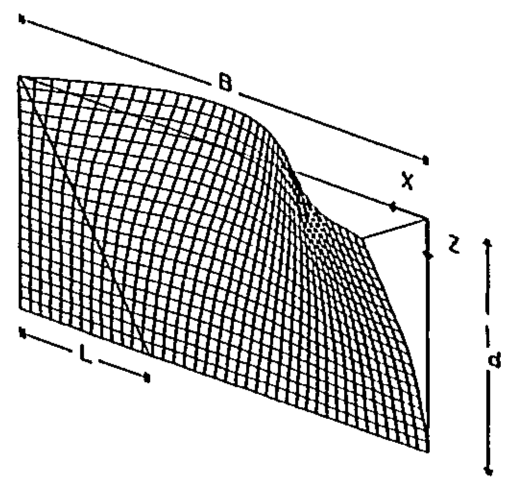

(c) Mode 1,2 - Period = 0.30 s

Fig. 2-13 Major modes from 2-D analysis
Soil profile : DS

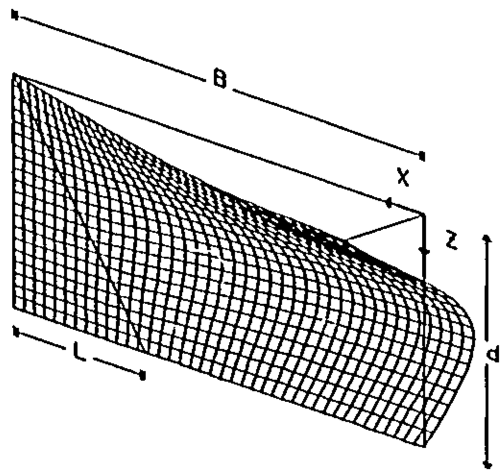

(d) Mode 2,1 - Period = 0.23 s

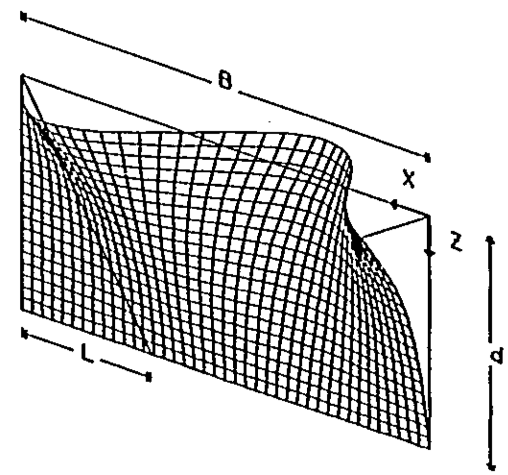

(e) Mode 1,3 - Period = 0.21 s

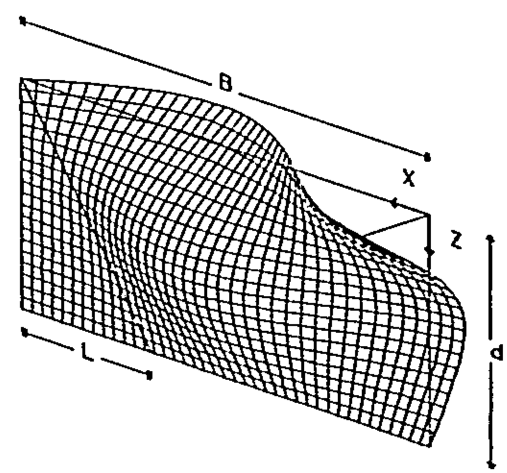

(f) Mode 2,2 - Period = 0.18 s

Fig. 2-13 (Cont'd) Major modes from 2-D analysis
Soil profile : DS

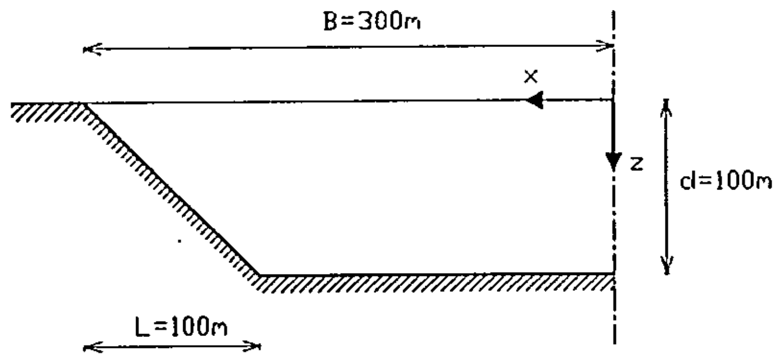

(a) Dimensions of valley (1)

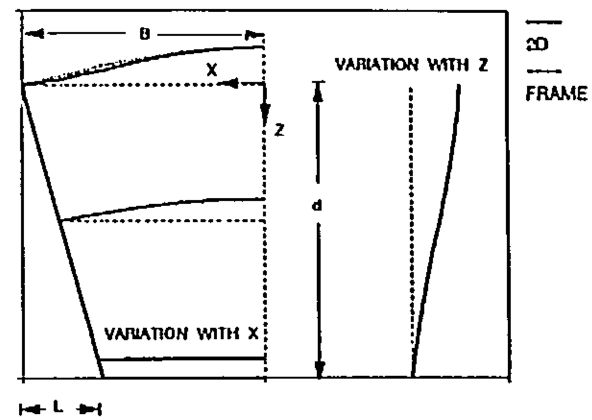

(b) Mode 1,1 - Period = 0.53 s

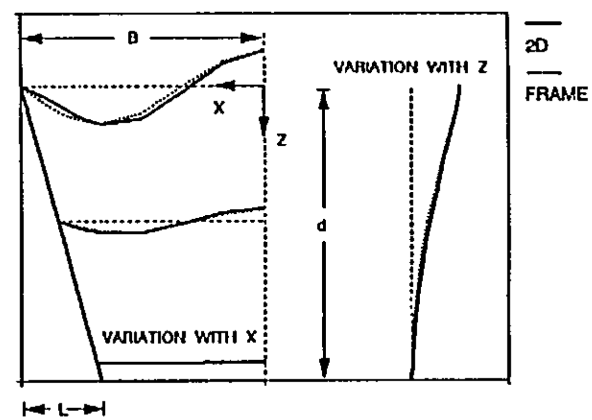

(c) Mode 1,2 - Period = 0.30 s

Fig. 2-14 Major modes of valley (1)
Soil profile : DS

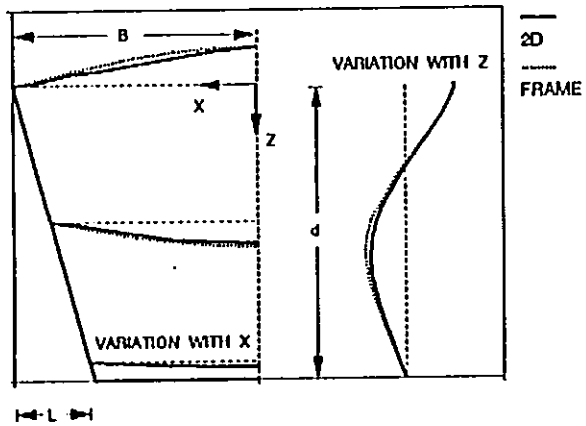

(d) Mode 2,1 - Period = 0.23 s

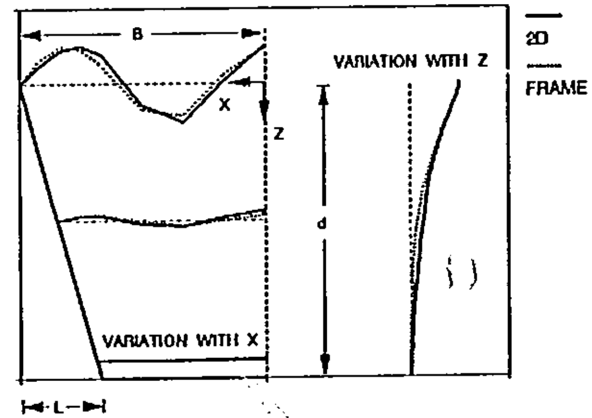

(e) Mode 1,3 - Period = 0.21 s

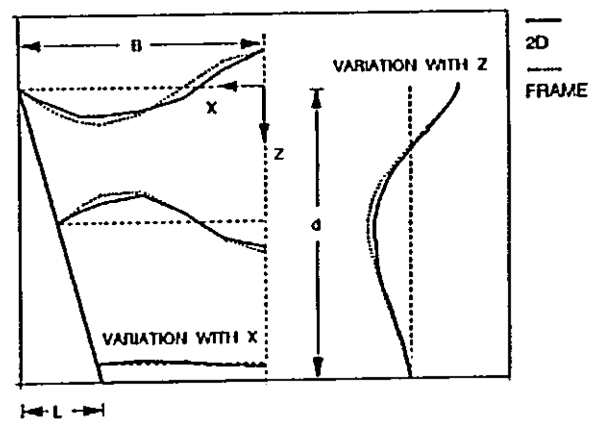

(f) Mode 2,2 - Period = 0.18 s

Fig. 2-14 (Cont'd) Major modes of valley (1)
Soil profile : DS

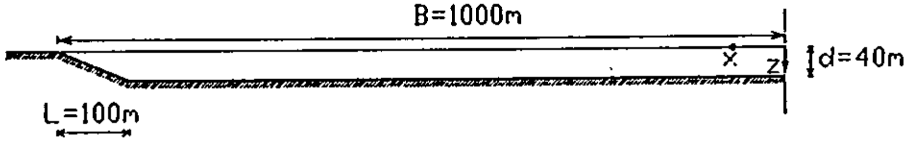

(a) Dimensions of valley (2)

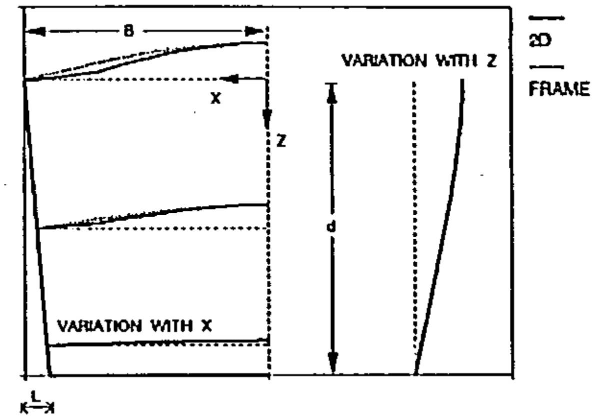

(b) Mode 1,1 - Period = 0.34 s

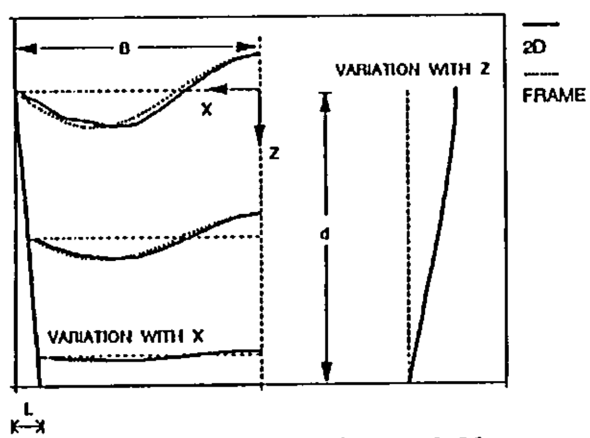

(c) Mode 1,2 - Period = 0.33 s

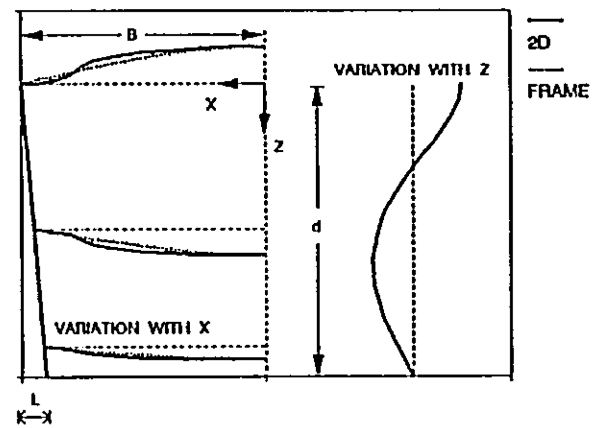

(d) Mode 2,1 - Period = 0.13 s

Fig. 2-15 Major modes of valley (2)
Soil profile : DS

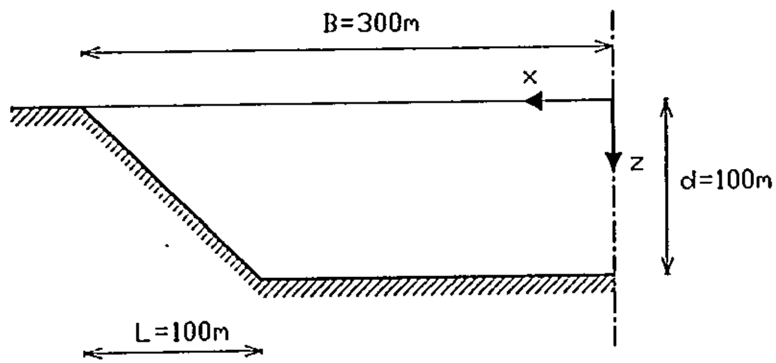

(a) Dimensions of valley (1)

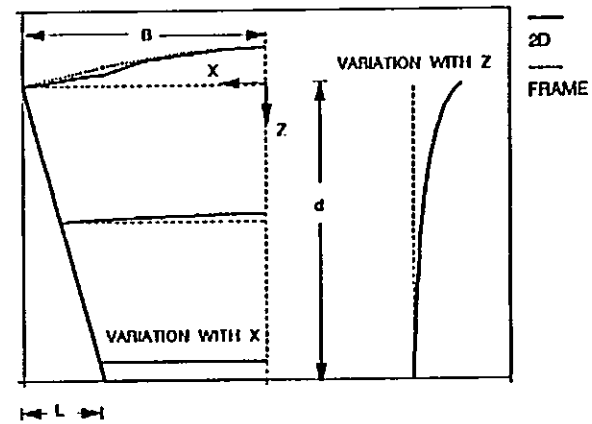

(b) Mode 1,1 - Period = 1.56 s

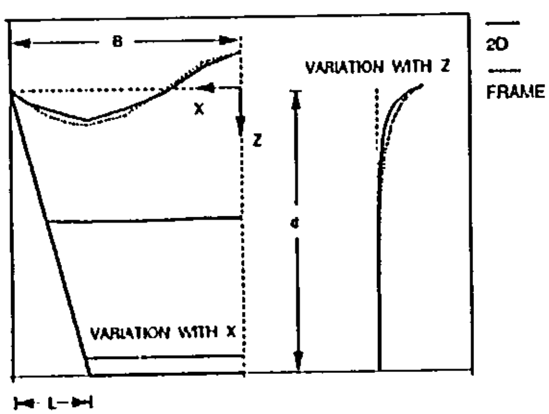

(c) Mode 1,2 - Period =1.26 s

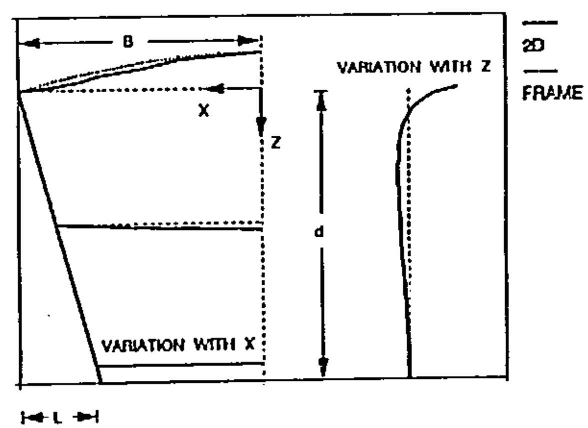

(d) Mode 2,1 - Period = 0.85 s

Fig. 2-16 Major modes of valley (1)
Soil profile : NC

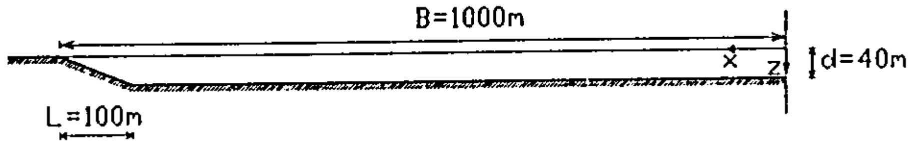

(a) Dimensions of valley (2)

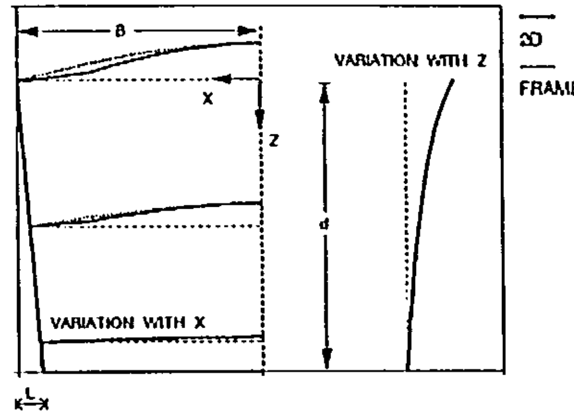

(b) Mode 1,1 - Period = 1.03 s

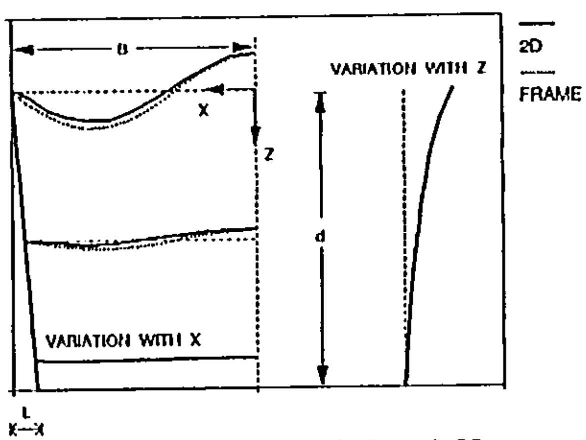

(c) Mode 1,2 - Period = 1.02 s

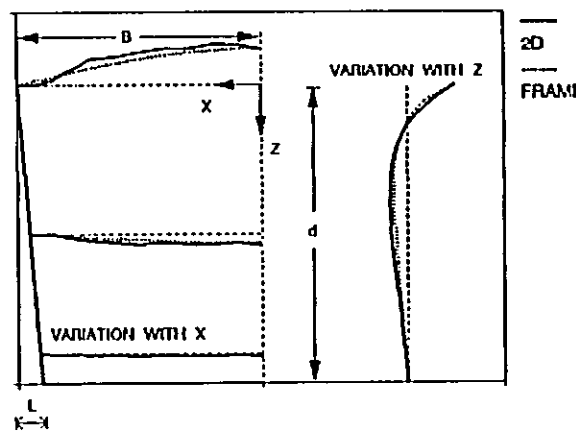

(d) Mode 2,1 - Period = 0.52 s

Fig. 2-17 Major modes of valley (2)
Soil profile : NC

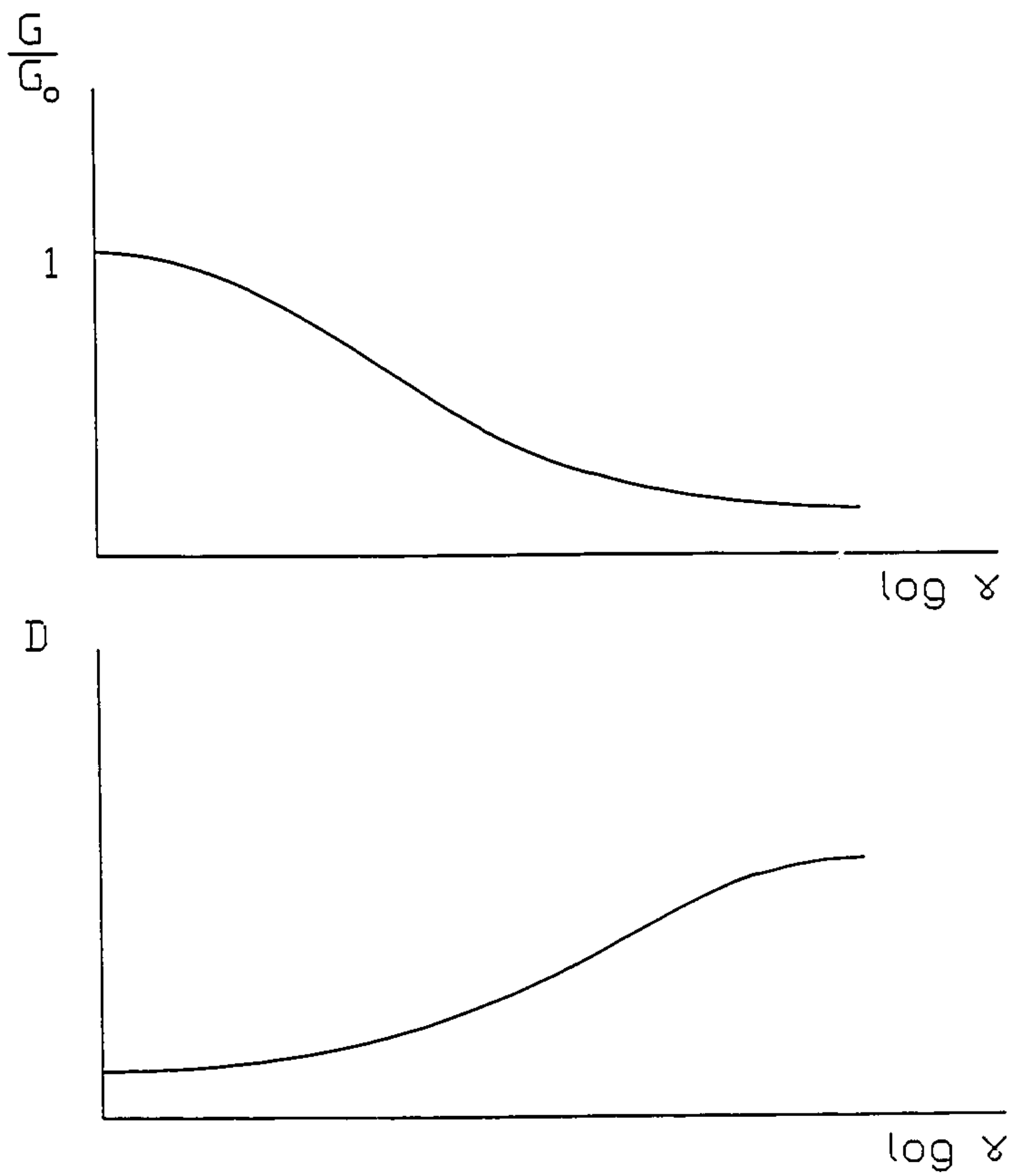

Fig. 2-18 Variation of secant shear modulus, G , and damping, D , with the shear strain, γ

CHAPTER 3

DESCRIPTION OF SITES AND INPUT ROCK MOTIONS

3.1 INTRODUCTION

The key parameters that are expected to govern the free-field seismic response of alluvial valleys are presented in this chapter. These include soil type, valley geometry and control motion in rock. The shape of the symmetrical valley is chosen to be a trapezoid with various dimensions, from wide and shallow to narrow and deep, along with different slopes of rock boundary. The soil types presented are normally to lightly over-consolidated clay (NC), heavily over-consolidated clay (OC), alluvial sand and silt (AS) and dense sand (DS). Variation of the shear modulus and damping ratio with strain level and with depth is presented for all soil categories.

The parameters of the seismic excitation input in rock, that are of main concern in this study, include the ratio of peak acceleration to peak velocity, a/v, and the peak velocity, v, which are measures of the frequency content and intensity of motion in rock, respectively. The peak velocity of a record can be used as an indicator of the motion intensity level provided that the duration and the frequency content of record do not change. Three artificial acceleration time histories are generated to match three target spectra. The artificial accelerations are used separately as horizontal components of uniform input motions in the rock. Each target spectrum is representative of one ensemble of records having a specific a/v ratio (high, intermediate and very low). The generated accelerations are scaled to three levels of intensity corresponding to peak velocities, v, equal to 0.05, 0.2 and 0.4 m/s. The purpose of these artificial excitations is to cover a wide range of frequency content and intensity of motion, as well as allow consistent examination of the valley effect on the amplification of rock motions.

3.2 THE VALLEY GEOMETRY

The shape of the symmetrical alluvial valley under consideration is simplified as the trapezoid shown in Fig.3-1. The dimensions of the trapezoidal valley are denoted as follows :

B = half the breadth at the top surface of the valley

d = depth of the valley at the axis of symmetry

L = length of the horizontal projection of the sloping rock boundary

s = slope of the rock boundary

The dimension B has values ranging from 100m to 1000m. Three thicknesses d = 20 , 40 and 100m are chosen for the soil deposits. The length L varies from 0 to 200m , where the zero length corresponds to a rectangular valley and the case L=B represents a triangular valley. The valley is assumed to constitute a plane-strain problem in the x-z plane with a unit thickness. Changes in the above dimensions of the valley will influence the surface seismic motions as well as the validity of the engineering models used in the analysis.

3.3 CATEGORIES OF SOIL PROFILES

A previous investigation on the seismic-response effects of eleven sites, by Henderson et al (1989b), has shown that all kinds of sites, soft or hard, deep or shallow, can produce magnification of rock motion. The eleven sites included eight actual sites, two artificial sites and one modified actual site. A more systematic approach, in which typical categories of soil deposits are considered, is applied in this study. These categories of soil deposits were described in detail in a site-response parametric study by Elhmadi et al (1990). They can be summarized as :

(a) Normally to lightly over-consolidated clay (NC)

(b) Heavily over-consolidated clay (OC)

(c) Alluvial sand and silt (AS)

(d) Dense sand (DS)

These types of soil combined with various thicknesses cover a wide range of sites. Their properties are based on measured data from actual sites which contain soils in the same category.

The soil properties required for the valley-response analysis by any of the engineering models discussed before are :

(a) Mass density of soil deposit ρ

(b) Initial shear modulus G_o as a function of depth, which is called the G_o profile

(c) Secant shear modulus G and hysteretic damping ratio D as a function of the shear strain amplitude γ

The mass-density values ρ and the G_o profiles for the above four soil categories are shown in Fig. 3-2. It is worth noticing that the zero G_o at the ground surface of the (NC) profile makes the top soil layers very soft. This, in turn, sets up a resonant oscillation which is a function of the discretization and is not a function of the soil deposit. For this reason, a modification was made, by Elhmadi et al (1990), for the G_o profile in the upper 1m , as shown in detail A in Fig.3-2, such that the profile is taken as constant equal to G_o at $z = 1m$. The curves recommended by Pappin et al (1989) and shown in Fig. 3-3 are used to represent the G/G_o versus γ variation for clay profiles (NC) and (OC) and sand profiles (AS) and (DS). The curves proposed by Seed and Idriss (1970) are used to describe the damping versus γ for clay and sand profiles. The damping-strain relationships are shown, along with their upper and lower bounds, in Fig. 3-4 for clays and in Fig. 3-5 for sands.

3.4 INPUT RECORDS IN THE ROCK BOUNDARY

Despite all the improvements in the methods of analysis, the uncertainty in the input motions is still a major problem for the dynamic analysis. The same control motion acting in the same control point can arise from different types of seismic waves. In general, identifying the wave pattern and its contribution to a given control motion is not yet satisfactorily understood. Hence, it will be assumed sufficiently accurate for engineering purposes to select the control motion as a given accelerogram representing a horizontal component of excitation and acting along the rock boundary of the alluvial valley.

Two of the significant features of earthquake motions in rock are the frequency content and the peak amplitude of motion which together can be presented by means of a response spectrum. Previous investigations (Idriss, 1978) have shown a decrease in the ratio of peak acceleration, a (in g), to peak velocity, v (in m/s), with increasing epicentral distance. This is due to the differences in the attenuation of acceleration and velocity ground motions. Hence, a/v is a measure of the frequency content of a recorded acceleration time history where the high frequency components are filtered out as the waves travel through the ground.

Based on the ratio a/v , a database of strong ground motions which includes 45 horizontal accelerograms recorded on rock or stiff soil (Naumoski et al, 1988) is classified into three ensembles each containing 15 records. Records with $a/v > 1.2$ belong to the high ensemble (H). The second ensemble is termed intermediate (I) and includes records with $0.8 < a/v < 1.2$. The third ensemble termed very low (V) contains records with $a/v < 0.6$. These 45 accelerograms are selected from the McMaster University Seismological Executive (MUSE) Database System and were used by Henderson et al (1989b) and Elhmadi et al (1990) to evaluate site-response effects. It should be mentioned that the 1990 edition of the National Building Code of Canada

(NBCC 1990) uses three ranges of a/v ratio to define force coefficients :

H high a/v ratios ($Z_a > Z_v$)

I intermediate a/v ratios ($Z_a = Z_v$)

V very low a/v ratios ($Z_a < Z_v$)

in which Z_a and Z_v represent the acceleration and velocity related seismic zones for a particular location, respectively.

In order to study the frequency content effect of each a/v ratio ensemble (H, I and V) on the seismic response of the valley, one target acceleration spectrum is created to represent each range of frequency with uniform spectral values over the dominant period range observed in each ensemble of records from the McMaster database (Elhmadi et al, 1990). Thus, the first target spectrum has its maximum spectral values uniform in the dominant period range of the (H) ensemble : $0.1 \leq T \leq 0.24$s. Similarly, the uniform spectral values of the second and third target spectra are in the dominant period ranges of the (I) and (V) ensembles, which are respectively: $0.26 \leq T \leq 0.6$ s and $0.8 \leq T \leq 2.0$ s . One accelerogram is chosen from each ensemble of the McMaster database and used as an initial accelerogram to generate the artificial time-history record compatible with the target spectrum proposed for the same ensemble. SYNTH computer program, prepared by Naumoski (1985), is utilized for this purpose. The three selected accelerograms are :

(a) Parkfield, California, June 27, 1966, component N65W, a/v = 1.86 (H) , recorded on rock

(b) Kern County, California, July 21, 1952, component S69E, a/v = 1.01 (I) , recorded on rock

(c) Long Beach, California, Mar. 10, 1933, component N51W, a/v = 0.41 (V) , recorded on rock

The acceleration spectra of the three generated records, representative of the three ensembles of a/v ratio, are scaled to $v = 0.2$ m/s and plotted in Fig. 3-6 for a critical damping ratio of 2%. The generated accelerations are used as horizontal input excitations in the rock boundary, thus covering a wide variety of frequency content ranges of real earthquake records. Furthermore, the smooth shapes of the spectra allow more consistent investigation of the valley effect on the amplification of rock motions.

The effect of the intensity of rock motion on the non-linear seismic site response can be studied by scaling each of the three generated records to three levels of peak velocity without altering the duration or frequency content of motion. The three levels of intensity correspond to peak velocities: $v = 0.05$, 0.2 and 0.4 m/s . This range of scaling is representative of the range of zonal velocities defined in the NBCC 1990.

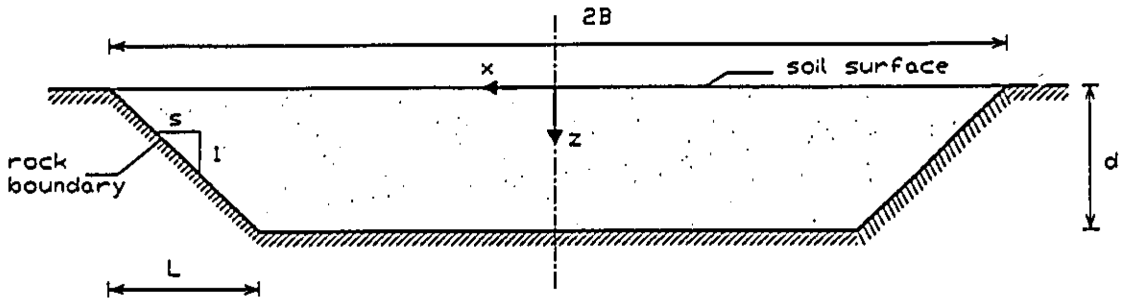

Fig. 3-1 The valley geometry

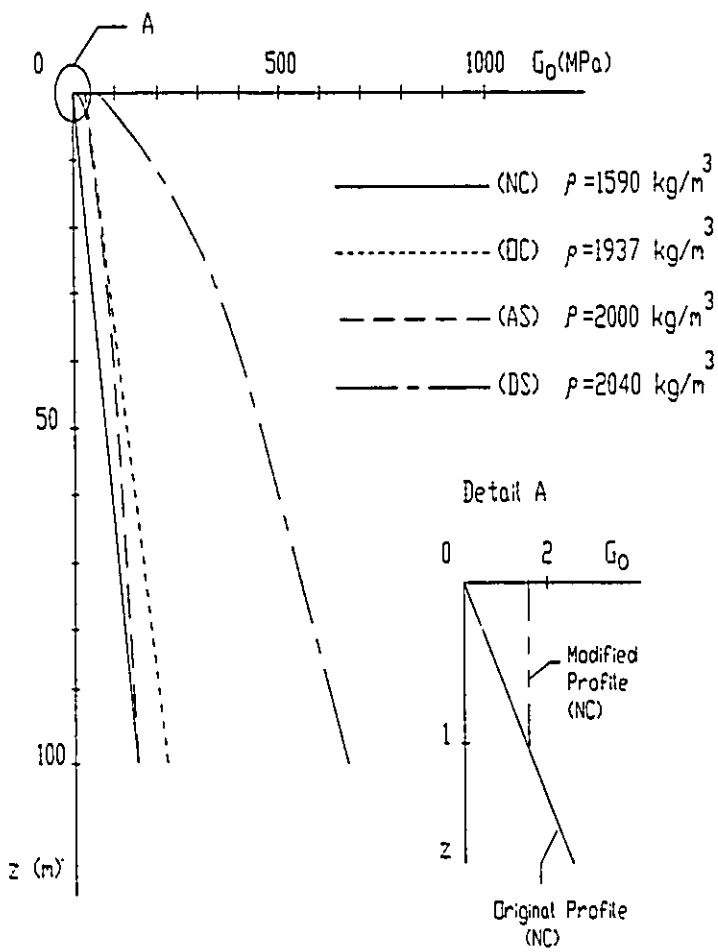

Fig. 3-2 G_o profiles of four soil categories

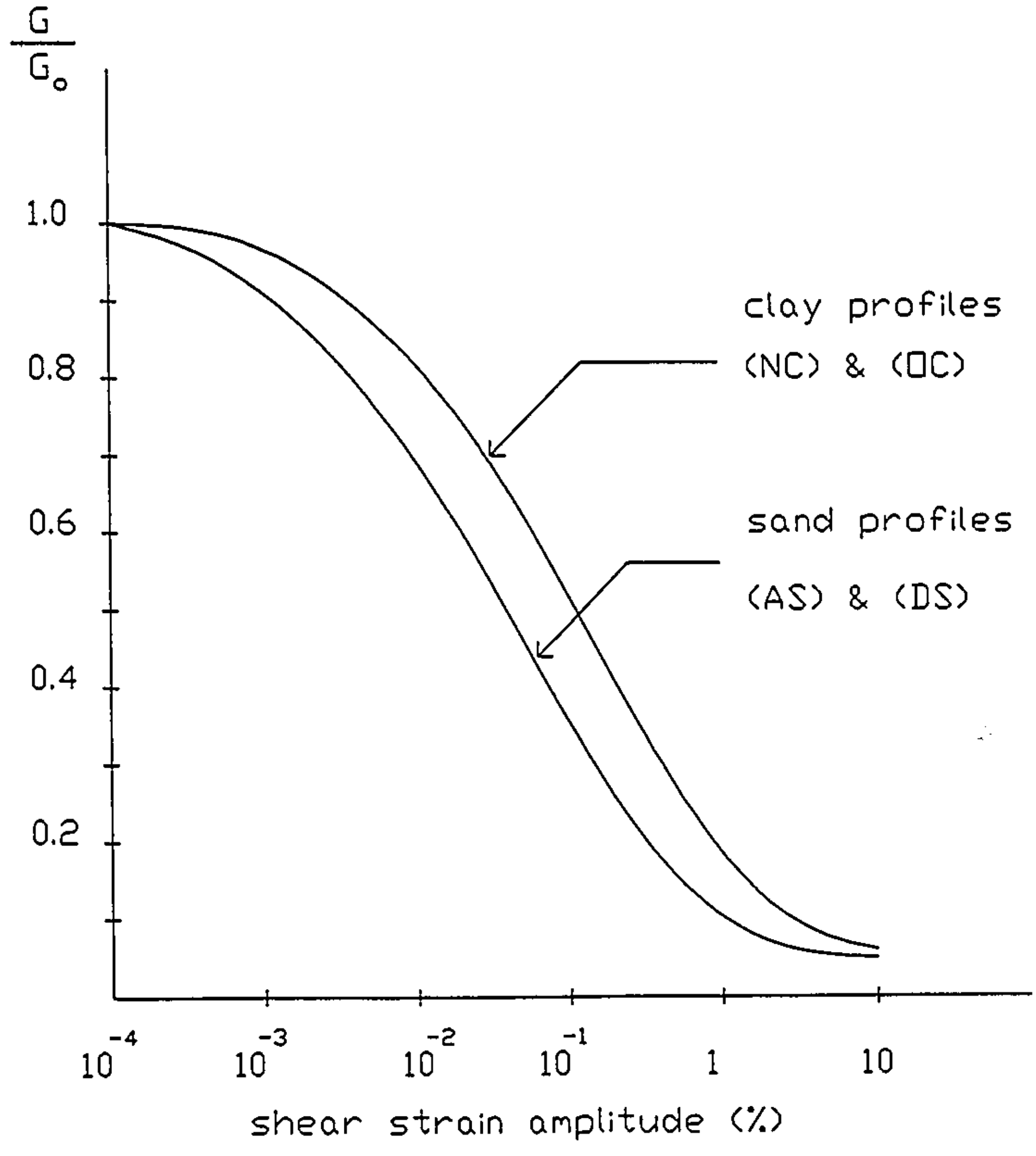

Fig. 3-3 Design values of G/G_o for various soils

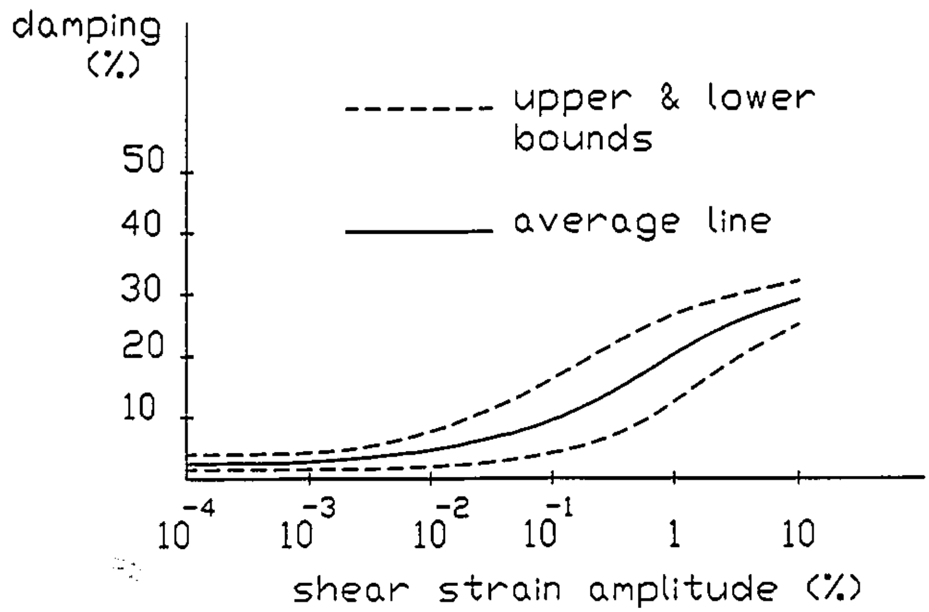

Fig. 3-4 Damping ratios for clay profiles (NC) and (OC)

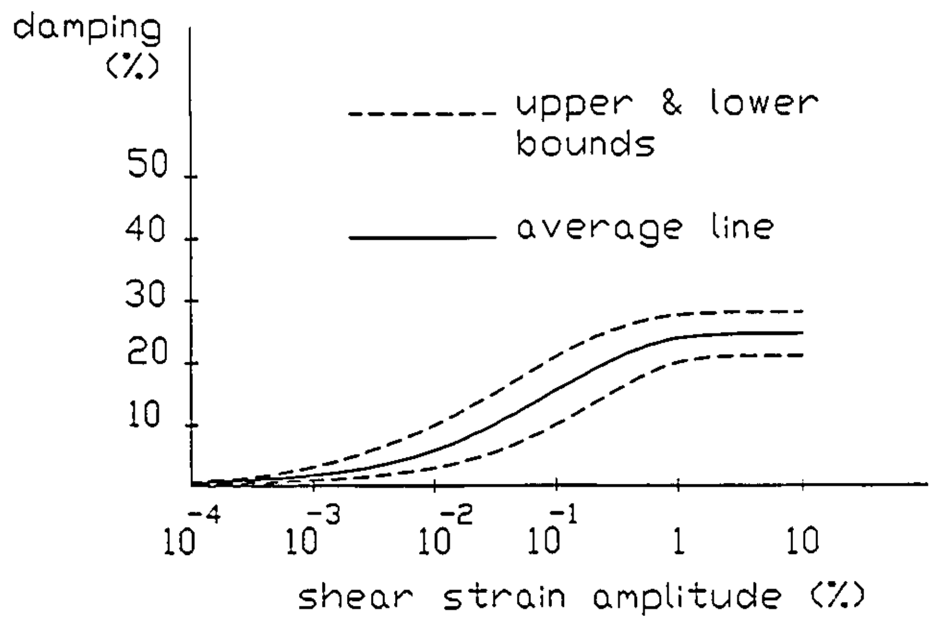

Fig. 3-5 Damping ratios for sand profiles (AS) and (DS)

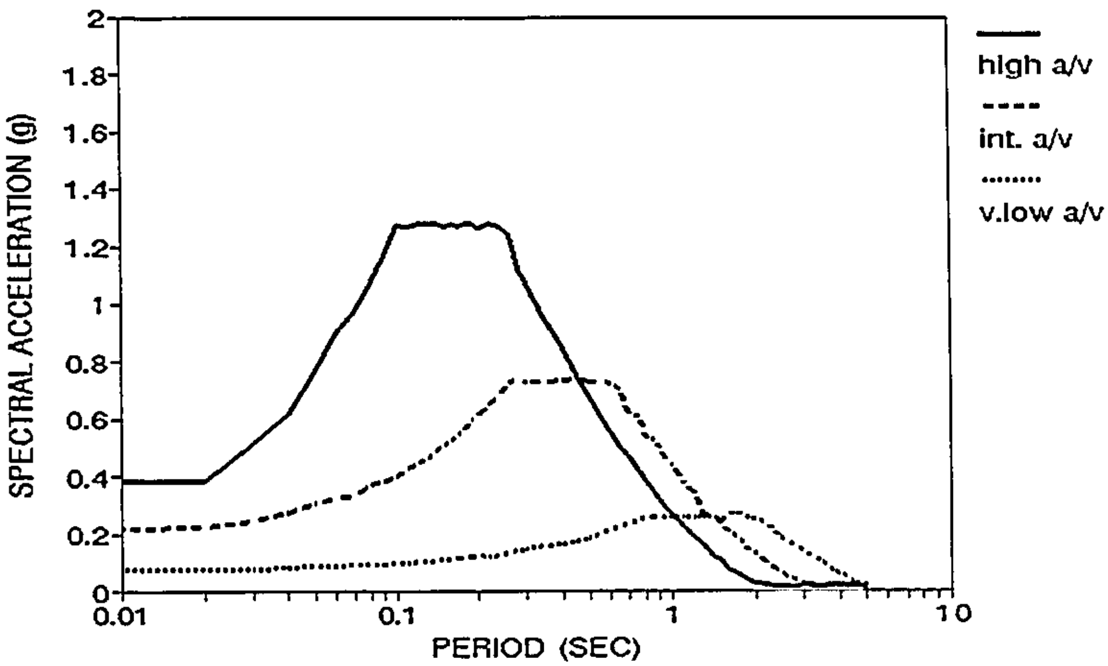

Fig. 3-6 Acceleration spectra of input rock motions scaled to v = 0.2 m/s

CHAPTER 4
SENSITIVITY ANALYSIS

4.1 INTRODUCTION

The sensitivity analysis is used to evaluate the effect of variations in various modelling parameters on the horizontal seismic response of the valley. This includes studying the effects of the variation in soil-layer discretization on the response results, for the purpose of modelling the soil continuum in the valley. The sensitivity of the response to the variation in the G_o profile as well as to the variation in the damping-strain relationship is also addressed to account for the uncertainty in establishing dynamic soil properties.

In this analysis, the valley dimensions are shown in Fig. 4-1, with B = 200 m, d = 40 m and L = 80 m. The engineering models utilized are :

(a) The one-dimensional (1-D) model using program SHAKE by Schnabel et al (1972)

(b) The two-dimensional (2-D) model using program FLUSH by Lysmer et al (1975)

(c) The proposed frame model using the modified version of program SAP IV. SAP IV program was originally presented by Bathe et al (1973)

The valley response from the above models is compared to examine their sensitivity to parameter variation and validity of the approach.

The response results are presented in the form of surface acceleration spectral ratios which are obtained by dividing the surface acceleration spectra by the input rock motion acceleration spectrum. This has the advantage of discarding some of the effects of the applied record in rock, which means that the spectral-ratio curve calculated at a site (surface point) represents the soil amplification of the rock motion at this site. In other words, the spectral ratio is a direct indicator of the site-response effect. Hence, the period at which the largest peak of amplification occurs at a site will be termed the local-amplification period of the site. However, one has to distinguish between the fundamental period of the valley which is associated with the fundamental mode and the so-called "local- amplification periods" which are meant, in this study, to be location-dependent characteristics related to the amplification at different surface points in the valley. Being the furthest surface point from the stiffening effect of the sloping rock boundary, the centre point has the longest local-amplification period which thus occurs at the fundamental period of the valley. The acceleration spectral ratios are calculated at three sites (surface points) with coordinates $x = 0$, $0.5\,B$ and $0.8\,B$ to cover the response at the middle and near the edge of the valley.

4.2 VARIATION IN THE SOIL - LAYER DISCRETIZATION

The soil deposit must be represented in the discrete engineering models by a set of homogeneous layers, each with a constant value of shear modulus and damping and constant breadth. For this reason, the thickness of each layer must be limited, based on the variation in the soil properties and the slope of the rock boundary at the valley edges. Of concern in this study is the vertical dimension of the soil elements or layers. The horizontal dimension of the elements in the 2-D analysis can usually be chosen several times the vertical dimension. This is the case because the major part of the motion consists of vertically propagating waves with horizontal fronts.

The softest soil profile (NC) is selected for this study since its lack of stiffness tends to make it more susceptible to discretization errors. Stiffer soil profiles are generally less sensitive to the soil-layer discretization and thus are not addressed in this analysis. The three generated acceleration time histories with $a/v = H$, I and V are scaled to peak velocity $v = 0.2$ m/s and used as input rock motions. In order to study the effect of the model discretization on the response, the soil thickness, 40 m, is divided as shown in Fig. 4-1 into:

(a) 10 layers (10 x 4 m = 40 m)

(b) 27 layers (10 x 1 m + 8 x 1.5 m + 9 x 2 m = 40 m)

The surface response is mainly affected by the top soil-layer thicknesses, since they are the softest layers, rather than the number of layers. The purpose of the 27-layer discretization is to reflect the effect of top layers on the response by using smaller thicknesses.

The resulting surface acceleration spectral ratios using the above two discretization schemes with the frame model are compared in Fig. 4-2. It is evident that the 10-layer and the 27-layer discretization produce more or less the same amplification at the soil surface regardless of the a/v ratio of the input rock motion or the location of the surface point in the valley. However, the finer top layers, in the 27-layer case capture and amplify the response from the higher modes of the valley which increases the amplification slightly more than in the 10-layer case, particularly in the short-period range, below the local-amplification period of the site.

The resulting amplification from the frame model is compared with those from the 1-D and 2-D models in Fig. 4-3 for the 27-layer discretization using the generated rock acceleration with a/v = V and in Fig. 4-4 for the 10-layer discretization using the generated rock acceleration with a/v = I. While the agreement is good between the frame and the two-dimensional models at different surface locations, the 1-D analysis, that ignores the limited lateral extent of soil, provides a poorer approximation, which is particularly evident near the edge of the valley.

It may be generally concluded that the 10-layer discretization can be utilized by the frame model or the 2-D model to obtain the surface response in the valley, as it provides reliable results when compared with the much finer discretization.

4.3 VARIATION IN THE G_o PROFILE

The regulatory practice in nuclear power plant design requires that the proposed G_o profile be varied between (1.5 G_o) and (G_o/1.5) (Valera et al, 1977). This is used to account for the uncertainty in establishing dynamic soil properties. Accordingly, results are compared using the frame model for the (1.5 G_o), (G_o) and (G_o/1.5) profiles of soil type (NC) in Fig. 4-5 and of soil type (DS) in Fig. 4-6. The input rock motion is the generated acceleration with $a/v = 1$, scaled to $v = 0.2$ m/s.

The effect of variation in the G_o profile on the acceleration spectral ratios is a shift to the left for the (1.5 G_o) profile and a shift to the right for the (G_o/1.5) profile. These shifts indicate changes in the local-amplification periods at the three surface locations $x = 0$, 0.5 B and 0.8 B. On the other hand, the peak spectral ratios are less affected by the change in the G_o profile, which is particularly evident near the edge of the valley, where the soil formation is stiffer and thus less sensitive to the variation in stiffness. Generally, higher G_o values lead to shorter periods and slightly higher peaks of amplification. The shorter periods are due to the larger stiffness and the slightly higher peaks are mainly because of the lower shear strain levels and consequently the lower damping associated with the larger G_o profiles. It is further observed that the (NC) profile, due to its softness especially in the top layers, is more sensitive to the variations in G_o than the (DS) profile.

The results from the frame model compare well with those from the 2-D model, as shown in Fig. 4-7 (a), (b) for the (G_o/1.5) profile of (NC) and in Fig. 4-7 (c), (d) for the (1.5 G_o) profile of (DS). The given cases in Fig. 4-7 represent two extreme cases of soil stiffness. The fundamental periods of the valley corresponding to the variation in the G_o profiles of (NC) and (DS) are given in Table 4-1. It is noticed that the stiffer profile (DS) results in shorter fundamental periods than the softer profile (NC).

4.4 VARIATION IN THE DAMPING - STRAIN RELATIONSHIP

The upper and lower bounds along with the average line of the damping-strain relationships, shown in Fig. 3-4 and Fig. 3-5, are used to obtain the acceleration spectral ratios for soil types (NC) and (DS), respectively. Results are presented in Fig. 4-8 for (NC) and in Fig. 4-9 for (DS), using the frame model. The input rock motion is the generated acceleration time history with $a/v = 1$, scaled to peak velocity $v = 0.2$ m/s.

The variation in the damping-strain relationship for the same soil type leads to significant changes in the spectral ratio peaks. This is because more energy is dissipated in the soil as the damping increases at the same strain level, resulting in lower amplification values of rock motion. On the other hand, there are hardly any noticeable shifts in the local-amplification periods of sites due to unchanged G/G_o values. It is further observed that the surface response at the sites $x = 0.5$ B and 0.8 B is less sensitive to the damping variation than that at the site $x = 0$. This may be attributed to the shallower depths and consequently the stiffer formation of soil beneath the edge surface points in the valley. This lack of sensitivity at the edge sites is more apparent in the case of the stiffer profile (DS).

The general agreement of the results from the frame model and the 2-D model is emphasized again in Fig. 4-10 (a), (b) for the upper damping bound of (NC) and in Fig. 4-10 (c), (d) for the lower damping bound of (DS).

4.5 SUMMARY

The sensitivity of the horizontal seismic response of the valley resulting from the engineering models was examined for the variation in the soil-layer discretization, the variation in the $G_o^{\cdot}$ profile and the variation in the damping-strain relationship. The response results were presented as surface acceleration spectral ratios which represent the soil amplification of the input rock motion.

The surface seismic motions proved not to be sensitive to the soil-layer discretization, under different conditions of soil properties and control motions in the rock, except in the short-period range due to the top-layer amplification of the higher modes. It is concluded that a finer discretization may be replaced by a coarser one for the analysis of soil amplification without losing accuracy.

The variation in the G_o profile (stiffness) leads to significant changes in the local-amplification periods of sites and minor changes in the spectral ratio peaks. Higher G_o values result in shorter periods due to larger stiffness and slightly higher peaks of amplification because of lower values of associated damping. Furthermore, the soft (NC) profile is more sensitive to variations in G_o than the stiffer (DS) profile.

The variation in the damping-strain relationship for the same soil type leads to significant changes in the amplification values of the rock motion and hardly any noticeable shifts in the local-amplification periods of sites. The higher the damping is the lower the amplification becomes, due to the higher energy dissipation associated. Having a stiffer soil formation, the edge sites of the valley are less sensitive to the damping variation than the sites near the middle, which is more pronounced in the stiffer (DS) profile.

In general, the results from the frame model and from the 2-D model are in good agreement at different surface locations in the valley. On the other hand, the 1-D model fails in approximating the response, particularly near the edge of the valley, where the sloping boundary effect is significant.

Table 4-1 Fundamental periods of the valley

($a/v = 1$, $v = 0.2$ m/s)

G_o profile	soil type	period (sec)
1.5 G_o	NC DS	1.46 0.46
G_o	NC DS	1.83 0.63
$G_o/1.5$	NC DS	2.29 0.82

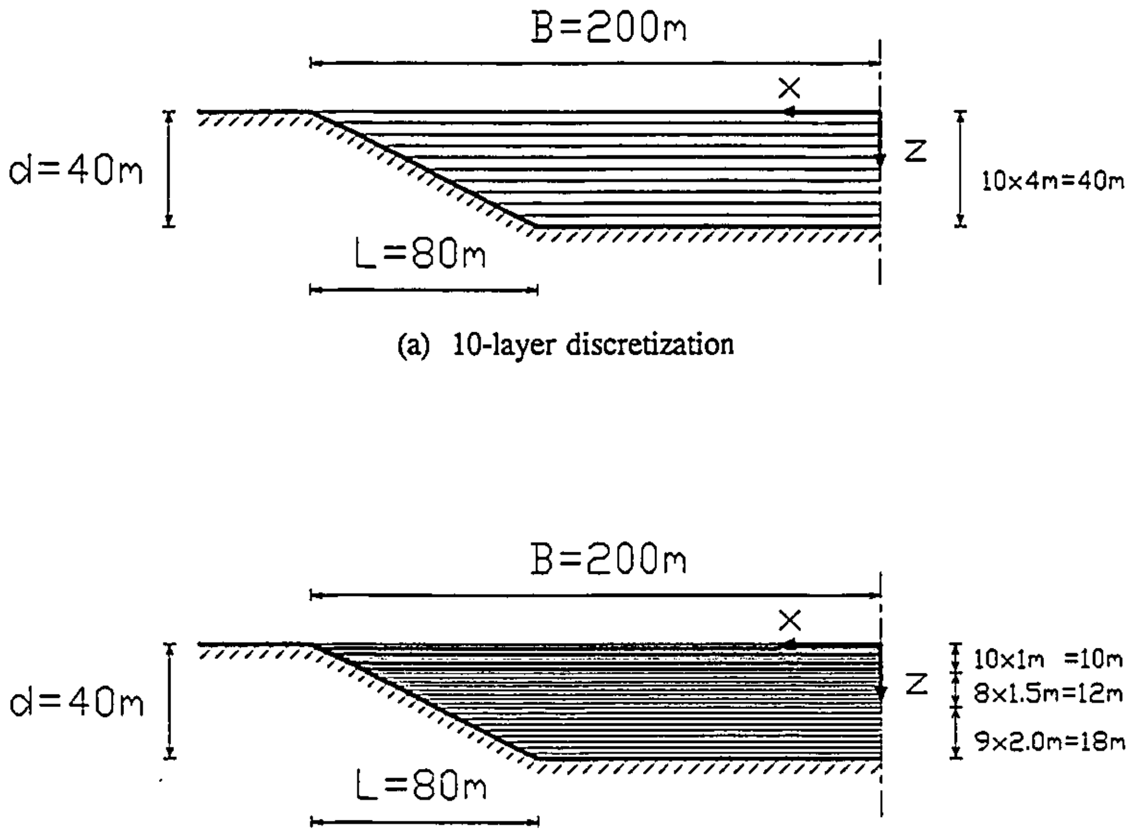

(a) 10-layer discretization

(b) 27-layer discretization

Fig. 4-1 Valley dimensions and soil-layer discretization

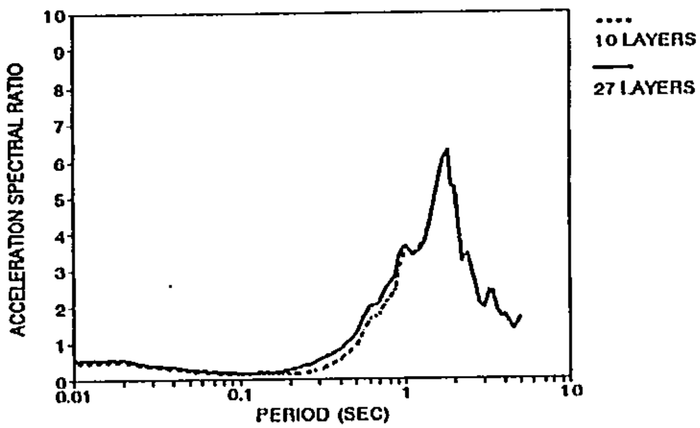

(a) a/v = H, v = 0.2 m/s, x = 0

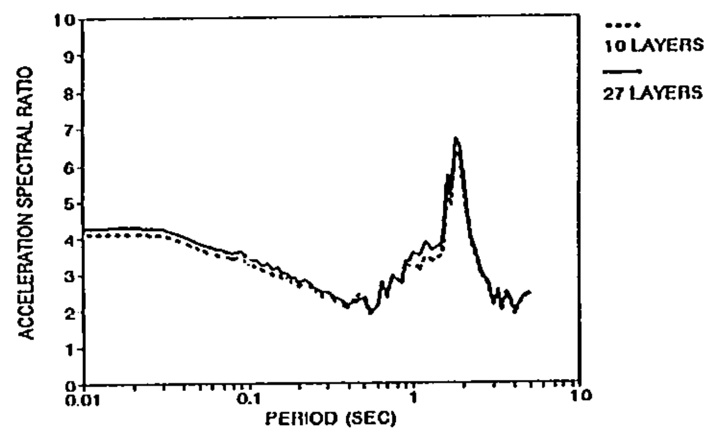

(b) a/v = V, v = 0.2 m/s, x = 0

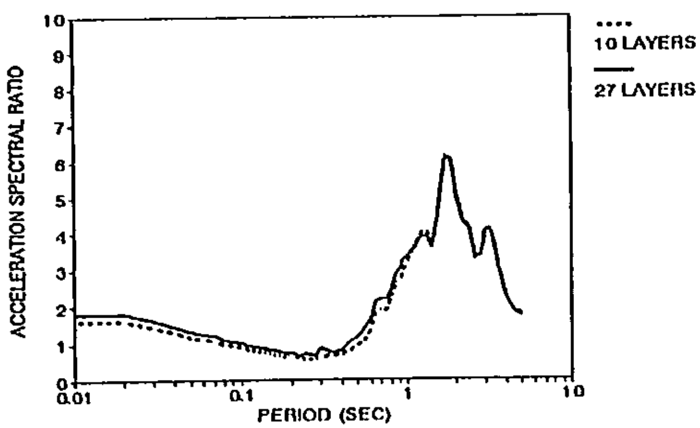

(c) a/v = I, v = 0.2 m/s, x = 0

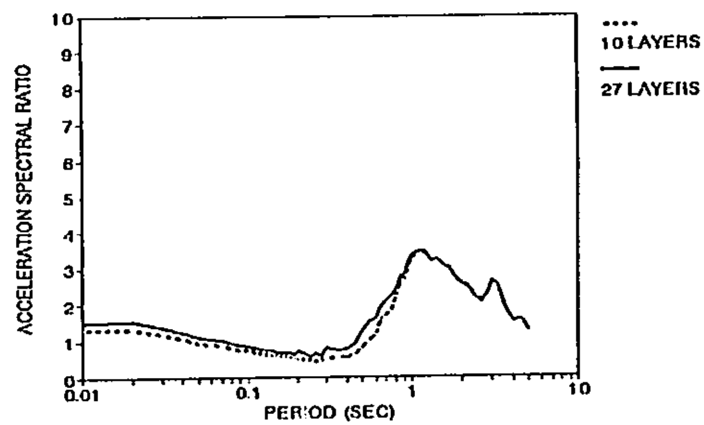

(d) a/v = I, v = 0.2 m/s, x = 0.8B

Fig. 4-2 Effect of variation in the soil-layer discretization
Soil profile : NC, frame model

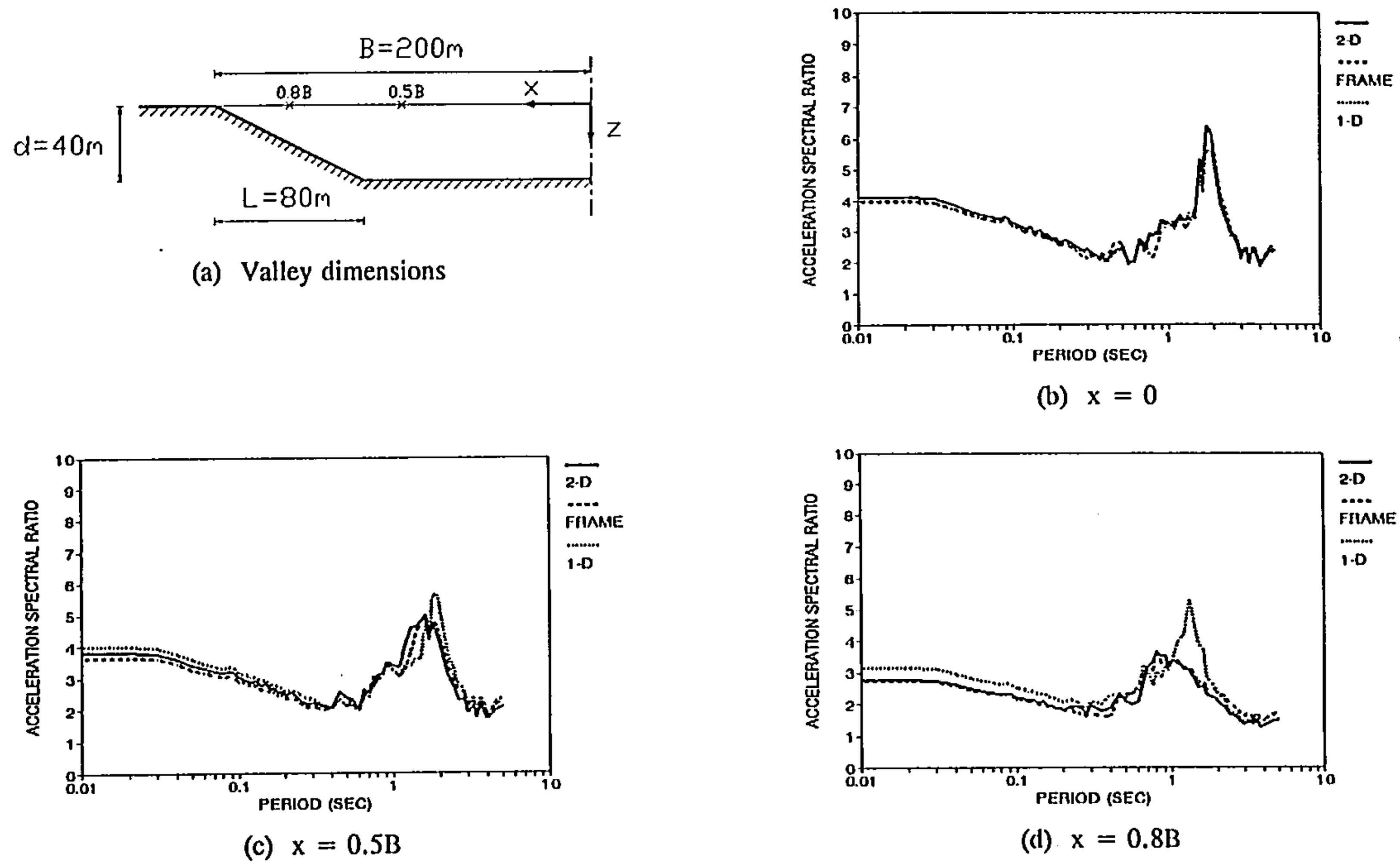

Fig. 4-3 Acceleration spectral ratios from 2-D, frame and 1-D models
Soil profile : NC, 27 layers, a/v = V, v = 0.2 m/s

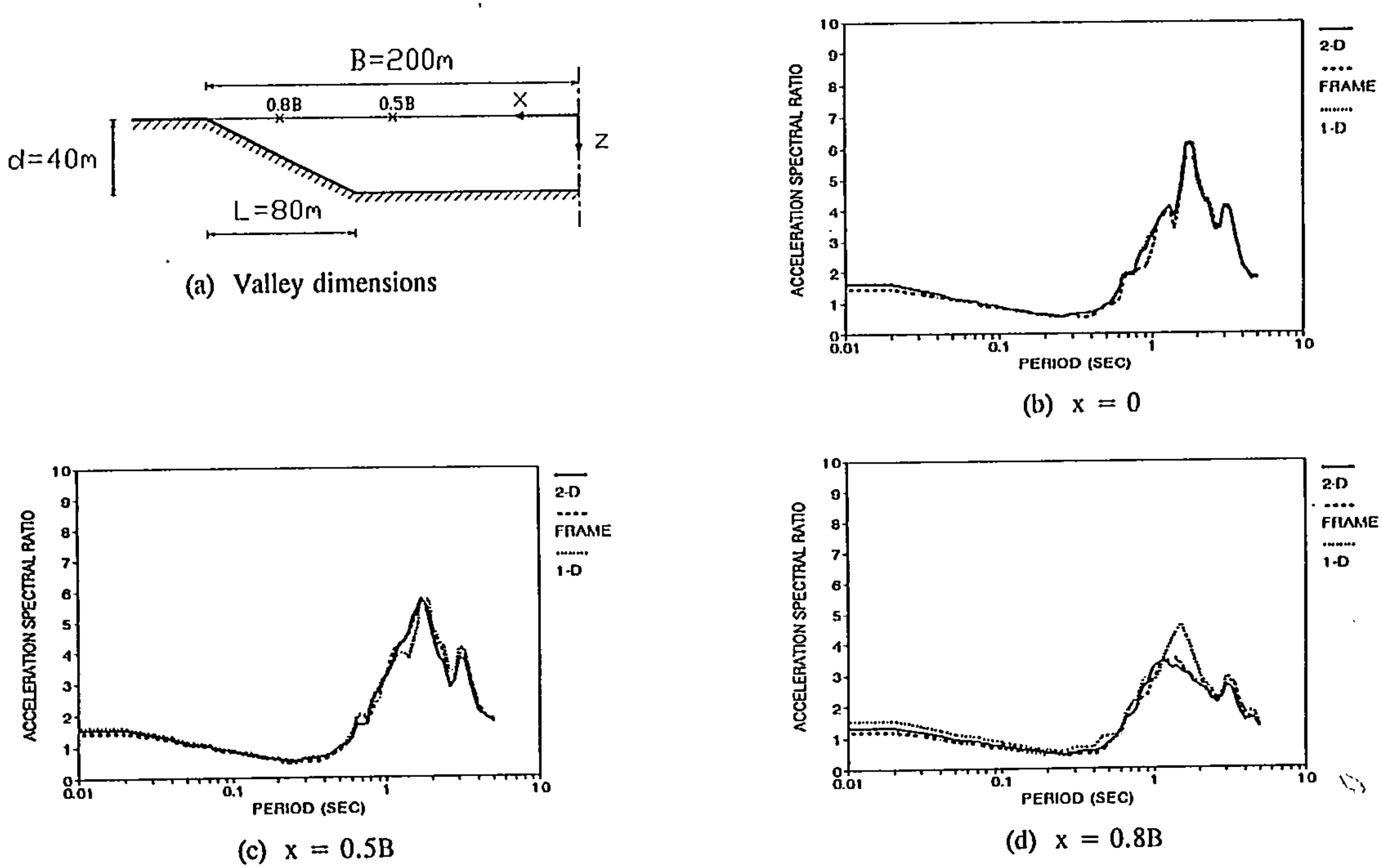

(a) Valley dimensions

(b) x = 0

(c) x = 0.5B

(d) x = 0.8B

Fig. 4-4 Acceleration spectral ratios from 2-D, frame and 1-D models
Soil profile : NC, 10 layers, a/v = I, v = 0.2 m/s

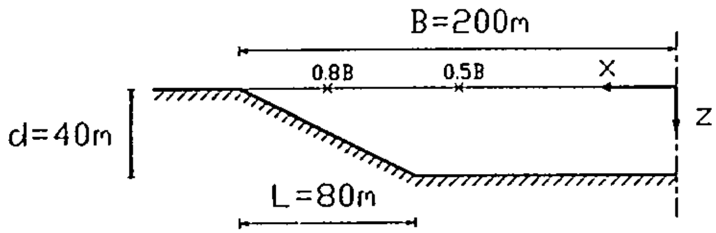

(a) Valley dimensions

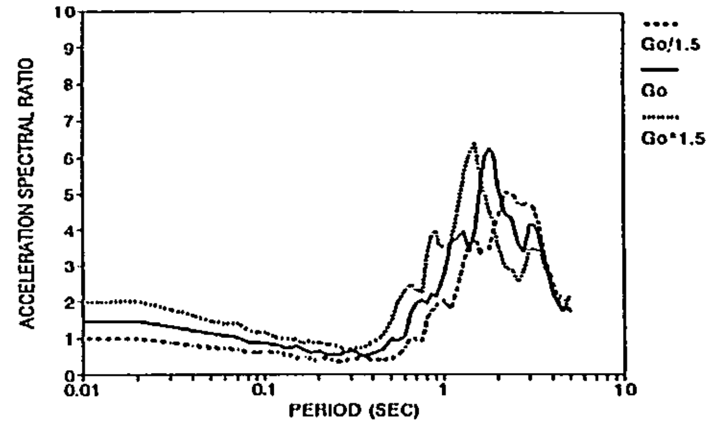

(b) x = 0

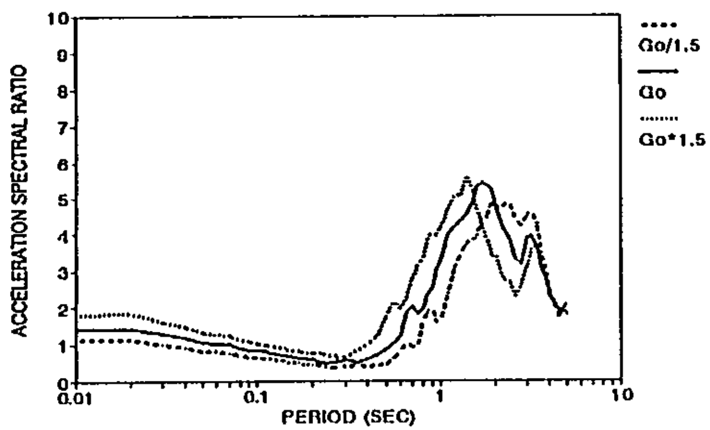

(c) x = 0.5B

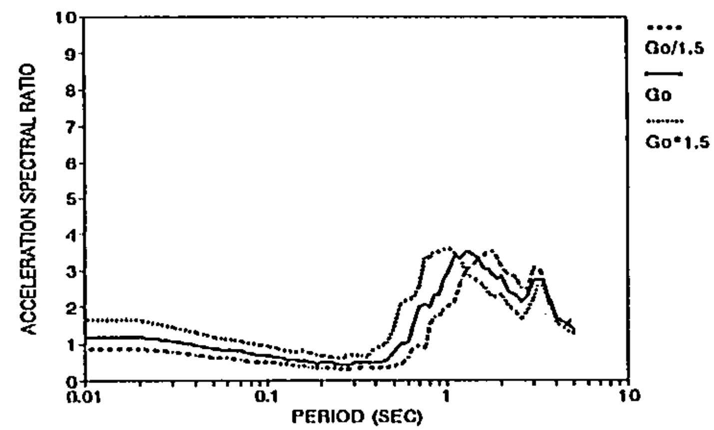

(d) x = 0.8B

Fig. 4-5 Effect of variation in the G_o profile
Soil profile : NC, frame model, a/v = I, v = 0.2 m/s

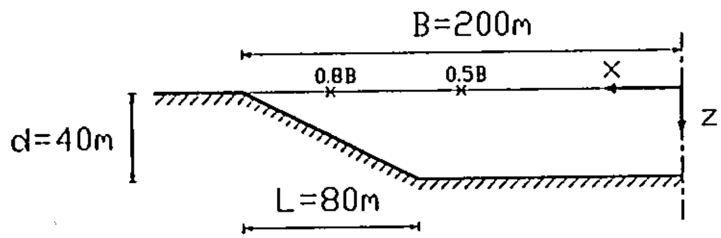

(a) Valley dimensions

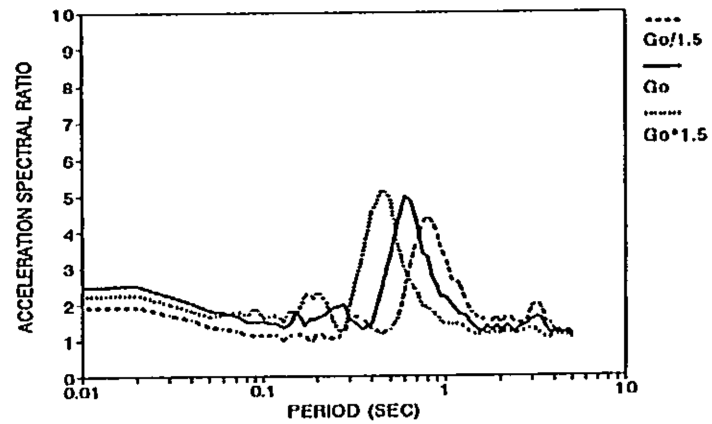

(b) x = 0

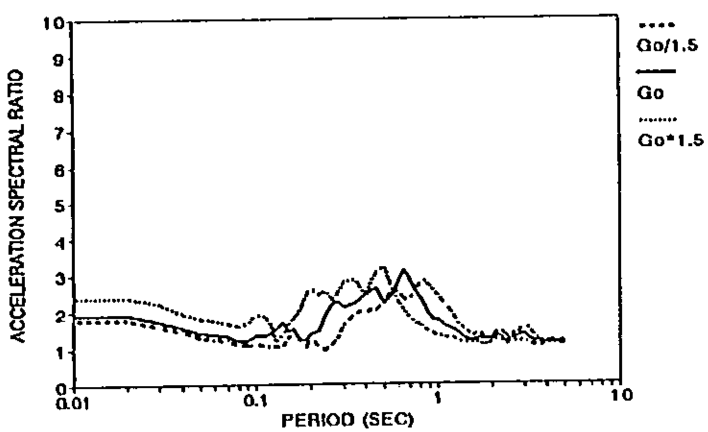

(c) x = 0.5B

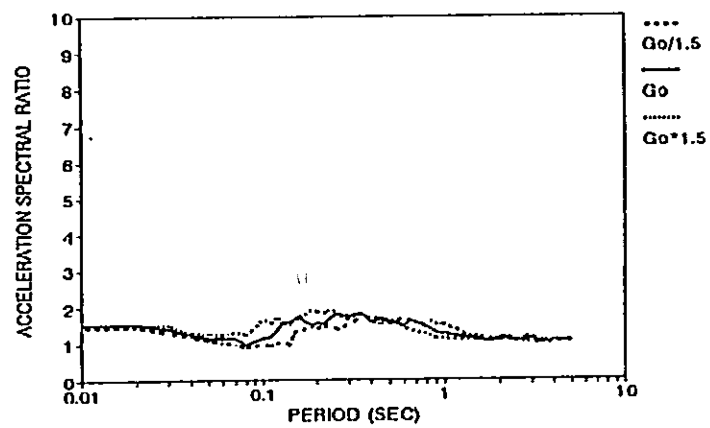

(d) x = 0.8B

Fig. 4-6 Effect of variation in the G_o profile
Soil profile : DS, frame model, a/v = I, v = 0.2 m/s

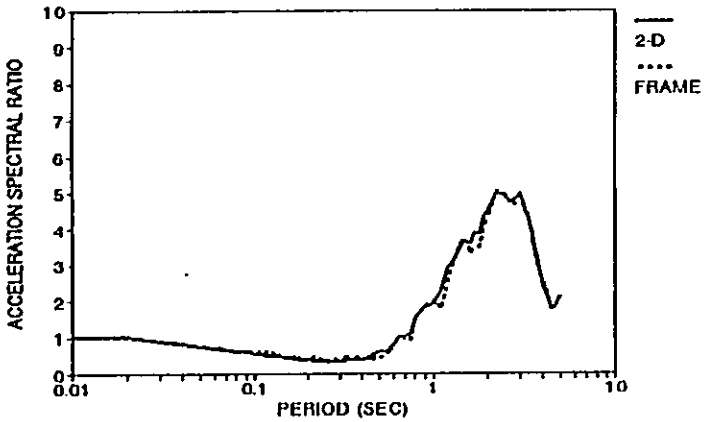

(a) Soil profile : NC, $G_o/1.5$, x = 0

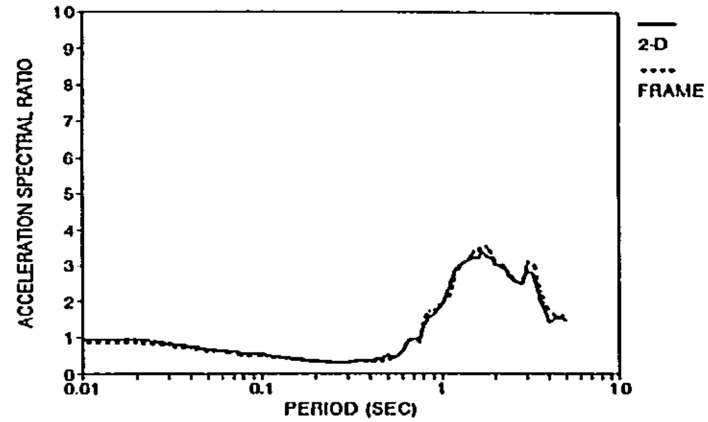

(b) Soil profile : NC, $G_o/1.5$, x = 0.8B

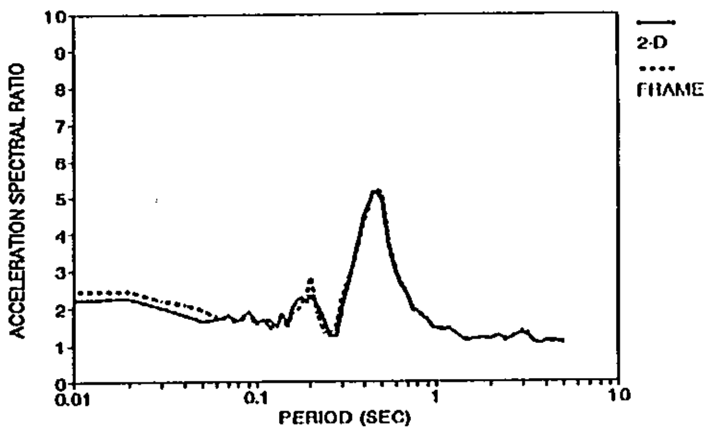

(c) Soil profile : DS, $1.5G_o$, x = 0

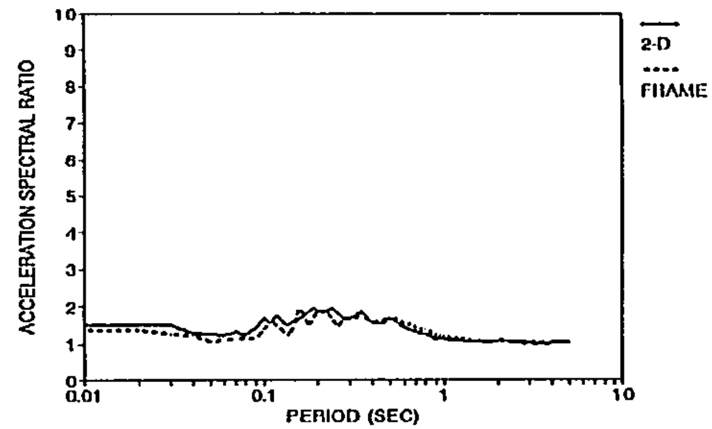

(d) Soil profile : DS, $1.5G_o$, x = 0.8B

Fig. 4-7 Acceleration spectral ratios from 2-D and frame models
a/v = I, v = 0.2 m/s

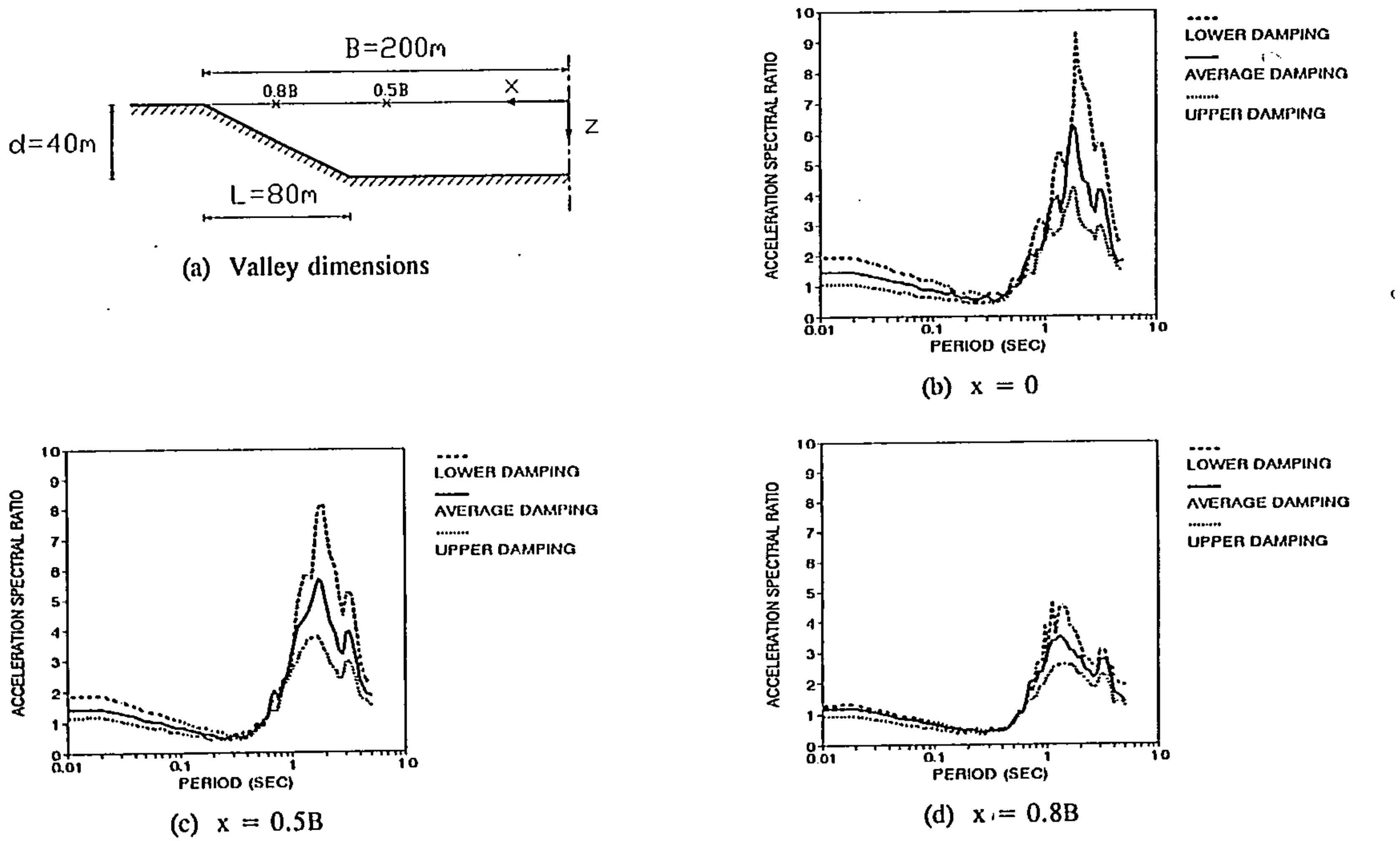

Fig. 4-8 Effect of variation in the damping-strain relationship
Soil profile : NC, frame model, a/v = I, v = 0.2 m/s

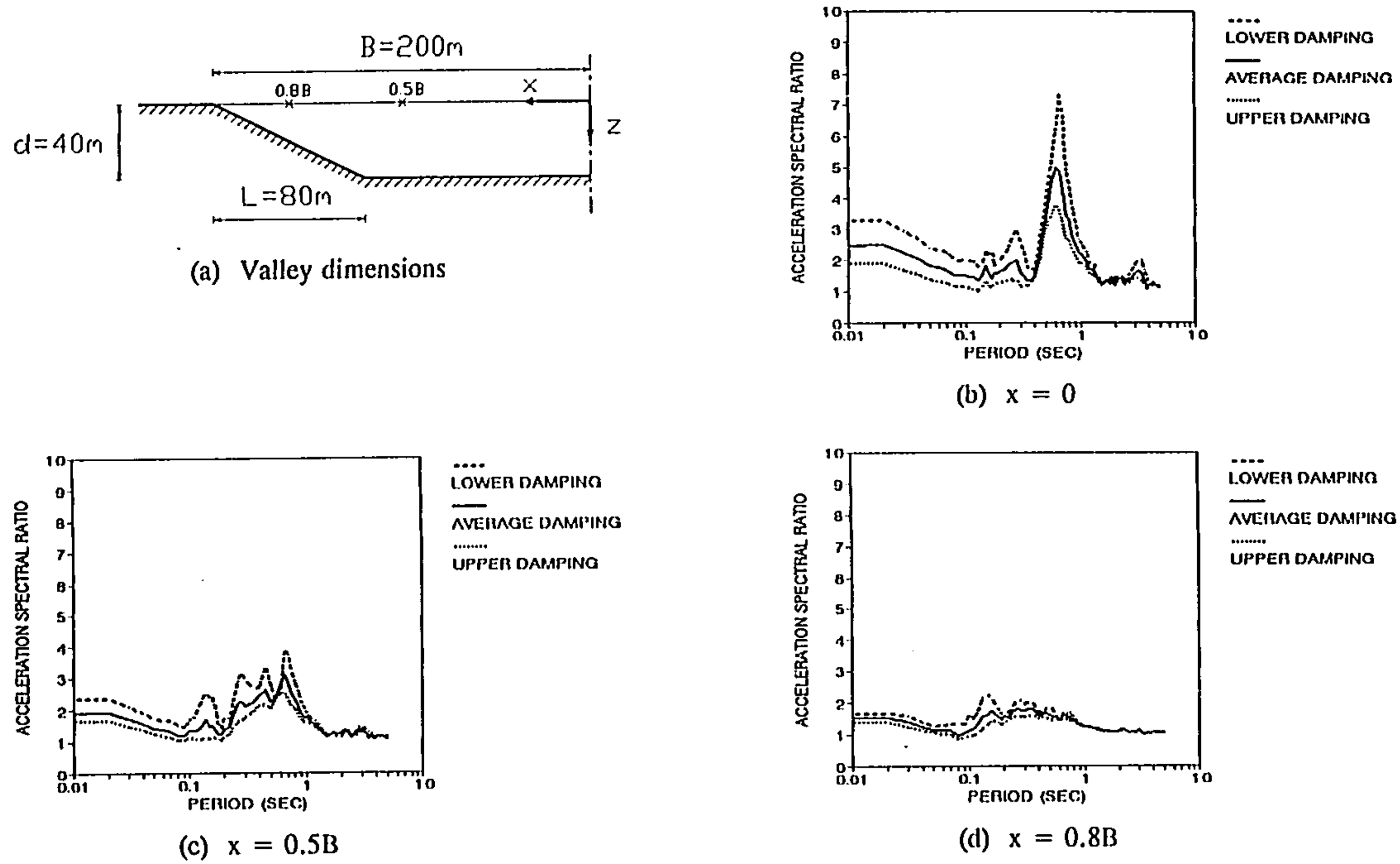

Fig. 4-9 Effect of variation in the damping-strain relationship
Soil profile : DS, frame model, a/v = I, v = 0.2 m/s

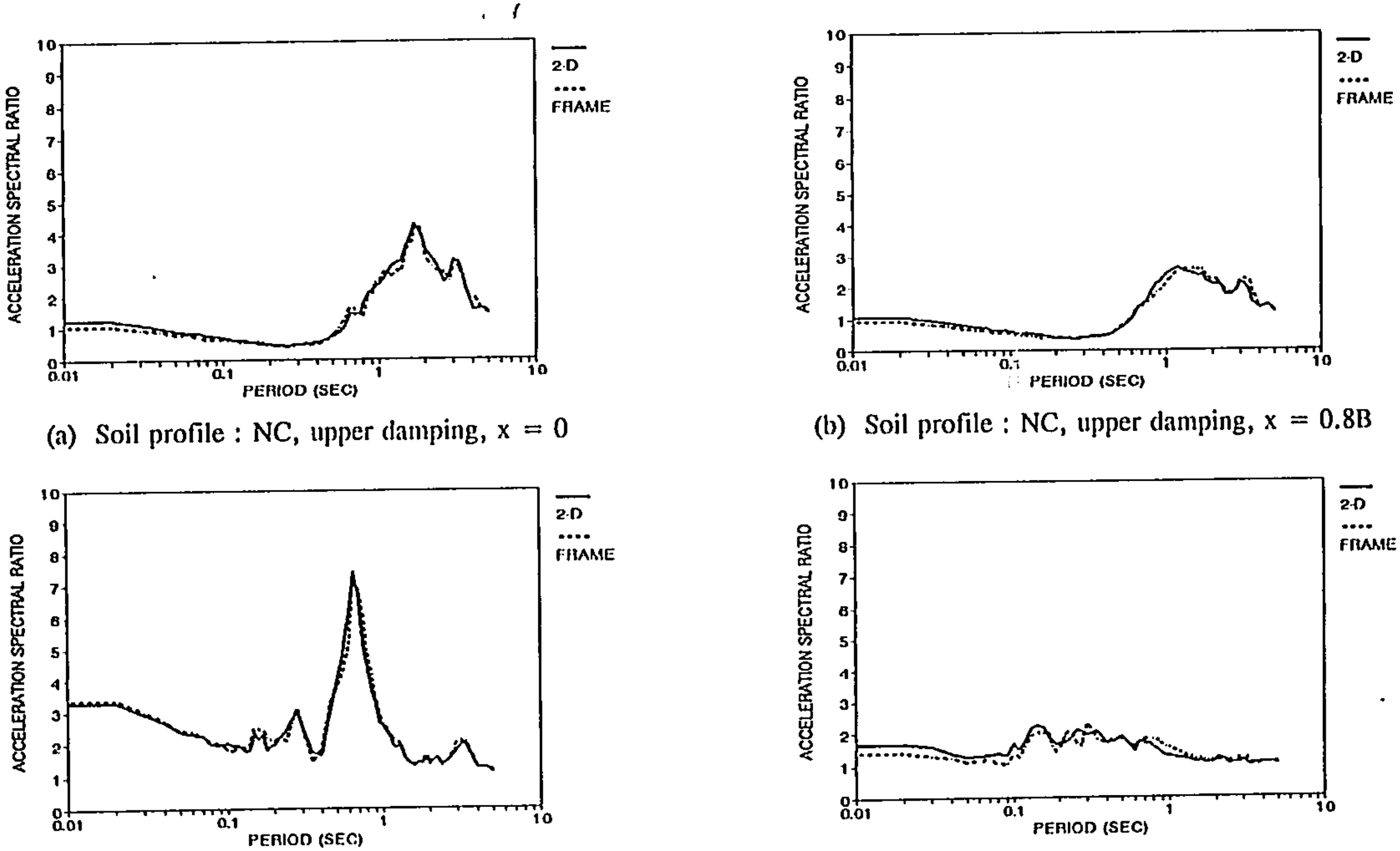

(a) Soil profile : NC, upper damping, x = 0

(b) Soil profile : NC, upper damping, x = 0.8B

(c) Soil profile : DS, lower damping, x = 0

(d) Soil profile : DS, lower damping, x = 0.8B

Fig. 4-10 Acceleration spectral ratios from 2-D and frame models
a/v = I, v = 0.2 m/s

CHAPTER 5

INFLUENCE OF VALLEY DIMENSIONS ON THE SEISMIC SITE RESPONSE

5.1 INTRODUCTION

The shape of the symmetrical valley is selected to be trapezoidal with various dimensions, from wide and shallow to narrow and deep, along with different slopes of rock boundary (Fig. 3-1). Effect of changes in the dimensions B , d and L of the valley on the horizontal surface seismic motions as well as on the validity of the engineering models (1-D, 2-D and frame) will be examined.

The examples provided in this chapter are for soil types (NC) and (DS), which are representative of a soft profile and a stiff profile, respectively. The horizontal input rock motion applied to soil profiles (NC) and (DS) are the generated accelerations with very low a/v ratio and intermediate a/v ratio, respectively. The input rock motions are so selected to have their dominant periods in the proximity of the fundamental periods of (NC) and (DS) valleys. They are scaled to peak velocity $v = 0.2$ m/s. The soil surface response is calculated using the frame model and compared with that from the 2-D and 1-D models. Response results are presented in the form of acceleration spectral ratios at sites in the middle and near the edge of the valley to reflect the soil amplification of rock motion at different locations.

The variation in the fundamental period of the valley is given in tables 5-1 and 5-2 for soil profiles (NC) and (DS), respectively, for several valley dimensions. The case of $B = \infty$ corresponds to the resulting fundamental periods when the limited valley breadth is ignored in the 1-D analysis. It is evident from the tables that the fundamental periods are more sensitive to the change in the depth d than to the variation in B or L.

5.2 EFFECT OF THE CHANGE IN DEPTH

The site-amplification curves for various depth values are plotted in figures 5-1, 5-2, 5-3 and 5-4. The figures show that increasing the depth d leads to higher local-amplification periods of sites because of the decrease in the overall stiffness. In general, the variation in depth leads to significant shifts in the fundamental period of the valley and little changes in the magnitude of amplification peak at the valley centre. This is particularly demonstrated in the case of wide valleys, as shown in Fig. 5-4.

Due to its lack of stiffness, soil type (NC) is more sensitive than (DS) to changes in the shear modulus values. (NC) sites with larger depths produce higher shear strains in the top layers which increase their softness. This results in larger top-layer amplification of the higher modes for larger depths, which is evident in the short-period range in figures 5-1 and 5-2 at all surface points. On the other hand, being of stiff profile, (DS) sites are associated with low shear strains during excitation and consequently damping values, especially in the top layers, are smaller than those associated with (NC). This results in (DS) being more vulnerable to changes in the damping, particularly in the top layers. (DS) sites with smaller depths produce lower shear strains in the top layers which in turn lead to lower damping values. Hence, smaller depths result in larger top-layer amplification of the higher modes. This is illustrated in Fig. 5-3 and Fig. 5-4 (c) in the short-period range.

The increase in the depth d leads to a larger sloping rock area. This causes the effect of the sloping rock boundary to extend further towards the valley centre. Hence, larger depths result in higher amplification peaks at or near the middle of the valley, as shown in figures 5-1 (c), 5-2 (d) and 5-3 (d), due to more focusing of the incoming waves from the sloping rock boundary toward the valley centre. This also explains the amplification peaks being higher near the centre than at sites near the edge of the valley, as shown in Fig. 5-5 for $d = 40$ m and Fig. 5-6 for $d = 100$ m. There are more variations in the amplification values in the case of the larger depth $d = 100$ m in Fig. 5-6 than those in the case when $d = 40$ m in Fig. 5-5. For example, in the case of $d = 40$ m in Fig. 5-5 (d), the amplification peaks increase from one surface point to another until point c is reached, from the left edge, where the highest effect of the wave focusing is obtained. The amplification is hardly altered beyond point c until point e, at the centre of the valley, is reached. When $d = 100$m in Fig. 5-6 (d) the largest effect of the wave focusing from the sloping rock boundary is shifted, further from the edge, to point d. Beyond point d the amplification peaks decrease slightly as the centre of the valley is approached. It is further observed from figures 5-5 and 5-6 that the periods associated with the local-amplification peaks differ from one site (surface point) to another, depending on the relative location in the valley. The local-amplification period at the middle surface point of the valley is the longest and thus occurs at the fundamental period of the valley. As the selected site approaches the edge of the valley, the local-amplification period becomes shorter due to the stiffening effect from the sloping rock boundary. This amplifies the higher modes at the edge sites more than the fundamental mode.

5.3 EFFECT OF THE CHANGE IN ROCK BOUNDARY SLOPE

It is observed from tables 5-1 and 5-2 that the fundamental periods of wide valleys ($B \geq 300$ m) are not affected by the change in the length L while B and d are fixed. For narrower valleys, where B/d is small, increasing the length L adds to the stiffness of the valley which results in a decrease in the fundamental period.

The effect of the wave focusing from the sloping rock boundary increases towards the valley centre as the length L increases for the same B and d. This results in slightly higher amplification near the middle of the valley for larger L, as shown in figures 5-7 (d) and 5-8 (d). For wider valleys, where the ratio L/B is small, the amplification ratios at surface points located away from the sloping rock area are not affected by the change in the length L.

Increasing the length L leads to a decrease in the depth under the edge surface points which adds to the stiffness of the soil in the area underlying these points. This stiffening effect causes shorter local-amplification periods at the edge surface points for larger L, as shown in Fig. 5-7 (b), (c) for (NC) and Fig. 5-8 (b), (c) for (DS). Furthermore, the decrease in depth under edge points due to the increase of L results in lower top-layer amplification of the higher modes in the case of (NC), as shown in Fig. 5-7 (b), (c). On the other hand, larger top-layer amplification of the higher modes is associated with larger L in the case of (DS), as shown in Fig. 5-8 (b), (c). The reason for this behaviour is as discussed before in section 5.2.

5.4 EFFECT OF THE CHANGE IN BREADTH

By examining the variation in the fundamental periods of the valleys in tables 5-1 and 5-2, it is noticed that the fundamental period is not altered by the change of B for the same d and L. When B = 100 m the stiffening effect of the sloping rock becomes substantial and results in a decrease in the fundamental period of the valley. As the valley approaches the triangular shape by decreasing B for the same L and d, amplification peaks near the middle of the valley become higher, as shown in Fig. 5-9. This is because of the increase of the wave focusing effect toward the valley centre.

Increasing B from 300 to 1000 m does not affect the amplification at the edge surface points a and b, as shown in Fig. 5-10. This means that the amplification at the edge sites is mainly affected by the incoming waves from the surrounding area (the sloping rock boundary). In other words, for relatively wide valleys (B $\geq$ 300 m) the edge-site amplification is a function of the depth and the slope underneath and is independent of the breadth B.

5.5 VALIDITY OF THE ENGINEERING MODELS

It is believed that the 2-D finite-element model of the valley provides a reliable analytical approximation to the surface response, since the irregularities of the rock boundaries and soil properties are best simulated using this model. Hence, in order to judge the validity of other models, the resulting acceleration spectral ratios will be compared with those from the 2-D model.

It is observed that the 1-D model fails in approximating the soil amplification, particularly near the peaks, in narrow triangular valleys. This is true whether the triangular valleys are shallow as in Fig. 5-11 or deep as in Fig. 5-12. The 1-D model also provides a poor approximation to the response at surface points near the edge of the valley. This is illustrated in Fig. 5-13 for a wide and shallow valley and in Fig. 5-14 for a narrow and deep valley. These edge sites are the spots mostly affected by the sloping rock boundary which is disregarded by the one-dimensional analysis. For narrow and deep valleys (B/d < 10), the response approximation provided by the 1-D model is not good even at surface points right in the middle of the valley. Predictions of motions by the 1-D analysis are conservative near the edges of deep and narrow valleys, as shown in Fig. 5-14. On the other hand, the 1-D analysis underpredicts the response in the middle of the deep valley, particularly in the neighbourhood of the fundamental period, as evident from Fig. 5-15. This is because the effect of the wave focusing from the sloping rock boundary, which is not considered by the 1-D approach, extends toward the centre of the valley due to the large depth and tends to increase the 2-D amplification. The only sites where the 1-D analysis succeeds in approximating the response of the 2-D model are those located near or at the centre of wide and shallow valleys ($B/d \geq 10$), far from the focusing effect of the sloping rock boundary, as shown in Fig. 5-16.

Examination of figures 5-11 through 5-16 indicates that the frame model succeeds in providing reliable results when compared with the response from the 2-D model. This proves to be true for the symmetrical valleys under consideration, with rectangular, trapezoidal or even triangular shapes at surface points either in the middle or near the edge of the valley. The computing time required by the finite-element model for valleys of small width (e.g. $B = 100$ m) is twice that required by the frame model. For valleys with larger breadth (e.g. $B = 1000$ m), the finite-element model requires computing time which is 12 times that required by the frame model. The substantial increase in the ratio of computing time from 2 to 12 occurs because a much larger mesh of finite elements is required by the 2-D model for a larger breadth. When the frame model is used, changing the breadth requires only a change in the stiffness of the horizontal links without altering the dimensions of the model. This may only affect the number of modes with significant participation in the response.

5.6 SUMMARY

Influence of the valley dimensions on the horizontal seismic site response as well as on the validity of the engineering models was analyzed. The fundamental period of the valley and the local-amplification periods at different surface locations are more susceptible to the change in the underlying depth of soil than to the change in other dimensions of the valley (i.e. B and L). Increasing the depth leads to longer local-amplification periods of sites due to the decrease in the overall stiffness. The change in the length L alters the depth below the edge sites and consequently affects their local-amplification periods. For narrow valleys, the added stiffness due to the decrease in B or increase in L becomes noticeable and is reflected in a lower fundamental period of the valley. As the edge of the valley is approached, the local-amplification periods of sites become shorter due to the stiffening effect from the sloping rock boundary. This results in larger amplification of the higher modes at sites near the edge.

The top layers of smaller depths of soil profile (DS) are associated with lower damping values and thus produce larger amplification for the higher modes. On the other hand, softer top layers are associated with larger depths of soil profile (NC), which results in larger amplification for the higher modes.

As the valley approaches a triangular shape by decreasing B or increasing d or L, the magnitude of the amplification peaks near the middle of the valley increases due to more focusing of the incoming waves from the sloping rock boundary toward the valley centre. The focusing effect results in increasing the amplification peaks as the middle of the valley is approached from the edge until one site is reached where the highest effect of the wave focusing is obtained. The position of this site depends on the ratio L/B and the depth d. Beyond this site, as the centre of the valley is approached, amplification peaks may slightly decrease for a distance, as the focusing effect diminishes, after which they remain unaltered and the one-dimensional approach may apply. The spectral ratios at the edge surface locations in the valley are independent of the breadth B. They are rather a function of the underlying depth of soil and slope of rock, since they are mainly affected by the incoming waves from the surrounding area.

The surface locations where the 1-D model provides a poor approximation of the response are those where the effect of the sloping rock boundary is significant. These locations include edge sites in any valley and almost all sites in deep and narrow valleys where $B/d < 10$. For shallow and wide valleys with $B/d \geq 10$ and $B/L \geq 2$, the one-dimensional analysis may be used to obtain the surface response at sites located at least 10 times the depth d, away from the edge of the valley. This is where the wave focusing effect from the sloping rock boundary vanishes and the one-dimensional resonance dominates the response. The frame model, on the other hand, provides results which are in good agreement with those obtained using the 2-D model. This proved to be true for the valleys under consideration, regardless of the location of the surface point.

Table 5-1 Fundamental periods of the valley

Normally consolidated clay (NC), very low a/v, v = 0.2 m/s

d (meter)	L (meter)	T (sec)				
		B=100m	B=300m	B=500m	B=1000m	B = ∞
20	100	1.18	1.35	1.35	1.35	1.35
40	0	1.73	1.88	1.89	1.90	1.90
	100	1.45	1.87	1.89	1.90	1.90
	200	——	1.86	1.89	1.90	1.90
100	100	1.75	2.57	2.70	2.73	2.73

Table 5-2 Fundamental periods of the valley

Dense sand (DS), Intermediate a/v, v = 0.2 m/s

d (meter)	L (meter)	T (sec)				
		B=100m	B=300m	B=500m	B=1000m	B = ∞
20	100	0.29	0.37	0.37	0.37	0.37
40	0	0.52	0.67	0.68	0.69	0.69
	100	0.39	0.67	0.68	0.68	0.68
	200	——	0.66	0.68	0.69	0.69
100	100	0.51	1.08	1.24	1.28	1.28

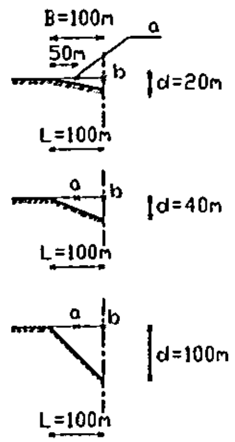

(a) Valley dimensions

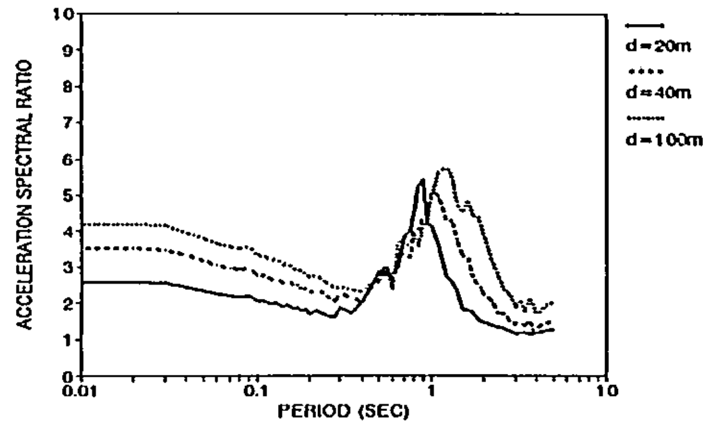

(b) Site a

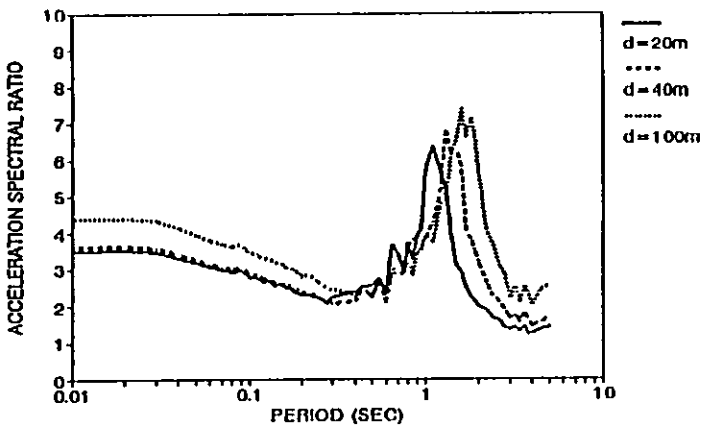

(c) Site b

Fig. 5-1 Effect of the change in depth
Soil profile : NC, a/v = V, v = 0.2 m/s

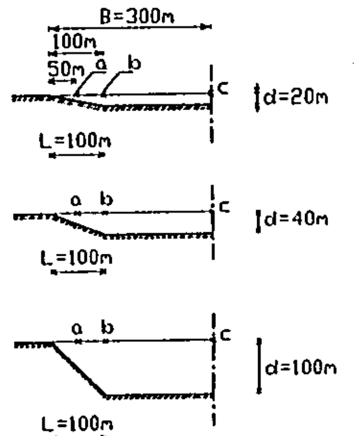

(a) Valley dimensions

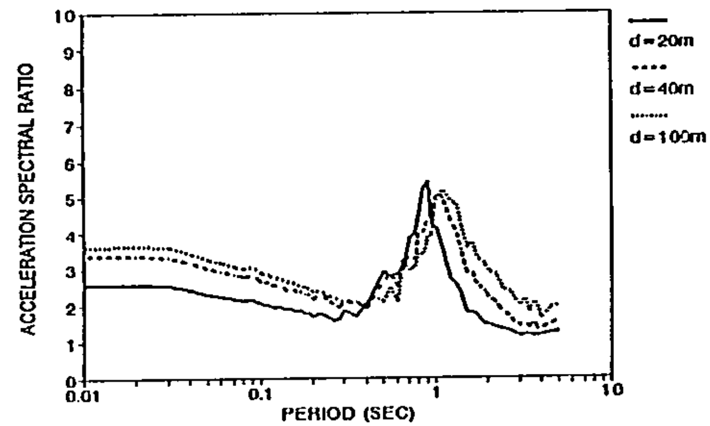

(b) Site a

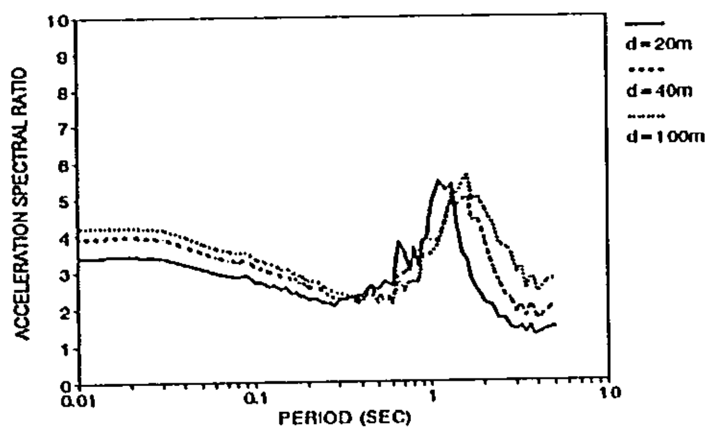

(c) Site b

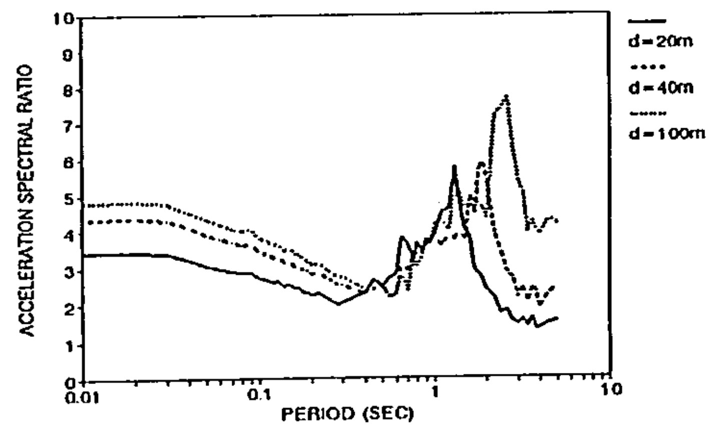

(d) Site c

Fig. 5-2 Effect of the change in depth
Soil profile : NC, a/v = V, v = 0.2 m/s

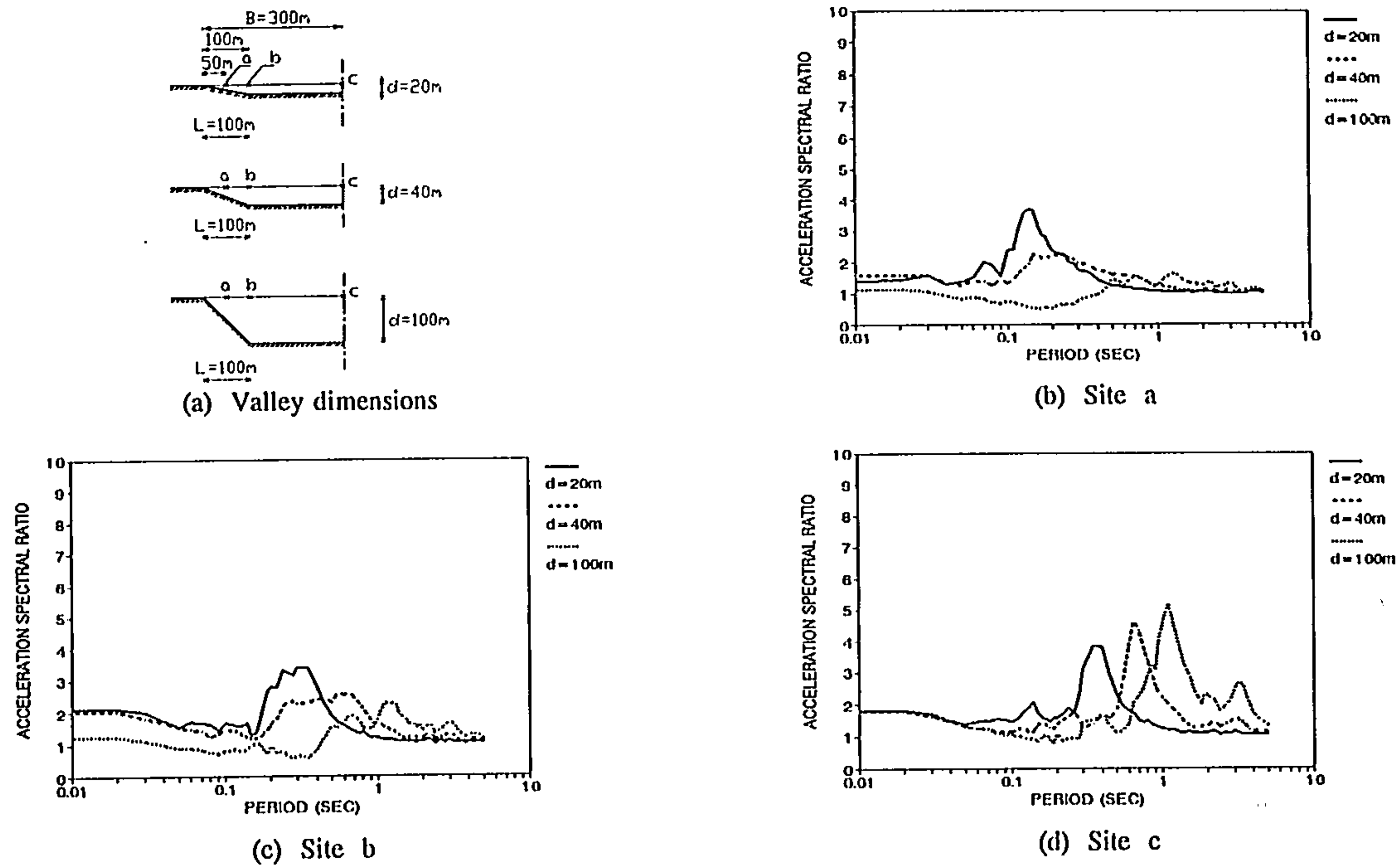

Fig. 5-3 Effect of the change in depth
Soil profile : DS, a/v = 1, v = 0.2 m/s

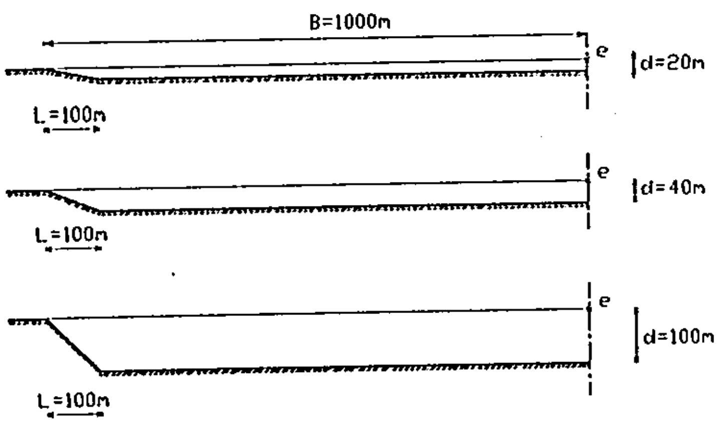

(a) Valley dimensions

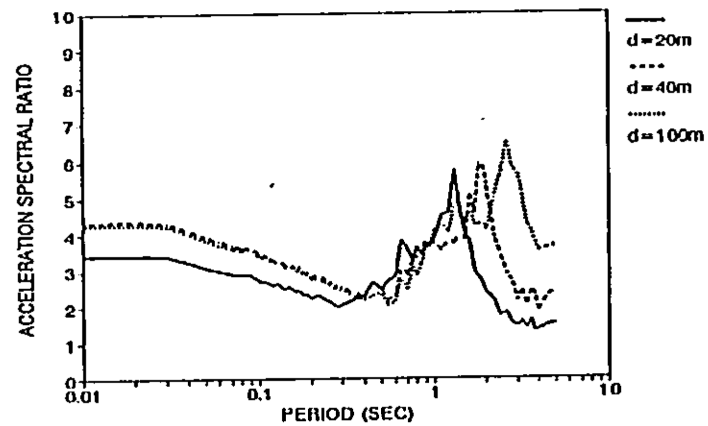

(b) Site e, profile (NC), a/v = V, v = 0.2 m/s

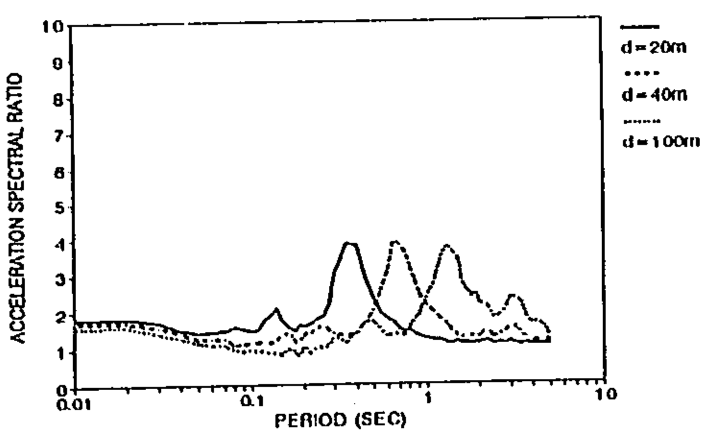

(c) Site e, profile (DS), a/v = I, v = 0.2 m/s

Fig. 5-4 Effect of the change in depth

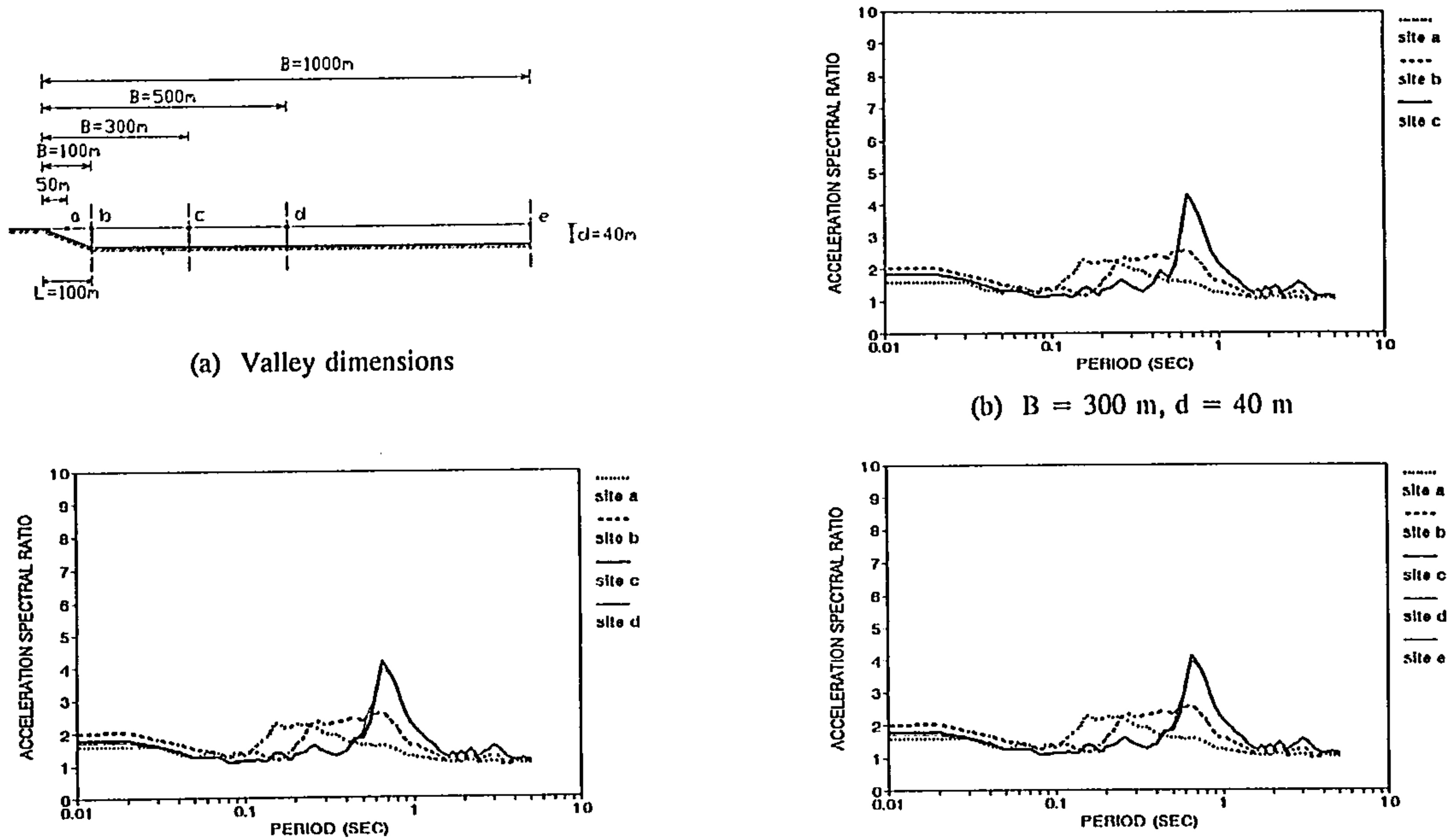

(a) Valley dimensions

(b) B = 300 m, d = 40 m

(c) B = 500 m, d = 40 m

(d) B = 1000 m, d = 40 m

Fig. 5-5 Variation of site amplification at different locations in the valley
Soil profile : DS, a/v = I, v = 0.2 m/s

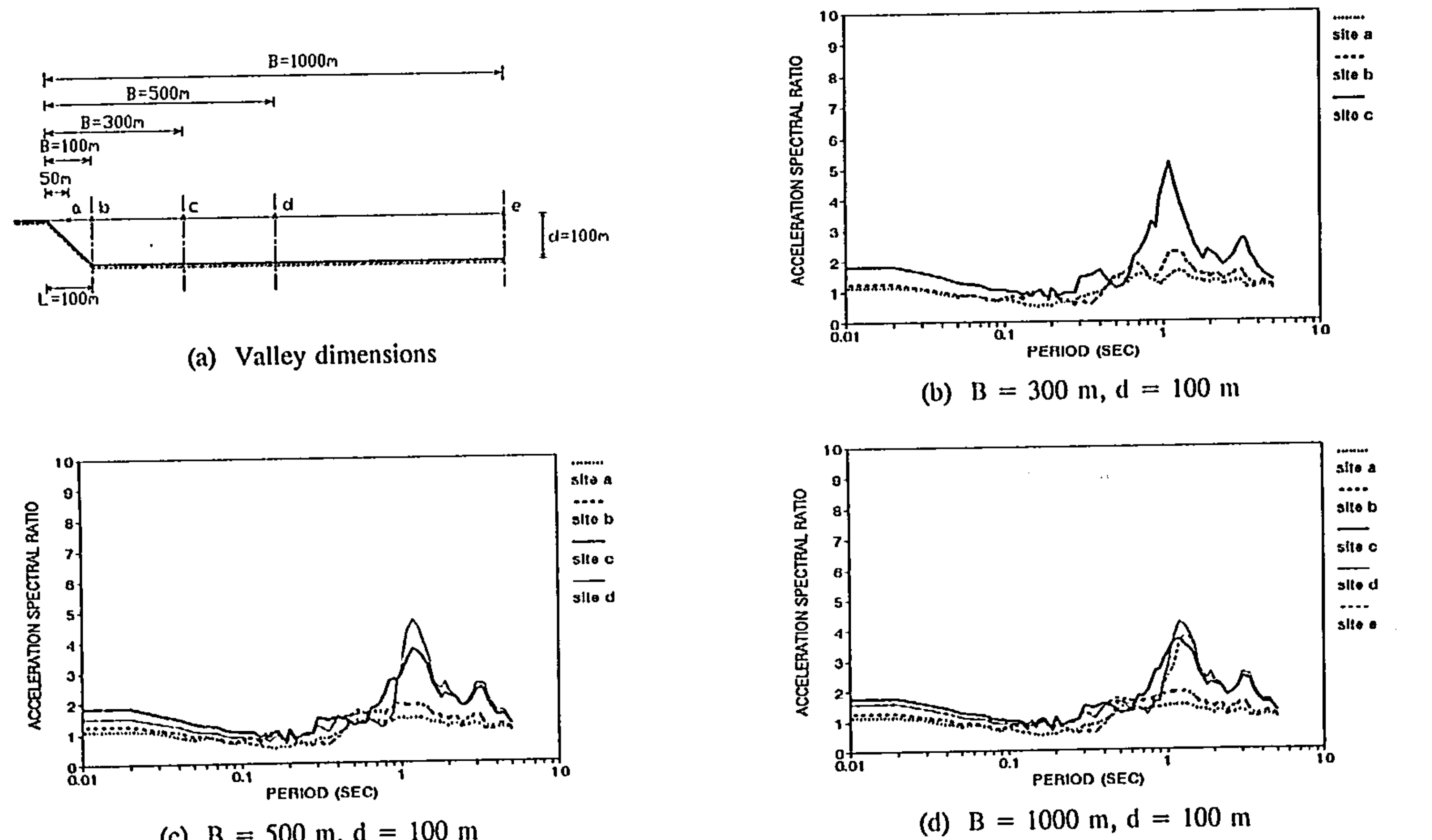

(a) Valley dimensions

(b) B = 300 m, d = 100 m

(c) B = 500 m, d = 100 m

(d) B = 1000 m, d = 100 m

Fig. 5-6 Variation of site amplification at different locations in the valley
Soil profile : DS, a/v = I, v = 0.2 m/s

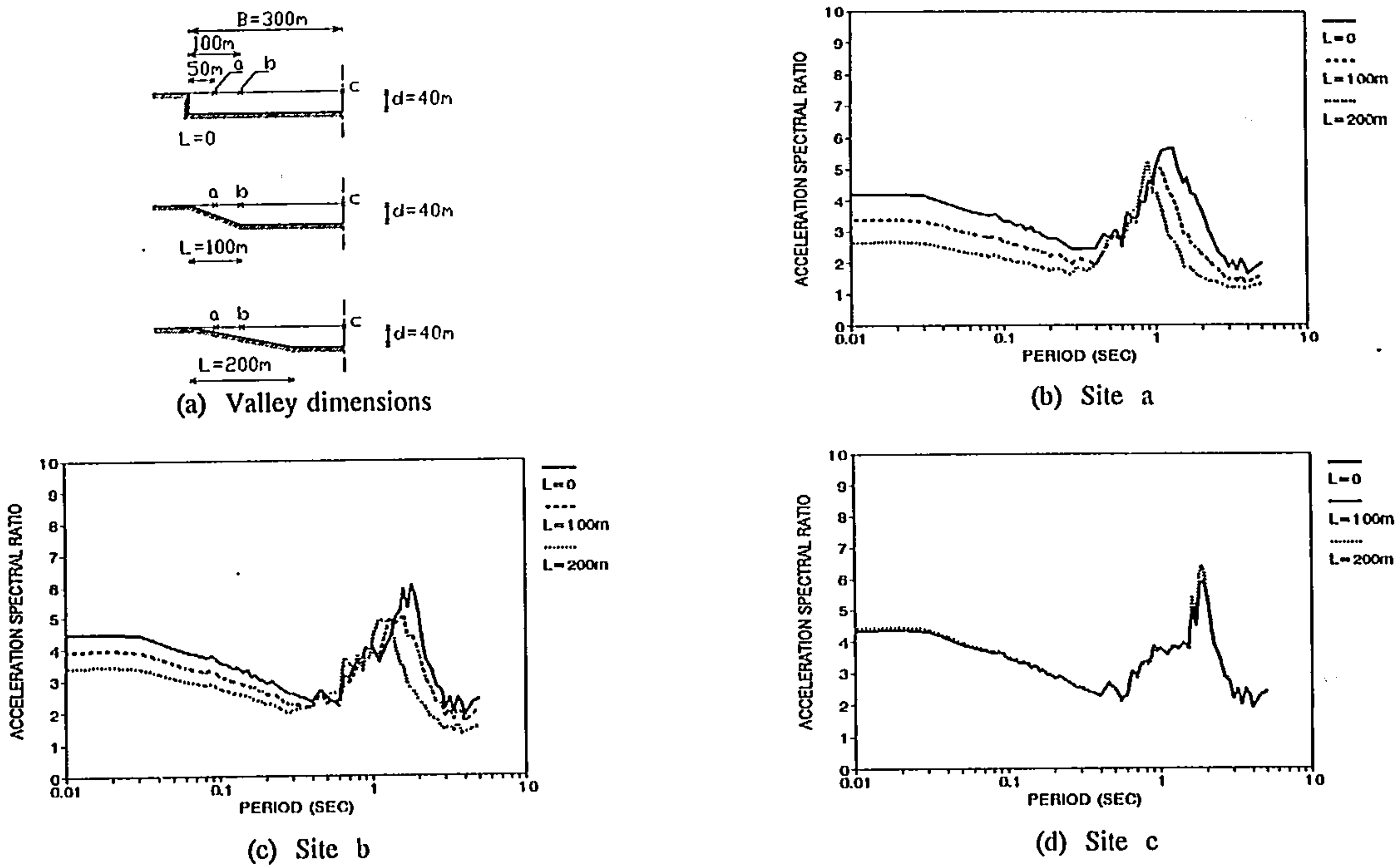

Fig. 5-7 Effect of the change in rock boundary slope
Soil profile : NC, a/v = V, v = 0.2 m/s

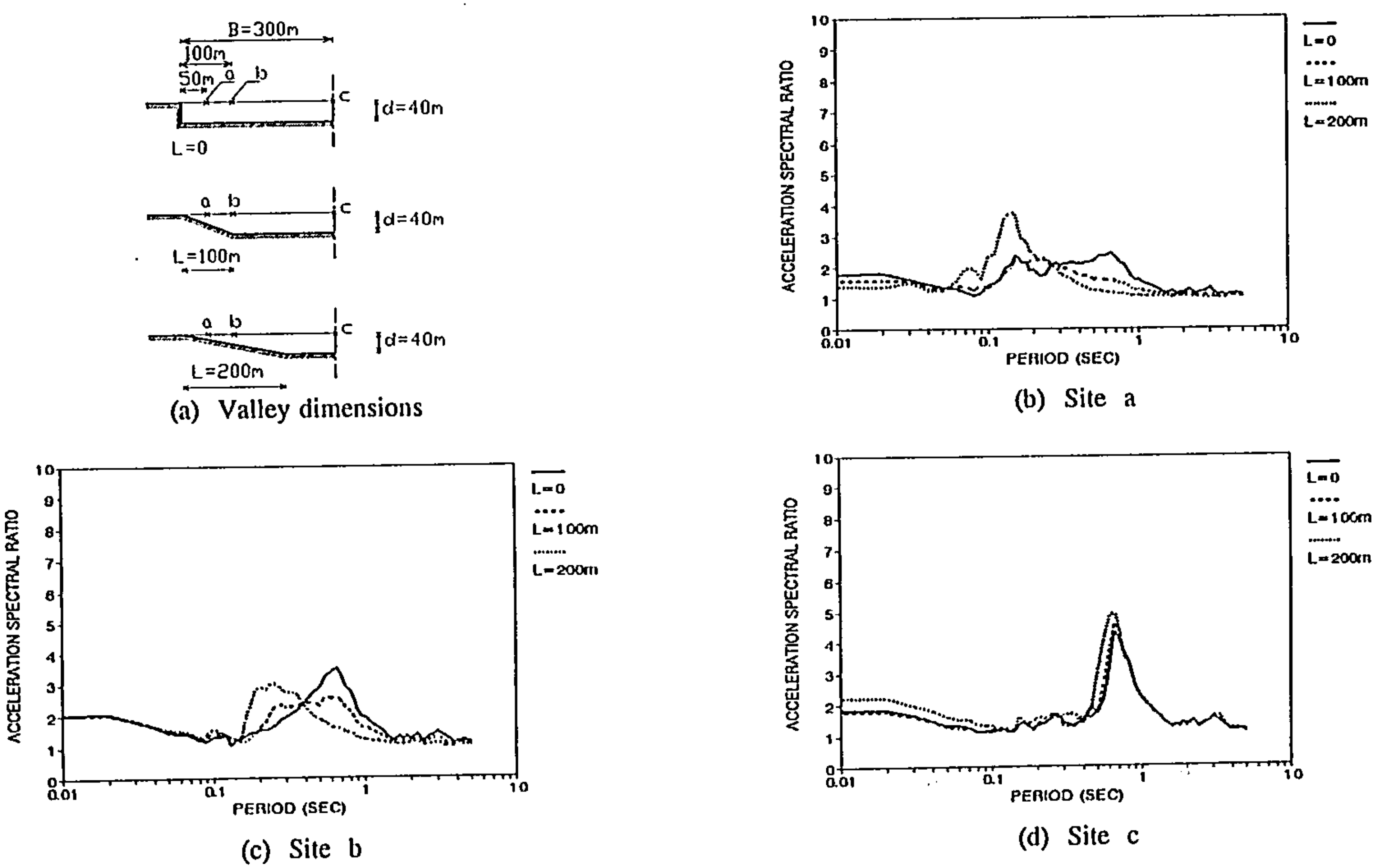

Fig. 5-8 Effect of the change in rock boundary slope
Soil profile : DS, a/v = I, v = 0.2 m/s

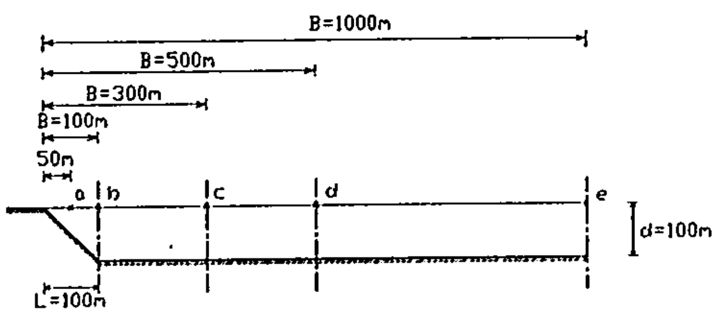

(a) Valley dimensions

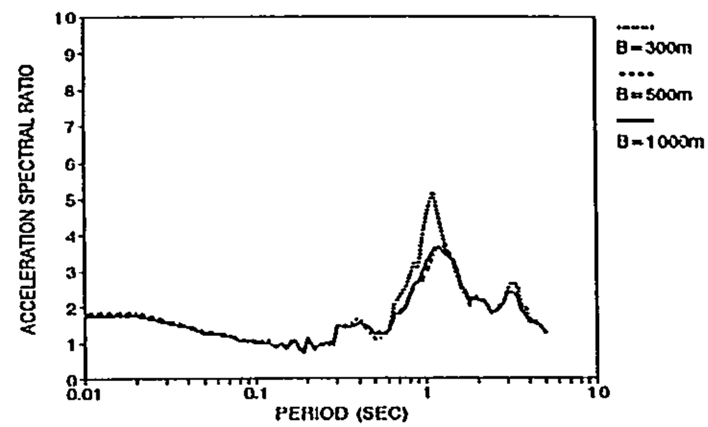

(b) Site c

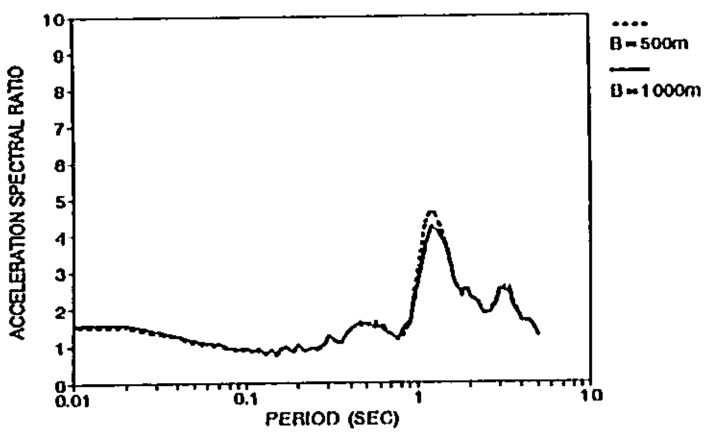

(c) Site d

Fig. 5-9 Effect of the change in breadth
Soil profile : DS, a/v = I, v = 0.2 m/s

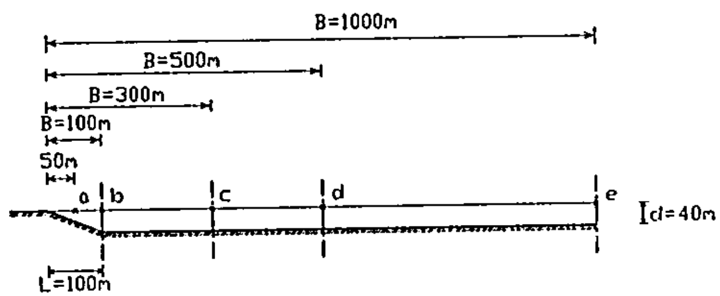

(a) Valley dimensions

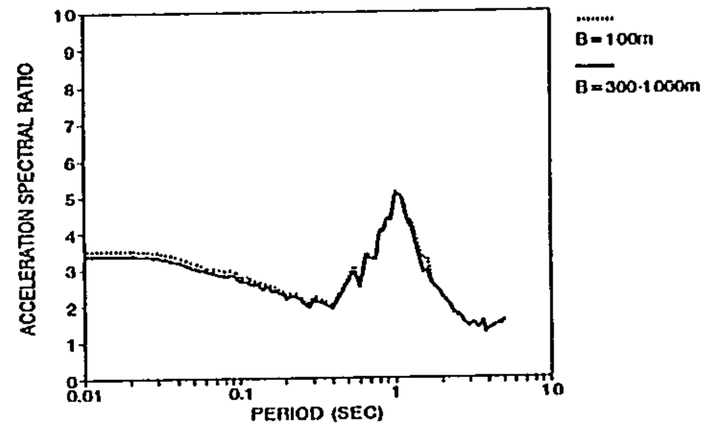

(b) Site a

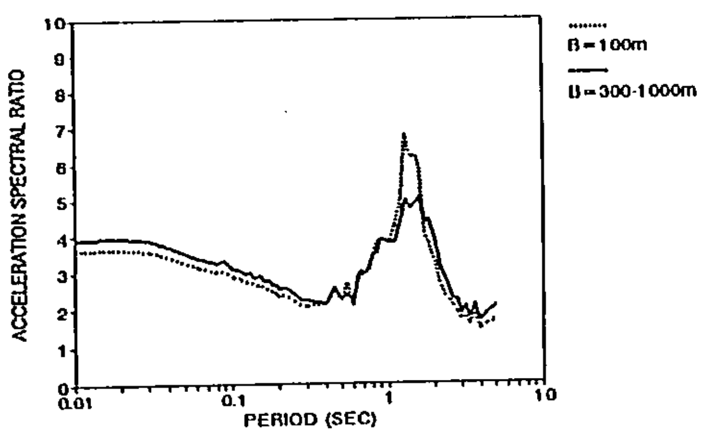

(c) Site b

Fig. 5-10 Effect of the change in breadth
Soil profile : NC, a/v = V, v = 0.2 m/s

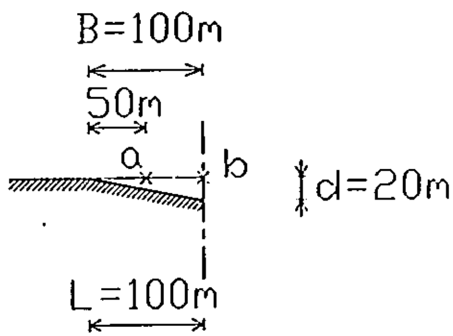

(a) Valley dimensions

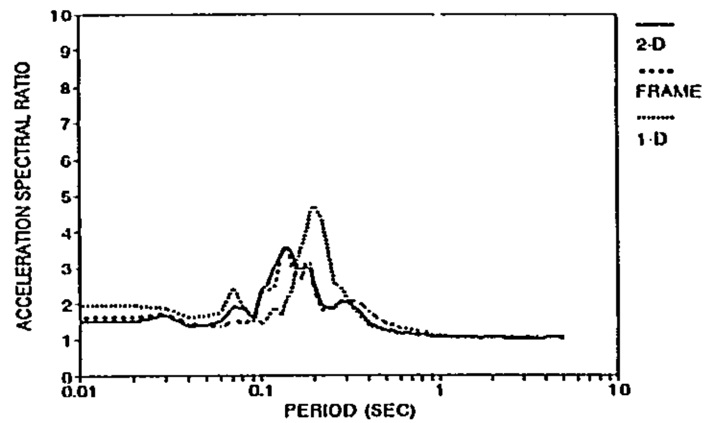

(b) Site a

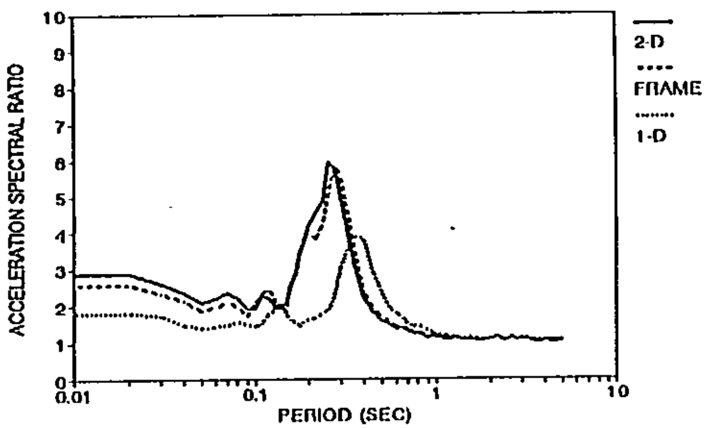

(c) Site b

Fig. 5-11 Validity of the engineering models in a triangular valley
Soil profile : DS, a/v = I, v = 0.2 m/s

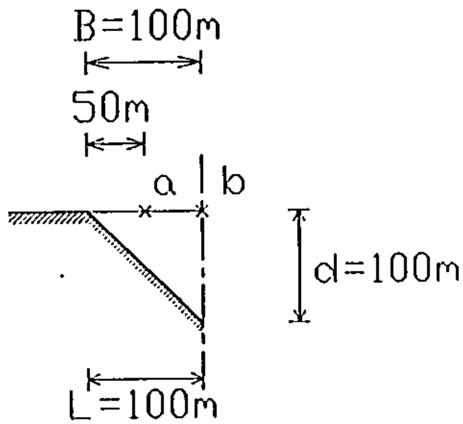

(a) Valley dimensions

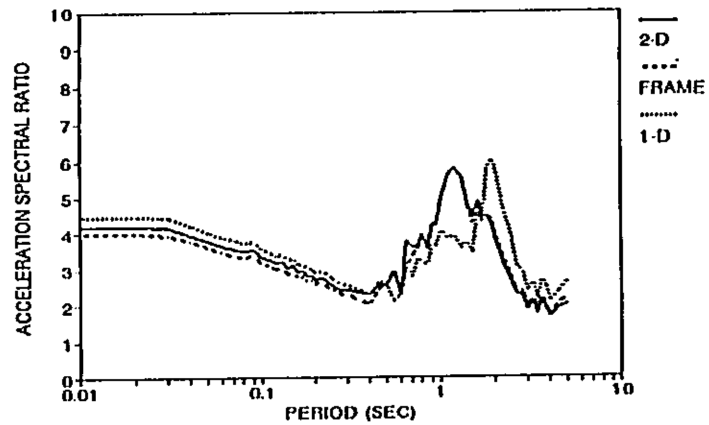

(b) Site a

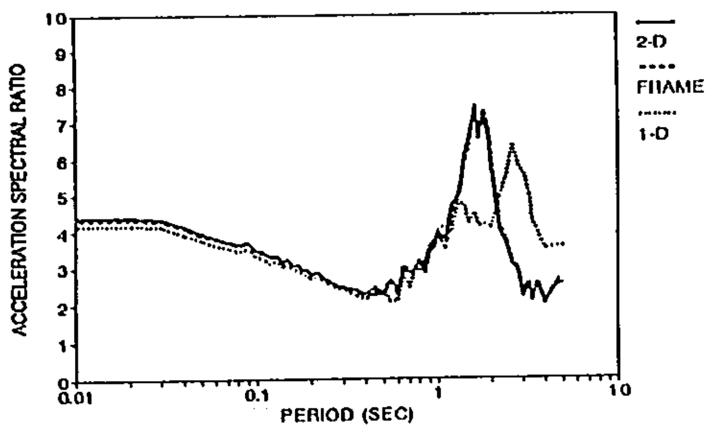

(c) Site b

Fig. 5-12 Validity of the engineering models in a triangular valley
Soil profile : NC, a/v = V, v = 0.2 m/s

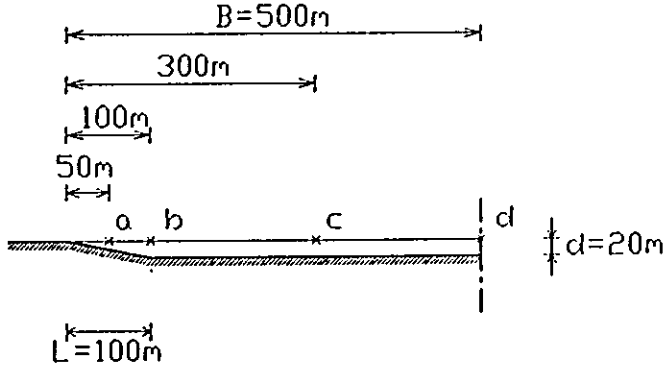

(a) Valley dimensions

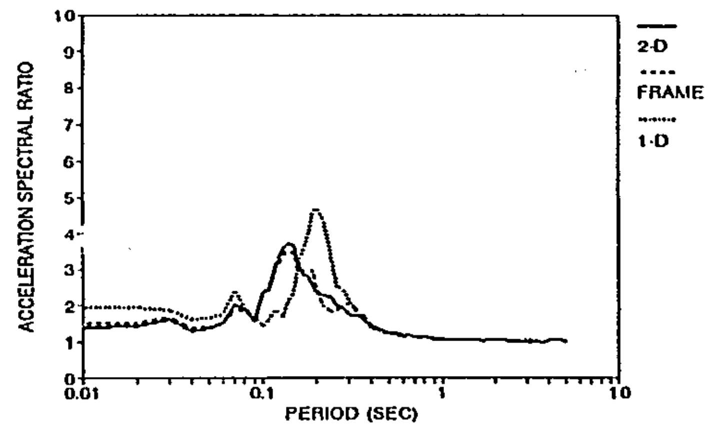

(b) Site a

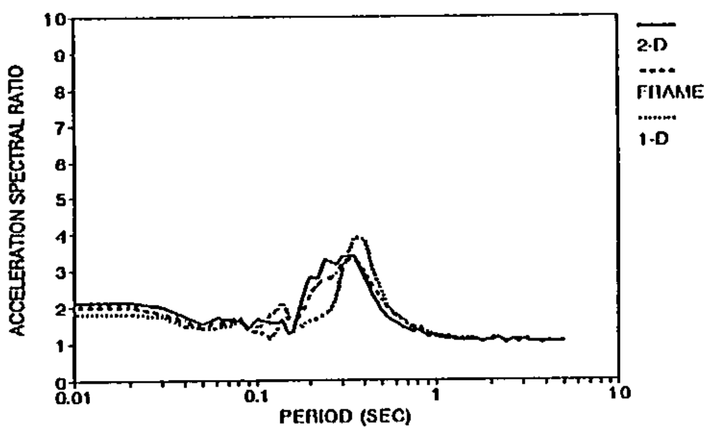

(c) Site b

Fig. 5-13 Validity of the engineering models at edge sites (B/d = 25)
Soil profile : DS, a/v = I, v = 0.2 m/s

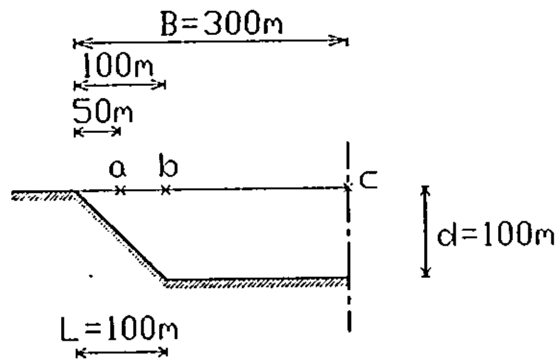

(a) Valley dimensions

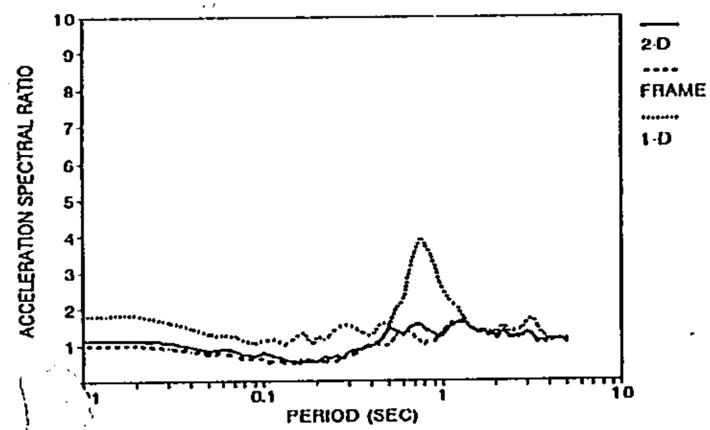

(b) Site a

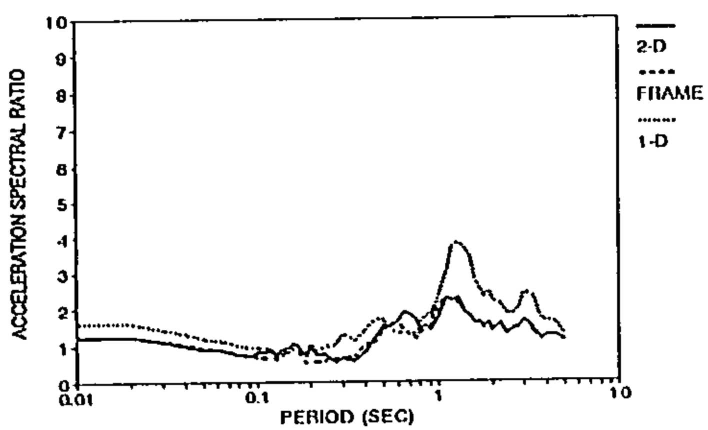

(c) Site b

Fig. 5-14 Validity of the engineering models at edge sites (B/d = 3)
Soil profile : DS, a/v = I, v = 0.2 m/s

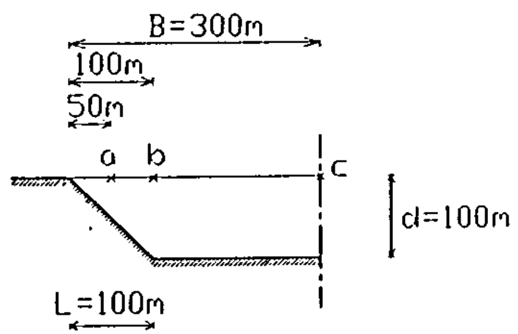

(a) Valley dimensions

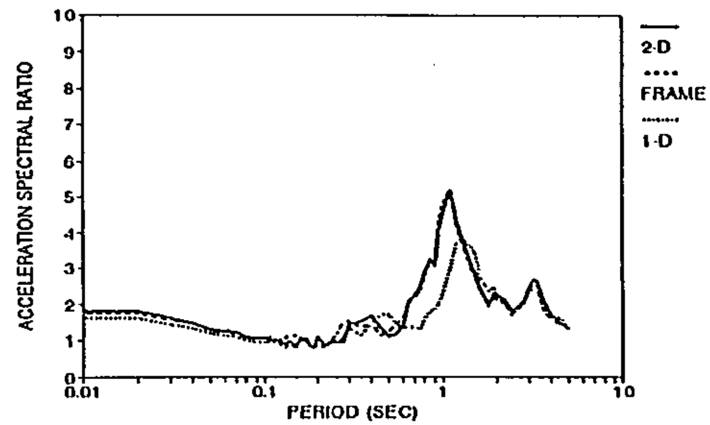

(b) Site c, B = 300 m, d = 100m

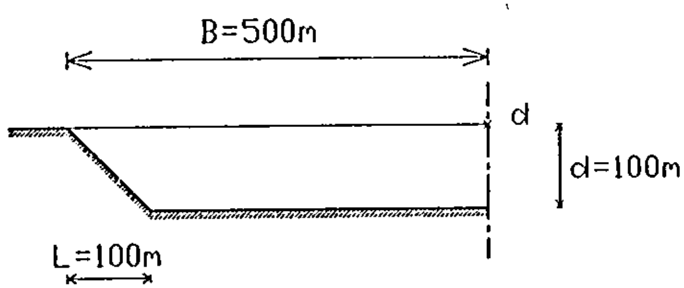

(c) Valley dimensions

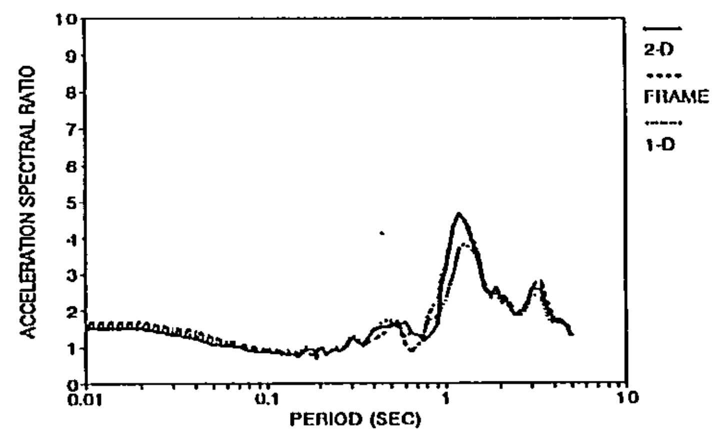

(d) Site d, B = 500 m, d = 100 m

Fig. 5-15 Validity of the engineering models at centre sites (B/d < 10)
Soil profile : DS, a/v = 1, v = 0.2 m/s

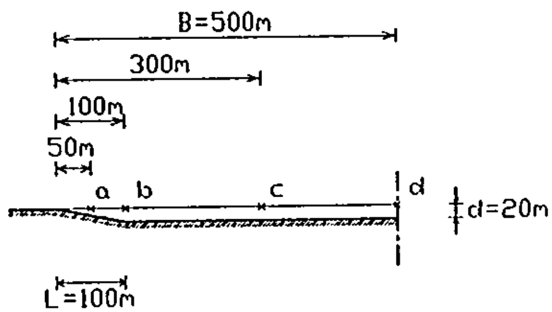

(a) Valley dimensions

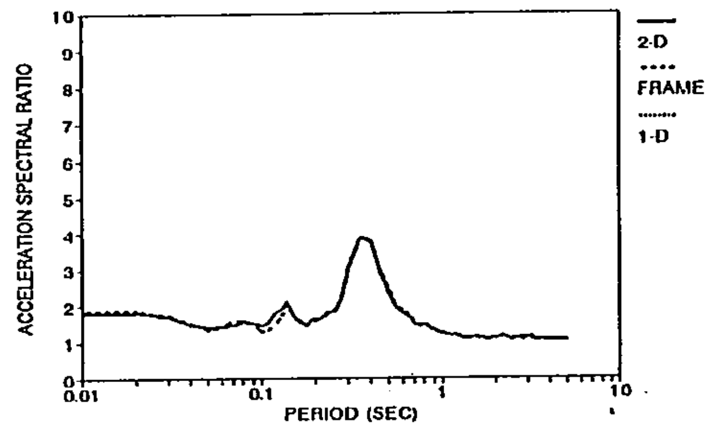

(b) Sites c and d, B = 500 m, d = 20 m

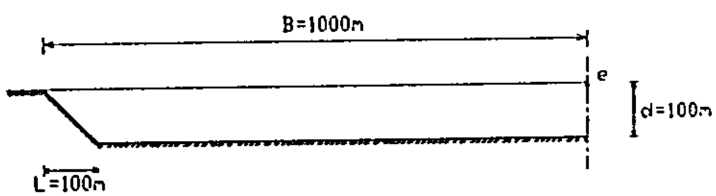

(c) Valley dimensions

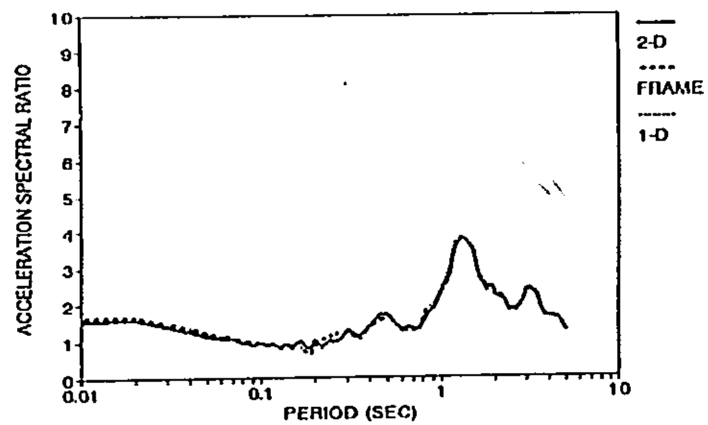

(d) Site e, B = 1000 m, d = 100m

Fig. 5-16 Validity of the engineering models at centre sites (B/d $\geq$ 10)
Soil profile : DS, a/v = I, v = 0.2 m/s

CHAPTER 6

INFLUENCE OF SOIL TYPE AND ROCK MOTION VARIATIONS ON THE SEISMIC SITE RESPONSE

6.1 INTRODUCTION

The horizontal seismic site response of the valley is analyzed for different soil types and rock motion variations. Four soil categories, with various stiffness variations along soil depth, are used in the analysis:

(a) Normally to lightly over-consolidated clay (NC)

(b) Heavily over-consolidated clay (OC)

(c) Alluvial sand and silt (AS)

(d) Dense sand (DS)

The mass-density values ρ and the G_o profiles for the above four soil types are shown in Fig. 3-2. Influence of input rock motion variations on the seismic response includes the effect of two characteristics of uniform rock motion, namely the frequency content and the peak amplitude of motion. In addition, it includes the effect of assuming non-uniform excitation along the rock boundary in wide valleys.

The three generated records, described in chapter 3, with high (H), intermediate (I) and very low (V) a/v ratios will be utilized as horizontal uniform motions in the rock to examine the effect of changing the frequency content on the seismic response. The peak amplitude of motion may be used as an indicator of the motion intensity level for the same frequency content and duration of motion. The peak amplitude of uniform rock motion is varied by scaling the record such that the peak velocity v is 0.05, 0.2 and 0.4 m/s. Peak accelerations and dominant periods of the uniform rock motions are given in table 6-1 for different a/v ratios and peak velocity values. A trapezoidal valley is selected for the analysis . The seismic site response for the above soil types under uniform conditions of rock motion is evaluated. The valley dimensions are taken to be: B = 300 m, d = 40 m and L = 100 m, as shown in Fig. 6-1 (a). Sites a, b and c are located at distances 50, 100 and 300 m from the left edge of the valley. The horizontal surface motions at these sites are obtained using the frame model. The seismic response is presented in the form of surface spectral accelerations and spectral ratios, calculated at a critical damping ratio of 2%. The spectral acceleration is a measure of the intensity of surface motion while the spectral ratio defines the soil amplification of rock motion. The period at which the largest peak of spectral acceleration occurs is the dominant period of the resulting surface motion. The dominant period at a site depends on both the dominant period of the input rock motion and the local-amplification period at that site. The local-amplification periods at sites a, b and c for various soil profiles are provided in table 6-2 under different a/v ratios and peak velocity values of uniform rock motion.

The non-uniform rock motion will be approximated as a single acceleration time history travelling along the rock boundary with different speeds. Two wide valleys are selected to study the effects of non-uniform control motion in the rock on the valley response. The surface motions are obtained by modifying and using program SAP IV to perform a multiple-support time-history analysis on the valley.

6.2 EFFECT OF SOIL TYPE UNDER UNIFORM ROCK MOTION

The soil profiles in an increasing order of stiffness are (NC), (AS), (OC) and (DS), as evident from Fig. 3-2. Table 6-2 shows that the stiffer the soil profile is, the shorter the local-amplification periods at sites become. In general, the magnitudes of the amplification peaks associated with soil profile (NC) are higher than those resulting from other soil types. This is illustrated in Fig. 6-1 for the case of high a/v rock motion and in Fig. 6-2 under the very low a/v rock motion, where v = 0.2 m/s. This behaviour is mainly because (NC) has the softest profile. The stiffest soil profile (DS) is usually associated with the lowest damping values, as discussed before in section 5.2. This causes the amplification peaks at (DS) sites to be slightly higher than those at (AS) sites, as shown in figures 6-1 and 6-2. The magnitude of the amplification peak from (DS) is even higher than that from (NC) at site c in the case of the very low a/v rock motion, as shown in Fig. 6-2 (d). The reason is that the local-amplification period at that site in the case of (DS) is far from the dominant period of the very low a/v rock record. This means lower intensity of motion in (DS) and consequently lower damping and higher amplification. The soil amplification of rock motion thus depends on the stiffness of soil and the amount of damping existing during excitation.

The intensity of surface motion for different soil profiles is illustrated in Fig. 6-3 under the rock motion with high a/v and in Fig. 6-4 under the rock motion with very low a/v. It is observed that the proximity of the local-amplification period at a site to the dominant period of the input rock record increases the resulting surface motion intensity. This accounts for the higher peaks of spectral accelerations in the case of stiffer soils (e.g. DS and OC) when a/v of the input record is high, as shown in Fig. 6-3. On the other hand, the softer profiles (e.g. NC) develop higher peaks of spectral accelerations for the very low a/v input record, as shown in Fig. 6-4.

6.3 EFFECT OF UNIFORM ROCK MOTION CHARACTERISTICS

6.3.1 Effect of Frequency Content

The three generated records with a/v = H, I and V, as defined in chapter 3, are scaled such that the peak ground velocity v = 0.2 m/s. They are used as input rock motions to examine the influence of the variation in frequency content on the seismic site response. The effect of different a/v ratios of the input record on the surface spectral accelerations is illustrated in Fig. 6-5 for soil profile (NC) and in Fig. 6-6 for soil profile (DS). The lowest intensity of surface motion at the three sites a, b and c occurs when a/v = H in the case of the soft profile (NC). For the stiff profile (DS), the lowest intensity of surface motion occurs when a/v = V. This takes place whenever the dominant period of the input motion is far from the local-amplification period at the site.

The acceleration spectral ratios are plotted in figures 6-7 and 6-8 for soil profiles (NC) and (DS), respectively, when using the three a/v ratios of ground motion as input records. It is observed that the variation in the a/v ratio has the least influence among other parameters on the local-amplification periods at sites. This observation is also emphasized in table 6-2. However, the small variations that may occur in the local-amplification periods are attributed to the change in intensity of motion in the soil, when the frequency content of input record varies. In the case of (DS) under very low a/v input record the low intensity of motion in the soil is associated with low damping values. This leads to higher amplification at (DS) sites under a/v = V, when compared with results under other a/v ratios, as shown in Fig. 6-8. In addition, the soil stiffness increases with the decrease of soil motion intensity causing slightly lower local-amplification periods, as illustrated for (DS) sites under a/v = V in Fig. 6-8. There is a substantial amplification at very low periods, which is particularly evident under the input record with very low a/v, as shown in figures 6-7 and 6-8. This is mainly because of the top-layer amplification of the soil deposit higher modes.

The effect of site location under various a/v ratios on the spectral response is demonstrated in Fig. 6-9 for soil profile (NC) and Fig. 6-10 for soil profile (DS). The surface spectral accelerations are shown in parts (a) and (c) of each figure, while parts (b) and (d) show the resulting spectral ratios under high and very low a/v input records, respectively. The input records in the rock are scaled to peak velocity v = 0.2 m/s. Parts (a) and (c) of Fig. 6-9 show that the magnitudes of spectral acceleration peaks at the three sites a, b and c do not differ substantially for soil profile (NC) under the same a/v ratio, although the dominant periods may vary. Parts (b) and (d) of Fig. 6-9 show that the magnitudes of amplification peaks and the periods at which they occur differ from one site to another, as discussed before in section 5.2.

Parts (a) and (c) of Fig. 6-10 show two contrasting patterns of behaviour for (DS) sites under rock motions with two different a/v ratios. In Fig. 6-10 (a) the magnitudes of spectral acceleration peaks increase from site c in the middle of the valley to site a near the edge, under high a/v ratio. In Fig. 6-10 (c) the magnitudes of spectral acceleration peaks decrease as the selected site approaches the edge of the valley, under very low a/v ratio. The reason for the contrasting behaviour is that the stiffening effect from the sloping rock boundary increases as the edge of the valley is approached. This causes the local-amplification periods of edge sites to become closer to the dominant period of the high a/v input record which leads to higher intensity of surface motion at site a than that at site c in Fig. 6-10 (a). In the case of very low a/v input record, the local-amplification period at site c is closer to the dominant period of the input record, which causes higher intensity of motion at site c than that at site a, as shown in Fig. 6-10 (c). However, the magnitudes of amplification peaks in both cases (a/v = H and a/v = V) become higher and the periods at which they occur get longer as the middle of the valley is approached, as shown in parts (b) and (d) of Fig. 6-10. The reason for this common behaviour is as discussed before in section 5.2.

6.3.2 Effect of Motion Peak Amplitude

The effect of the peak amplitude of rock motion on the soil amplification values is studied by scaling the generated record with a/v = I to three levels of peak velocity:

v = 0.05, 0.2 and 0.4 m/s. As the peak velocity, v, of the input record increases, the intensity of motion in soil becomes higher for the same duration and frequency content of input record. This develops higher shear strains in the soil and leads to higher surface spectral accelerations, as shown in Fig. 6-11. The higher shear strains are associated with higher damping values and more softening in the soil. Consequently, increasing the intensity of motion leads to lower amplification due to the higher damping and causes longer local-amplification periods at the sites due to the smaller stiffness. This is illustrated in Fig. 6-12 for soil profile (NC) and Fig. 6-13 for soil profile (DS). A similar behaviour is observed in the case of input rock records with high and very low a/v, when the peak velocity changes.

6.4 SEISMIC SITE RESPONSE UNDER NON-UNIFORM ROCK MOTION

It has been assumed in the above analyses in sections 6.2 and 6.3 that the input excitation along the rock boundary is uniform. However, this may not be accurate in valleys with large horizontal dimensions where a differential motion may occur along the rock boundary. The input excitation may vary from one point to another due to time shift, change in amplitude and/or change in frequency content. The problem of deriving the differential motion of adjacent points along the rock boundary from a single earthquake time history, recorded at one point, is a very difficult one. This is mainly because very little is known about the extent of spatial correlation of the ground motion. Consequently, the only parameter considered in this analysis will be the time shift. That is, the rock motion will be approximated as travelling waves of constant shape, with no variation in amplitude or frequency. The time shift between two input motions at two points is a function of the separation distance between them and the wave propagation velocity. The travelling wave assumption, presented by Newmark and Rosenblueth (1971), is a very convenient one, since it substitutes the known temporal variations of the rock motion for the unknown spatial variations. This will make a single acceleration time history sufficient to describe the differential motion by using various speeds of propagation along the rock boundary. This assumption requires an estimate of the horizontal propagation velocity of the waves which is believed to be in the order of the shear wave velocity of the rock.

Since the input rock motion differs from one point to another, program SAP IV, by Bathe et al (1973), is modified to perform a 2-D multiple-support excitation analysis of the valley. The input data to the modified SAP IV program is provided in appendix I. Program SAP IV requires that soil properties be linear throughout the analysis. Soil properties will be thus selected as those properties which result under uniform rock motion conditions and are obtained from the last linear iteration in program FLUSH, by Lysmer et al (1975) . Consequently, soil properties will correspond to the case of infinite speed of propagation in rock and will be the same for all travelling speeds.

Two valleys are selected with large breadths, B = 500 m and B = 1000 m, as shown in figures 6-14 (a) and 6-15 (a), respectively. Both valleys have the same d = 40 m and L = 200 m. The generated acceleration with intermediate a/v ratio is scaled to v = 0.2 m/s and applied to the rock boundary, as a wave travelling from left to right with different speeds of propagation. Propagation speeds are chosen as 500, 1000 m/s and infinity. The infinite speed corresponds to the uniform rock motion case.

The effect of variation in travelling wave speed on the surface spectral accelerations at different locations in the valleys is illustrated in figures 6-14 and 6-15 for the (DS) profile. As shown in the two figures, lower speeds of propagation are associated with lower spectral accelerations. This is mainly because input motions at different points along the rock boundary are less likely to have coinciding peaks when the speed of propagation decreases, which will reduce the intensity of surface motion. The surface motion intensity at sites near the edge (e.g. site a) is less sensitive to the variation in speed of propagation than that at sites near the middle of the valley. This occurs since most of the motion at these edge locations arises from the small surrounding area of rock and thus is less affected by variation of speeds. Figures 6-14 and 6-15 also show that the dominant periods of the surface motions are slightly affected by the variation in travelling wave speeds. By comparing Fig. 6-14 (d) and Fig. 6-15 (d), it is evident that the dominant period of the surface motion at the centre site in the broader valley is more affected by the change in speed of propagation than that at the centre of the smaller valley. This is because the differential rock motion works on a larger area in the broader valley.

6.5 SUMMARY

Influence of soil type and uniform rock motion characteristics on the horizontal seismic site response was evaluated for four soil types: (NC), (OC), (AS) and (DS). The uniform horizontal rock motions were the three generated accelerations with different frequency contents (a/v = H, I and V). Intensity of the uniform motion was varied by using three scales of peak velocity: v = 0.05, 0.2 and 0.4 m/s. Surface motions were obtained using the frame model.

Results from the model indicate that stiffer soil is associated with shorter local-amplification periods at various sites. The soil amplification of rock motion varies from one soil type to another, depending on two parameters: the stiffness of soil and the amount of damping existing during excitation. Soil profile (NC) provides the highest magnitudes of amplification peaks because it has the softest profile among other soil categories. Associated with lower damping values, soil profile (DS) produces higher peaks of amplification than does soil profile (AS).

The surface spectral acceleration is taken as a measure of the intensity of surface motion in the soil. The magnitudes of spectral acceleration peaks depend on the local-amplification period at the site and its proximity to the dominant period of the input rock record. The closer the two periods are, the more intense the soil surface motion is. Consequently, the lowest intensity of surface motion occurs in (NC) sites when $a/v = H$ and in (DS) sites when $a/v = V$. As the intensity of motion in soil increases, higher shear strains are developed leading to higher damping values and more softening of soil. The higher damping causes lower amplification of rock motion and the lower stiffness results in longer local-amplification periods at different sites.

The edge sites of valleys with stiff soil (e.g. DS) are more vulnerable to rock excitations with high a/v ratio because their local-amplification periods are close to the dominant period of the high a/v records. This leads to higher intensity of surface motions near the edge. On the other hand, for a stiff soil profile under a very low a/v input record, the intensity of surface motion is higher near the middle of the valley. This is because the local-amplification period near the middle is closer to the dominant period of the very low a/v record. There is considerable soil amplification at very low periods, particularly under the input record with very low a/v due to the top-layer amplification of the soil deposit higher modes.

Under the travelling wave assumption, the surface spectral accelerations are lower than those resulting from the case of uniform rock excitation. This is expected since speeds of propagation less than infinity make the input motions at different points along the rock boundary less likely to be in phase. The surface motions at sites in the middle of the valley are the most to be affected by the differential motion in rock. This is more pronounced in broader valleys where the effects of non-uniform rock motion should be considered if more accurate results are desired.

Table 6-1 Characteristics of uniform rock motions

a/v	peak acceleration "a" (g)			dominant period (sec)
	v = 0.05 m/s	v = 0.20 m/s	v = 0.40 m/s	
H	0.095	0.382	0.764	0.10 - 0.24
I	0.055	0.220	0.440	0.26 - 0.60
V	0.019	0.077	0.155	0.80 - 2.00

Table 6-2 Local-amplification periods at sites a, b and c

a/v	v m/s	local-amplification period at site (sec)											
		soil (NC)			soil (AS)			soil (OC)			soil (DS)		
		a	b	c	a	b	c	a	b	c	a	b	c
H	.05	.85	1.2	1.4	.45	1.2	1.2	.18	1.0	1.0	.17	.20	.50
	.20	1.4	1.5	1.8	.60	1.5	1.6	.26	1.2	1.2	.24	.55	.70
	.40	1.5	1.6	2.0	.80	1.6	1.9	.55	1.4	1.4	.30	.80	.80
I	.05	.80	1.1	1.5	.40	1.1	1.2	.22	.95	.95	.12	.20	.50
	.20	1.4	1.7	1.8	.65	1.7	1.7	.26	1.0	1.2	.16	.65	.65
	.40	1.7	1.9	2.2	1.0	1.8	1.9	.55	1.3	1.5	.24	.80	.80
V	.05	.70	1.0	1.4	.28	1.0	1.1	.19	.90	.90	.11	.17	.40
	.20	1.0	1.6	1.9	.70	1.6	1.6	.20	1.1	1.1	.17	.40	.45
	.40	1.6	1.9	2.2	.80	1.9	2.2	.26	1.1	1.3	.17	.45	.60

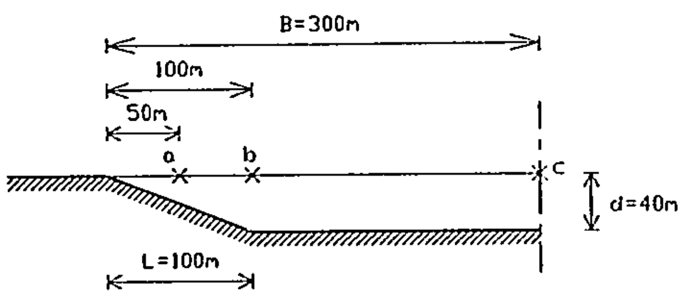

(a) Valley dimensions

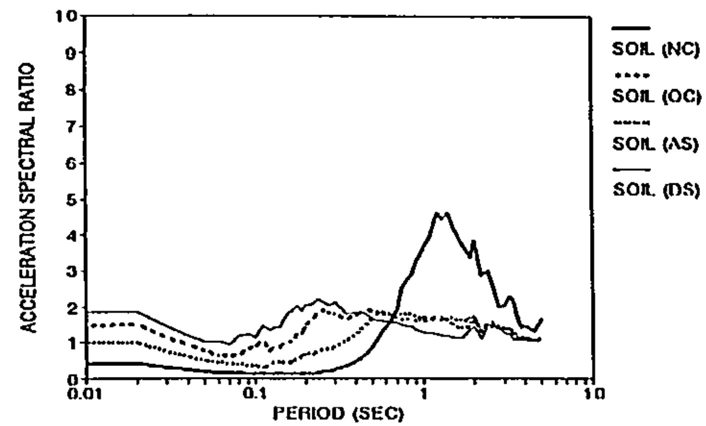

(b) Site a

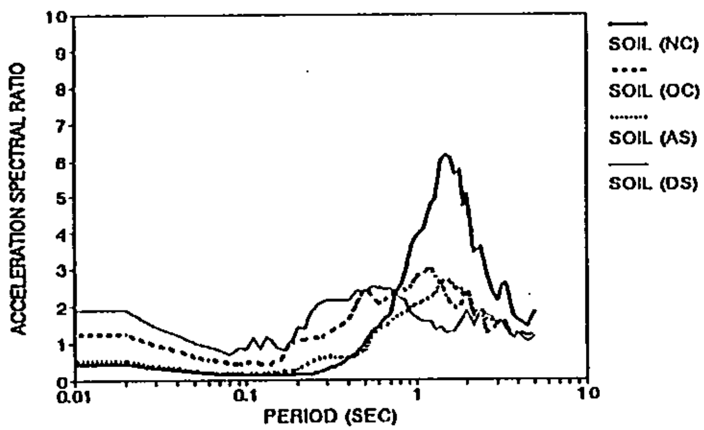

(c) Site b

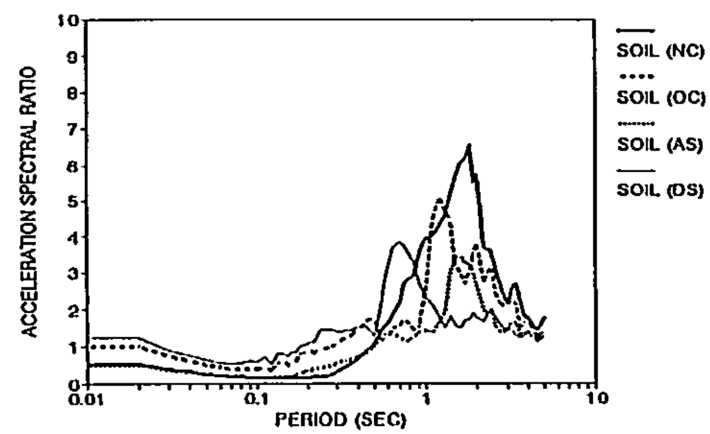

(d) Site c

Fig. 6-1 Effect of soil type on the spectral ratios
High a/v, v = 0.2 m/s

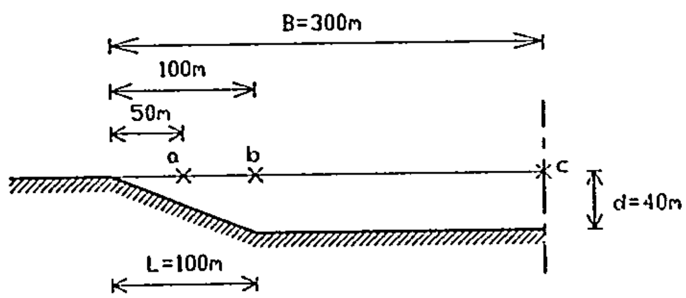

(a) Valley dimensions

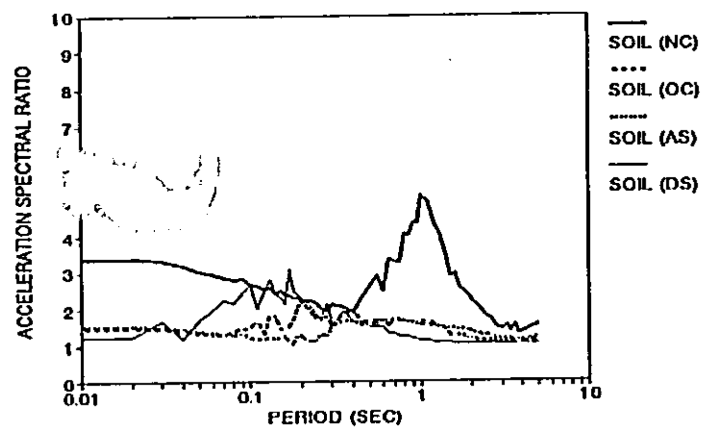

(b) Site a

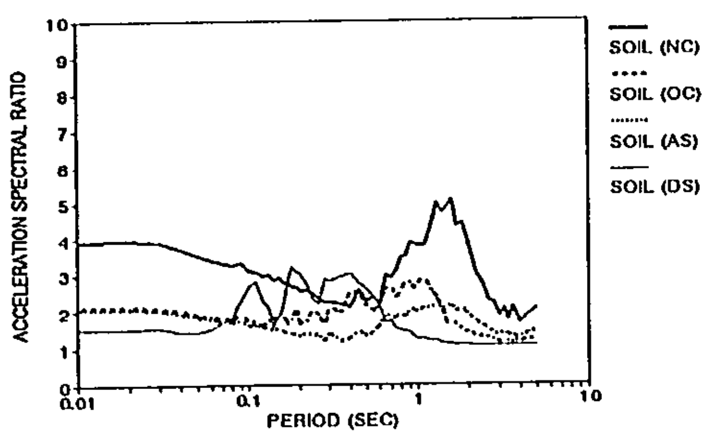

(c) Site b

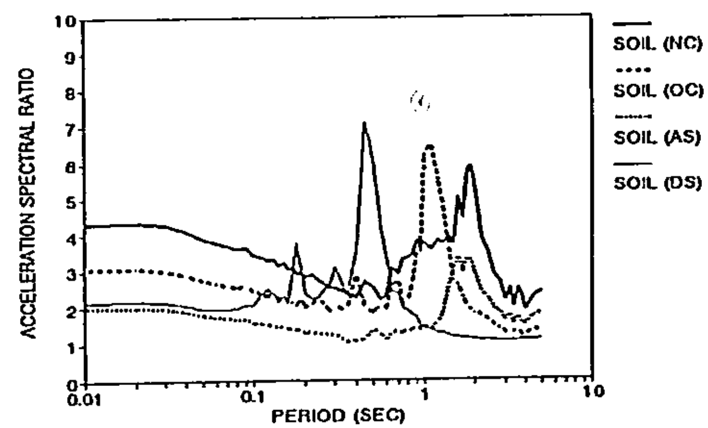

(d) Site c

Fig. 6-2 Effect of soil type on the spectral ratios
Very low a/v, v = 0.2 m/s

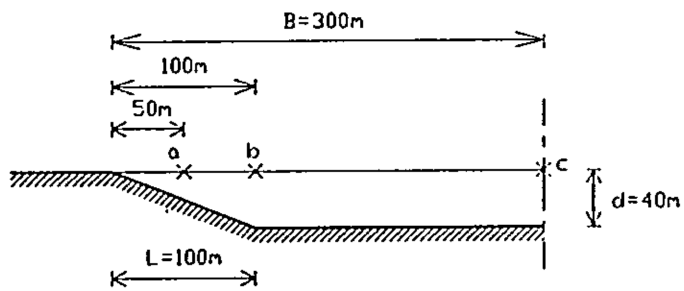

(a) Valley dimensions

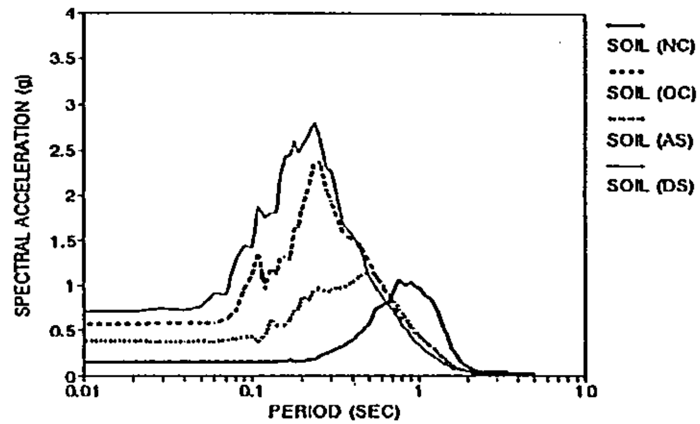

(b) Site a

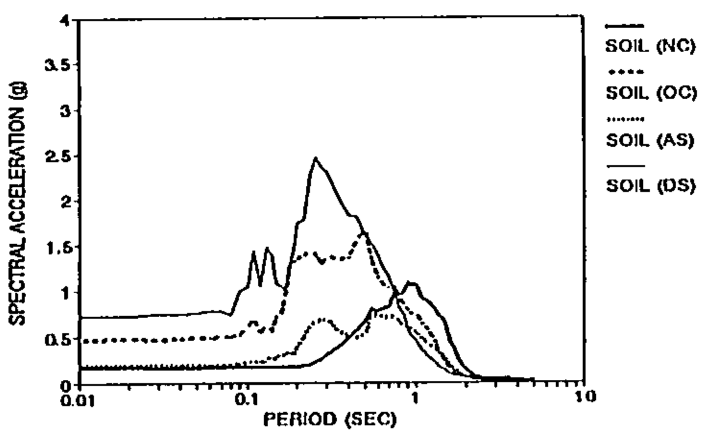

(c) Site b

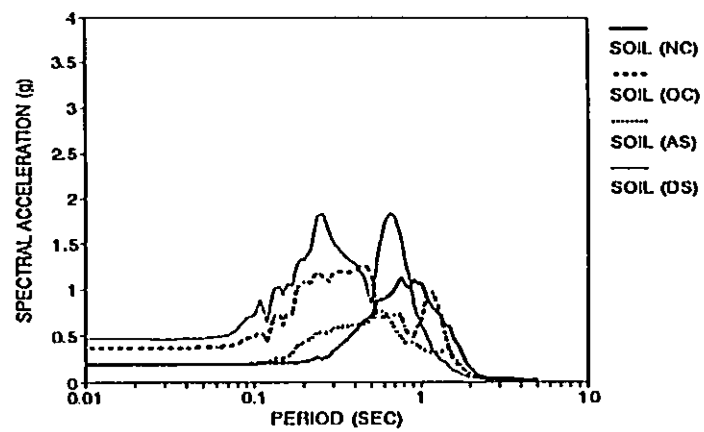

(d) Site c

Fig. 6-3 Effect of soil type on the spectral accelerations
High a/v, v = 0.2 m/s

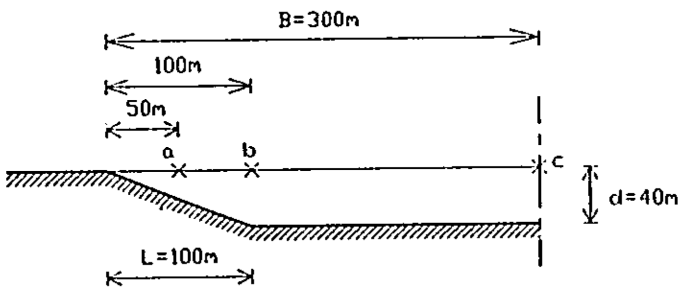

(a) Valley dimensions

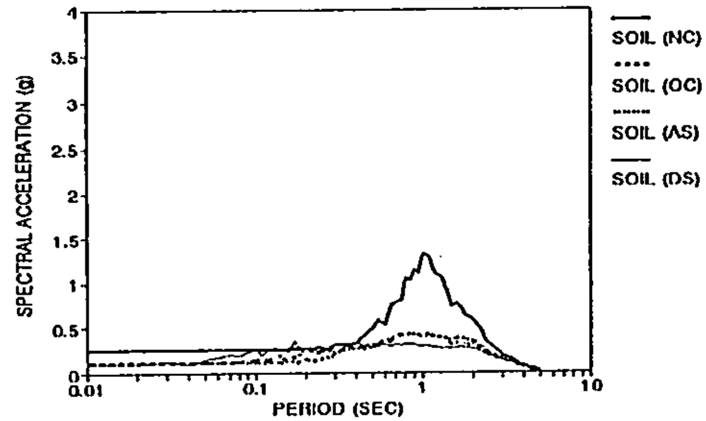

(b) Site a

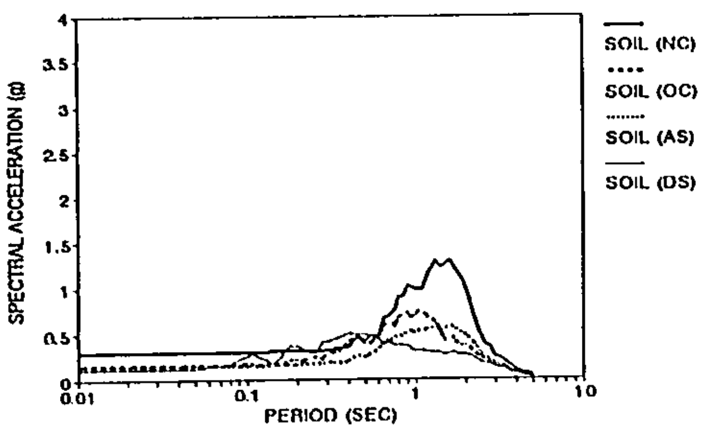

(c) Site b

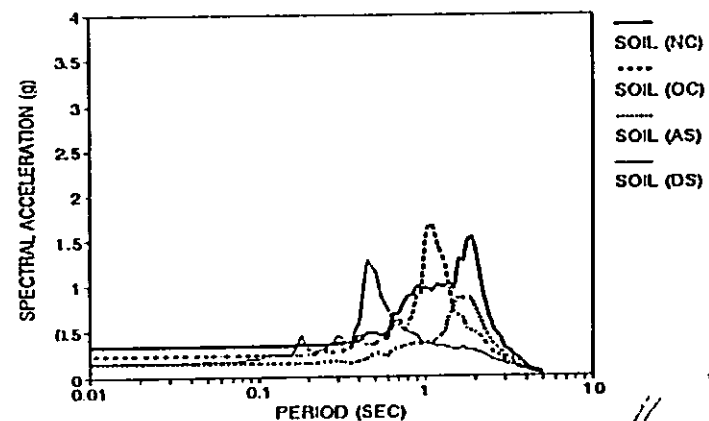

(d) Site c

Fig. 6-4 Effect of soil type on the spectral accelerations
Very low a/v, v = 0.2 m/s

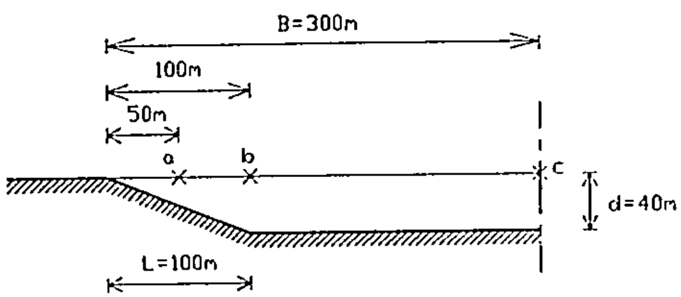

(a) Valley dimensions

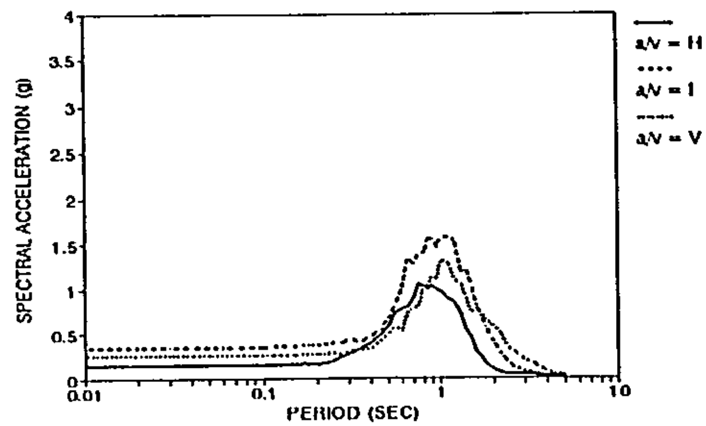

(b) Site a

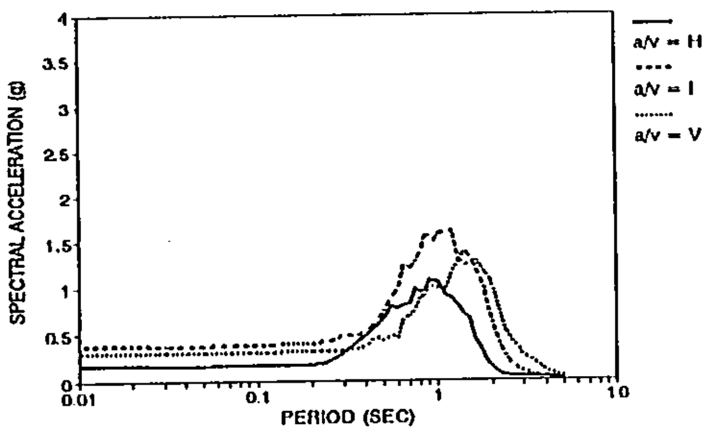

(c) Site b

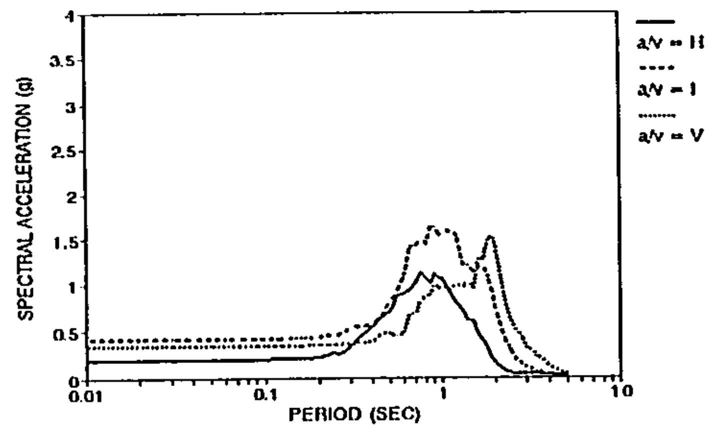

(d) Site c

Fig. 6-5 Effect of a/v ratio on the spectral accelerations
Soil profile (NC), v = 0.2 m/s

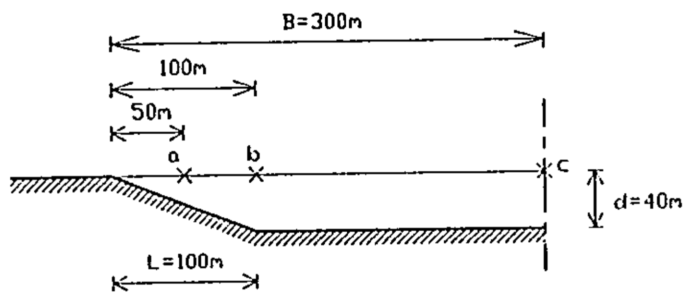

(a) Valley dimensions

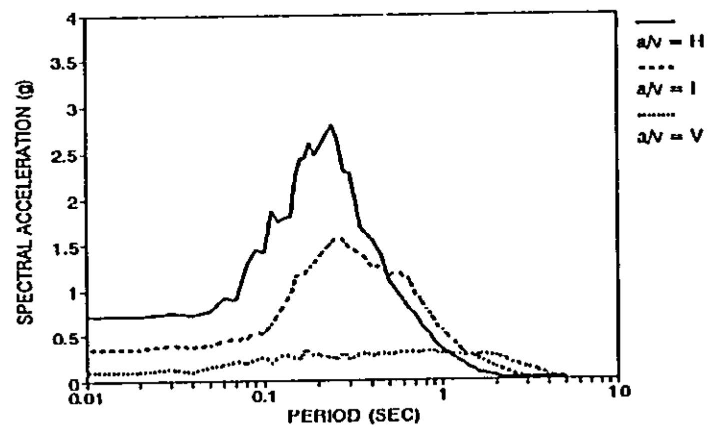

(b) Site a

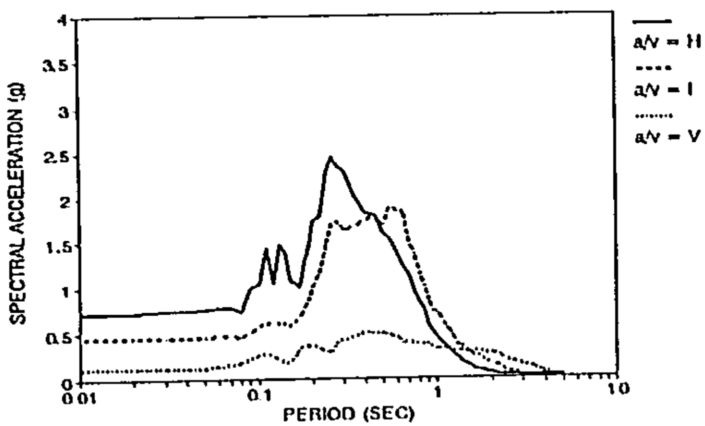

(c) Site b

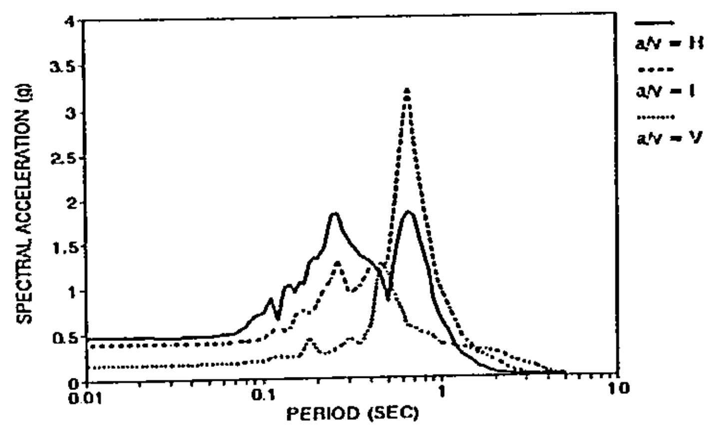

(d) Site c

Fig. 6-6 Effect of a/v ratio on the spectral accelerations
Soil profile (DS), v = 0.2 m/s

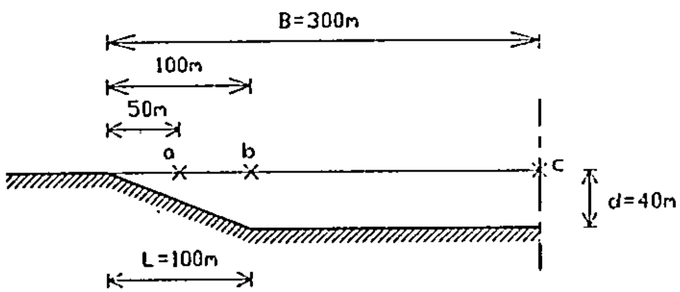

(a) Valley dimensions

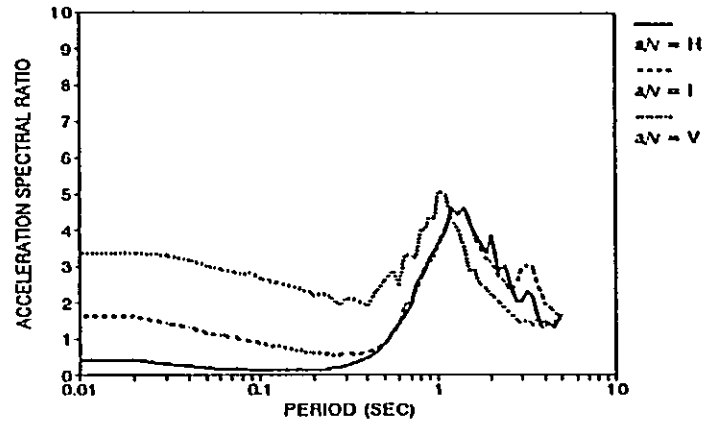

(b) Site a

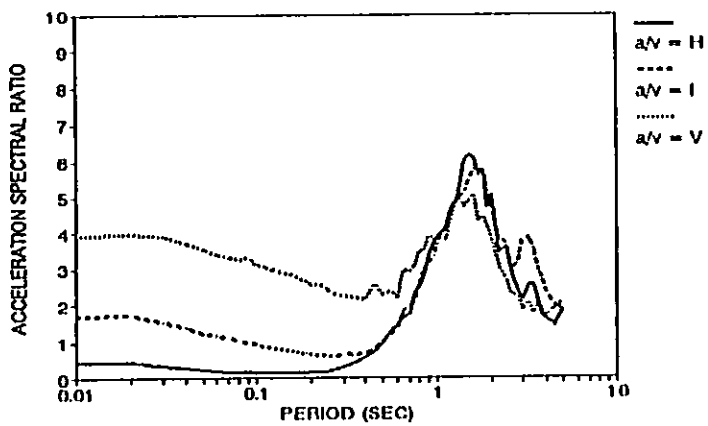

(c) Site b

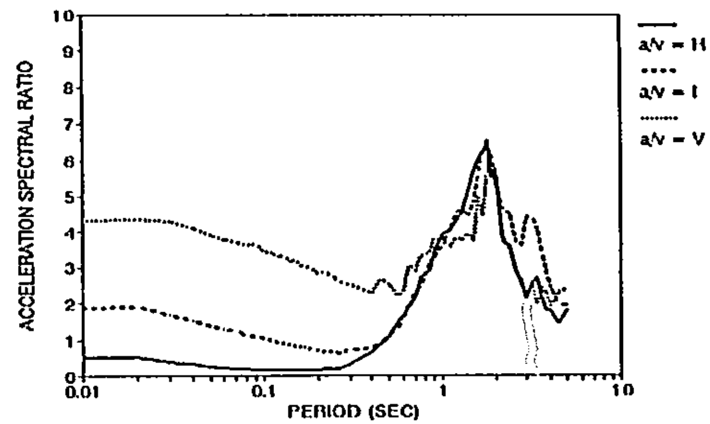

(d) Site c

Fig. 6-7 Effect of a/v ratio on the spectral ratios
Soil profile (NC), v = 0.2 m/s

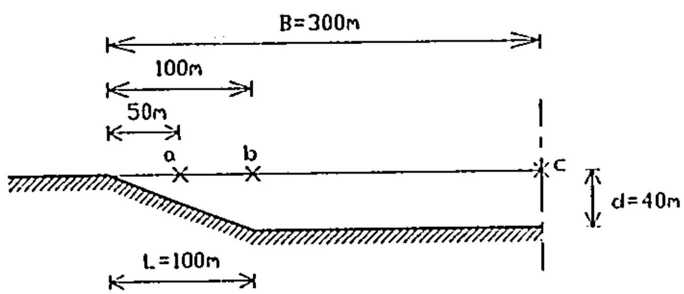

(a) Valley dimensions

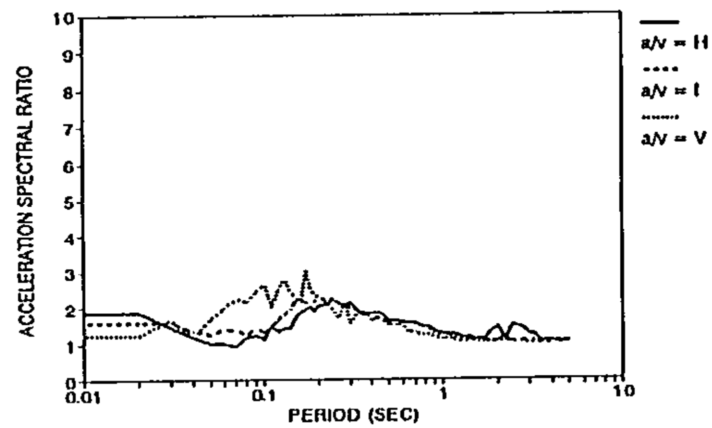

(b) Site a

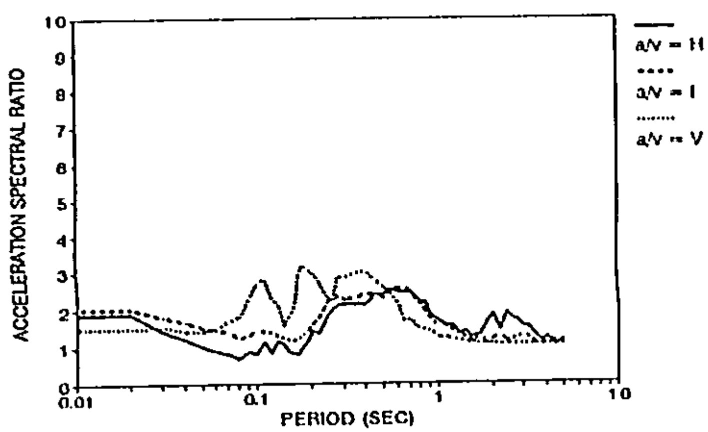

(c) Site b

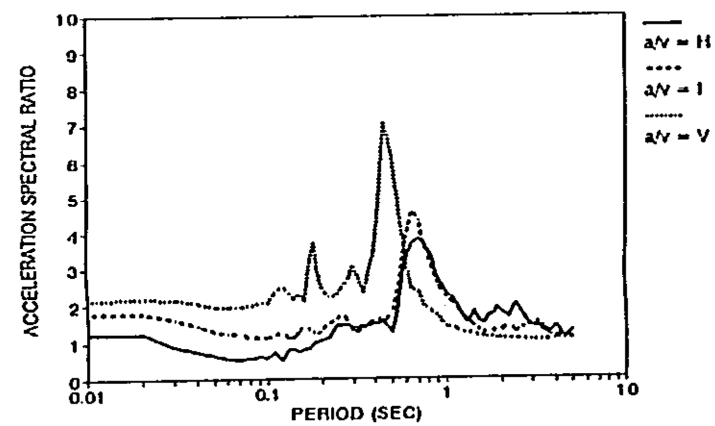

(d) Site c

Fig. 6-8 Effect of a/v ratio on the spectral ratios
Soil profile (DS), v = 0.2 m/s

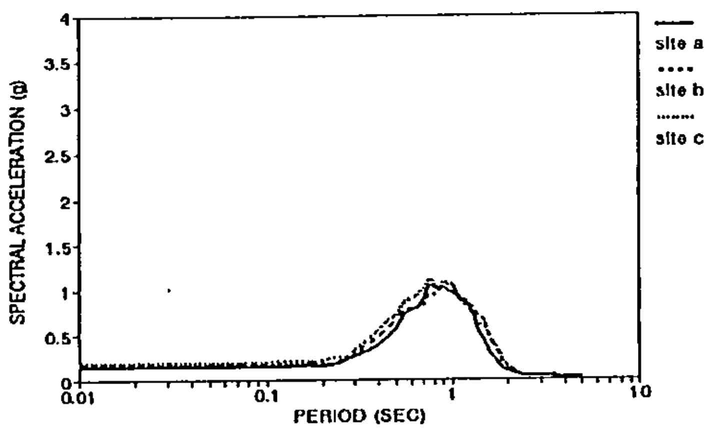

(a) Spectral acceleration, a/v = H, v = 0.2 m/s

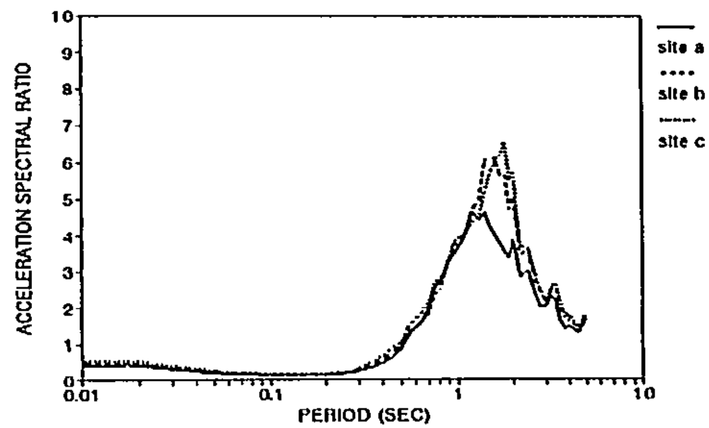

(b) Spectral ratio, a/v = H, v = 0.2 m/s

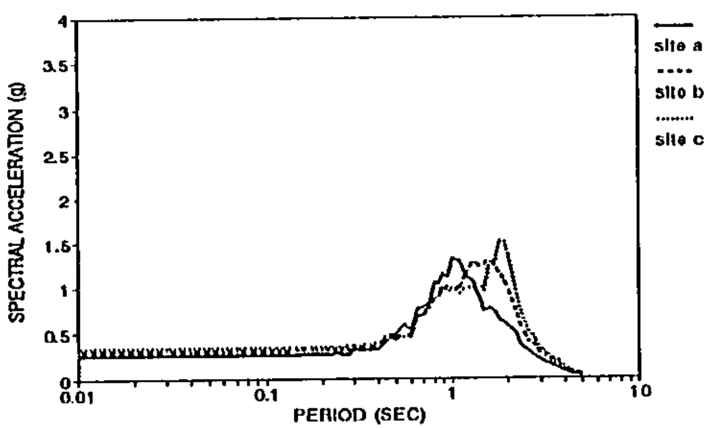

(c) Spectral acceleration, a/v = V, v = 0.2 m/s

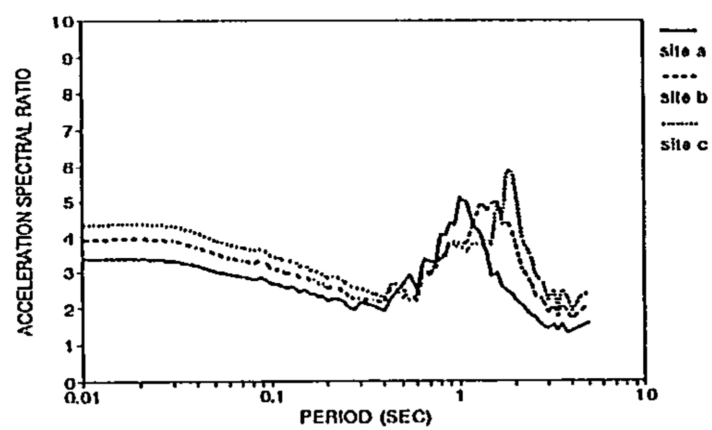

(d) Spectral ratio, a/v = V, v = 0.2 m/s

Fig. 6-9 Effect of site location on the spectral response
Soil profile (NC)

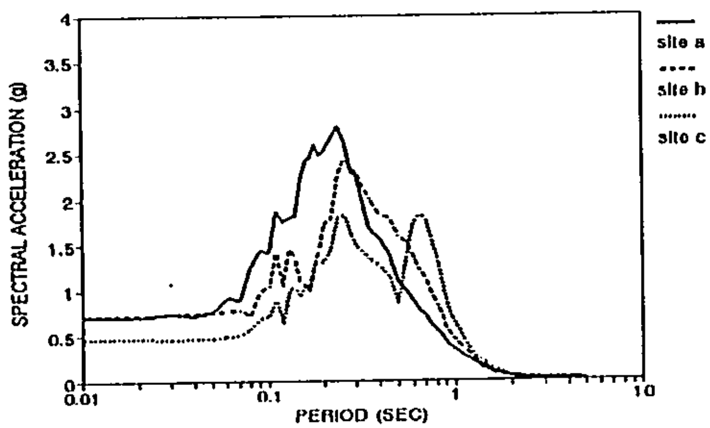

(a) Spectral acceleration, a/v = H, v = 0.2 m/s

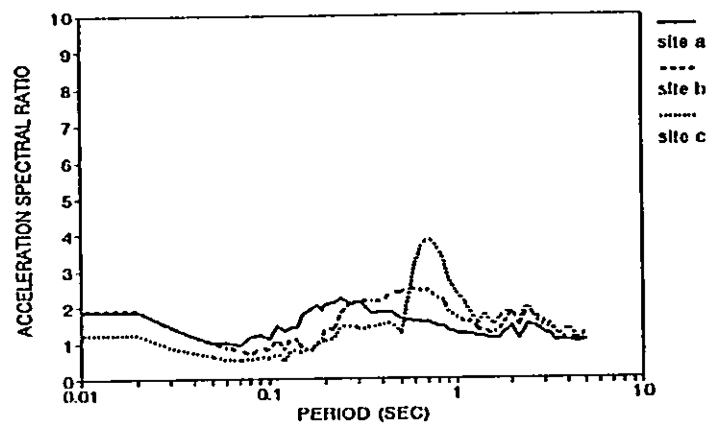

(b) Spectral ratio, a/v = H, v = 0.2 m/s

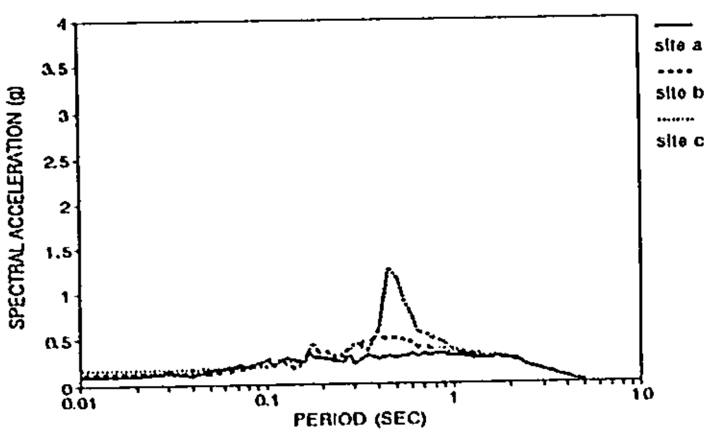

(c) Spectral acceleration, a/v = V, v = 0.2 m/s

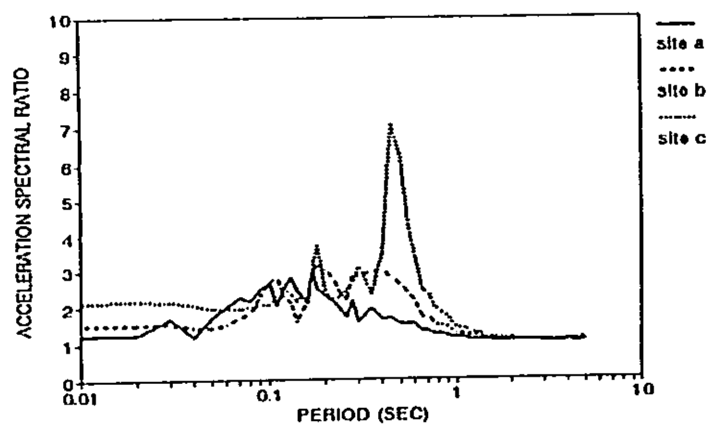

(d) Spectral ratio, a/v = V, v = 0.2 m/s

Fig. 6-10 Effect of site location on the spectral response
Soil profile (DS)

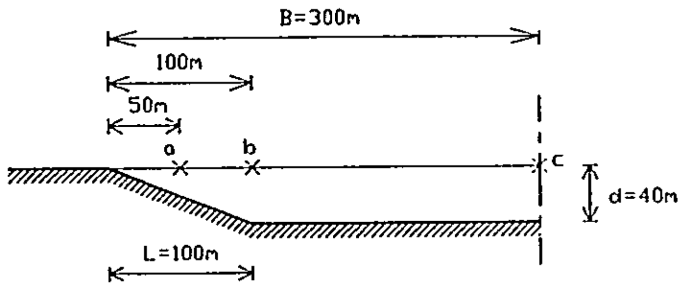

(a) Valley dimensions

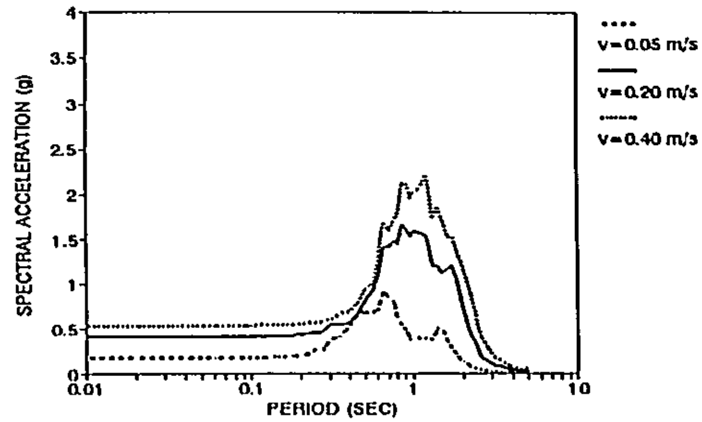

(b) Soil profile (NC), site c

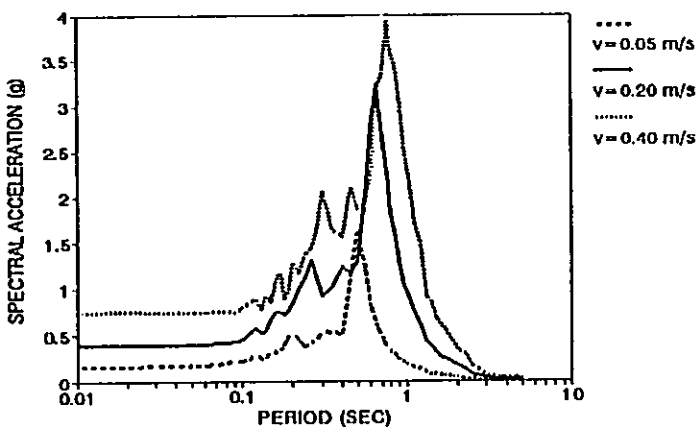

(c) Soil profile (DS), site c

Fig. 6-11 Effect of rock motion intensity on the spectral accelerations
a/v = 1

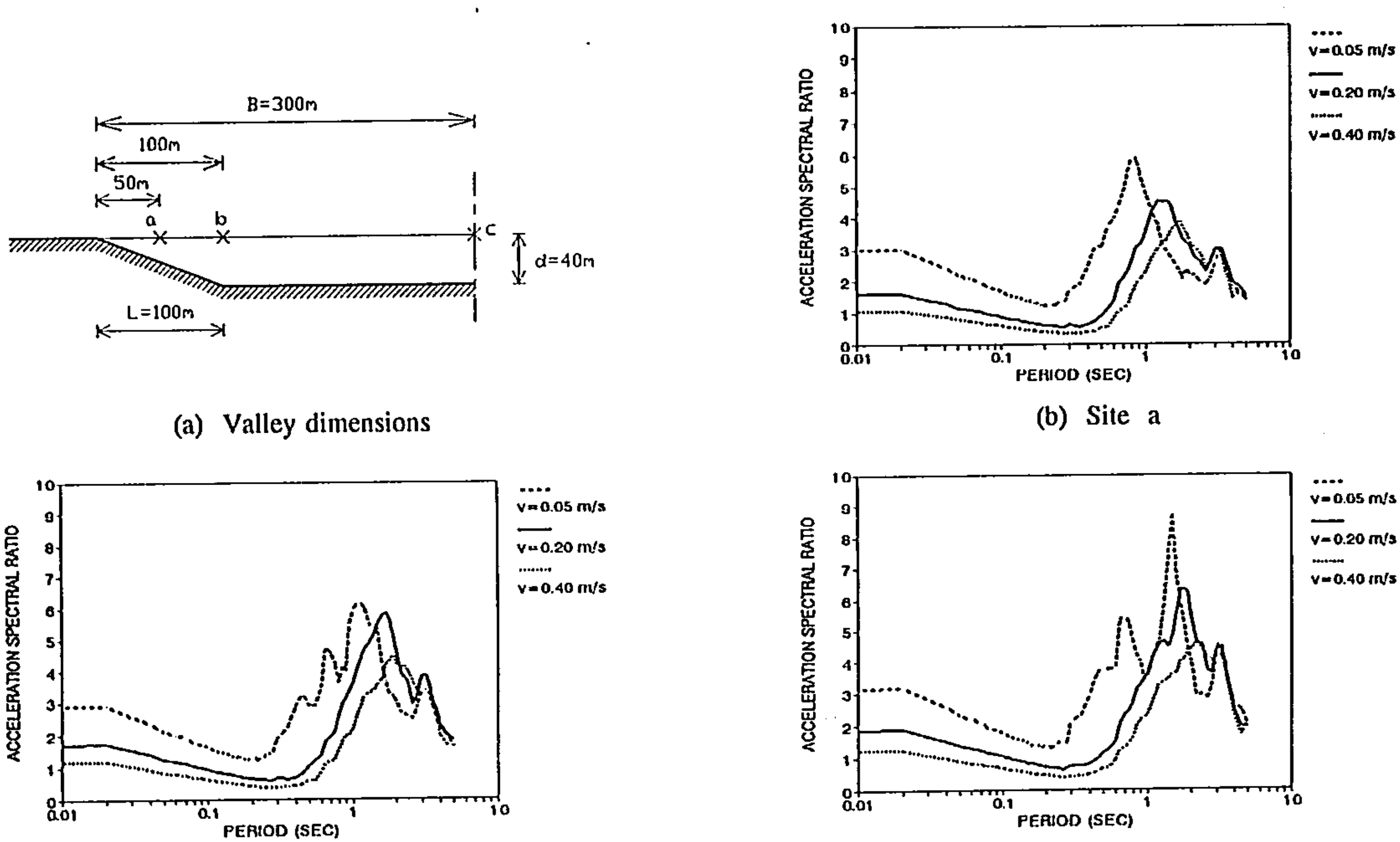

(a) Valley dimensions

(b) Site a

(c) Site b

(d) Site c

Fig. 6-12 Effect of rock motion intensity on the spectral ratios
Soil profile (NC), a/v = I

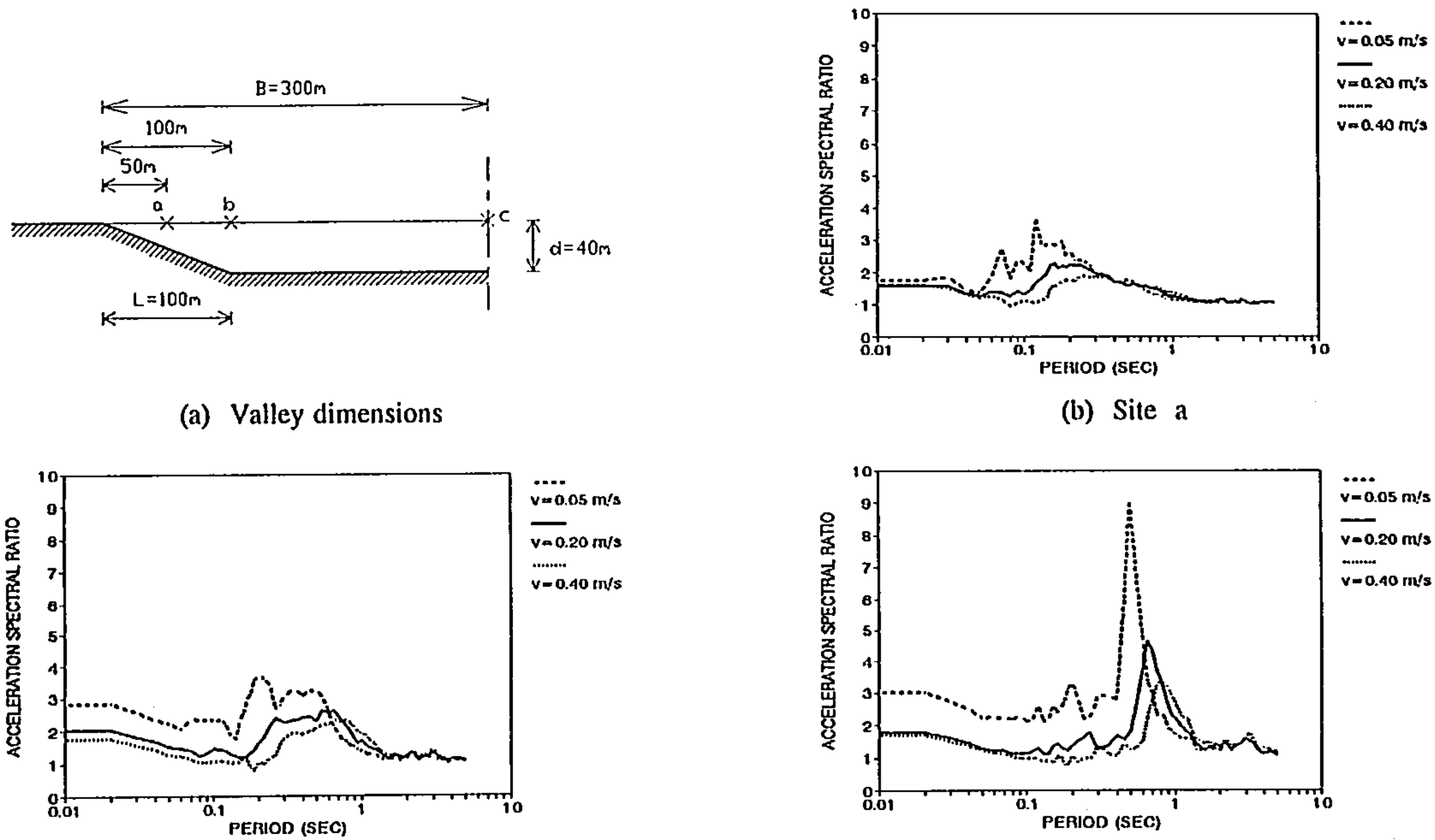

(a) Valley dimensions

(b) Site a

(c) Site b

(d) Site c

Fig. 6-13 Effect of rock motion intensity on the spectral ratios
Soil profile (DS), a/v = I

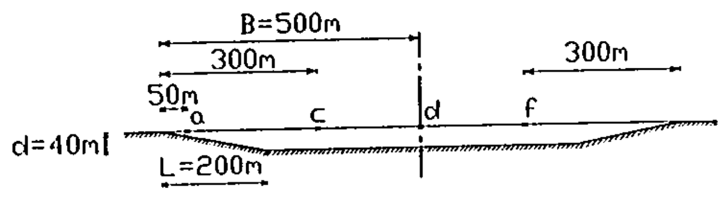

(a) Valley dimensions

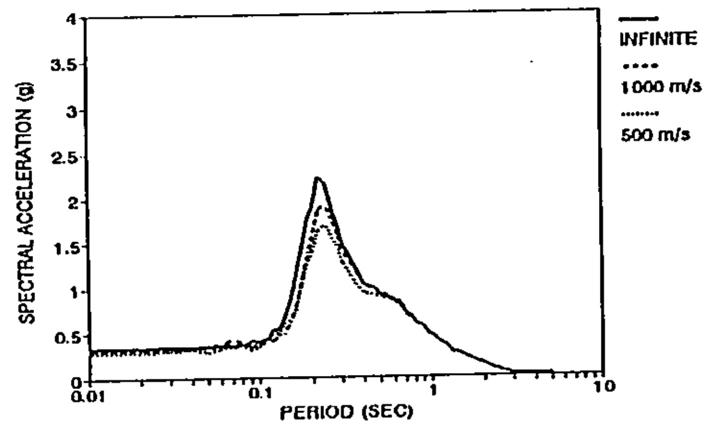

(b) Site a

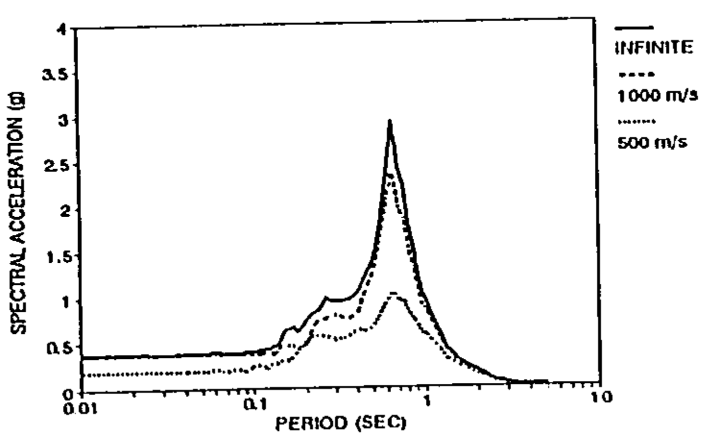

(c) Site c

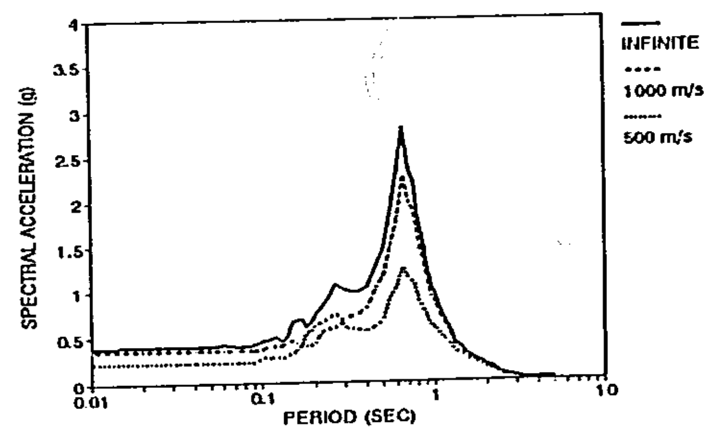

(d) Site d

Fig. 6-14 Effect of variation in travelling wave speed in the rock
Soil profile (DS), B = 500 m

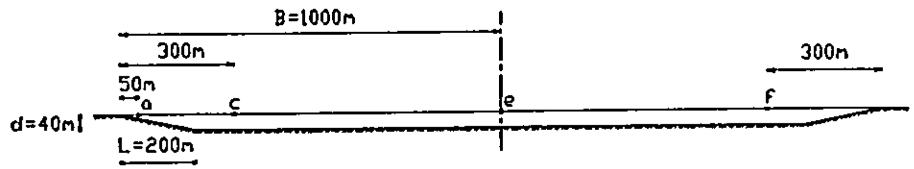

(a) Valley dimensions

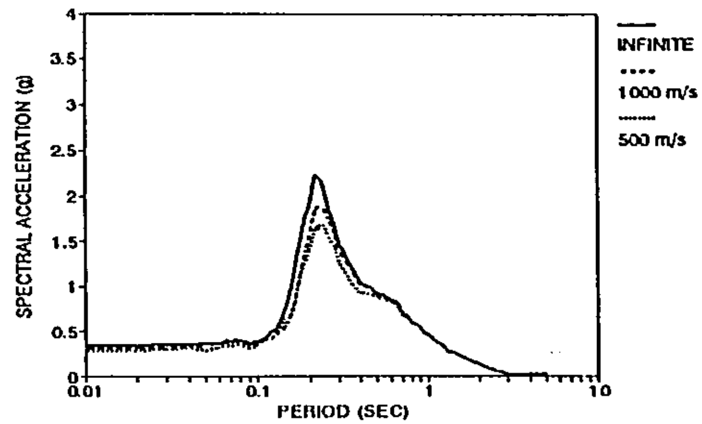

(b) Site a

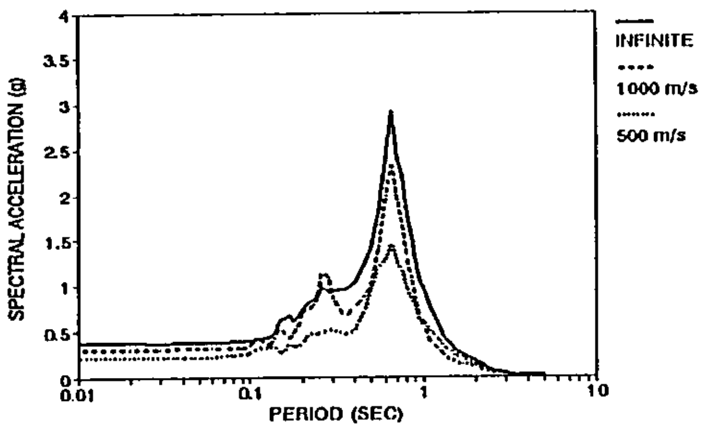

(c) Site f

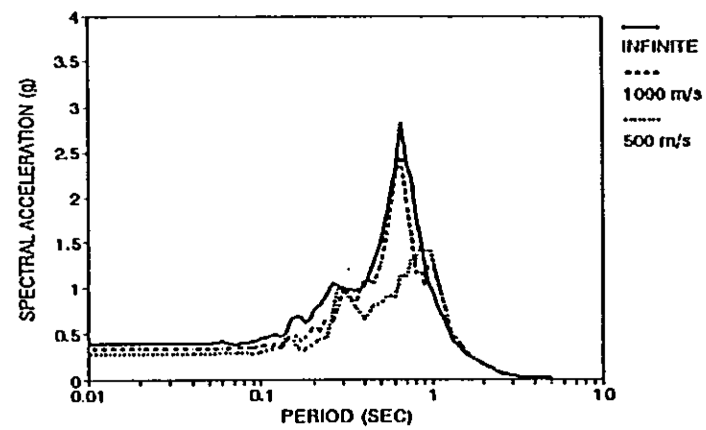

(d) Site e

Fig. 6-15 Effect of variation in travelling wave speed in the rock
Soil profile (DS), B = 1000 m

CHAPTER 7

APPLICATION OF THE VALLEY SURFACE MOTION TO THE HUMBER SUSPENSION BRIDGE

7.1 INTRODUCTION

In most analyses of the response of structures to earthquake ground motions, the seismic excitation is assumed to be identical at all points along the base of the structure. This assumption is reasonable for structures where the foundation occupies only a localized region. However, for structures with large horizontal dimensions, such as long-span suspension bridges, the above assumption ignores the spatial variations of ground motion inputs at different support points. These spatial variations cause the various foundations along the length of the bridge to be subjected to excitations that differ in both amplitude and phase. The variation in the input excitations can have significant effect on the bridge response.

Because of the complex phenomena that affect spatially varying ground motions and the scarcity of closely spaced strong-motion records that could provide insight into these phenomena, there is considerable uncertainty involved in defining spatially varying input motions for seismic response analyses of such extended structures. One method to define varying input motions is to approximate the input motion as travelling waves of constant shape which propagate from one support to another with no variation in amplitude or frequency. Only the time lag between input support motions is considered under this assumption. Dumanoglu and Severn (1985b, c, d) applied the travelling wave approach to the multiple-support excitation of the Bosporus suspension bridge in Turkey and the Humber bridge in U.K. They showed that the finite speed of travelling wave produced quasi-static displacements caused by the differential movement of the foundations in addition to the normal dynamic displacement. They concluded that for lower speeds of wave propagation the quasi-static effect is more significant and may lead, when added to the dynamic response, to total response values in some parts of the bridge that are higher than those obtained under the uniform support excitation assumption.

The travelling wave assumption, however, does not account for support motion variations in amplitude and frequency. These variations will take place in the resulting free-field surface motions in a valley. Although the input excitation may be assumed uniform along the rock boundary, the resulting surface motions will vary from one location to another due to different patterns of site amplification at different locations. Hence, the response analysis of a suspension bridge to spatially varying excitation can be made possible by applying the free-field surface motions obtained at different locations in the valley to the foundations of the bridge. This will create a multiple-support excitation condition in the bridge, which involves more realistic representation of the varying support motions.

The Humber suspension bridge in the U.K. is taken as an example of the modern type of suspension bridges, having slender towers, steel box-decks and inclined hangers. The structural configuration of the bridge is shown in Fig. 7-1. The computer input data for the structural modelling of the bridge using SAP IV computer program was made available by Dumanoglu (1987). For the purpose of this analysis the bridge will be assumed to be located on a hypothetical valley condition. A symmetric trapezoidal wide valley of the dimensions shown in Fig. 7-2 is selected for the calculation of the horizontal surface motions that will be applied to the supports of the Humber bridge. The artificial time-history record, generated in chapter 3, with very low a/v ratio is applied as the horizontal input uniform motion along the rock boundary. Two parameters will be of main interest in analyzing the response of the bridge to the multiple-support excitation. These are the location of bridge supports in the valley and the soil type producing the surface motions. The purpose of this analysis is to investigate the parameters that influence the multiple-support input motion which cause significant variation in the bridge response. SAP IV computer program by Bathe et al (1973) is modified to perform a multiple-support time-history analysis on the bridge, using the modal analysis technique.

7.2 MULTIPLE - SUPPORT EXCITATION ANALYSIS OF THE HUMBER BRIDGE

7.2.1 Description of the Bridge Model

The Humber suspension bridge in the U.K. connects the towns of Barton and Hessle across the Humber estuary upstream from Hull. The bridge was opened to traffic in July 1981. The structural configuration of the bridge is shown in Fig. 7-1 with main span of 1410 m and side spans of 530 m and 280 m. The general arrangement of the Humber bridge and a summary of material properties, dimensions and modelling are contained in four reports by Dumanoglu and Severn (1985a). They modelled the bridge by using two-dimensional beam elements for the deck, cables and towers in the vertical plane, as shown in Fig. 7-1. At each node, three degrees of freedom are allowed, two translations in y and z directions and a rotation about the x-axis. The deck over the three spans is supported by the cables and is free to move in the longitudinal (y-axis) direction at support points. The deck is only restrained vertically at the towers and anchor blocks. The towers are assumed fixed at the base (supports S2 and S3) and so are the cables at the two anchor blocks (supports S1 and S4). The element stiffness matrices for the various components contain both elastic and geometric stiffness terms. The geometric stiffness matrices account for the effects of the initial stresses in the bridge elements on the bridge dynamic behaviour. These initial stresses are the result of the bridge deformation under the action of the existing dead loads. The structural model presented in the reports by Dumanoglu and Severn (1985a) is used in this chapter to model the bridge for multiple-support excitation analysis under the applied surface motions in the valley.

7.2.2 Vibration Modes of the Bridge

SAP IV computer program was modified to include the effects of geometric stiffness matrices and utilized to obtain the mode shapes and periods of free vibration of the bridge. The first 20 modes of vibration are presented in Fig. 7-3. They are reproduced from the first report on free vibration by Dumanoglu and Severn (1985a), after being confirmed by the present analysis. Periods and modal participation factors of the modes having major contribution to the response are listed in table 7-1. The modes in the table are classified under two headings: major vertical (z-direction) modes and major longitudinal (y-direction) modes. The modal participation factors are presented in the table as absolute ratios $|\Gamma_{iy} / \Gamma_{max}|$ and $|\Gamma_{iz} / \Gamma_{max}|$. The factors Γ_{iy} and Γ_{iz} are portions of the modal participation factor of the i^{th} mode associated with the y and z directions, respectively. Listed in the table are those modes having $|\Gamma_{iy} / \Gamma_{max}|$ or $|\Gamma_{iz} / \Gamma_{max}| > 10\%$. The modal participation factor of the i^{th} mode, Γ_i, can be obtained by simply adding Γ_{iy} and Γ_{iz}. The maximum modal participation factor, Γ_{max}, is found to be associated with the longitudinal mode number 12. The major vertical modes appear among the first few modes, followed by the major longitudinal modes. Mode number 4 occurs at a period of 4.84 s and has the largest participation in the vertical response. Mode number 12 with the largest participation in the longitudinal response occurs at a period of 2.07 s.

Fig. 7-3 shows that most vertical modes with major contribution reflect vertical vibration of the deck in all three spans, which is particularly symmetrical in the main span (see modes 2, 3, 4, 6, 7 and 10). On the other hand, major longitudinal modes show large vibration of the towers and longitudinal movement of the deck in the three spans (see modes 11, 12, 13, 14, 16 and 19). Because the deck in all three spans is free to move longitudinally at the support points, the coupled motion of the complete bridge is only taking place through the cables. The three spans demonstrate independent mode patterns because of the vertical restraint of the deck at the supports. In general, the Humber mode shapes indicate close coupling between the vertical and longitudinal degrees of freedom. Excitation of the bridge in the longitudinal direction will thus induce vertical as well as longitudinal displacements in the different bridge components.

7.2.3 Equation of Motion for Multiple-Support Excitation

The large distances between support points of the bridge will cause different base points to experience different acceleration inputs according to their locations. The bridge is then subjected to multiple-support excitation. This will create what is called a quasi-static displacement, in addition to the normal dynamic displacement. Whereas the latter is caused by inertia of the structure, the former is caused by the differential movement between support points. These additional quasi-static displacements are time-dependent and cause stresses which depend on the stiffness of the structure and not its mass. These quasi-static stresses are added to the dynamic stresses caused by inertia forces.

The mass of the bridge can be lumped at the nodes between different beam elements. The equation of motion for this lumped-mass representation of the bridge under multiple-support excitation (Clough and Penzien, 1975) can be written as

$$[M]\,\{\ddot{u}\} + [C]\,\{\dot{u}\} + [K]\,\{u\} = -\,[M]\,[R]\,\{\ddot{u}_g(t)\} \qquad [7.1]$$

in which,

[M]	=	lumped-mass matrix (n x n)
[C]	=	damping matrix (n x n)
[K]	=	overall stiffness matrix (n x n)
{ u }	=	vector of nodal dynamic components of displacement (n x 1) (dots denote differentiation with respect to time)
$\{\ddot{u}_g\}$	=	vector of ground acceleration inputs at support points (m x 1)
[R]	=	quasi-static influence matrix (n x m)

The dimensions n and m of the above vectors and matrices refer to the number of active degrees of freedom of the structure and number of degrees of freedom associated with the support movements, respectively. In the case of the Humber bridge which has four supports, the value of m will equal 4 when the excitation is applied at each support in one direction only (longitudinal direction). The quasi-static influence matrix will thus consist of four columns $\{r_1\}$ through $\{r_4\}$. Each column corresponds to one support and represents the resulting displacements in the bridge nodes in the direction of the active degrees of freedom due to unit ground displacement of that support in the direction of excitation. Hence, the determination of matrix [R] requires the deformed shape of the bridge to be calculated for each longitudinal unit displacement at each support point. A static analysis of the bridge can be performed using SAP IV computer code to obtain the required deformed shapes which are illustrated in Fig. 7-4. Because the towers are flexible, any longitudinal movement of an anchor block (supports S1 and S4) causes a vertical movement at mid-span almost double in size. In general, the longitudinal movement of the anchor blocks produces appreciable longitudinal and vertical displacements. Movement in the tower supports is found to have little effect beyond the tower itself. This is mainly because the deck spans are supported by the cables and they are assumed to be simply resting on the tower cross-beams.

Using modal analysis technique (Clough and Penzien, 1975), the unknown dynamic displacement vector {u} in equation [7.1] can be obtained as the sum of the modal displacement vectors of the system

$$\{u\} = \sum_{i=1}^{n} y_i(t)\ \{\phi_i\} \tag{7.2}$$

where, i denotes the mode number, $y_i(t)$ is the modal amplitude associated with the i^{th} mode and $\{\phi_i\}$ is the i^{th} mode shape. The summation in equation [7.2] may be truncated by including only the modes of significant contribution to the response. Applying orthogonality conditions, the equation of motion [7.1] can be decoupled into modal equations associated with different modes. The equation of motion corresponding to the i^{th} mode can be written as

$$\ddot{y} + 2\ \beta_i\ \omega_i\ \dot{y}_i + \omega_i^2\ y_i = -\ \frac{\{\phi_i\}^T\ [M]\ [R]}{\{\phi_i\}^T\ [M]\ \{\phi_i\}}\ \{\ddot{u}_g(t)\} \tag{7.3}$$

in which, ω_i and β_i are the natural circular frequency and the modal damping ratio of mode i, respectively.

SAP IV computer program, by Bathe et al (1973), is modified to include the effect of the [R] matrix on the calculation of the unknown modal amplitude $y_i(t)$. Moreover, it is modified to calculate the quasi-static displacement vector $\{u^s\}$ using the formula:

$$\{u^s\} = [R]\ \{u_g\} \tag{7.4}$$

where, $\{u_g\}$ is the vector of ground displacement inputs at support points. The total displacement vector $\{u^t\}$ can be thus obtained by adding the dynamic displacement vector to the quasi-static displacement vector as:

$$\{u^t\} = \{u\} + \{u^s\} \qquad [7.5]$$

In the modified SAP IV program, the total displacement vector is used in the calculation of the internal forces in the bridge elements. The input data to the modified program is provided in appendix I.

7.3 CASES OF EXCITATION AND SUPPORT MOTIONS

Since the main concern of this study is to focus on the dynamic behaviour of the suspension bridge structural system under different cases of multiple-support excitations, it will be assumed that the soil-foundation interface is at the top surface of the valley. In other words, the dynamic analysis is performed on the bridge due to the free-field surface motions applied to the supports regardless of the actual foundation level. Since the suspension bridge is a relatively flexible structure, it is more vulnerable to support excitations with low frequency contents. This is the reason for selecting the generated record with very low a/v as the horizontal input uniform motion along the rock boundary. The rock record is scaled such that its peak velocity v = 0.2 m/s.

Surface motions to be applied to the bridge supports are calculated using two types of soil in the valley: soft clay (NC) and dense sand (DS). A description of the properties of these soil types was given in chapter 3. These two categories of soil represent two extreme cases of soil stiffness. Hence, they are expected to produce different patterns of amplification for the same input rock motion. Since the input rock motion is applied in the horizontal (y-axis) direction, the frame model of the valley may calculate the resulting surface motions only in the horizontal direction. These surface motions will be thus applied in the longitudinal (y-axis) direction of the bridge. Although vertical components of excitation at the support bridges are as significant as horizontal components, it will be considered sufficient for the purpose of this chapter to analyze the bridge response to a multiple horizontal excitation at the supports.

Five excitation cases are provided by moving the bridge supports to different locations relative to the valley. The five positions of the bridge along with the spectral accelerations of the resulting surface motions at support locations are illustrated in figures 7-5 through 7-9, for the two soil types. In each excitation case, some supports are located on rock and others on soil surface. The supports located on rock will be subjected to the input rock excitation without amplification. The motions at other supports on soil surface will vary depending on their location in the valley. These variations will depend on the pattern of soil amplification at each location. For example, compare the spectral accelerations of support motions at S3 (near the valley centre) and S4 (near the valley edge) for soil profiles (NC) and (DS) in Fig. 7-5. Being near the centre of the valley, the site will have longer local-amplification period. This leads to longer dominant period of motion and higher spectral acceleration values in the long-period range at such site. This occurs due to proximity of the local-amplification period at the site and the dominant period of the input rock motion with very low a/v. As the site location approaches the edge of the valley, the dominant period of the resulting surface motion decreases and the spectral acceleration values become lower in the long-period range.

The spectral acceleration values of support motions that are most significant to the Humber bridge response are those obtained in the long-period range, where $T > 1.5$ s. This is the range of periods at which the vibration modes of the bridge with major participation in the response occur. By comparing spectral acceleration curves of surface motions at supports located on soil with those at supports located on rock in figures 7-5 through 7-9, it is observed that there is remarkable soil amplification at support locations on soft soil profile (NC) in the long-period range of interest for the bridge response. On the other hand, the amplification of the input rock motion at support locations on stiff soil profile (DS) occurs at periods far below that period range of interest. Consequently, the intensity of input motion for the bridge at supports located on soil profile (DS) will be similar to that at supports located on rock. In addition, the intensity of input motion for the bridge is higher at supports located on soil profile (NC) than that at supports located on soil profile (DS) or on rock.

7.4 BRIDGE RESPONSE TO SPATIALLY VARYING SUPPORT EXCITATIONS

The longitudinal support motions resulting from the above five excitation cases are applied to the Humber suspension bridge. The bridge response is calculated assuming a uniform damping ratio of 2.5%. The modified version of SAP IV computer program, which considers multiple-support excitation effects, is utilized to perform the response calculations. Envelopes of maximum response values are presented for the deck and towers under the five excitation cases of the bridge as well as under a uniform excitation case. The uniform excitation case corresponds to the case when all four supports of the bridge are located on rock. It is to be noted that the maximum response values represent the total response which is obtained by adding the dynamic and quasi-static components of response.

As an example of the results, the envelopes of maximum displacements and maximum bending moments resulting in the towers are presented in Fig. 7-10 for the case of soil profile (NC). For each case of excitation, the maximum horizontal displacement at the tower base represents the peak ground displacement of the surface motion applied to that base. The overall maximum displacement occurs at about half-way up the tower height. The top deflection of the tower is reduced due to the restraining influence of the cables supporting the side span. The envelopes of maximum bending moments in Fig. 7-10 are plotted on one side of the towers since they reflect the maximum absolute values. At about one third up the tower height, the bending moment should reverse signs.

It is observed in Fig. 7-10 that the most critical case of excitation for the Hessle tower is case 5 while for the Barton tower it is case 1. This is expected since case 5 is the case when the Hessle (left) tower is at its nearest position to the centre of the valley and so is the Barton (right) tower in case 1. At these positions, the intensity of surface motion is at its highest level around the period range of interest for the bridge response. As the tower position moves towards the edge of the valley, the intensity of motion in that period range decreases leading to a decrease in the resulting responses of the towers.

Fig. 7-11 shows the envelopes of maximum displacements and maximum bending moments resulting in the deck for the case of soil profile (NC). It is observed in the figure that excitation case 5 induces the highest bending moment values in the Hessle (left) side span. In addition, case 1 does the same in the Barton (right) side span. This is because in case 5 the Hessle side span is at its closest position to the middle of the valley, where the highest intensity of surface motion in the long-period range occurs. A similar explanation applies to the Barton side span under excitation case 1. It is also shown in Fig. 7-11 that excitation case 3 causes the largest values of displacement and bending moments in the main span. This can be explained by referring to Fig. 7-7 showing excitation case 3 where the two towers of the bridge are located at nearly equal distances on both sides from the centre line of the symmetric valley. This case causes similar excitations with the highest intensity of motion in the long-period range at the two towers. Hence, case 3 will represent the most critical excitation case for the main span. It is to be noted that the uniform case of excitation induces the lowest values of displacements and bending moments in the bridge elements, since it corresponds to the case when all bridge supports are excited by the rock motion without amplification.

The total responses of the towers and of the deck in the case of soil profile (DS) are shown in figures 7-12 and 7-13, respectively. It is evident that the five cases of excitation cause similar responses to those resulting from the uniform excitation case when all supports are on rock. This is because the input rock motion to the valley is not amplified by soil profile (DS) in the period range of interest for the bridge response. This means that the given case of stiff soil profile (DS) does not create a significant multiple-support excitation case for the Humber suspension bridge, wherever the support locations are.

7.5 SUMMARY

The free-field surface motions in a symmetric wide valley, due to horizontal input uniform excitation in rock with very low a/v, are applied to the support points of the Humber suspension bridge in the U.K. The purpose is to analyze the response of the bridge to the longitudinal spatially varying excitations at its supports which differ in amplitude and frequency due to variations in soil patterns of amplification at different valley sites. The two-dimensional model of the bridge, presented by Dumanoglu and Severn (1985a), is utilized. SAP IV computer program is modified to perform the multiple-support time-history analysis on the bridge, using the modal analysis technique.

The vibration mode of the bridge with the largest participation in the vertical response occurs at a period of 4.84 s, while the mode with the largest participation in the longitudinal response occurs at a period of 2.07 s. The Humber bridge mode shapes indicate close coupling between the vertical and longitudinal degrees of freedom. In general, excitation of the bridge supports in the longitudinal direction will induce vertical as well as longitudinal displacements. The multiple-support excitation of the bridge creates quasi-static displacements and stresses due to the differential movement between the support points. The quasi-static response is to be added to the normal dynamic response to obtain the total response of any bridge element.

Two soil types are used to produce the surface motions to be applied to the bridge supports: soft clay (NC) and dense sand (DS). Five cases of loading are applied to the bridge by moving its supports to different locations relative to the valley, such that some supports are located on rock and others on soil surface. There is considerable amplification observed at supports located on soft soil profile (NC) in the long-period range of interest for the bridge response ($T > 1.5$ s). On the other hand, no amplification occurs at any surface location in this range of periods in the case of stiff soil profile (DS). Consequently, the valley with soil profile (DS) does not create a significant multiple-support excitation case for the Humber suspension bridge, wherever the support locations are. The bridge response in the (DS) profile case is thus equivalent to that resulting when all bridge supports are on rock (uniform excitation case). The lowest values of displacements and bending moments in the bridge elements are expected when all bridge supports are excited by the rock motion without amplification. In the case of (NC) profile, supports which are located near the valley centre are subjected to surface motions with higher intensity in the long-period range. This causes larger values of displacements and bending moments in the tower or the side span of the bridge when it is closer to the middle of the valley. In addition, the most critical excitation case for the main span occurs when the two towers of the Humber bridge are both subjected to the highest intensity of surface motion. This takes place when the two towers are at about equal distances on both sides from the centre line of the symmetrical valley.

It is concluded that the analysis of the multiple-support excitation case for the Humber bridge does not always produce significant variation in the bridge response from the uniform input case. The amplitude and frequency variation in the input support motions may be too small or may be affecting frequencies that are far from the natural period range of the bridge modes of vibration. The inclusion of the multiple-support excitation case in the bridge analysis is significant when there are noticeable variations in the intensity of support motions in the period range of interest for the bridge response. If the support motions are of equal intensity in that period range, a multiple-support excitation case should only be considered when the input support motions are not in phase, as confirmed in the literature (e.g. Dumanoglu and Severn, 1985b, c, d) under the travelling wave assumption.

Table 7-1 Periods and modal participation factors of major modes of the Humber suspension bridge

Major vertical modes			Major longitudinal modes		
mode number	period (sec)	$\lvert \Gamma_{iz} / \Gamma_{max} \rvert$	mode number	period (sec)	$\lvert \Gamma_{iy} / \Gamma_{max} \rvert$
			1	9.23	0.29
2	8.72	0.31			
3	5.96	0.15	3	5.96	0.10
4	4.84	0.77	4	4.84	0.12
6	3.25	0.26	6	3.25	0.13
7	3.20	0.52	7	3.20	0.12
			9	2.64	0.18
10	2.17	0.14	10	2.17	0.13
			11	2.15	0.86
12	2.07	0.08	12	2.07	0.92
			13	1.95	0.21
14	1.92	0.15	14	1.92	0.26
			16	1.76	0.19
			19	1.38	0.19
			22	1.16	0.23
25	0.91	0.11			
28	0.77	0.12			
			38	0.52	0.32
			41	0.49	0.13

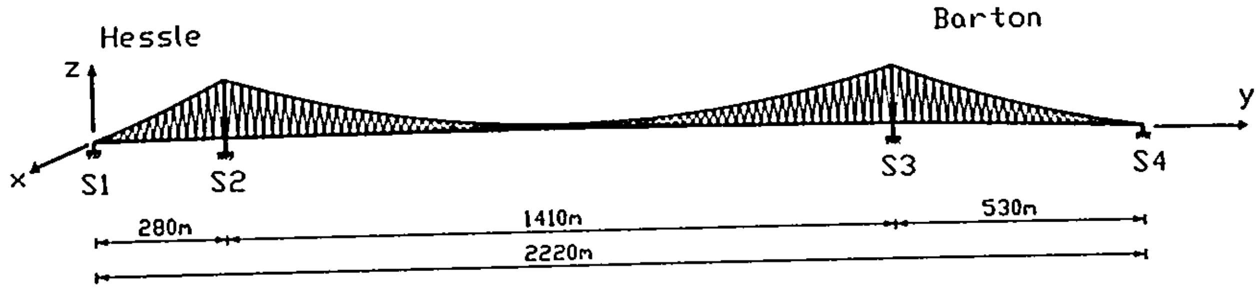

Fig. 7-1 Structural model of the Humber bridge

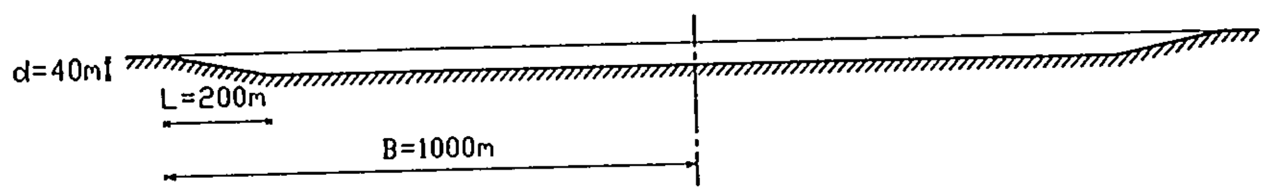

Fig. 7-2 Assumed Valley dimensions

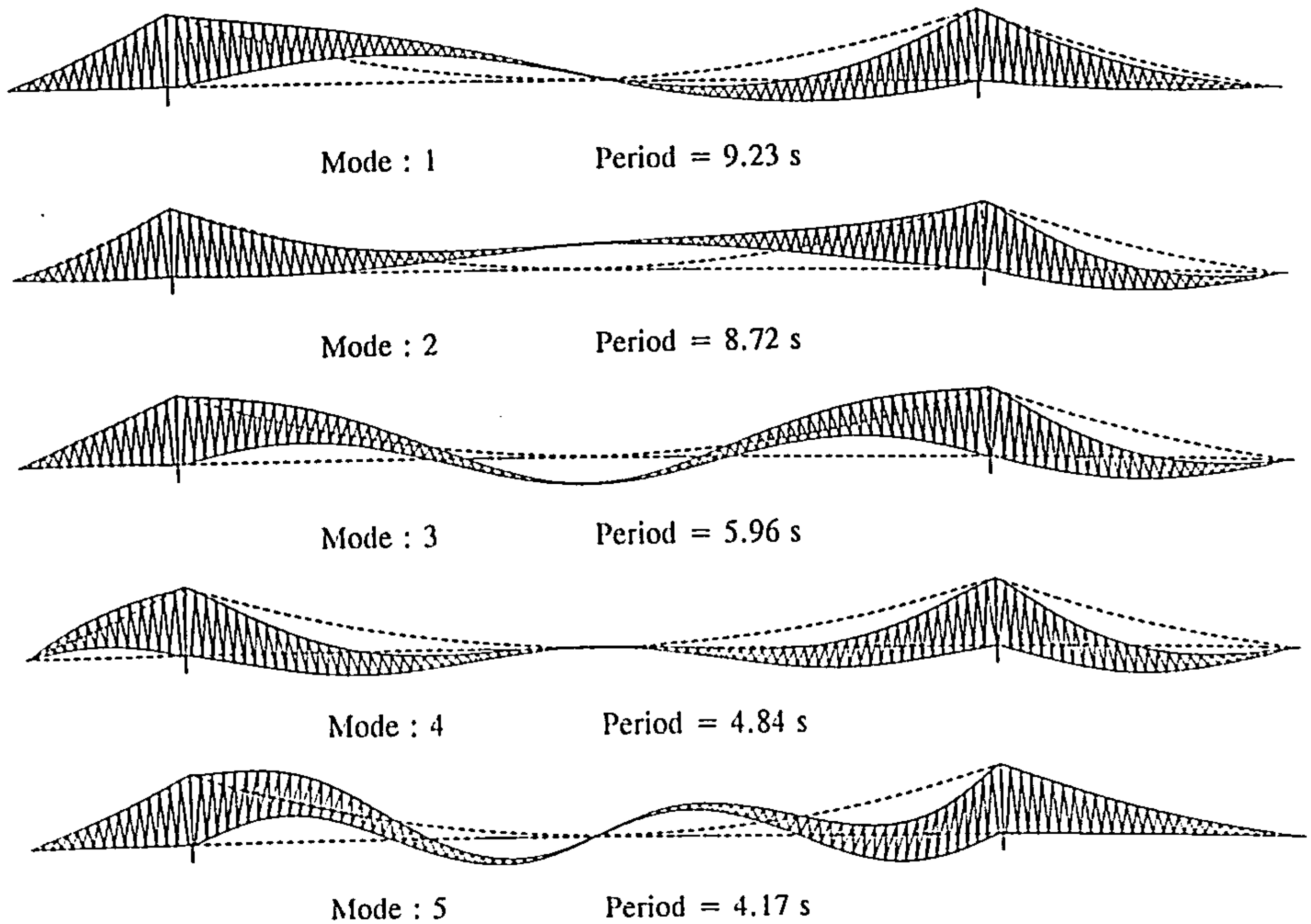

Fig. 7-3 Vibration modes of the Humber bridge (from Dumanoglu and Severn, 1985, part I)

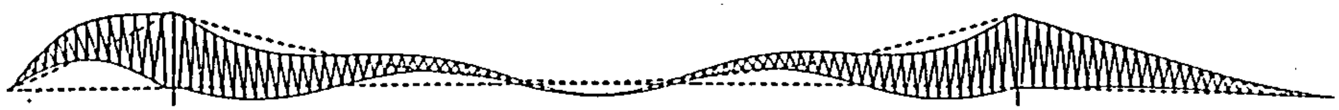

Mode : 6 Period = 3.25 s

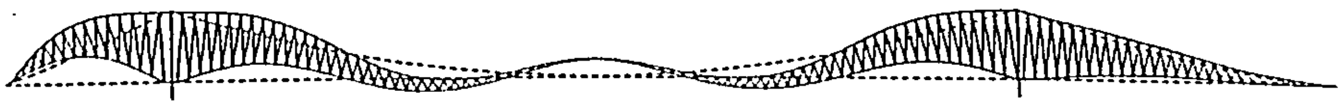

Mode : 7 Period = 3.20 s

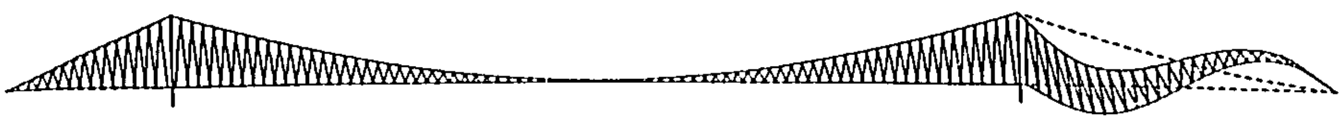

Mode : 8 Period = 3.08 s

Mode : 9 Period = 2.64 s

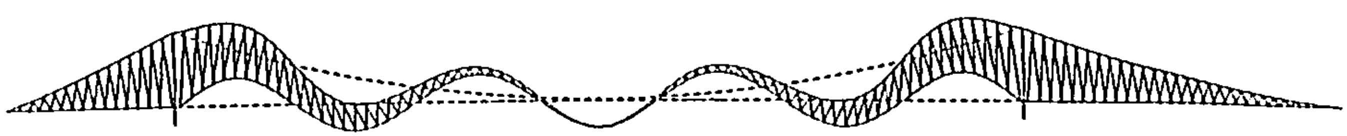

Mode : 10 Period = 2.17 s

Fig.7-3 (Cont'd) Vibration modes of the Humber bridge

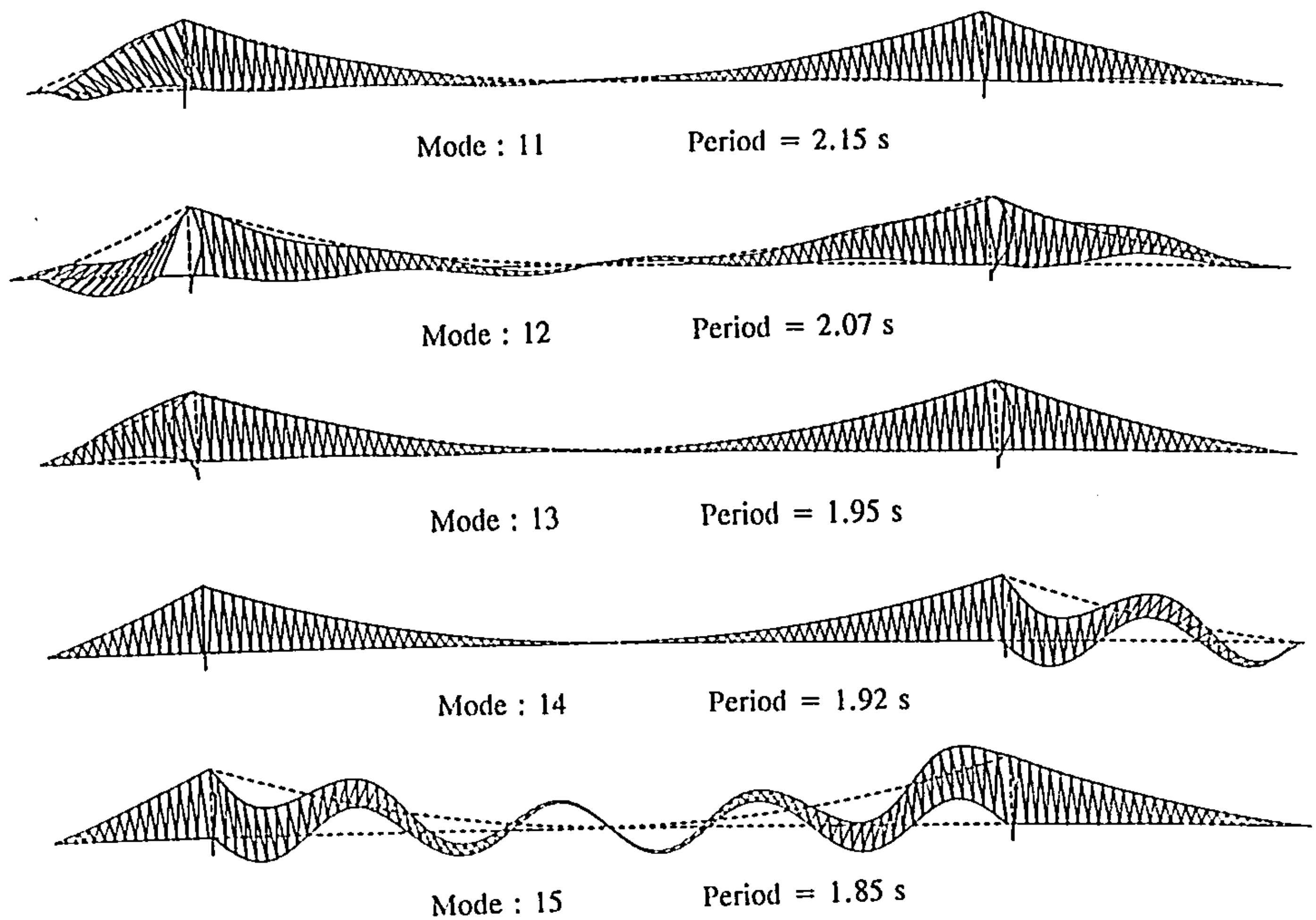

Fig.7-3 (Cont'd) Vibration modes of the Humber bridge

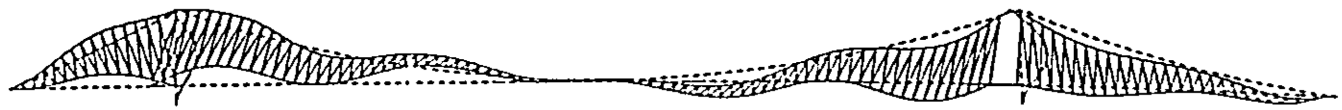

Mode : 16 Period = 1.76 s

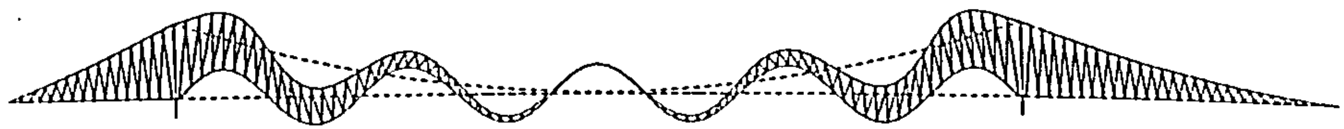

Mode : 17 Period = 1.59 s

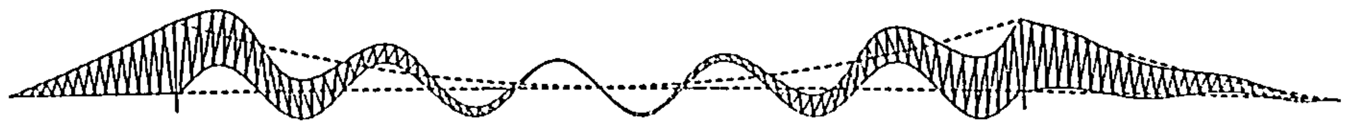

Mode : 18 Period = 1.40 s

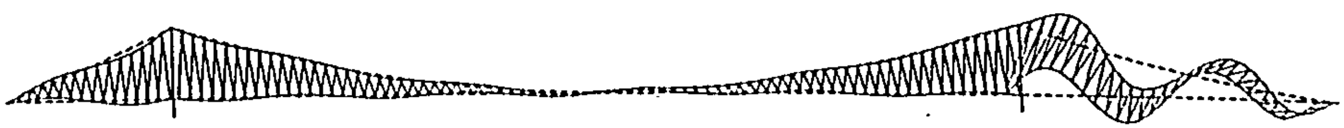

Mode : 19 Period = 1.38 s

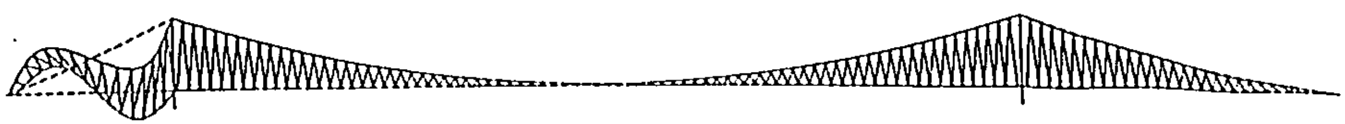

Mode : 20 Period = 1.37 s

Fig.7-3 (Cont'd) Vibration modes of the Humber bridge

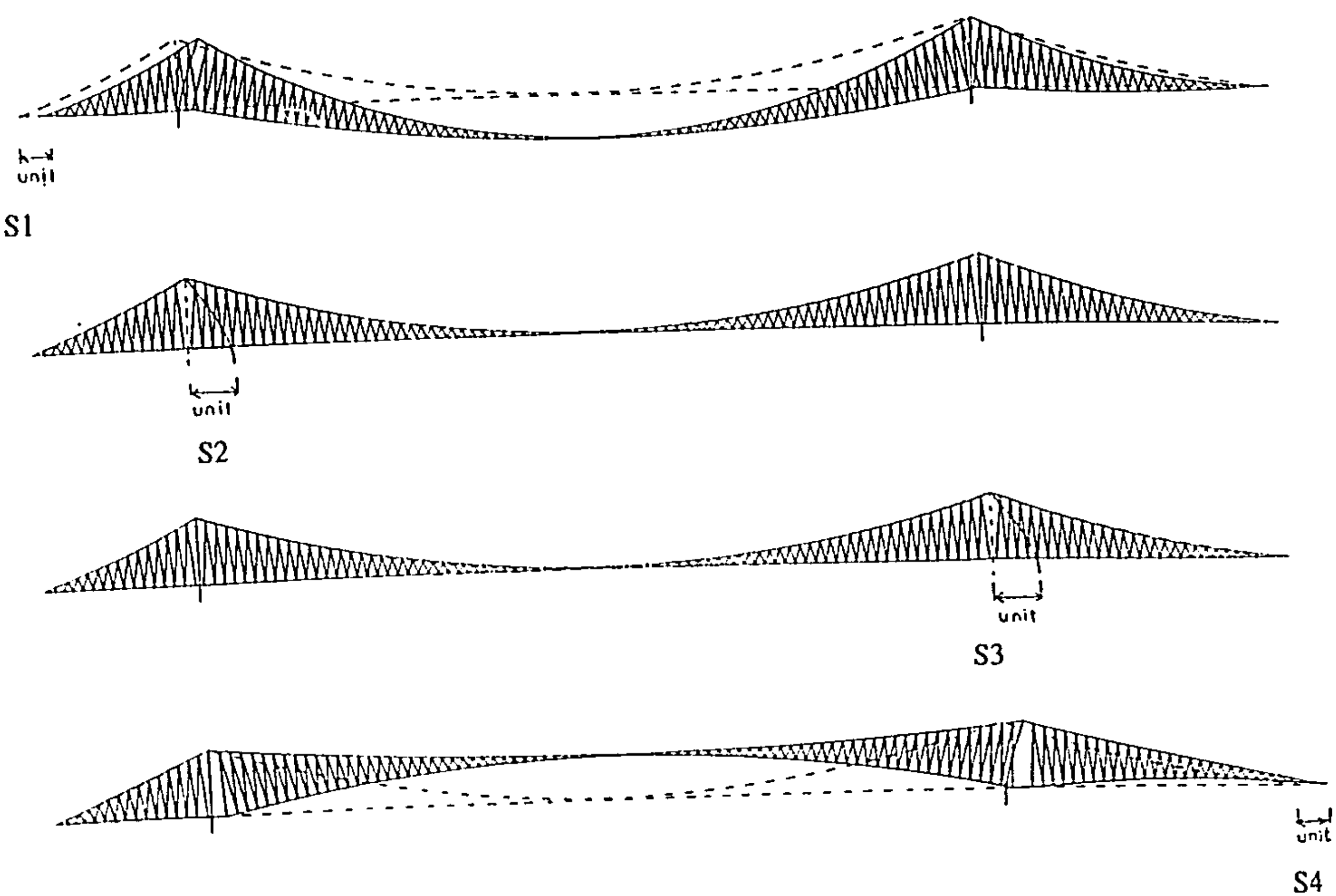

Fig. 7-4 Deformed shapes of the Humber bridge under unit displacements of supports
(matrix [R])

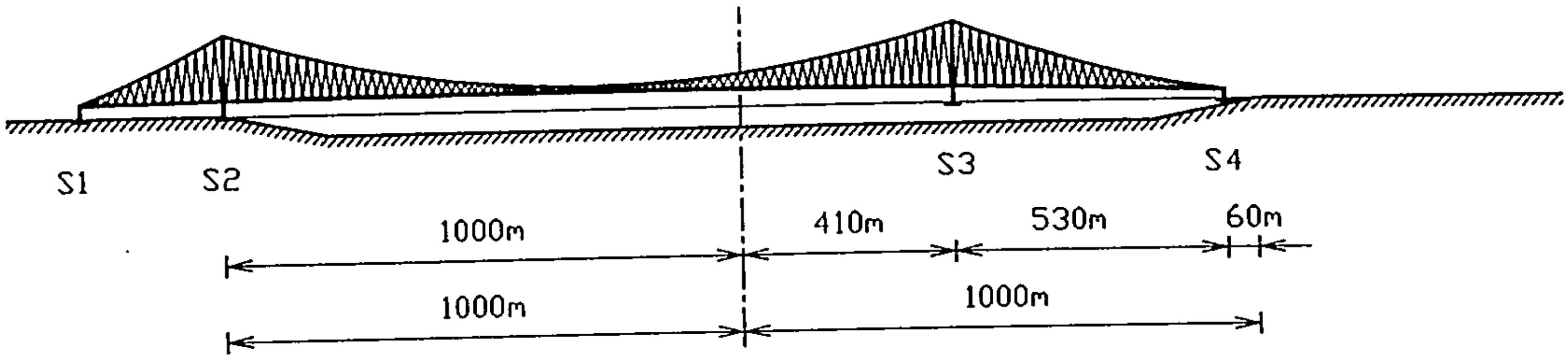

(a) Location of bridge supports in the valley

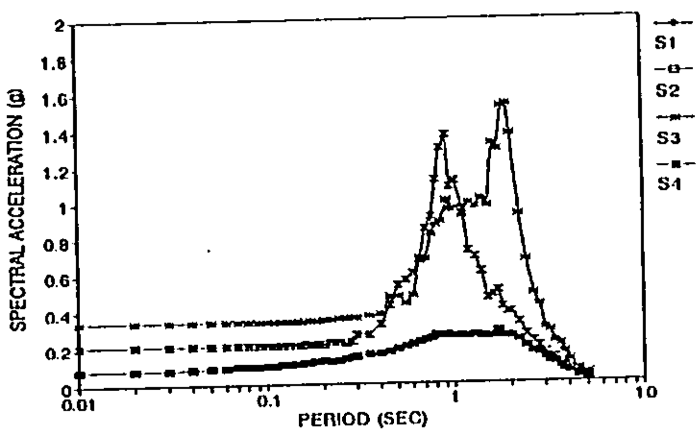

(b) Spectral accelerations of support motions
Soil profile (NC), a/v = V

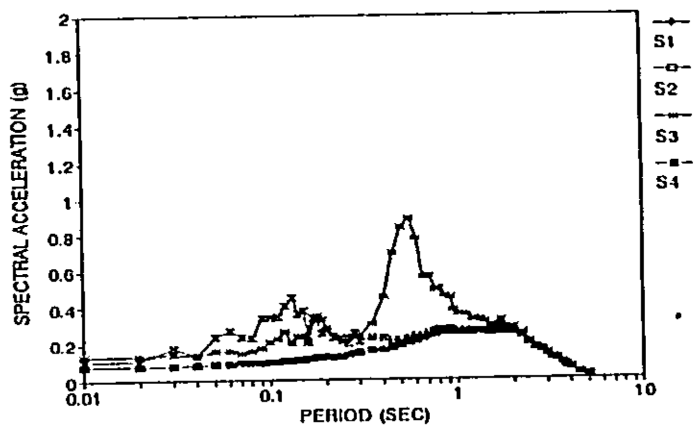

(c) Spectral accelerations of support motions
Soil profile (DS), a/v = V

Fig. 7-5 Excitation case 1

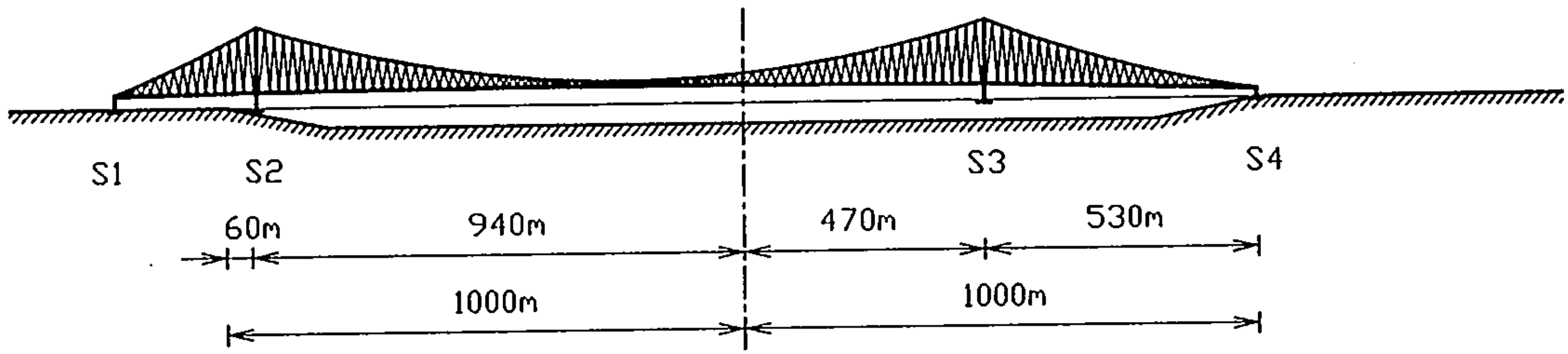

(a) Location of bridge supports in the valley

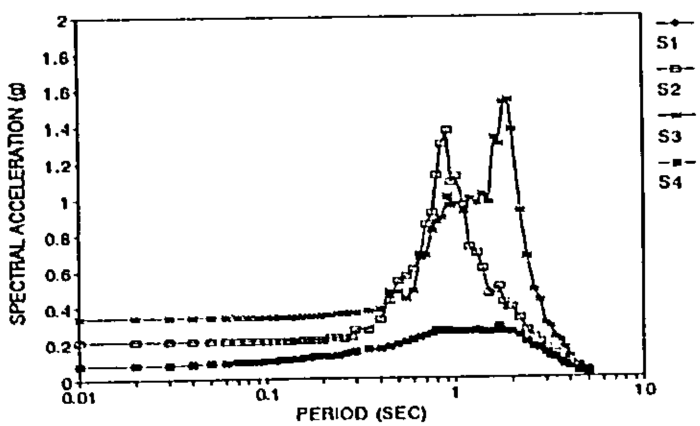

(b) Spectral accelerations of support motions
Soil profile (NC), a/v = V

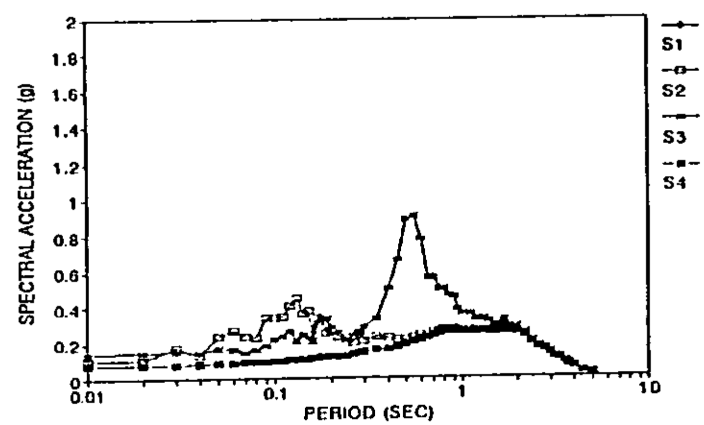

(c) Spectral accelerations of support motions
Soil profile (DS), a/v = V

Fig. 7-6 Excitation case 2

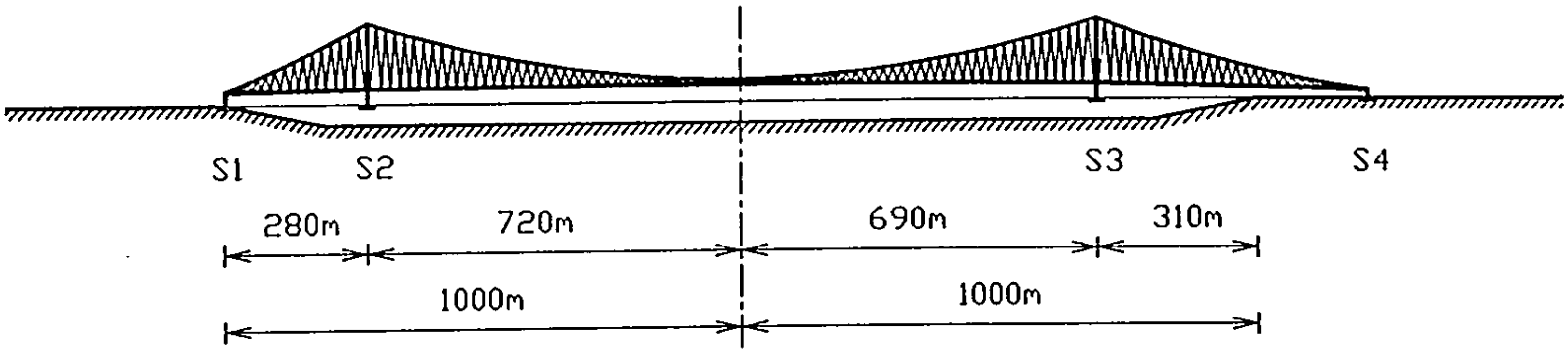

(a) Location of bridge supports in the valley

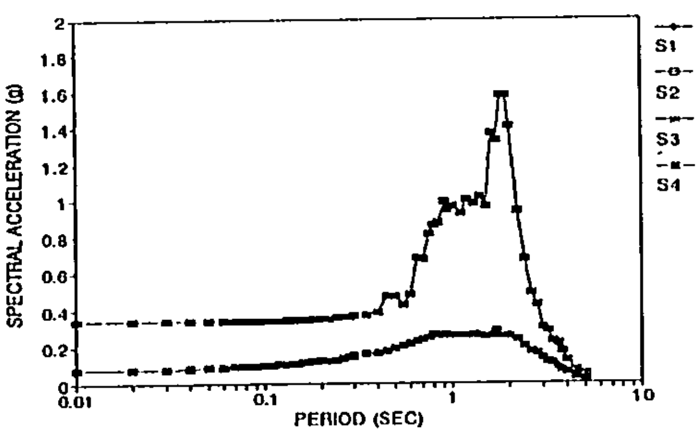

(b) Spectral accelerations of support motions
Soil profile (NC), a/v = V

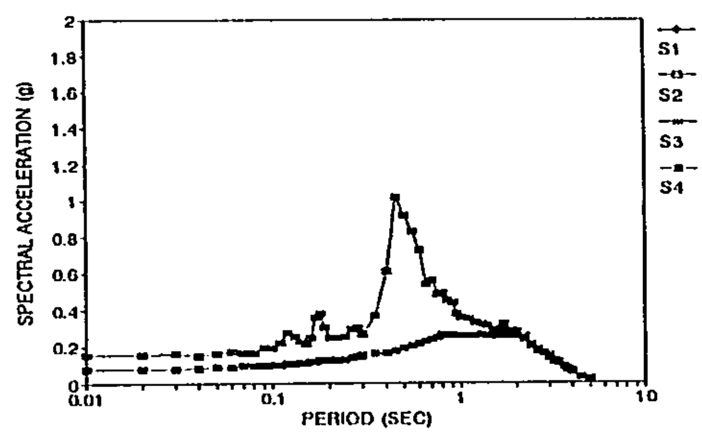

(c) Spectral accelerations of support motions
Soil profile (DS), a/v = V

Fig. 7-7 Excitation case 3

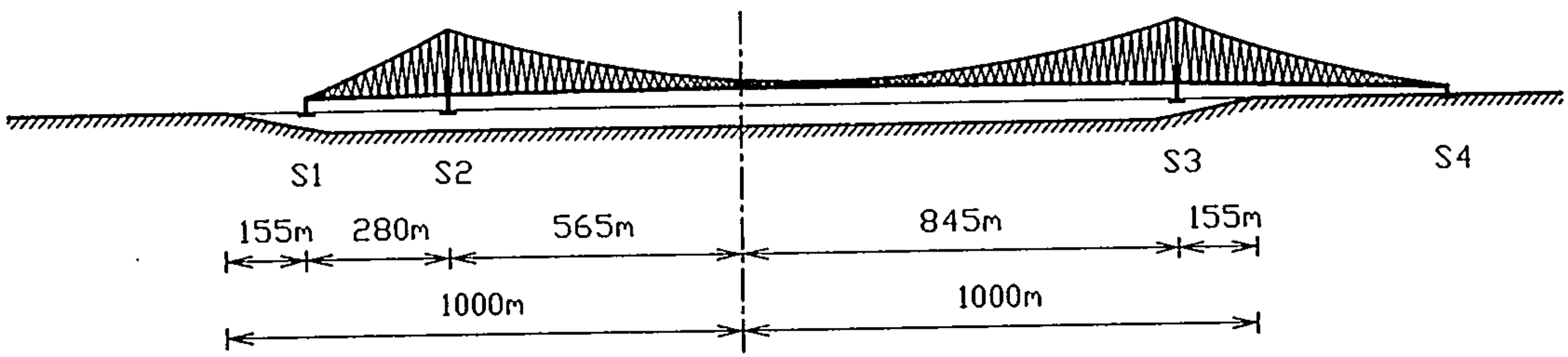

(a) Location of bridge supports in the valley

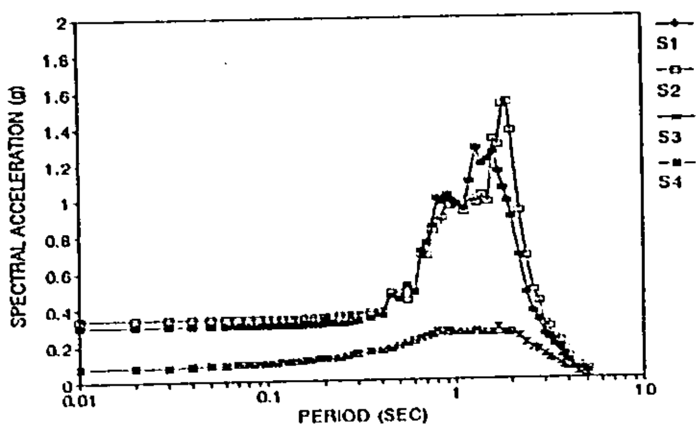

(b) Spectral accelerations of support motions
Soil profile (NC), a/v = V

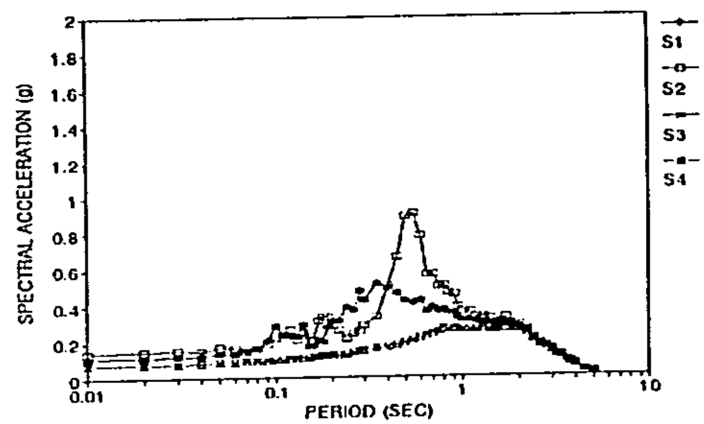

(c) Spectral accelerations of support motions
Soil profile (DS), a/v = V

Fig. 7-8 Excitation case 4

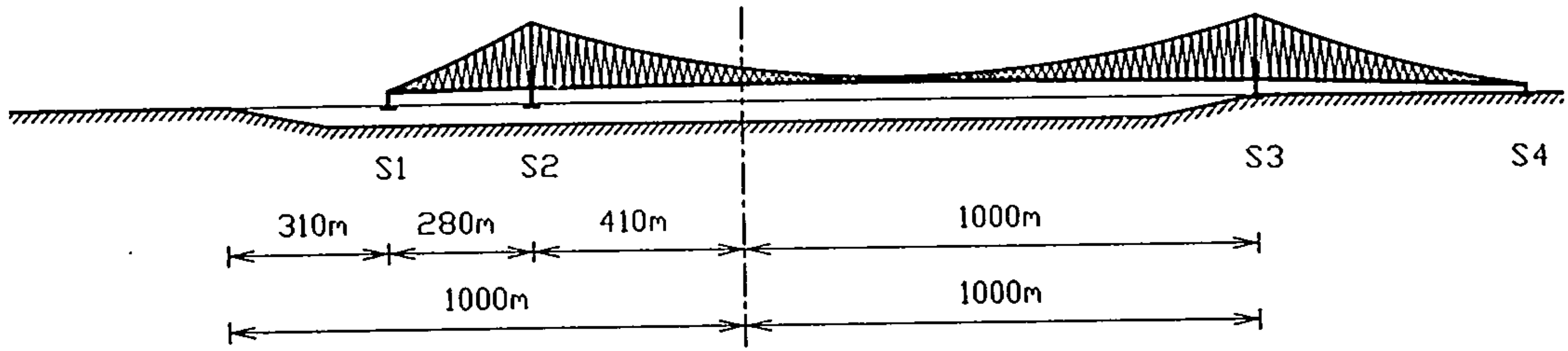

(a) Location of bridge supports in the valley

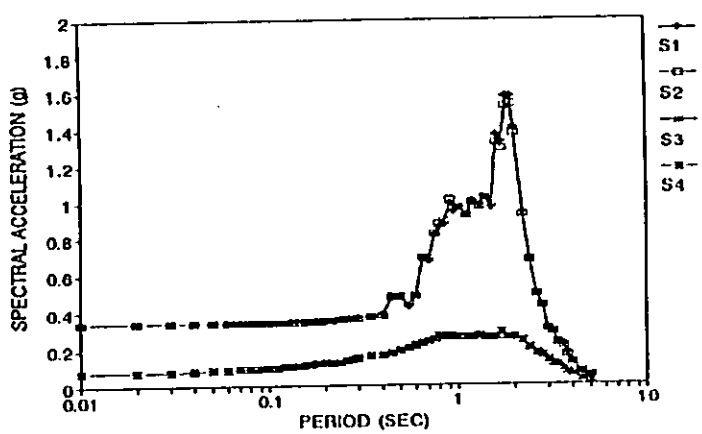

(b) Spectral accelerations of support motions
Soil profile (NC), a/v = V

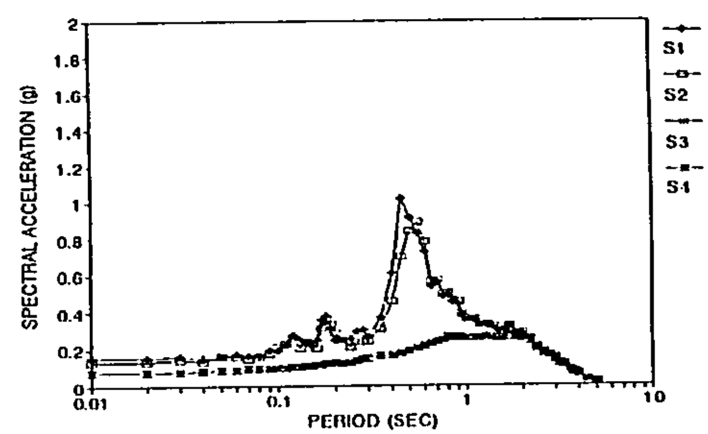

(c) Spectral accelerations of support motions
Soil profile (DS), a/v = V

Fig. 7-9 Excitation case 5

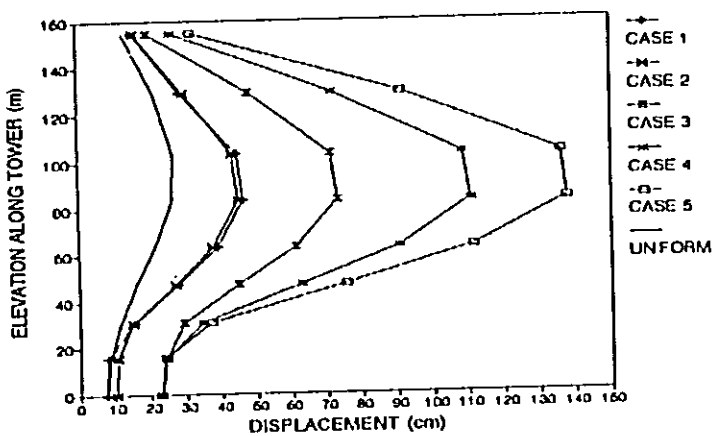

(a) Max. horizontal displacement of Hessle tower

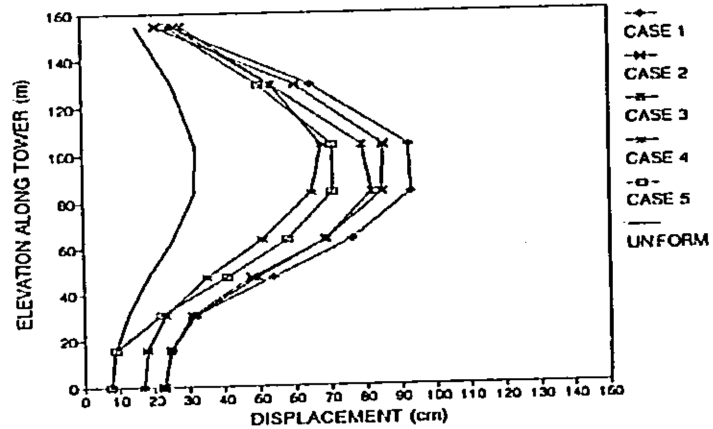

(b) Max. horizontal displacement of Barton tower

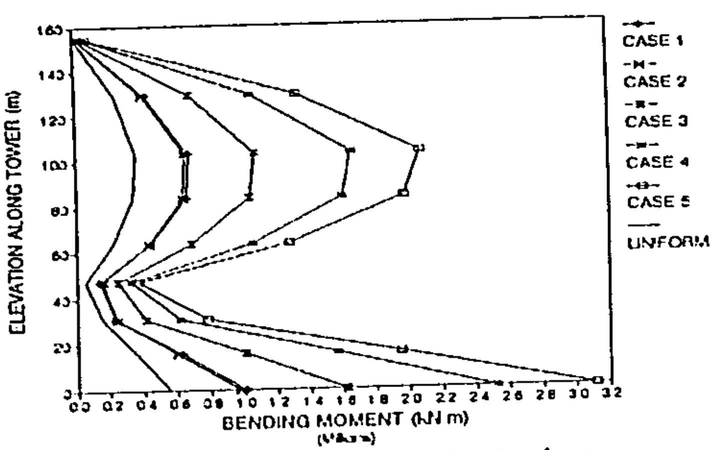

(c) Max. bending moment in Hessle tower

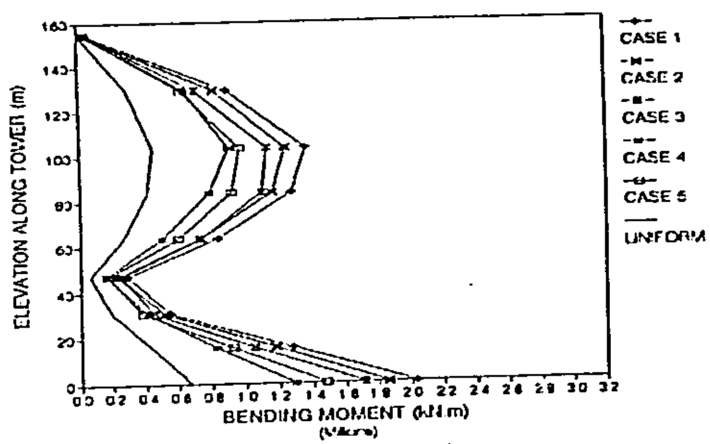

(d) Max. bending moment in Barton tower

Fig. 7-10 Total (dynamic + quasi-static) response of the towers
Soil profile (NC)

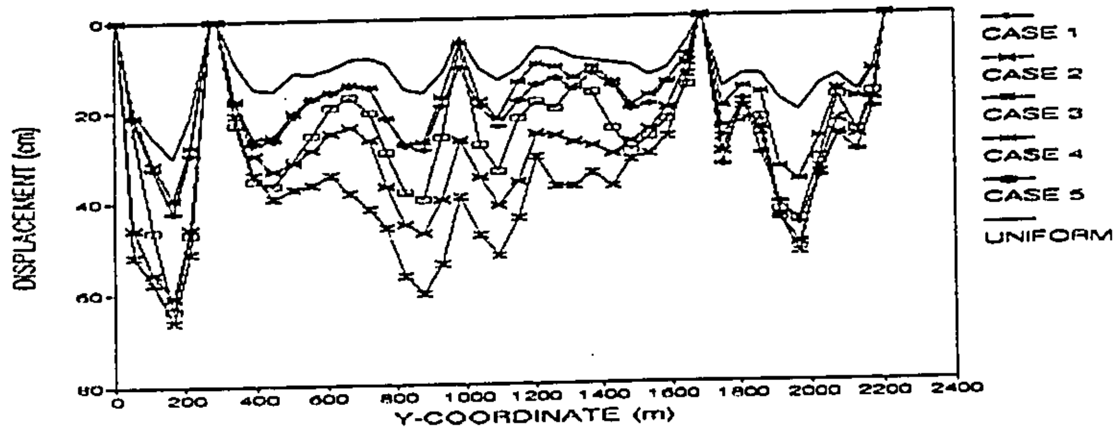

(a) Max. vertical displacement of the deck

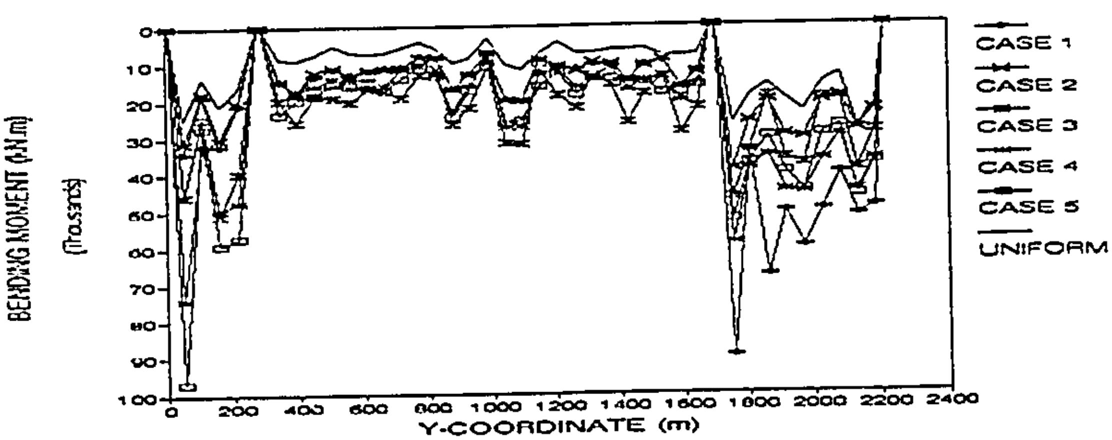

(b) Max. bending moment in the deck

Fig. 7-11 Total (dynamic + quasi-static) response of the deck
Soil profile (NC)

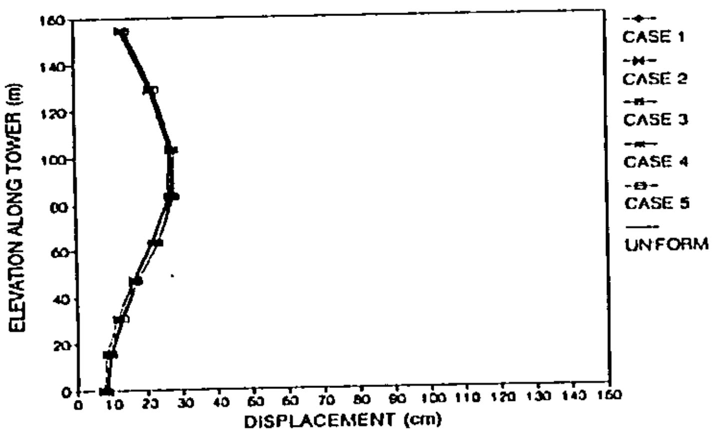

(a) Max. horizontal displacement of Hessle tower

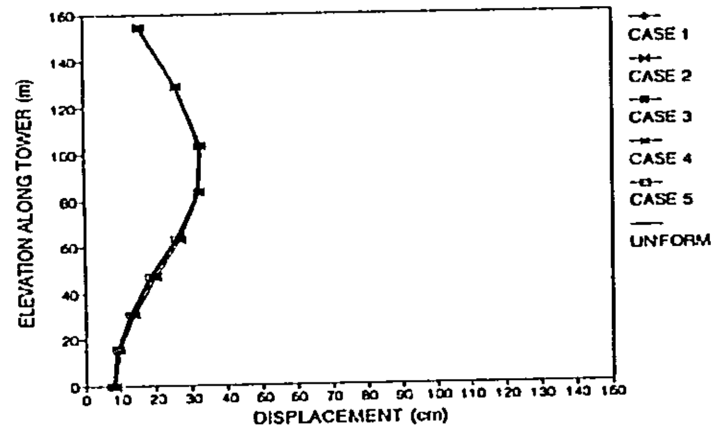

(b) Max. horizontal displacement of Barton tower

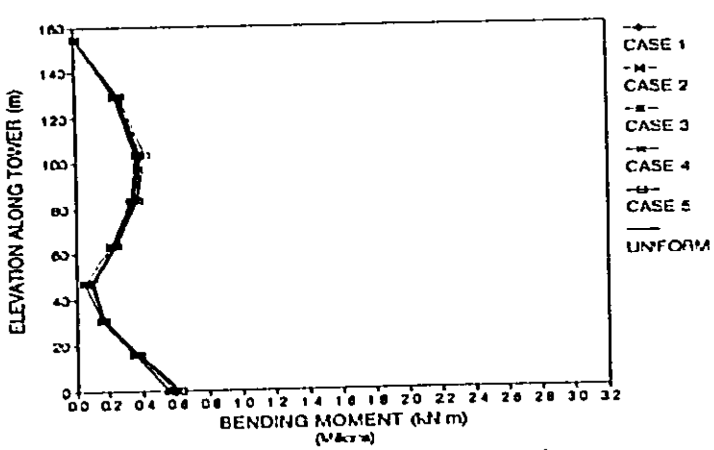

(c) Max. bending moment in Hessle tower

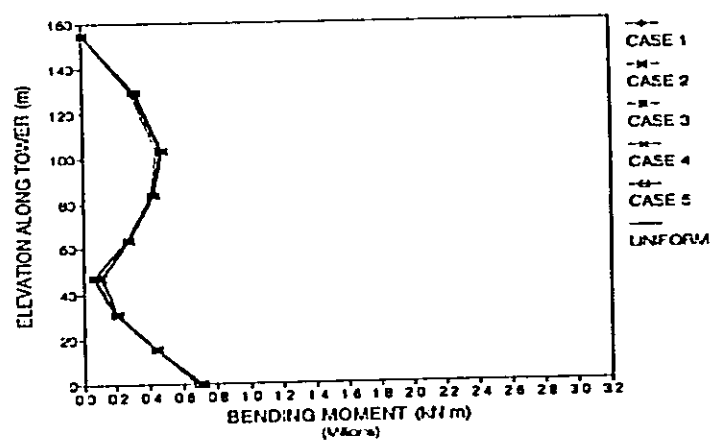

(d) Max. bending moment in Barton tower

Fig. 7-12 Total (dynamic + quasi-static) response of the towers
Soil profile (DS)

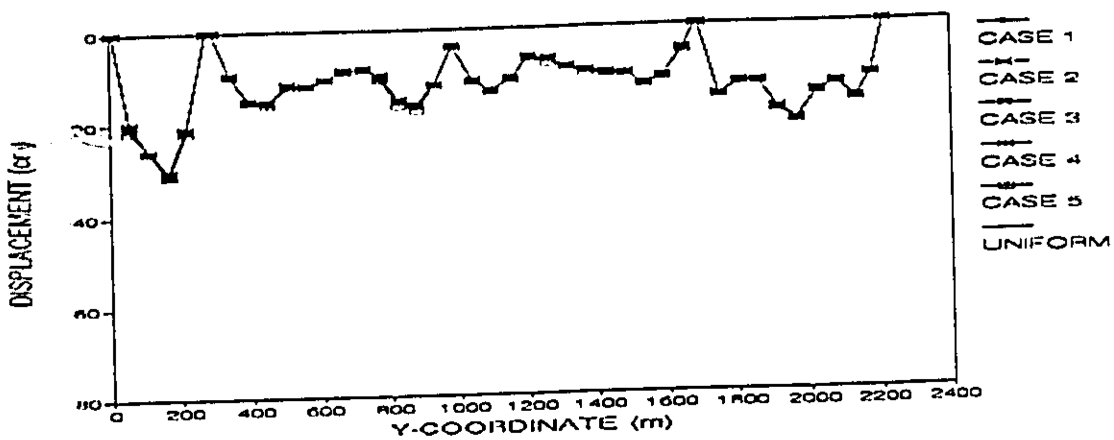

(a) Max. vertical displacement of the deck

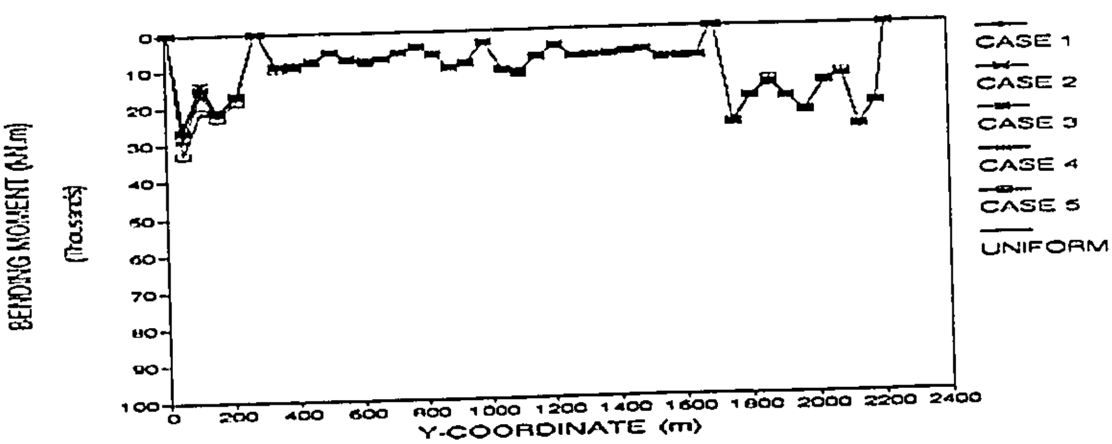

(b) Max. bending moment in the deck

Fig. 7-13 Total (dynamic + quasi-static) response of the deck
Soil profile (DS)

CHAPTER 8
SUMMARY AND CONCLUSIONS

8.1 SUMMARY

A study has been conducted on the seismic site response of alluvial valleys with limited width and the effects of spatially varying surface motions in these valleys on the response of a suspension bridge. The intent of this investigation was to extend the work carried out by seismologists on the two-dimensional seismic response of alluvial valleys to include the effects of stiffness variation with depth and non-linear behaviour of soils. These effects are of much interest to engineers but were mainly considered in a one-dimensional perspective. One objective of this study was to provide engineers with useful guidelines to predict the valley response at different sites, by identifying the main parameters governing the spatial variations of surface seismic motions in alluvial valleys and their influence on the response. Another objective was to develop more realistic multiple-support input motions to a suspension bridge using the computed valley surface motions which vary in amplitude and frequency as well as analyze the potential of soil conditions and subsurface topographic structure in alluvial valleys for producing significant variations in the bridge response.

The assumptions and methods of analysis of two existing engineering models of the valley problem were reviewed. The two models include the simple one-dimensional (1-D) model and the elaborate two-dimensional (2-D) finite-element model. Since a large amount of computation is involved in such parametric studies, a simplified engineering model (frame model) has been developed to predict the non-linear seismic response of symmetrical alluvial valleys which are bounded by rigid rock and have limited width.

The new model was introduced to compensate for the deficiency of the regular one-dimensional approach without sacrificing its simplicity. The separation of the valley mode shapes into variations with depth (the k-variations) and variations with the horizontal direction (the j-variations) led to the development of the model. To evaluate the horizontal valley response to a given horizontal rock motion, the frame model was obtained by replacing the second dimension of the valley by a set of horizontal axial links attached to the lumped masses of the one-dimensional model. The horizontal links introduce the effect of the limited valley width to the 1-D model by representing the lateral axial stiffness that arise due to the finite lateral extent of soil in plane.

SAP IV computer program was modified to accommodate the frame model and calculate the linear response using the modal analysis technique. The resulting motions from the frame model reflect the valley response at the centroidal axis. The response at other points in the valley can be obtained by utilizing the modal variations in the horizontal direction. The non-linear behaviour of soil was accounted for by using the equivalent linear method to ensure strain-compatible soil properties. The validity of the frame model was verified through the comparison of the results with those from the 2-D finite-element model.

The key parameters involved in characterizing the seismic response of alluvial valleys include the soil type, valley geometry and control motion characteristics in rock. Four soil types were selected for this study to cover the behaviour of soft soil profiles as well as stiff soil profiles with different properties. The symmetrical valley shape was simplified as a trapezoid with different dimensions, from wide and shallow to narrow and deep, along with different slopes of rock boundary at the valley edges.

The input control motion in the rock boundary of the alluvial valley was selected as a given accelerogram representing a horizontal or vertical component of excitation. Two characteristics of rock motion were of main concern in this study: the frequency content, represented by the ratio of peak acceleration to peak velocity, a/v, and the peak amplitude of motion, which was varied by changing the peak velocity, v. Three artificial time histories were generated to match three target spectra representative of three different a/v ratios: high (H), intermediate (I) and very low (V). The generated records were scaled to various levels of intensity corresponding to different values of peak velocity and used as input motions in the rigid rock.

The response results at different site locations in the valley were presented in the form of surface spectral accelerations and spectral ratios. The spectral acceleration is a measure of the intensity of surface motion while the spectral ratio defines the soil amplification of rock motion. The "local-amplification period" at a site is defined as the period at which the largest peak of amplification occurs at that site.

Finally, the free-field surface motions in a symmetric hypothetical valley were applied to the supports of the Humber suspension bridge in U.K. The purpose was to analyze the linear dynamic response of the bridge to simultaneous longitudinal excitations which vary in amplitude and frequency due to differences in soil patterns of amplification at different valley sites. This creates a multiple-support excitation condition in the bridge, which involves more realistic representation of the varying support motions. SAP IV computer program was modified to perform the multiple-support time-history analysis on the bridge, using the modal analysis technique. The analysis was performed for different soil conditions and support locations in the valley.

8.2 RESULTS AND GUIDELINES

The study of the frame model and its viability as a tool for evaluating the seismic site response of alluvial valleys shows the following results:

1. The proposed frame model can only compute one component of motion in soil in the same direction as the input component in rock (horizontal or vertical). This is

similar to the one-dimensional model. However, the proposed model accounts for the effect of the limited horizontal extent of soil in the valley.

2. Due to its simplicity, the frame model provides valuable insight into the dynamic behaviour of the alluvial valley by identifying the vibration modes of significance, their variations in the horizontal and vertical directions, and their contribution to the response. The number of modes that have significant participation in the response and the shapes of their k- and j-variations depend on the valley dimensions and the soil profile. The frame model selects those modes with major participation faster than does the finite-element model.

3. Response from the frame model shows good agreement at different surface locations in the valley when compared with the response based on the two-dimensional finite-element model.

4. Considerable saving in computing time can be achieved by using the frame model as compared to the finite-element model. This is mainly because the second dimension of the valley is represented by a large mesh in the case when finite element is used, while it is only represented by links in the frame model.

Based on the sensitivity analysis of the horizontal seismic response of the valley to variation in the soil-layer discretization and variation in the dynamic soil properties, the following results can be used as useful guidelines:

5. The surface seismic motions proved not to be sensitive to the soil-layer models of discretization, used in this analysis. A finer discretization may be replaced by a coarser one without losing significant accuracy.

6. The variation in the G_o profile (stiffness) leads to significant changes in the local-amplification periods and minor changes in the magnitudes of spectral ratio peaks. On the other hand, the variation in the damping-strain relationship for the same soil type causes significant changes in the amplification values and hardly any noticeable

shifts in the local-amplification periods at sites.

7. Higher G_o values result in shorter local-amplification periods due to larger stiffness and slightly higher peaks of amplification because of lower values of associated damping. Softer soil profiles are more sensitive to variations in G_o values.
8. For a stiffer soil formation, the valley edge sites are less sensitive to the damping variation than the sites near the middle.

Based on the investigation of the influence of valley dimensions on the seismic site response at different surface locations, the following guidelines can be concluded:

9. The local-amplification periods at different surface locations in the valley are more susceptible to the change in the underlying depth of soil than to the change in other dimensions of the valley.
10. Increasing the valley depth, d, leads to longer local-amplification periods due to the decrease in the overall stiffness.
11. The effects of variations in the breadth, B, or the length of the sloping rock boundary, L, on the fundamental period become noticeable only in the case of narrow valleys. In such case, a decrease in B or increase in L results in a lower fundamental period of the valley due to the added lateral stiffness.
12. The focusing of the incoming waves from the two sloping edges toward the valley centre results in increased amplification as the middle of the valley is approached from the edge. The distance from the site where the highest wave focusing effect takes place to the edge increases as the ratio L/B and/or the depth d increase. Beyond this site, as the valley centre is approached, the focusing effect diminishes and the amplification decreases slightly for a distance, after which the amplification remains unaltered and the one-dimensional approach may apply.
13. The local-amplification periods at valley edge sites are shorter due to the stiffening effect from the sloping rock boundary. This results in larger amplification of the

higher modes at sites near the edge.

14. The soil amplification at edge sites in the valley is independent of the breadth B. It is rather a function of the underlying depth of soil and slope of rock, since edge sites are mainly affected by the incoming waves from the surrounding area.
15. The top layers of smaller depths of stiff soil are associated with lower damping values which lead to larger amplification of the higher modes. In soft soil, larger depths are associated with softer top layers which result in larger amplification of the higher modes.
16. The surface locations where the 1-D model provides a poor approximation of the response are those where the effect of the sloping edge of valley is significant. Consequently, the one-dimensional approach may be used, in shallow and wide valleys with $B/d \geq 10$ and $B/L \geq 2$, to obtain the surface response at sites located at least 10 times the depth d, away from the valley edge.

Based on the evaluation of the influence of soil type and rock motion variations on the seismic site response of the valley, the following guidelines can be indicated:

17. The soil amplification varies from one soil type to another, depending on the stiffness of soil and the amount of damping existing during excitation. Softer soil profiles and lower damping values produce higher magnitudes of amplification peaks. Stiffer soil profiles lead to shorter local-amplification periods at various sites.
18. The magnitude of the spectral acceleration peak depends on the local-amplification period at the site and its proximity to the dominant period of the input rock record. The closer the two periods are, the more intense the soil surface motion is. As a consequence, the lowest intensity of surface motion occurs in soft soil sites when they are subjected to rock motion with high frequency content and in stiff soil sites when the rock motion has a very low frequency content.
19. As the intensity of motion in soil increases, higher shear strains are developed

leading to higher damping values and more softening of soil. The higher damping causes lower amplification of rock motion and the lower stiffness results in longer local-amplification periods at sites.

20. The edge sites of valleys with stiff soil are more vulnerable than the centre sites to rock excitations with high a/v ratio because the local-amplification periods at edge sites are closer to the dominant period of the high a/v rock records. This leads to higher intensity of surface motions near the edge.
21. For a stiff soil profile under a very low a/v input record, the intensity of surface motion is higher near the middle of the valley. This is because the local-amplification period near the middle is closer to the dominant period of the very low a/v record.
22. Under the assumption of travelling excitation in rock, the surface spectral accelerations are lower than those resulting from the case of uniform rock excitation. This is because speeds of propagation less than infinity make the input motions at different points along the rock boundary less likely to be in phase.

Based on the multiple-support excitation analysis of the Humber suspension bridge in this study, the following guidelines can be deduced:

23. Excitation of the bridge supports in the longitudinal direction induces vertical as well as longitudinal displacements in the bridge elements because of the close coupling between the vertical and longitudinal modes of vibration.
24. The inclusion of the multiple-support excitation case in the bridge analysis is significant when there are noticeable variations in the intensity of support motions in the period range of interest for the bridge response ($T > 1.5$ s), as in the case when some bridge supports are on soft soil. The stiff soil does not alter the motion amplitudes at any surface location in this range of periods and thus does not create a significant multiple-support excitation case for the Humber bridge.

25. If the support motions are of equal intensity in the period range of interest for the bridge response, a multiple-support excitation case should only be considered when the input support motions are not in phase.
26. In the case when the bridge is supported on soft soil, supports which are located near the valley centre are subjected to surface motion with higher intensity in the long-period range. This causes more critical values of response in the tower or the side span of the bridge which is closer to the middle of the valley.
27. The most critical excitation case for the main span occurs when the two towers of the Humber bridge are both subjected to the highest intensity of surface motion. This occurs when the two towers are at about equal distances on both sides from the centre line of the valley with soft soil profile.

8.3 CONCLUSIONS

The present investigation of the seismic site response of alluvial valleys and effects on the dynamic analysis of a suspension bridge leads to the following conclusions:

1. The limitations on the use of one-dimensional approach to obtain the free-field motions in valleys with limited width were demonstrated.
2. A simple engineering model, that accounts for the effect of the valley limited width, is developed to evaluate the non-linear seismic response of a sedimentary valley. The new model provides more physical insight into the valley dynamic behaviour. Response from the model was verified against the 2-D finite element solution.
3. The valley dimensions, soil type and input rock motion characteristics were found to have significant effects on the valley response.
4. Soil type, site topography and the location of the supports of a long-span suspension bridge in a valley are all factors that must be considered for more realistic evaluation of the ground motions affecting the bridge.

8.4 RECOMMENDATIONS

Further work is still needed to enhance the understanding of the seismic behaviour of alluvial valleys and the accuracy of the analytical models in predicting the spatial variations of surface motions in such valleys and their effects on the design of long structures. The following aspects require further investigation:

1. Analysis of the effects of the elasticity of rock base formation on the alluvial valley response.
2. Identification of the contribution of various seismic waves which propagate with different velocities and angles of incidence to the characteristics of a given control motion at the rock boundary and their effect on the soil amplification.
3. Study of the variations in excitations at different points along the rock boundary that arise due to the differences in seismic wave propagation. The effects of non-uniform rock motion on the seismic site response in wide valleys are to be examined.
4. Investigation of the influence of the valley parameters on the duration of strong-phase shaking of surface motions at different locations.
5. Consideration of the three-dimensional subsurface structure of the valley, particularly when it has a limited out-of-plane dimension. The double curvature of the sediment-rock interface is expected to lead to three-dimensional resonance patterns which increase the amplitude of motion, especially near the centre of the valley due to more focusing of the seismic energy.
6. Analysis of recorded data from instrumented alluvial valleys to check the validity of assumptions and results from the analytical models when applied to the same valleys, considering their actual shapes.
7. Incorporation of the variations in site and topographical effects in the design of long-span bridges.

REFERENCES

Abdel-Ghaffar, A.M. and Rubin, L.I. 1983a. "Vertical seismic behaviour of suspension bridges," International Journal of Earthquake Engineering and Structural Dynamics, Vol.11, pp.1-19.

Abdel-Ghaffar, A.M. and Rubin, L.I. 1983b. "Lateral earthquake response of suspension bridges," Journal of Structural Engineering, ASCE, Vol.109, pp.664-675.

Abdel-Ghaffar, A.M. and Stringfellow, R.G. 1984a. "Response of suspension bridges to travelling earthquake excitations: Part I. Vertical response," Soil Dynamics and Earthquake Engineering, Vol.3, pp.62-72.

Abdel-Ghaffar, A.M. and Stringfellow, R.G. 1984b. "Response of suspension bridges to travelling earthquake excitations: Part II. Lateral response," Soil Dynamics and Earthquake Engineering, Vol.3, pp.73-81.

Abdel-Ghaffar, A.M. and Trifunac, M.D. 1977. "Antiplane dynamic soil-bridge interaction for incident plane SH-waves," International Journal of Earthquake Engineering and Structural Dynamics, Vol.5, pp.107-129.

Aki,K. 1988. "Local site effects on ground motion," in Earthquake Engineering and Soil Dynamics II- Recent Advances in Ground Motion Evaluation, J.L. Von. Thun (Editor), Geotechnical Special Publication No.20, ASCE, New York, pp. 103-155.

Aki, K. and Larner, K.L. 1970. "Surface motion of a layered medium having an irregular interface due to incident plane SH waves," Journal of Geophysical Research, Vol.75, pp.933-954.

Altinisik, D. and Severn, R.T. 1981. "Multiple-support and asynchronous base excitation of structures," Proceedings of the Institution of Civil Engineers, London, Vol.71, pp.407-426.

Astaneh, A., Bertero, V.V., Bolt, B.A., Mahin, S.A., Moehle, J.P. and Seed, H.B. 1990. "Preliminary report on the seismological and engineering aspects of the October 17, 1989 Santa Cruz (Loma Prieta) earthquake," Report No. EERC 89-14, Earthquake Engineering Research Center, University of California, Berkeley, California.

Bard, P.Y. and Bouchon, M. 1980a. "The seismic response of sediment-filled valleys, Part I. The case of incident SH waves," Bulletin of the Seismological Society of

America, Vol.70, pp.1263-1286.

Bard, P.Y. and Bouchon, M. 1980b. "The seismic response of sediment-filled valleys, Part II. The case of incident P and SV waves," Bulletin of the Seismological Society of America, Vol.70, pp.1921-1941.

Bard, P.Y. and Bouchon, M. 1985. "The two-dimensional resonance of sediment-filled valleys," Bulletin of the Seismological Society of America, Vol.75, pp.519-541

Bard, P.Y., Campillo, M., Chaves-Garcia, F.J. and Sanchez-Sesma, F.J. 1988. "The Mexico earthquake of September 19, 1985: A theoretical investigation of large and small amplification effects in the Mexico City Valley," Earthquake Spectra, Vol.4, pp.609-633.

Bard, P.Y. and Gariel, J.C. 1986. "The seismic response of two-dimensional sedimentary deposits with large vertical velocity gradients," Bulletin of the Seismological Society of America, Vol.76, pp.343-366.

Bathe, K.J., Wilson, E.L. and Peterson, F.E. 1973. "SAP IV : A structural analysis program for static and dynamic response of linear systems," Report No. EERC 73-11, Earthquake Engineering Research Center, University of California, Berkeley, California.

Bogdanoff, J.L. Goldberg, J.E. and Schiff, A.J. 1965. "The effect of ground transmission time on the response of long structures," Bulletin of the Seismological Society of America, Vol.55, pp.627-640.

Bravo, M.A., Sanchez-Sesma, J. and Chaves-Garcia, F.J. 1988. "Ground motions on stratified alluvial deposits for incident SH waves," Bulletin of the Seismological Society of America, Vol.78, pp.436-450.

Clough, R.W. and Chopra, A.K. 1966. "Earthquake stress analysis in earth dams," Journal of the Engineering Mechanics Division, ASCE, Vol.92, No.EM2, pp.197-211.

Clough, R.W. and Penzien, J. 1975. "Dynamics of structures," McGraw Hill, New York.

Cooley, J.W. and Tukey, J.W. 1965. "An algorithm for the calculation of complex Fourier series," Mathematics of Computation, Vol.19, No.90, pp.297-301.

Der Kiureghian, A. and Neuenhofer, A. 1992. "Respnse spectrum method for incoherent support motions," Proceedings of the Tenth World Conference on Earthquake Engineering, Spain, Vol.8, pp.4757-4762.

Desai, C. and Christian, J.T. 1977. "Numerical methods in geotechnical engineering," McGraw Hill, New York.

Dibaj, M. and Penzien, J. 1969. "Nonlinear seismic response of earth structures," Report No. EERC 69-2, Earthquake Engineering Research Center, University of California, Berkeley, California.

Dravinski, M. 1983. "Amplification of P, SV and Rayleigh waves by two alluvial valleys," Soil Dynamics and Earthquake Engineering, Vol.2, pp.66-77.

Dumanoglu, A.A. 1987. Private Communication from "Dr. A.A. Dumanoglu," Department of Civil Engineering, Karadeniz Technical University, Trabzon, Turkey.

Dumanoglu, A.A. and Severn, R.T. 1984. "Dynamic response of dams and other structures to differential ground motions," Proceedings of the Institution of Civil Engineers, London, Vol.71, pp.333-352.

Dumanoglu, A.A. and Severn, R.T. 1985a. "Asynchronous seismic analysis of modern suspension bridges, Part I: Free vibration," Research Report, Department of Civil Engineering, University of Bristol, Bristol, United Kingdom.

Dumanoglu, A.A. and Severn, R.T. 1985b. "Asynchronous seismic analysis of modern suspension bridges, Part II: Response to travelling vertical ground motion," Research Report, Department of Civil Engineering, University of Bristol, Bristol, United Kingdom.

Dumanoglu, A.A. and Severn, R.T. 1985c. "Asynchronous seismic analysis of modern suspension bridges, Part III: Response to travelling longitudinal ground motion," Research Report, Department of Civil Engineering, University of Bristol, Bristol, United Kingdom.

Dumanoglu, A.A. and Severn, R.T. 1985d. "Asynchronous seismic analysis of modern suspension bridges, Part IV: Response to travelling lateral ground motion," Research Report, Department of Civil Engineering, University of Bristol, Bristol, United Kingdom.

Dumanoglu, A.A. and Severn, R.T. 1990. "Stochastic response of suspension bridges to earthquake forces," International Journal of Earthquake Engineering and Structural Dynamics, Vol.19, pp.133-152.

Elhmadi, K., Heidebrecht, A.C. and Hosni, S. 1990. "Parametric study of seismic site response effects," EERG Report 90-01, Earthquake Engineering Research Group, McMaster University, Hamilton, Ontario.

Faccioli, E. 1991. "Seismic amplification in the presence of geological and topographic irregularities," Proceedings of the second International Conference on Recent Advances in Geotechnical Earthquake Engineering and Soil Dynamics, St. Louis, Missouri, Vol.II, pp. 1779-1797.

Finn, W.D. 1991. "The effects of site conditions on ground motions," Proceedings of the Sixth Canadian Conference on Earthquake Engineering, Toronto, Ontario, pp.17-33.

Finn, W.D. and Nichols, A.M. 1988. "Seismic response of long-period sites: Lessons from the September 19, 1985 Mexican Earthquake," Canadian Geotechnical Journal, Vol.25, pp.128-137.

Gutenberg, B. 1957. "Effects of ground on earthquake motion," Bulletin of the Seismological Society of America, Vol.47, pp. 221-250.

Hanks, T.C. 1975. "Strong ground motion of San Fernando, California, earthquake ground displacements," Bulletin of the Seismological Society of America, Vol.65, pp.193-225.

Hao, H. 1989. "Effects of spatial variation of ground motions on large multiply-supported structures," Report No. EERC 89-06, Earthquake Engineering Research Center, University of California, Berkeley, California.

Harmsen, S.C. and Harding, S.T. 1981. "Surface motion over a sedimentary valley for incident plane P and SV waves," Bulletin of the Seismological Society of America, Vol.72, pp.655-670.

Haskell, N.A. 1960. "Crustal reflection of plane SH waves," Journal of Geophysical Research, Vol.65, pp.4147-4150.

Haskell, N.A. 1962. "Crustal reflection of plane P and SV waves," Journal of Geophysical Research, Vol.67, pp.4751-4767.

Heidebrecht, A.C., Henderson, P., Naumoski, N. and Pappin, J.W. 1990. "Seismic response and design for structures located on soft clay sites," Canadian Geotechnical Journal, Vol.27, pp.330-341.

Henderson, P., Heidebrecht, A.C., Naumoski, N. and Pappin, J.W. 1989a. "Site response study - Methodology, calibration and verification of computer programs," EERG Report 89-01, Earthquake Engineering Research Group, McMaster University, Hamilton, Ontario.

Henderson, P., Heidebrecht, A.C., Naumoski, N. and Pappin, J.W. 1989b. "Site response study - Presentation of results," EERG Report 89-03, Earthquake Engineering Research Group, McMaster University, Hamilton, Ontario.

Henderson, P., Heidebrecht, A.C., Naumoski, N. and Pappin,J.W. 1990. "Site response effects for structures located on sand sites," Canadian Geotechnical Journal, Vol.27, pp.342-354.

Hong, T.L. and Helmberger, D.V. 1977. "Glorified optics and wave propagation in non-planar structures," Bulletin of the Seismological Society of America, Vol.68, pp.1313-1330.

Huang, M. 1984. "Investigation of local geology effects on strong earthquake ground motions," Report EERL 83-03, Earthquake Engineering Research Laboratory, California Institute of Technology, Pasadena, California.

Idriss, I.M. 1978. "Characteristics of earthquake ground motions," Proceedings of the ASCE Conference on Earthquake Engineering and Soil Dynamics, Pasadena, California, pp.1151-1265.

Idriss, I.M., Lysmer, J., Hwang, R. and Seed, H.B. 1973. "QUAD-4 : A computer program for evaluating the seismic response of soil structures by variable damping finite element procedures," Report No. EERC 73-16, Earthquake Engineering Research Center, University of California, Berkeley, California.

Idriss, I.M. and Seed, H.B. 1966. "The response of earth banks during earthquakes," Research Report, Soil Mechanics and Bituminous Materials, Research Laboratory, University of California, Berkeley, California.

Idriss, I.M. and Seed, H.B. 1968. "Seismic response of horizontal soil layers," Journal of the Soil Mechanics and Foundations Division, ASCE, Vol.94, pp.1003-1031.

Joyner, W.B. 1975. "A method for calculating nonlinear seismic response in two dimensions," Bulletin of the Seismological Society of America, Vol.65, pp.1337-1357.

Joyner, W.B. and Chen, A.T.F. 1975. "Calculation of nonlinear ground motion response in earthquakes," Bulletin of the Seismological Society of America, Vol.65, pp.1315-1336.

Kanai, K. 1952. "Relation between the nature of surface layer and the amplitudes of earthquake motions," Bulletin of Earthquake Research Institute, Tokyo, Vol.30, pp.31-37.

Khair, K.R., Datta, S.K. and Shah, A.H. 1989. "Amplification of obliquely incident seismic waves by cylindrical alluvial valleys of arbitrary cross-sectional shape. Part I: Incident P and SV waves," Bulletin of the Seismological Society of America, Vol.79, pp.610-630.

Khair, K.R., Datta, S.K. and Shah, A.H. 1991. "Amplification of obliquely incident seismic waves by cylindrical alluvial valleys of arbitrary cross-sectional shape. Part II: Incident SH and Rayleigh waves," Bulletin of the Seismological Society of America, Vol.81, pp.346-357.

King, J.L. and Tucker, B.E. 1984. "Observed variations of earthquake motion over a sediment-filled valley," Bulletin of the Seismological Society of America, Vol.74, pp.137-152.

Lee, V.W. 1984. "Three-dimensional diffraction of plane P, SV and SH waves by a hemispherical alluvial valley," Soil Dynamics and Earthquake Engineering, Vol.3, pp. 133-144.

Lysmer, J., Udaka, T., Tsai, C. and Seed, H.B. 1975. "FLUSH : A computer program for approximate 3-D analysis of soil-structure interaction problems," Report No. EERC 75-30, Earthquake Engineering Research Center, University of California, Berkeley, California.

National Building Code of Canada. 1990, Associate Committee on the National Building Code, National Research Council of Canada, Ottawa, Ontario.

Naumoski, N. 1985. Private Communication from "Dr. Nove Naumoski," Department of Civil Engineering and Engineering Mechanics, McMaster University, Hamilton, Ontario.

Naumoski, N., Tso, W.K. and Heidebrecht, A.C. 1988. "A selection of representative strong motion earthquake records having different a/v ratios," EERG Report 88-01, Earthquake Engineering Research Group, McMaster University, Hamilton, Ontario.

Newmark, N.M. and Rosenblueth, E. 1971. "Fundamentals of earthquake engineering," Prentice-Hall, Englewood Cliffs, N.J.

Ohtsuki, A. and Harumi, K. 1983. "Effect of topography and subsurface inhomogeneities on seismic SV waves," International Journal of Earthquake Engineering and Structural Dynamics, Vol.11, pp.441-462.

Pappin, J.W., Heidebrecht, A.C., Henderson, P. and Naumoski, N. 1989. "Site response study - Soil modelling," EERG Report 89-02, Earthquake Engineering Research Group, McMaster University, Hamilton, Ontario.

Pyke, R. 1979. "Non-linear soil models for irregular cyclic loadings," Journal of the Geotechnical Engineering Division, ASCE, Vol.105, pp.715-726.

Rassem, M., Heidebrecht, A.C. and Ghobarah, A. 1990. "Approximate spectral multiple-support analysis applied to the Humber suspension bridge," Proceedings of the

1990 Annual Conference of the Canadian Society for Civil Engineering, Hamilton, Ontario, Vol. IV-1, pp.27-38.

Roesset, J.M., Whitman, R.V. and Dobry, R. 1973. "Modal analysis for structures with foundation interaction," Journal of the Structural Division, ASCE, Vol.99, No.ST3, pp.399-416.

Romo, M.P. and Seed, H.B. 1986. "Analytical modelling of dynamic soil response in the Mexico earthquake of September 19, 1985," Proceedings of International Conference on the 1985 Mexico Earthquake, pp.148-162.

Rutenberg, A. and Heidebrecht, A.C. 1987. "Approximate spectral multiple-support seismic analysis: Travelling wave approach," Research report, Department of Civil Engineering, McMaster University, Hamilton, Ontario.

Sanchez-Sesma, F.J. 1987. "Site effects on strong ground motion," Soil Dynamics and Earthquake Engineering, Vol.6, pp.124-132.

Sanchez-Sesma, F.J., Chaves-Garcia, F.J. and Bravo, M.A. 1988. "Seismic response of a class of alluvial valleys for incident SH waves," Bulletin of the Seismological Society of America, Vol.78, pp.83-95.

Sanchez-Sesma, F.J. and Esquivel, J.A. 1979. "Ground motion on alluvial valleys under incident plane SH waves," Bulletin of the Seismological Society of America, Vol.69, pp.1107-1120.

Schnabel, P.B., Lysmer, J. and Seed, H.B. 1972. "SHAKE : A computer program for earthquake response analysis of horizontally layered sites," Report No. EERC 72-12, Earthquake Engineering Research Center, University of California, Berkeley, California.

Seed, H.B. 1986. "Influence of local soil conditions on ground motions and building damage during earthquakes," The eighth Nabor Carrillo Lecture, Presented at the Mexican Society for Soil Mechanics XIII National Meeting, Mazatlan, Sinaloa, Mexico.

Seed, H.B., Dezfulian, H. and Idriss, I.M. 1970. "Relationships between soil conditions and building damage in the Caracas earthquake of July 29, 1967," Report No. EERC 70-2, Earthquake Engineering Research Center, University of California, Berkeley, California.

Seed, H.B. and Idriss, I.M. 1969. "Influence of soil conditions on ground motions during earthquakes," Journal of the Soil Mechanics and Foundations Division, ASCE, Vol.95, pp.99-137.

Seed, H.B. and Idriss, I.M. 1970. "Soil moduli and damping factors for dynamic response analysis," Report No. EERC 70-10, Earthquake Engineering Research Center, University of California, Berkeley, California.

Seed, H.B., Romo, M.P., Sun, J., Jaime, A. and Lysmer, J. 1987. "Relationship between soil conditions and earthquake ground motions in Mexico City in the earthquake of September 19, 1985," Report No. EERC 87-15, Earthquake Engineering Research Center, University of California, Berkeley, California.

Seed, H.B., Whitman, R.V., Dezfulian, H., Dobry, R. and Idriss, I.M. 1972. "Soil conditions and building damage in 1967 Caracas earthquake," Journal of the Soil Mechanics and Foundations Division, ASCE, Vol.98, pp.787-806.

Silva, W. 1976. "Body waves in a layered anelastic solid," Bulletin of the Seismological Society of America, Vol.66, pp.1539-1554.

Thomson, W.T. 1950. "Transmission of elastic waves through a stratified solid medium," Journal of Applied Physics, Vol.21, pp.89-93.

Trifunac, M.D. 1971. "Surface motion of a semi-cylindrical alluvial valley for incident plane SH waves," Bulletin of the Seismological Society of America, Vol.61, pp.1755-1770.

Tsai, N.C. and Housner, G.W. 1970. "Calculation of surface motions of a layered half-space," Bulletin of the Seismological Society of America, Vol. 60, pp.1625-1651.

Tucker, B.E. and King, J.L. 1984. "Dependence of sediment-filled valley response on input amplitude and valley properties," Bulletin of the Seismological Society of America, Vol.74, pp.153-166.

Uebayashi, H., Takeuchi, Y. and Horike, M. 1992. "Study on characteristics of near-field seismic motions in a three-dimensional sedimentary basin due to a fault source using Aki and Larner method," Proceedings of the Tenth World Conference on Earthquake Engineering, Spain, Vol.2, pp.751-756.

Valera, J.E., Seed, H.B., Tsai, C.F. and Lysmer, J. 1977 "Seismic soil-structure interaction effects at Humboldt Bay power plant," Journal of the Geotechnical Engineering Division, ASCE, Vol.103, pp.1143-1161.

Vidale, J.E. and Helmberger, D.V. 1988. "Elastic finite-difference modelling of the 1971 San Fernando, California, earthquake," Bulletin of the Seismological Society of America, Vol.78, pp.122-141.

Werner, S.D., Lee, L.C., Wong, H.L. and Trifunac, M.D. 1979. "Structural response to travelling seismic waves," Journal of the Structural Division, ASCE, Vol.105, pp.2547-2564.

Wolf, J.P. 1985. "Dynamic soil-structure interaction," Prentice Hall, Englewood Cliffs, New Jersey.

Wong, H.L. 1982. "Effect of surface topography on the diffraction of P, SV and Rayleigh waves," Bulletin of the Seismological Society of America, Vol.72, pp.1167-1183.

Wong, H.L. and Trifunac, M.D. 1974. "Surface motion of a semi-elliptical alluvial valley for incident plane SH waves," Bulletin of the Seismological Society of America, Vol.64, pp.1389-1408.

Zahradnik, J. and Hron, F. 1987. "Seismic ground motion of sedimentary valleys: Example La Molina, Lima, Peru," Journal of Geophysics, Vol.62., pp.31-37.

APPENDIX I

INPUT DATA TO THE MODIFIED SAP IV PROGRAM FOR THE MULTIPLE - SUPPORT EXCITATION ANALYSIS

Five input data files are required for the multiple-support excitation analysis using the modified SAP IV computer program. These files include the main file SAP.DAT and four auxiliary new data files: SUPT.DAT, ELMT.DAT, DISP.DAT and ACCL.DAT.

I.1 MAIN INPUT FILE

The main input file SAP.DAT consists of two parts: static analysis input data (NDYN=0) followed by dynamic analysis input data (NDYN=2) for the given structural system. NDYN is the analysis type code defined in the master control card data in SAP IV user's guide (Bathe et al, 1973). Data for static or dynamic analysis is as given in the user's guide except for minor modifications that are required for the dynamic analysis input. The static analysis is performed to obtain the quasi-static influence matrix [R]. This is achieved by attaching axial-stiffness springs to the supports in the direction of the input excitation to allow the specification of unit displacements at these supports in that direction. The springs can be provided in the input file at the support positions using element type 7 data in SAP IV user's guide. The number of static load cases is equal to the number of degrees of freedom specified as unit displacements at the supports.

The dynamic analysis is carried out by mode superposition for the same structural system (with no springs attached to the supports). Some modifications are required in the input data provided for the dynamic analysis in SAP IV user's guide:

1. A number of ground motion control cards (VII.B.3 in the user's guide) should

be supplied equal to the number of support nodal points which are excited by ground motion.

2. The number (NLP) of time function definition points (VII.B.5.a in the user's guide) should be the same for all input acceleration time histories at the supports.

I.2 AUXILIARY DATA FILES

I.2.1 SUPT.DAT

The input file SUPT.DAT contains the support nodal point numbers which are excited by ground motion. The numbers may be punched in free format.

I.2.2 ELMT.DAT

The input data in ELMT.DAT is used by the program for the calculation of the quasi-static component of stress only in beam elements which have one of their end nodes as a support nodal point excited by ground motion. The input file has the following data which can be read in free format:

1. NELTOT
2. For I = 1 to NELTOT provide cards with the following data

   NELMT(I), NDG(I), (QD(I,J), J=1, NFN)

in which,

NELTOT = total number of beam elements that are requested for stress output and have one of their end nodes as a support nodal point excited by ground motion. If NELTOT = 0, this data file is skipped

NELMT(I) = Beam element number

NDG(I) = degree of freedom (DOF) local number that has been attached to a spring (i.e. released) during the static analysis phase (1 to 12; 6 DOF at each node)

NFN = number of static load cases

QD(I,J) = static displacement (unit or zero) associated with NDG(I) from different static load cases

I.2.3 DISP.DAT

The input file DISP.DAT contains a number of sets of data equal to the number of support nodal points which are excited by ground motion. Each set has the following data which can be read in free format:

1. Scaling factor to convert the time-history data into the required units or scale the record.
2. Ground displacement time-history data at one support which should be provided at equal intervals.

I.2.4 ACCL.DAT

The data format in the input file ACCL.DAT is similar to that in DISP.DAT except that the ground acceleration data replaces the ground displacement data. The data in DISP.DAT and ACCL.DAT is used only to calculate the quasi-static component of response.

the effect of the model discretization on the response, the soil thickness, 40 m, is divided as shown in Fig. 4-1 into:

(a) 10 layers (10 x 4 m = 40 m)

(b) 27 layers (10 x 1 m + 8 x 1.5 m + 9 x 2 m = 40 m)

The surface response is mainly affected by the top soil-layer thicknesses, since they are the softest layers, rather than the number of layers. The purpose of the 27-layer discretization is to reflect the effect of top layers on the response by using smaller thicknesses.

The resulting surface acceleration spectral ratios using the above two discretization schemes with the frame model are compared in Fig. 4-2. It is evident that the 10-layer and the 27-layer discretization produce more or less the same amplification at the soil surface regardless of the a/v ratio of the input rock motion or the location of the surface point in the valley. However, the finer top layers, in the 27-layer case capture and amplify the response from the higher modes of the valley which increases the amplification slightly more than in the 10-layer case, particularly in the short-period range, below the local-amplification period of the site.

The resulting amplification from the frame model is compared with those from the 1-D and 2-D models in Fig. 4-3 for the 27-layer discretization using the generated rock acceleration with a/v = V and in Fig. 4-4 for the 10-layer discretization using the generated rock acceleration with a/v = I. While the agreement is good between the frame and the two-dimensional models at different surface locations, the 1-D analysis, that ignores the limited lateral extent of soil, provides a poorer approximation, which is particularly evident near the edge of the valley.

It may be generally concluded that the 10-layer discretization can be utilized by the frame model or the 2-D model to obtain the surface response in the valley, as it provides reliable results when compared with the much finer discretization.

4.3 VARIATION IN THE G_o PROFILE

The regulatory practice in nuclear power plant design requires that the proposed G_o profile be varied between ($1.5\ G_o$) and ($G_o/1.5$) (Valera et al, 1977). This is used to account for the uncertainty in establishing dynamic soil properties. Accordingly, results are compared using the frame model for the ($1.5\ G_o$), (G_o) and ($G_o/1.5$) profiles of soil type (NC) in Fig. 4-5 and of soil type (DS) in Fig. 4-6. The input rock motion is the generated acceleration with $a/v = 1$, scaled to $v = 0.2$ m/s.

The effect of variation in the G_o profile on the acceleration spectral ratios is a shift to the left for the ($1.5\ G_o$) profile and a shift to the right for the ($G_o/1.5$) profile. These shifts indicate changes in the local-amplification periods at the three surface locations $x = 0$, 0.5 B and 0.8 B. On the other hand, the peak spectral ratios are less affected by the change in the G_o profile, which is particularly evident near the edge of the valley, where the soil formation is stiffer and thus less sensitive to the variation in stiffness. Generally, higher G_o values lead to shorter periods and slightly higher peaks of amplification. The shorter periods are due to the larger stiffness and the slightly higher peaks are mainly because of the lower shear strain levels and consequently the lower damping associated with the larger G_o profiles. It is further observed that the (NC) profile, due to its softness especially in the top layers, is more sensitive to the variations in G_o than the (DS) profile.

The results from the frame model compare well with those from the 2-D model, as shown in Fig. 4-7 (a), (b) for the ($G_o/1.5$) profile of (NC) and in Fig. 4-7 (c), (d) for the ($1.5\ G_o$) profile of (DS). The given cases in Fig. 4-7 represent two extreme cases of soil stiffness. The fundamental periods of the valley corresponding to the variation in the G_o profiles of (NC) and (DS) are given in Table 4-1. It is noticed that the stiffer profile (DS) results in shorter fundamental periods than the softer profile (NC).

4.4 VARIATION IN THE DAMPING - STRAIN RELATIONSHIP

The upper and lower bounds along with the average line of the damping-strain relationships, shown in Fig. 3-4 and Fig. 3-5, are used to obtain the acceleration spectral ratios for soil types (NC) and (DS), respectively. Results are presented in Fig. 4-8 for (NC) and in Fig. 4-9 for (DS), using the frame model. The input rock motion is the generated acceleration time history with $a/v = 1$, scaled to peak velocity $v = 0.2$ m/s.

The variation in the damping-strain relationship for the same soil type leads to significant changes in the spectral ratio peaks. This is because more energy is dissipated in the soil as the damping increases at the same strain level, resulting in lower amplification values of rock motion. On the other hand, there are hardly any noticeable shifts in the local-amplification periods of sites due to unchanged G/G_o values. It is further observed that the surface response at the sites $x = 0.5$ B and 0.8 B is less sensitive to the damping variation than that at the site $x = 0$. This may be attributed to the shallower depths and consequently the stiffer formation of soil beneath the edge surface points in the valley. This lack of sensitivity at the edge sites is more apparent in the case of the stiffer profile (DS).

The general agreement of the results from the frame model and the 2-D model is emphasized again in Fig. 4-10 (a), (b) for the upper damping bound of (NC) and in Fig. 4-10 (c), (d) for the lower damping bound of (DS).

4.5 SUMMARY

The sensitivity of the horizontal seismic response of the valley resulting from the engineering models was examined for the variation in the soil-layer discretization, the variation in the G_o profile and the variation in the damping-strain relationship. The response results were presented as surface acceleration spectral ratios which represent the soil amplification of the input rock motion.

The surface seismic motions proved not to be sensitive to the soil-layer discretization, under different conditions of soil properties and control motions in the rock, except in the short-period range due to the top-layer amplification of the higher modes. It is concluded that a finer discretization may be replaced by a coarser one for the analysis of soil amplification without losing accuracy.

The variation in the G_o profile (stiffness) leads to significant changes in the local-amplification periods of sites and minor changes in the spectral ratio peaks. Higher G_o values result in shorter periods due to larger stiffness and slightly higher peaks of amplification because of lower values of associated damping. Furthermore, the soft (NC) profile is more sensitive to variations in G_o than the stiffer (DS) profile.

The variation in the damping-strain relationship for the same soil type leads to significant changes in the amplification values of the rock motion and hardly any noticeable shifts in the local-amplification periods of sites. The higher the damping is the lower the amplification becomes, due to the higher energy dissipation associated. Having a stiffer soil formation, the edge sites of the valley are less sensitive to the damping variation than the sites near the middle, which is more pronounced in the stiffer (DS) profile.

In general, the results from the frame model and from the 2-D model are in good agreement at different surface locations in the valley. On the other hand, the 1-D model fails in approximating the response, particularly near the edge of the valley, where the sloping boundary effect is significant.

Table 4-1 Fundamental periods of the valley

(a/v = I , v = 0.2 m/s)

G_o profile	soil type	period (sec)
1.5 G_o	NC DS	1.46 0.46
G_o	NC DS	1.83 0.63
G_o/1.5	NC DS	2.29 0.82

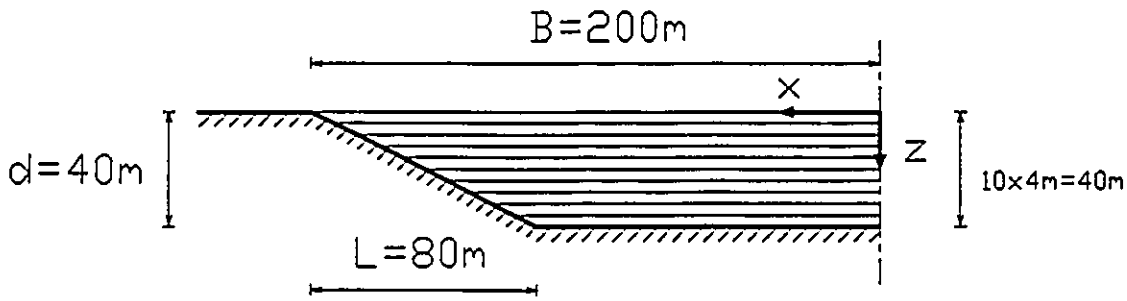

(a) 10-layer discretization

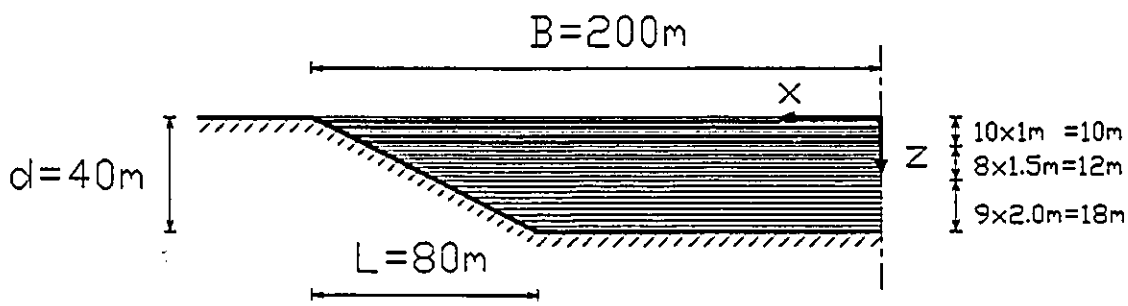

(b) 27-layer discretization

Fig. 4-1 Valley dimensions and soil-layer discretization

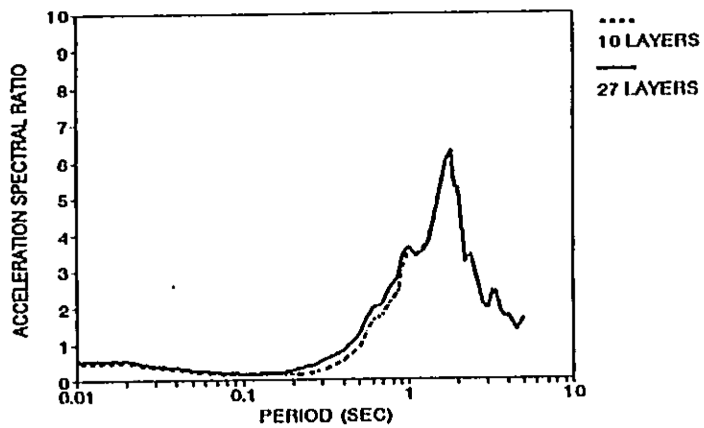

(a) a/v = H, v = 0.2 m/s, x = 0

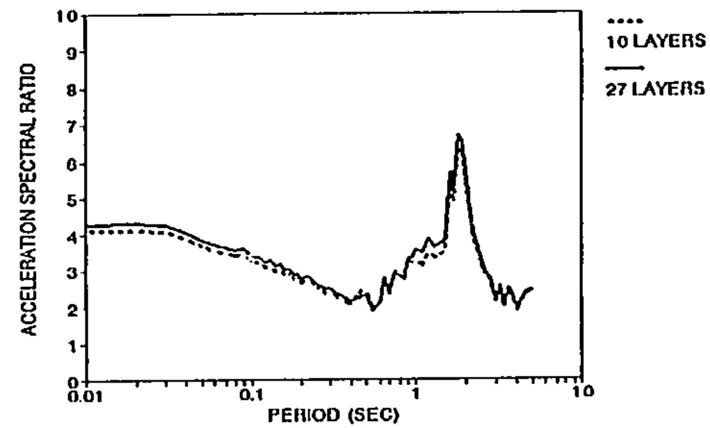

(b) a/v = V, v = 0.2 m/s, x = 0

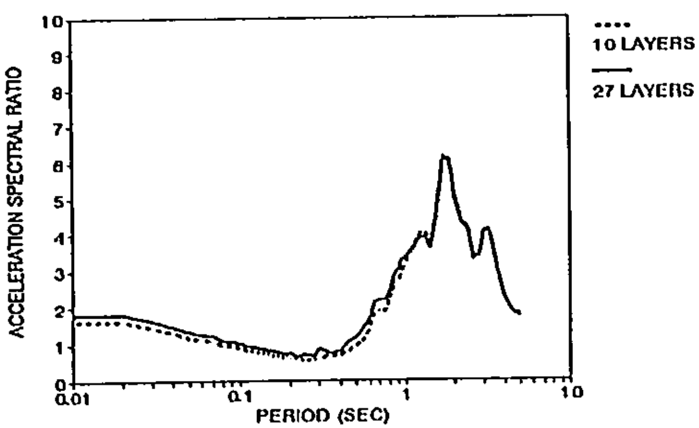

(c) a/v = I, v = 0.2 m/s, x = 0

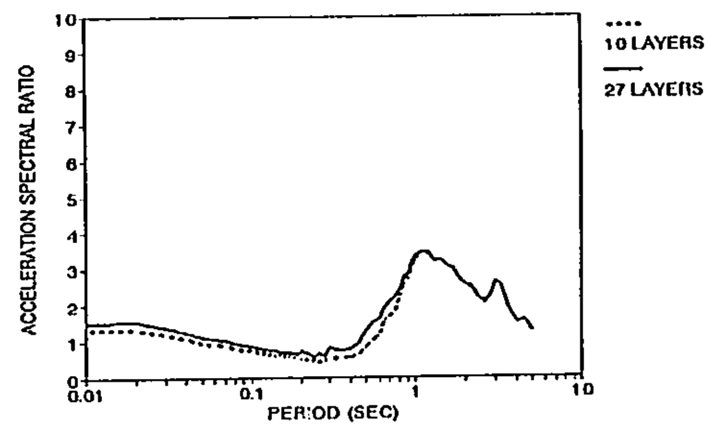

(d) a/v = I, v = 0.2 m/s, x = 0.8B

Fig. 4-2 Effect of variation in the soil-layer discretization
Soil profile : NC, frame model

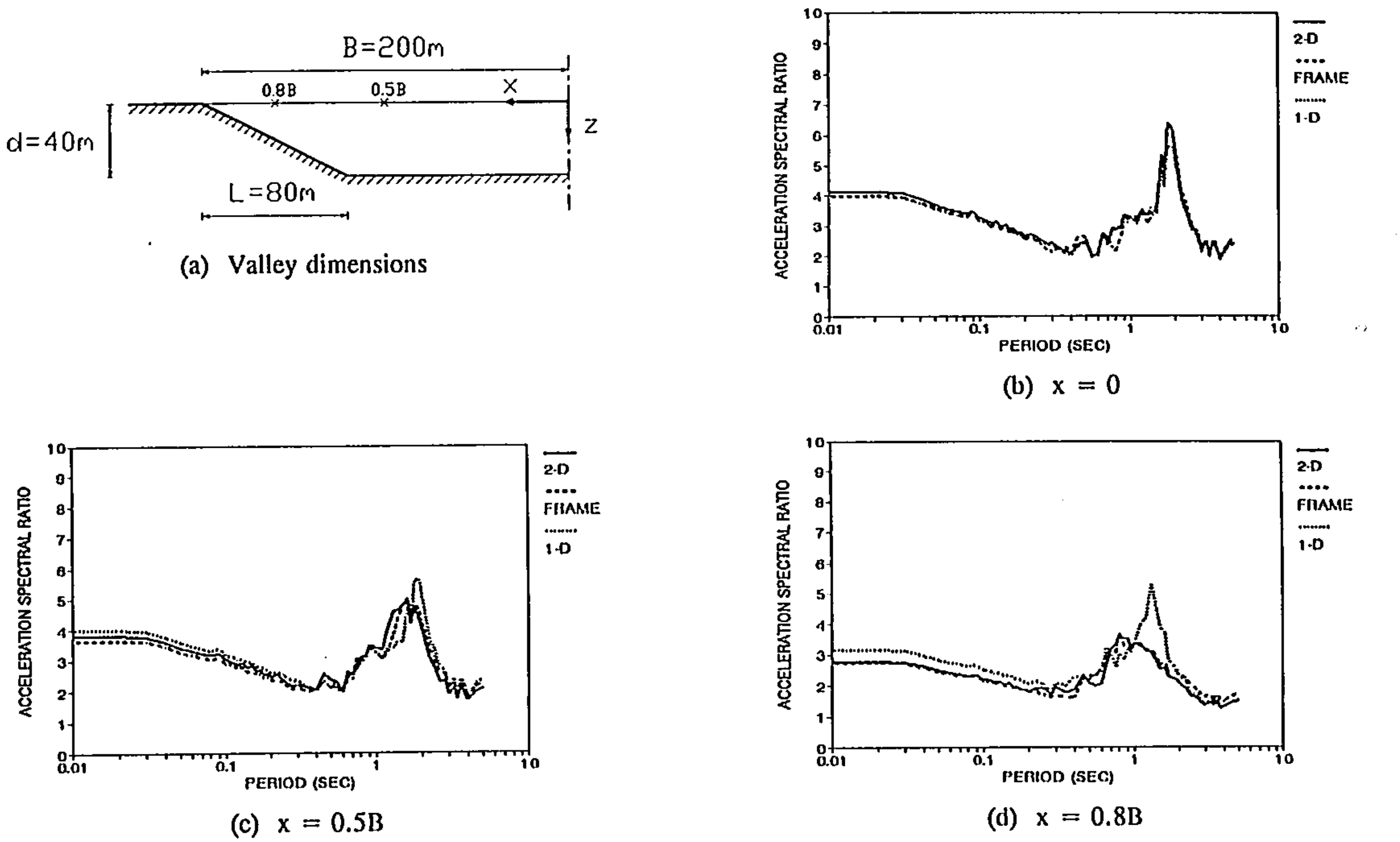

Fig. 4-3 Acceleration spectral ratios from 2-D, frame and 1-D models
Soil profile : NC, 27 layers, a/v = V, v = 0.2 m/s

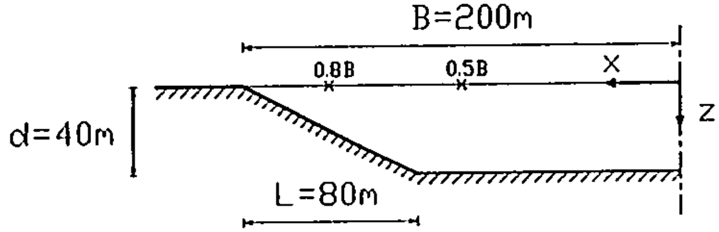

(a) Valley dimensions

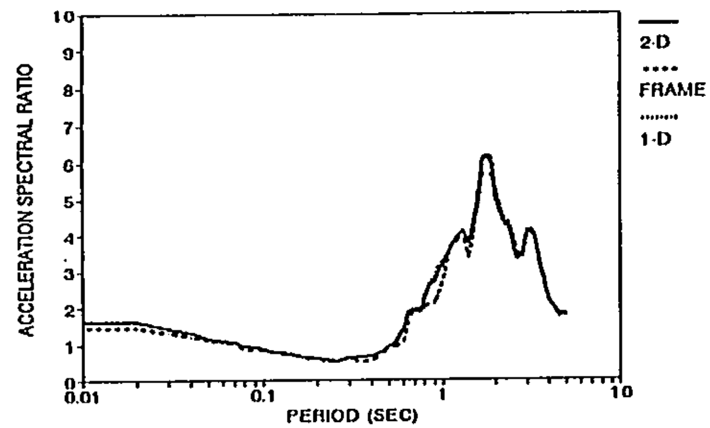

(b) x = 0

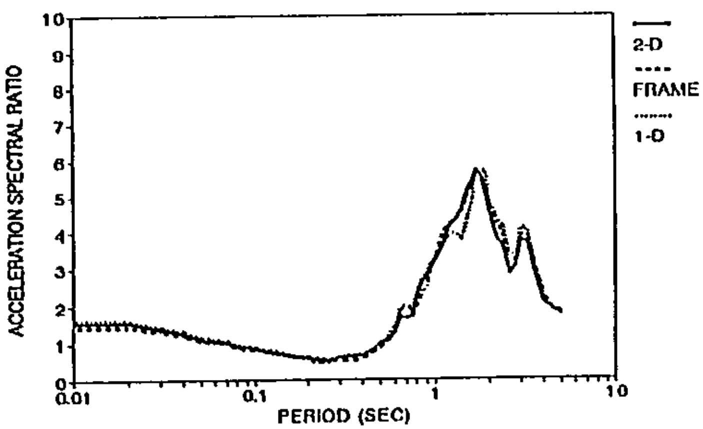

(c) x = 0.5B

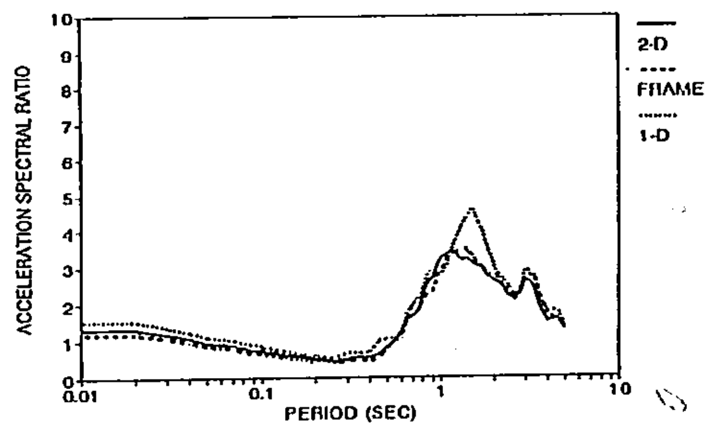

(d) x = 0.8B

Fig. 4-4 Acceleration spectral ratios from 2-D, frame and 1-D models
Soil profile : NC, 10 layers, a/v = 1, v = 0.2 m/s

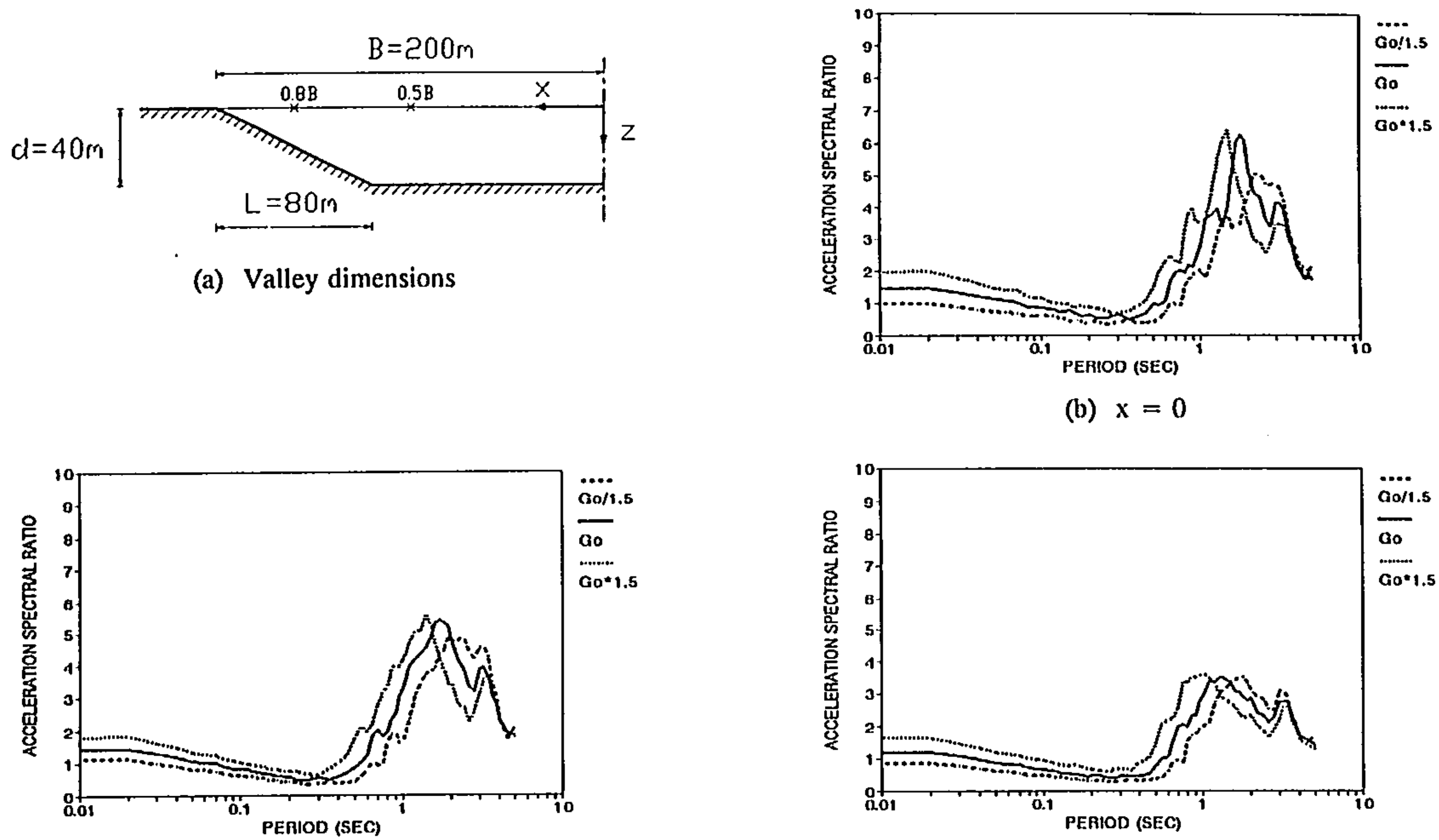

(a) Valley dimensions

(b) x = 0

(c) x = 0.5B

(d) x = 0.8B

Fig. 4-5 Effect of variation in the G_o profile
Soil profile : NC, frame model, a/v = I, v = 0.2 m/s

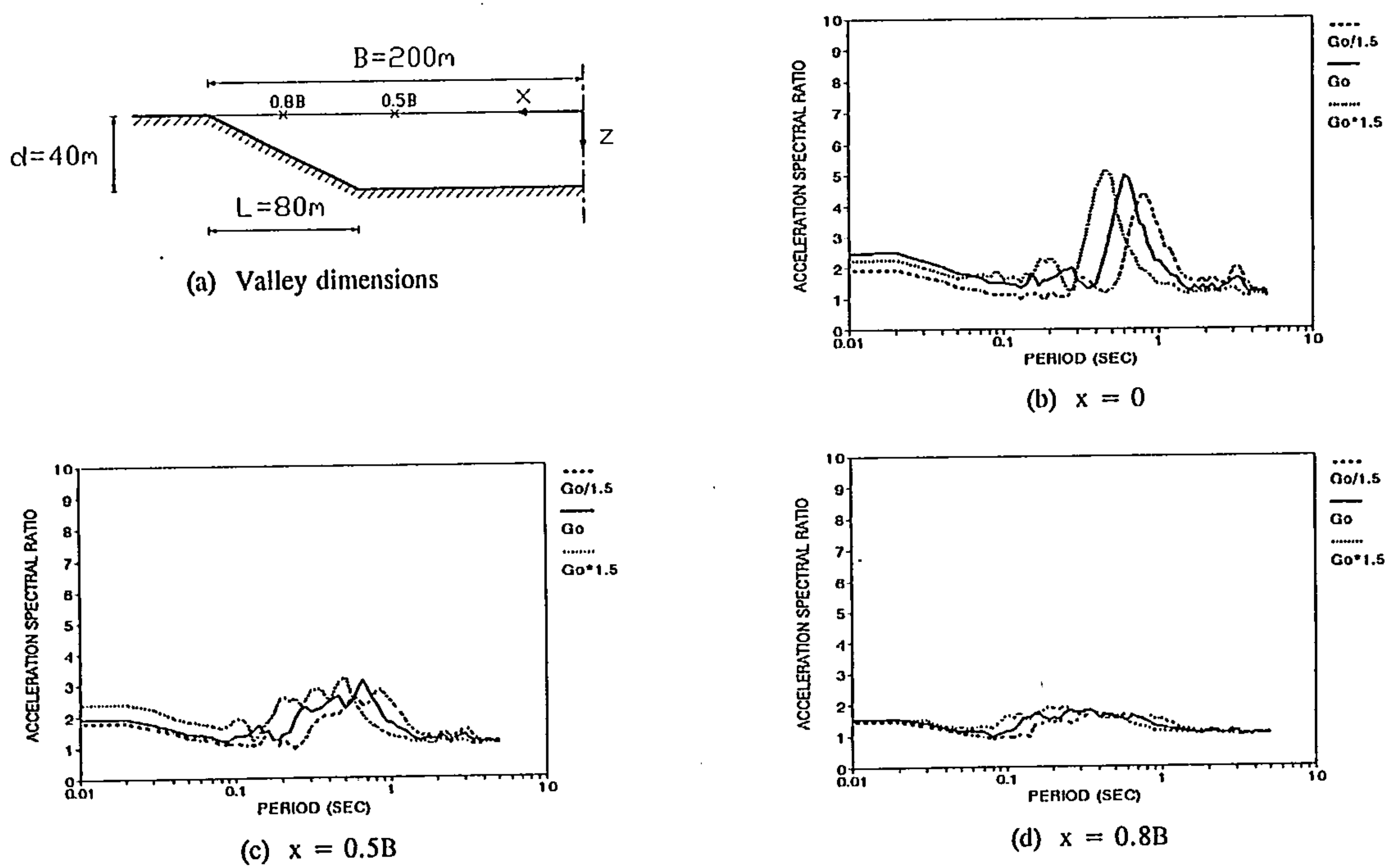

Fig. 4-6 Effect of variation in the G_o profile
Soil profile : DS, frame model, a/v = I, v = 0.2 m/s

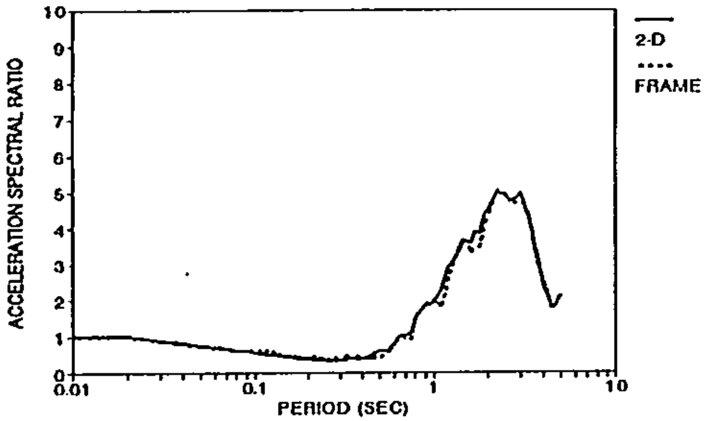

(a) Soil profile : NC, $G_o/1.5$, x = 0

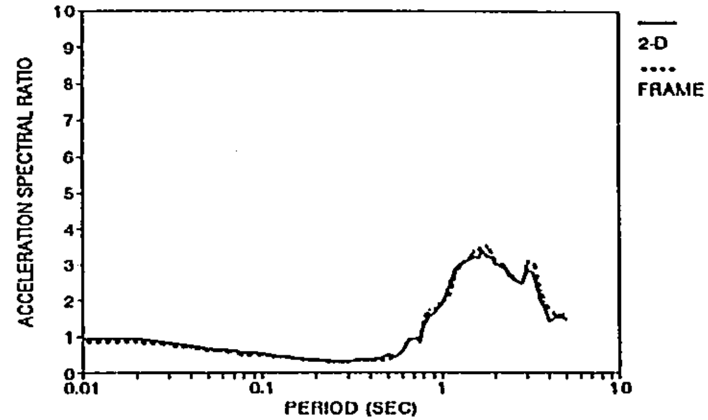

(b) Soil profile : NC, $G_o/1.5$, x = 0.8B

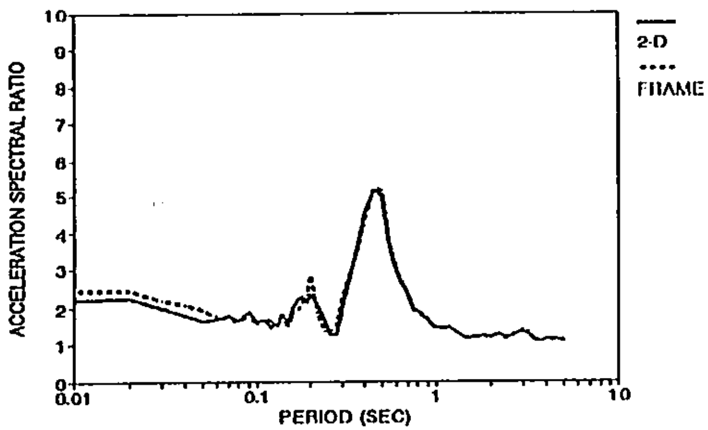

(c) Soil profile : DS, $1.5G_o$, x = 0

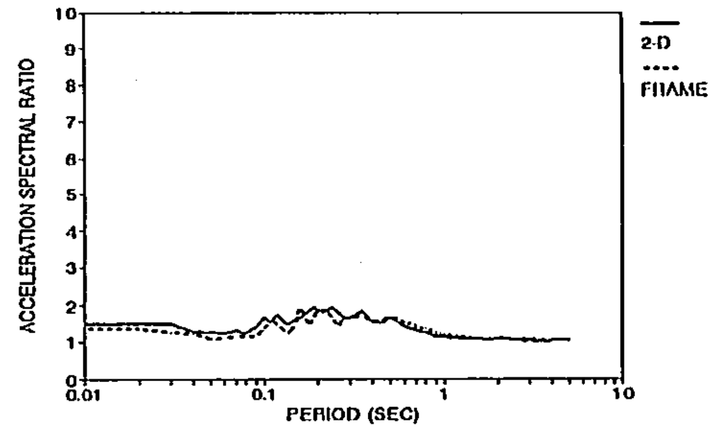

(d) Soil profile : DS, $1.5G_o$, x = 0.8B

Fig. 4-7 Acceleration spectral ratios from 2-D and frame models
$a/v = 1$, $v = 0.2$ m/s